博 士 論 文

STUDY ON THE ECONOMY POTENTIAL AND IMPLICATION OF HYDROGEN ENERGY SYSTEM WITH CARBON TAX INTRODUCTION

炭素税導入に基づく水素エネルギーシステムの経済的可能性と影響に関する研究

2020 年 07 月

钱　凡悦

FANYUE QIAN

Study on the Economy Potential and Implication of Hydrogen Energy System with Carbon Tax Introduction

ABSTRACT

The development of renewable energy is one of the cores of the current global energy transformation. Then due to the unstable supply of renewable energy, the development of the fastest growing photovoltaic and wind power has fallen into a bottleneck. The application and promotion of hydrogen energy can solve this problem well, but the current development of hydrogen energy is limited by the high equipment cost. Therefore, this study proposed the introduction of carbon tax to highlight the characteristics of zero carbon emission of hydrogen energy, and to transfer the environmental advantages of hydrogen energy into economic benefits. And from the three levels of equipment, system and region, the economic benefits of hydrogen energy system and conventional energy system are analyzed. Finally, based on Japan's electricity and energy consumption data, a prediction study was conducted to the effect on the energy structure and carbon emission reduction effect after considering the promotion of carbon tax and hydrogen energy.

In chapter 1, RESEARCH BACKGROUND AND PURPOSE OF THE STUDY. Firstly, the significance of hydrogen energy for renewable energy and global deep decarbonization were analyzed. Then the safety characteristics of hydrogen were compared with other fuels. After that, the process of producing, storing, transporting and using hydrogen energy was explained. Then, through the elaboration of the hydrogen energy development process and goals of the United States, the European Union, China and Japan, the importance of hydrogen energy in the energy strategies of various countries was highlighted. Finally, the research logic and content of the article were expounded.

In chapter 2, LITERATURE REVIEW OF HYDROGEN ENERGY SYSTEM. Firstly, through the review of the research on the development of hydrogen energy by the policies of various countries, the current status and trends of the cost reduction of hydrogen energy systems were explained. Next, since the core of development based on hydrogen energy is to combine with renewable energy, the literature and compares the characteristics of hydrogen storage and other energy storage technologies was reviewed. Finally, according to the research object of this article, the research and combing of the application of fuel cell, fuel cell vehicle and hydrogen energy in regional energy system were carried out.

In chapter 3, MODEL ESTABLISHMENT AND FORECASTING METHOD RESEARCH. Firstly, the research motivation and main research methods of the article were

expounded. Then the general load and equipment model to be used in the follow-up study were established. At the same time, different operating strategies based on regional energy systems were explained. Next, it was believed that load forecasting is the basis of follow-up research, so a new forecasting method of cold and hot load based on transfer learning was proposed and verified.

In chapter 4, UTILIZATION POTENTIAL AND ECONOMIC ANALYSIS OF HYDROGEN ENERGY EQUIPMENT. In this part, a 5kW methanol reforming PEMFC will be simulated based on a simulation software called TRNSYS to analyze the situation of the residual heat. Then, through the simulation models of the two waste heat recovery methods of refrigeration and hot water production, the comprehensive energy utilization potential of the fuel cell was studied. After introducing carbon tax restrictions, the economic comparison of fuel cells and fuel cell vehicles with conventional energy systems was explored.

In chapter 5, ECONOMIC AND POTENTIAL ANALYSIS OF FUEL CELL VEHICLE-TO-GRID SYSTEM. Firstly, this part choosed a large shopping mall in Japan as the research scenario, after obtaining its annual electricity consumption. The Monte Carlo simulation method was used to simulate the basic parameters such as vehicle visiting time, running kilometers and departure time, and to analyze the impact of FCV discharging on building energy consumption. Then, replacing part of the FCVs with EVs was considered, as well as the discharges of vehicles to buildings and power grids, using buildings as agents for all vehicles to provide V2G services for power grids. A genetic algorithm (GA) was used to find the best discharge price, the choice of vehicle discharging under the condition of the highest economic benefit, and to analyze the change of building income under different FCV ratios and EV charging demand. Through sensitivity analysis, the influence of six parameters on economic benefit was analyzed, including daily electricity price for buildings, battery cost, fuel cell cost, carbon emission price, electricity grid carbon emission and hydrogen cost.

In chapter 6, ECONOMIC AND POTENTIAL ANALYSIS OF REGION DISTRIBUTED HYDROGEN ENERGY SYSTEM. This part firstly selected ten buildings of different building types in the Higashida area of Kitakyushu City, Japan as the research goal, the hydrogen distributed energy system as the research object, and the conventional distributed energy system as the comparative reference. Secondly, based on the actual data of building power consumption, the hourly cooling and heating load was calculated using the index method and the hourly load sharing method. After that, a region distributed energy system (RDES) optimization model was established, and the genetic system was used to design and optimize the conventional system and the hydrogen energy system respectively, and the comparison of the two systems under different carbon taxes was obtained. Through the analysis of the results of different types of buildings, the adaptability of the hydrogen RDES was studied. After the lease, through the sensitivity analysis of electricity price, natural gas price, hydrogen price, and hydrogen energy equipment price, the future economic benefits of the hydrogen RDES were studied.

In chapter 7, STUDY ON THE HYDROGEN IMPLICATION OF ENERGY STRUCTURE WITH CARBON TAX INTRODUCTION. Firstly, the three energy storage technologies of battery, pumped storage and hydrogen storage were compared with the application in different renewable energy sources. Then ten power companies in Japan was selected and the weighted on-grid electricity price was used as the objective function to study the energy structure changes under different carbon taxes. According to the characteristics of long-distance and inter-seasonal storage, the effect of renewable energy coordination and scheduling in Japan was studied. Then through sensitivity analysis, the impact of price fluctuations of coal, LNG, photovoltaic equipment, wind power generation equipment and hydrogen energy production equipment on the research results was obtained. Finally, from the power generation field to the overall primary energy consumption, the effects of three kinds of hydrogen energy promotion measures for household fuel cells, fuel cell vehicles and natural gas dropped with hydrogen on CO2 emission reduction was carried out to explore the introduction of hydrogen energy to help Japan achieve its CO2 reduction goals.

In chapter 8, CONCLUSION AND PROSPECT. The conclusions of whole thesis is deduced and the future work of hydrogen energy has been discussed.

钱 凡悦 博士論文の構成

Study on the Economy Potential and Implication of Hydrogen Energy System with Carbon Tax Limitation

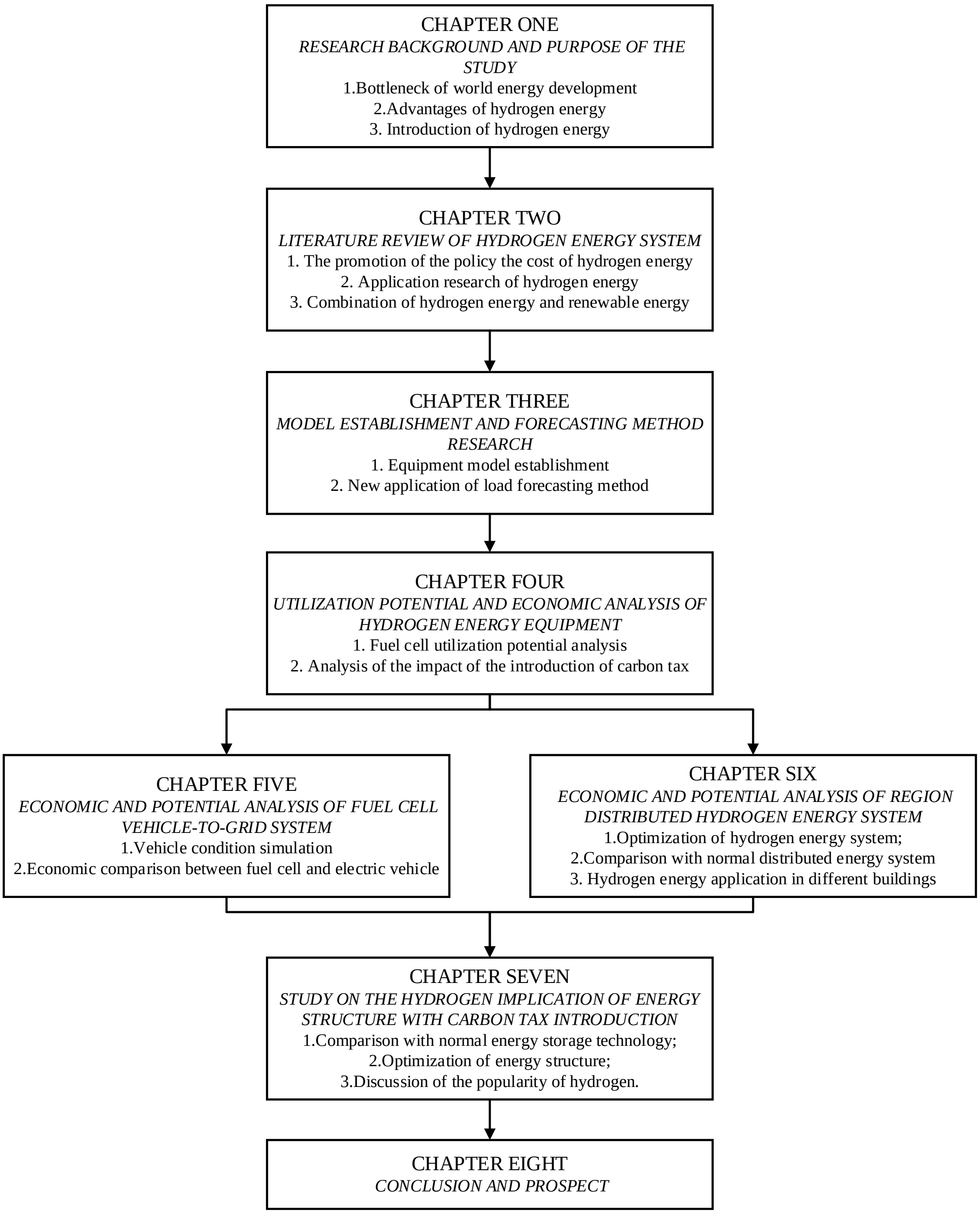

TABLE OF CONTENTS

CHAPTER 4: UTILIZATION POTENTIAL AND ECONOMIC ANALYSIS OF HYDROGEN ENERGY EQUIPMENT

CHAPTER 5: ECONOMIC AND POTENTIAL ANALYSIS OF FUEL CELL VEHICLE-TO-GRID SYSTEM

CHAPTER 6: ECONOMIC AND POTENTIAL ANALYSIS OF REGION DISTRIBUTED HYDROGEN ENERGY SYSTEM

CHAPTER 7: STUDY ON THE HYDROGEN IMPLICATION OF ENERGY STRUCTURE WITH CARBON TAX INTRODUCTION

CHAPTER 8: CONCLUSION AND PROSPECT

Chapter 1

RESEARCH BACKGROUND AND PURPOSE OF THE STUDY

CHAPTER ONE: RESEARCH BACKGROUND AND PURPOSE OF THE STUDY

1.1 Background

1.1.1 Current status and bottleneck of international energy development

(1) Renewable energy is still the focus of development

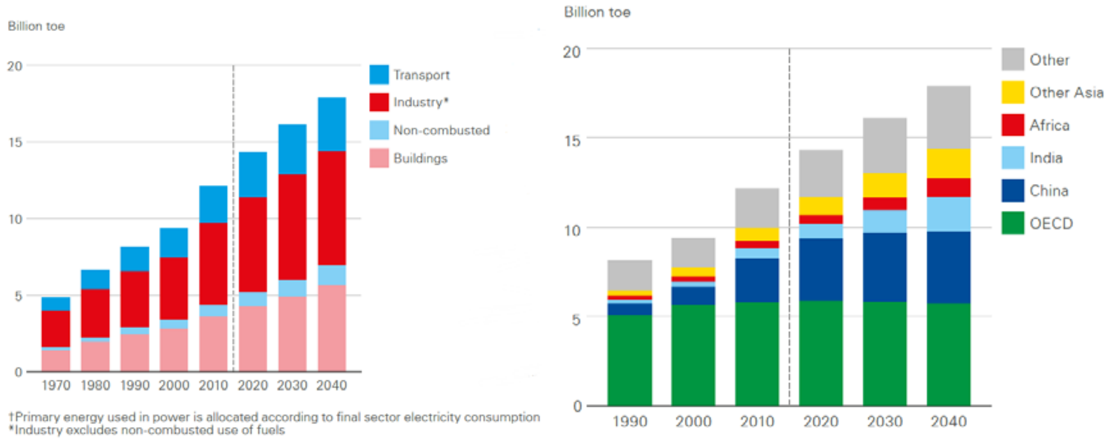

(a) By terminal industry **(b) By region**

Fig 1-1 Global primary energy consumption forecast by 2040 by terminal industry and region [1]

In order to achieve the goals in the Paris Agreement, all countries in the world are in the gradual transformation stage of the energy system. It is predicted that world GDP will more than double by 2040, but this increase will be offset by accelerated energy efficiency. In the next 25 years, energy demand will only increase by about one-third. Among them, the industrial demand growth of energy accounts for about half of the new energy consumption, and the growth rate of the transportation field will be greatly reduced due to the promotion of new energy vehicles (Fig 1-1).

At present, the global energy economy is still largely dependent on fossil energy, but the increasingly exhausted fossil energy is difficult to meet the sustainable growth of energy demand [2]. Moreover, the excessive consumption of fossil energy leads to a series of environmental pollution problems such as air pollution, acid rain, greenhouse effect [3]. The renewable energy represented by solar energy and wind energy has the advantages of inexhaustible and widely distributed resources, which is regarded as the main method to solve the energy crisis [4]. Therefore, all countries in the world have issued relevant laws and regulations to promote the promotion and use of renewable energy [5].

According to BP's "Energy Outlook 2019" forecast for the future energy development trend, renewable energy is the fastest growing of all energy sources, accounting for 40% of the primary energy growth. At the same time, with the deepening of the transformation process of renewable

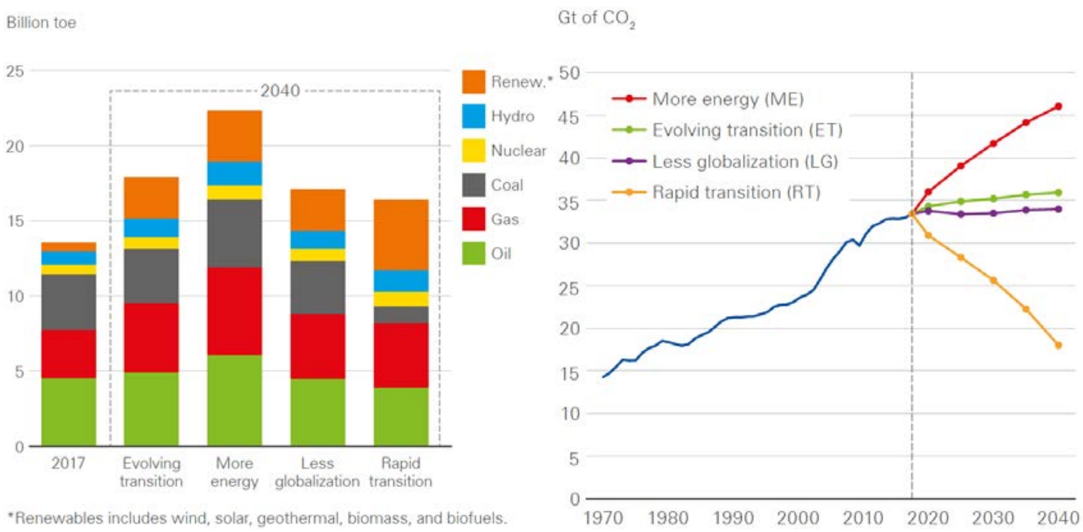

Fig 1-2 Forecast of global primary energy consumption and carbon emission in 2040 [1]

energy and energy system, the growth trend of primary energy consumption and carbon emissions will gradually slow down until it finally starts to reduce (Fig1-2). It can be seen that the development of renewable energy and efficient use of energy will be the key direction of energy system development in the future.

(2) Renewable energy consumption is the key obstacle

Renewable energy can replace traditional energy in four ways: power generation, heating / cooling, transportation fuel, and energy supply in remote villages. Among them, power generation is the most important and largest use. In recent years, many countries have achieved a high proportion of renewable energy power generation, most of which are mainly hydropower. Renewable electricity accounts for more than 50% in more than 20 countries, including Iceland (100%), Norway (96%), Brazil (85%), New Zealand (73%), Colombia (70%), Austria (68%) , Venezuela (66%), Switzerland (58%), Sweden (55%), etc. Since the 1990s, the development of the global renewable energy industry has continued to accelerate. The installed capacity of renewable energy power generation increased from 812 million kilowatts in 2004 to 1.712 billion kilowatts in 2014, an average annual increase of about 8%, of which hydropower, wind power and solar photovoltaic power generation accounted for the absolute leading position.[6]

As of 2016, global renewable energy power generation accounted for 24.5% of the total power, of which hydropower generation was the highest, accounting for 16.6%, followed by wind farms 4.0%, biomass power generation 2.0% and photovoltaic power generation 1.5%. According to the data of 2017 REN21 and the previous 7 years, they are compiled in Table 1-1 below.

Table 1-1 Global Power Production Structure 2009-2016 [7]

	2009	2010	2011	2012	2013	2014	2015	2016
Global power /TWh	20261	21562	22242	22797	23403	23844	24216	24816
Fossil fuel, nuclear energy /%	82.0	80.6	79.7	78.3	77.9	77.2	76.3	75.5
Renewable energy /%	18	19.4	20.3	21.7	22.1	22.8	23.7	24.5
Hydropower /%	15.0	16.1	15.3	16.5	16.4	16.6	16.6	16.6
Wind energy/%	3.0	3.3	5.0	5.2	2.9	3.1	3.6	5.0
Biomass energy /%					1.8	1.8	2.0	2.0
Photovoltaic /%					0.7	0.9	1.2	1.5
Geothermal etc. /%					0.4	0.4	0.4	0.4

As can be seen from the above table, although the current renewable energy is still dominated by hydropower, the reason for the rapid progress of renewable energy power generation in recent years is mainly due to the acceleration of wind farms and photovoltaic power generation. Among them, wind power has grown from 6% of renewable energy in 2004 to 24.1% in 2016. Photovoltaics has grown from 0.3% renewable energy in 2004 to 15% in 2016. At the same time, the global photovoltaic industry has a large workforce, accounting for 31.5% of global renewable energy.

With the rapid development of photovoltaic and wind power, the phenomenon of abandoning wind and light is becoming more and more serious. Among them, developed countries such as Germany and the United States encountered this phenomenon earlier and took measures to deal with it earlier. Mainly include: changing the operation mode of the electricity market, constructing power transmission channels (including mutual aid with neighboring countries), improving the electricity price mechanism (such as negative electricity prices), and adding flexible units such as hydropower and gas power. Some results have been achieved, which promoted the consumption of photovoltaic and wind power, but at the same time caused the slowdown of the development of renewable energy.

Even so, after a period of development, the share of renewable energy still reaches the bottleneck, unable to make further breakthroughs. It is mainly the low-grade and intermittent characteristics of renewable energy [8]. Solar energy only produces energy when the irradiance is high, and wind energy changes with the change of outdoor wind speed; such highly volatile renewable energy, in the process of power generation and grid connection, has great impact on the power grid, and it is difficult to ensure the stability of the power grid, making it more difficult to quickly match with the urban power grid [9]. In addition to improving the stability of renewable energy in the grid connection stage, the second solution to the utilization of renewable energy is energy storage integration. However, the low energy storage efficiency and high initial investment of traditional batteries slow the progress of this technology [10]. Hydrogen energy has the characteristics of high energy storage, convenient storage and transportation, and zero pollution. It is considered to be the most promising energy storage option in the future.

1.1.2 The significance of the development of hydrogen energy for renewable energy and energy environment

(1) Hydrogen energy will be an important way to absorb renewable energy

Since hydrogen must be produced from hydrogen-containing substances such as water and fossil fuels, it is a secondary energy source. At present, high-efficiency and low-cost hydrogen production is the focus of attention of countries around the world. Using renewable energy to produce hydrogen can both reduce production costs and achieve the purpose of protecting the environment. It is the most effective way to produce hydrogen. At the same time, this method can effectively alleviate the current consumption problems caused by the continuous development of renewable energy.

Hydrogen and electricity can be said to be complementary to each other during the transformation of the energy system. The use of electrolysis devices to achieve hydrogen production from renewable energy power is conducive to the integration of highly volatile renewable energy power (VRE) into the energy system. At the same time, large-scale use of solar energy, wind energy and other renewable energy to produce hydrogen, and the development of large-scale, low-cost VRE facilities in marginal areas with rich solar or wind energy resources, dedicated to hydrogen production, can realize the reuse of wind and light, and energy conversion, improve the utilization rate of renewable energy, reduce waste of clean energy.[11] Although batteries and demand-side measures can provide short-term flexibility, hydrogen is the only large-scale technology that can be used for long-term energy storage. It can use the existing natural gas network, salt caves and barren gas fields to store energy for a long time at a lower cost. Through the hydrogen produced from renewable energy, a large amount of renewable energy can be led from the power sector to the end-use sector. Renewable energy power can be used to produce hydrogen, which in turn can provide energy for sectors that are difficult to achieve decarbonization through electrification and achieve sustainable energy development.

(2) Hydrogen energy helps deep decarbonization in various industries

As a transportation medium for renewable energy, hydrogen can realize the long-distance transmission of renewable energy, promote the interconnection between electricity and construction, transportation and industry, and help in areas where electrification is difficult (transportation, industrial Construction departments that rely on existing natural gas pipeline networks, etc.) make more use of renewable energy to reduce carbon dioxide emissions.(Fig1-3)

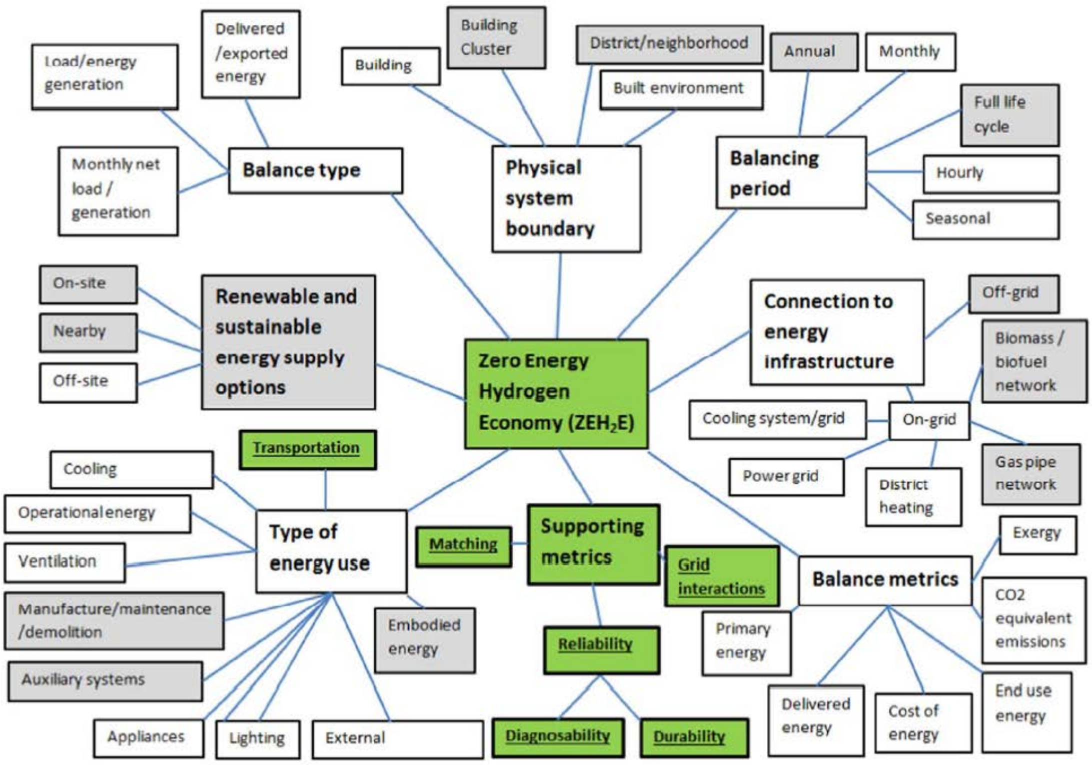

Fig 1-3 Mind map for the definition of zero-energy hydrogen economy [12]

In terms of transportation, hydrogen is the most promising decarbonization option for trucks, buses, large cars, and commercial vehicles. Among them, lower energy density (hence lower range), higher initial cost, and slow battery charging performance are The main disadvantage. Compared with batteries and internal combustion engines, fuel cells require less raw materials. Since the transportation sector accounts for nearly a quarter of global carbon dioxide emissions, decarbonization is a key factor in achieving energy transformation. In addition, hydrogen fuel replenishment facilities have a significant advantage: compared to fast charging, it only requires about one tenth of the city and highway space. Similarly, suppliers can flexibly supply hydrogen, and large-scale deployment of fast charging facilities requires major upgrades to the grid. Finally, once the smallest scale of promotion is achieved, hydrogen provides operators with an attractive business case. In addition to road transportation, in the longer term, hydrogen may also promote decarbonization in the fields of railway transportation, shipping, and aviation. In the aviation industry, hydrogen and hydrogen-based synthetic fuels are the only options for large-scale decarbonization.

Industry can burn hydrogen to produce high-grade heat, and use the fuel as a raw material in several processes, directly or together with carbon dioxide as a synthetic fuel / electric fuel. In steelmaking, for example, hydrogen can be used as a reducing agent to replace coal-based blast furnaces. When the refinery is used as a raw material for ammonia production and hydroprocessing, low-carbon sources can be used in the future. Along with carbon dioxide, hydrogen can also replace hydrocarbons such as natural gas in the chemical process, such as the production of olefins and hydrocarbon solvents (BTX), which form a major part of raw material uses. This provides a carbon sink, that is, an opportunity to use carbon dioxide instead of emissions. Large industrial sectors (such as oil refineries, ammonia production plants, etc.) that have more than ten years of experience in using hydrogen are expected to become the main early market for hydrogen production from electricity, because they can immediately produce scale effects, thereby quickly reducing costs.

In addition, injecting hydrogen produced from renewable energy power into the natural gas pipeline network will likely increase revenue and thus improve the economics of power generation. This measure can make the introduction of hydrogen energy smoother, and energy companies can directly use the existing pipeline to transport hydrogen or synthetic methane to natural gas power plants through electricity. Although eventually switching to 100% hydrogen requires equipment and piping upgrades, it still fits perfectly with the existing heating infrastructure in the building.

1.2 Hydrogen energy characteristics and application process

1.2.1 Characteristics of hydrogen energy

Hydrogen energy mainly appears in the form of a compound state on the earth. It is the most widely distributed substance in the universe. It constitutes 75% of the mass of the universe. The main characteristics of hydrogen are compared with other common fuels, and four coordinates are established to represent diffusion, buoyancy, lower explosion limit, and the reciprocal of combustion speed. As shown in the Fig1-4 below, the closer to the coordinate origin, the more dangerous. It can be seen that in terms of diffusion, buoyancy and lower explosion limit, hydrogen is far safer than other fuels, and it is not easy to form explosive aerosols. Therefore, as long as effective prevention and control measures are established, the safety of hydrogen is still very outstanding.

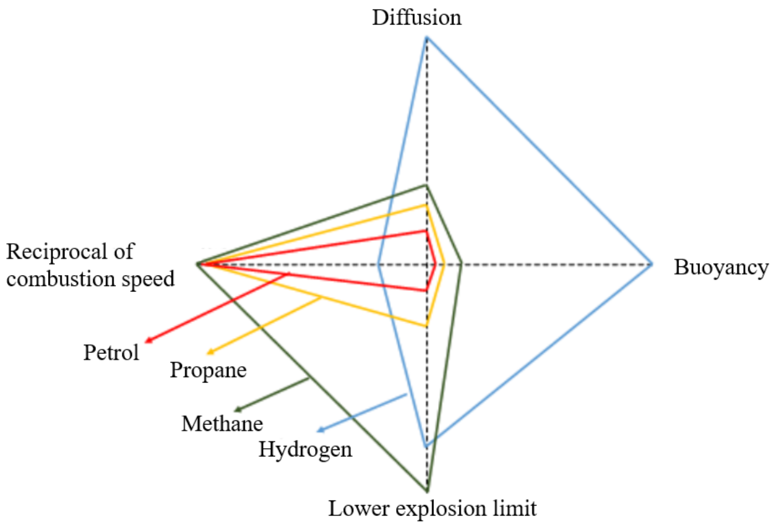

Fig 1-4 Hydrogen characteristic analysis diagram (Source: Guojin Securities Research Institute, fuel cell industry chain (4) | hydrogen: safety analysis http://www.china-nengyuan.com/news/136577.html)

It is difficult to accumulate high concentration of hydrogen in the air. If a leak occurs, the hydrogen will diffuse quickly, especially in an open environment, it is easy to escape quickly, unlike gasoline that stays in the air after volatilization. Dr. Swain of the University of Miami in the United States did a famous experiment, as shown in Fig 1-5. The two vehicles used hydrogen and gasoline as fuel, respectively, and then conducted a leak ignition test. After 3 seconds of ignition, the flame produced by the high-pressure hydrogen directly sprayed above, and gasoline ignited from the lower part of the car; by 1 minute, only hydrogen leaked from the car using hydrogen as fuel burned, the car has no major problems, and the gasoline car has already been Become a big fireball and burn out completely. Therefore, the volatile nature of hydrogen, compared with ordinary gasoline cars, is conducive to the safety of cars.

(a) 3 seconds **(b) 60 seconds**

Fig1-5 Combustion comparison test of hydrogen car and petrol car [13]

1.2.2 Application of hydrogen energy

The non-polluting, zero-emission hydrogen energy is often referred to as "the most promising secondary energy in the 21st century" and is also recognized as a clean energy. The whole process of the application of hydrogen energy is shown in Fig 1-6 below, including: the preparation, storage, transportation and utilization of hydrogen energy. In the following chapters, the development status of each link will be explained.

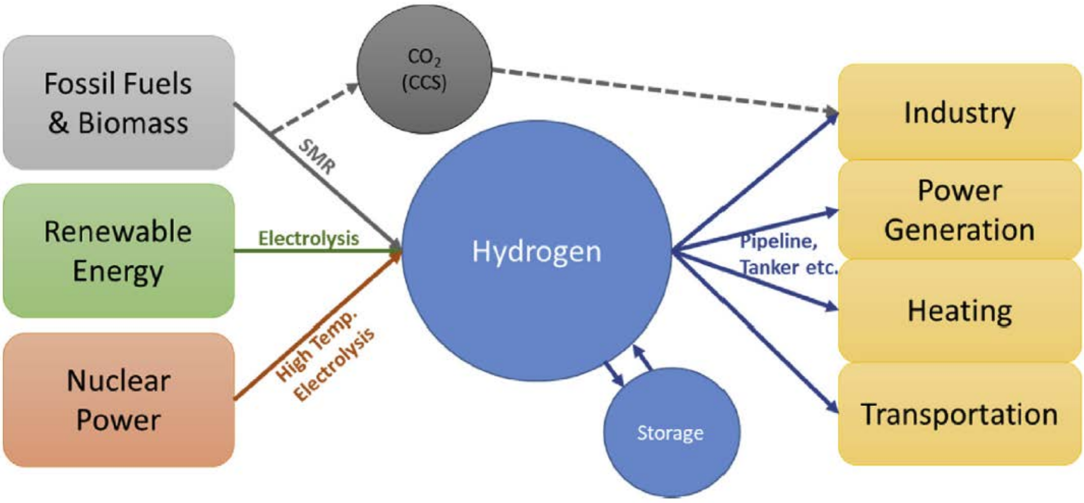

Fig 1-6 Hydrogen energy production and application flow chart [14-16]

1.2.2.1 Hydrogen production

At present, the production of hydrogen mainly has the following three more mature technical routes: (1) coal and natural gas are represented by fossil energy reforming to produce hydrogen; (2) coke oven gas, chlor-alkali tail gas and propane dehydrogenation are represented The industrial by-product gas produces hydrogen; (3) Electrolytic water produces hydrogen. At present, electrolytic hydrogen production can be produced on a small scale (<1 MW), and large-scale (up to 10 MW) demonstration projects are underway, with an annual hydrogen production ratio of about 3%. Technologies such as biomass direct hydrogen production and solar photocatalytic decomposition of water to produce hydrogen are still in the experimental and development stage, and have not yet reached the requirements for industrial-scale hydrogen production. Fig 1-7 shows various technical descriptions of hydrogen energy production

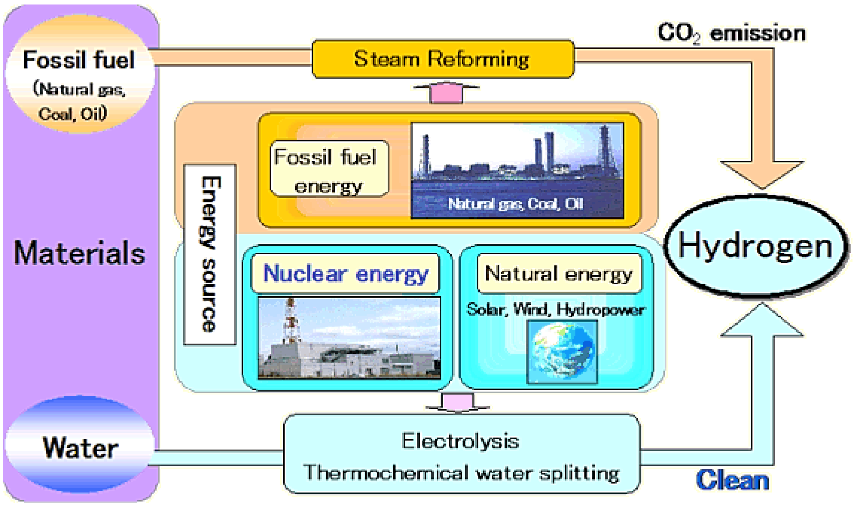

Fig 1-7 Various technical descriptions of hydrogen energy production (Source: Japan Atomic Energy Agency, HTGR Research and Development Center, Hydrogen Society in the Future https://www.jaea.go.jp/04/o-arai/nhc/en/data/data_10.html)

It can be seen that relying solely on fossil energy and industrial by-product hydrogen production cannot meet the transformation requirements of the energy system and cannot achieve the purpose of deep decarbonization. Therefore, the hydrogen production technology of renewable energy electrolysis and other renewable energy hydrogen production technologies are currently the development path of hydrogen energy that the government and industry must pay attention to.

(1) Hydrogen production from fossil fuel reforming

Hydrogen production from fossil fuel reformation is the main production path of industrial hydrogen at present due to its mature process and low cost. Currently the most used is hydrogen production by steam methane reforming (SMR). However, the process of producing hydrogen from fossil resources will emit a large amount of carbon dioxide and pollute the environment. Hydrogen production is difficult to become the main source of hydrogen for fuel cells.

(2) Hydrogen as a By-Product or Industrial Residual Hydrogen

Hydrogen production by industry is the use of hydrogen-rich industrial tail gas as a raw material, mainly using the pressure swing adsorption method (PSA method) to recover and purify hydrogen. At present, the main sources of tail gas include chlor-alkali industrial by-product gas, coke oven gas, and light hydrocarbon cracking by-product gas. Compared with other hydrogen production methods, the biggest advantage of industrial by-product hydrogen production is that almost no additional capital investment and fossil raw material investment are required, and the obtained hydrogen has significant advantages in terms of cost and emission reduction. Therefore, this method can be used as the main form of hydrogen energy development in the early stage. In the later period, due to the limitation of industrial production capacity, it will gradually transition to electrolytic hydrogen production.

(3) Electrolytic hydrogen production

Hydrogen production from electrolyzed water dissociates water molecules into hydrogen and oxygen through an electrochemical process and separates them at the anode and cathode. According to different diaphragms, it can be divided into alkaline water electrolysis, proton exchange membrane water electrolysis, and solid oxide water electrolysis.

The industrial application of industrialized water electrolysis technology began in the 1920s. The alkaline water electrolysis cell electrolysis water technology has achieved industrial scale hydrogen production and is used in industrial needs such as ammonia production and petroleum refining. After the 1970s, energy shortages, environmental pollution, and space exploration requirements drove the development of proton exchange membrane electrolysis water technology. At the same time, the high-pressure compact alkaline electrolyzed water technology required for the development of special fields has also been developed accordingly. At present, the practically applicable hydrogen production technology of electrolytic water mainly includes alkaline liquid water electrolysis and solid polymer water electrolysis.

At the same time, there are still many problems that need to be improved due to the alkaline liquid electrolyte electrolytic cell, which promotes the rapid development of solid polymer electrolyte (SPE) water electrolysis technology. The first practical SPE is proton exchange membrane (PEM), so it is also called PEM electrolysis. The proton exchange membrane replaces the asbestos membrane, conducts protons, and isolates the gas on both sides of the electrode, which avoids the disadvantages of using a strong alkaline liquid electrolyte in the alkaline liquid electrolyte electrolytic cell. At the same time, the PEM water electrolytic cell adopts a zero-gap structure, the volume of the electrolytic cell is more compact and streamlined, the ohmic resistance of the electrolytic cell is reduced, and the overall performance of the electrolytic cell is greatly improved. The operating current density of the PEM electrolyzer is usually higher than 1A / cm2, at least four times that of the alkaline water electrolyzer. It has high efficiency, high gas purity, green environmental protection, low energy consumption, no alkali solution, small size, safe and reliable, It can achieve higher gas production pressure and other advantages, and it is recognized as one of the most promising electrolytic hydrogen production technologies in the field of hydrogen production.

1.2.2.2 Hydrogen storage and transportation

The storage of hydrogen energy includes compressed hydrogen storage, liquid hydrogen storage, and storage using hydrogen storage media, as shown in Fig 1-8 below.

After storage, according to different storage forms, it will also be transported by the corresponding transportation method. In addition, pipeline transportation and manufacturing material transportation can also be used. As shown in Fig 1-9 is the hydrogen transport costs with different methods and distance.

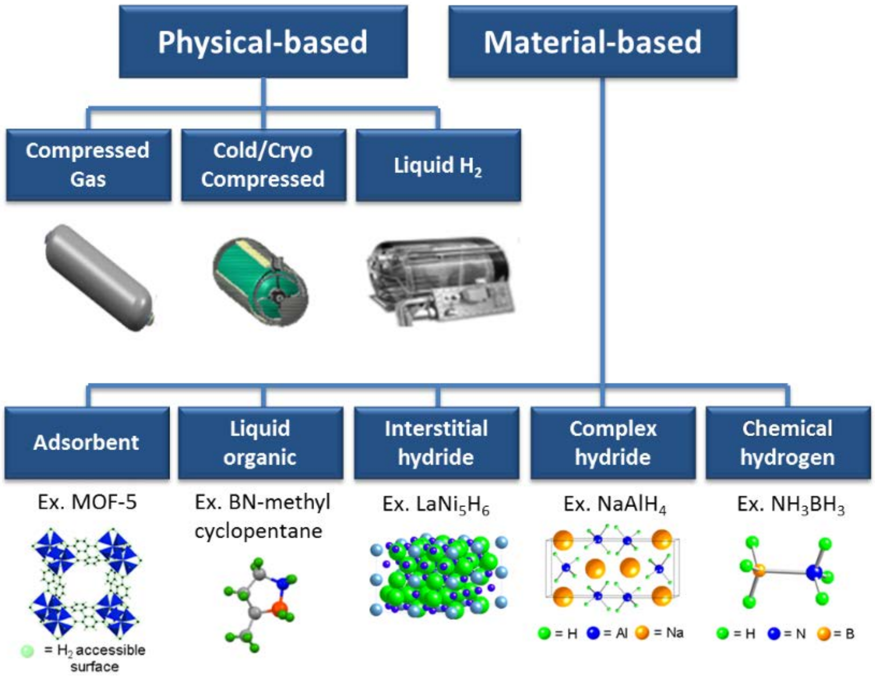

Fig 1-8 Various storage methods of hydrogen (Source: The Hydrogen and Fuel Cell Technologies Office (HFTO), Hydrogen Storage https://www.energy.gov/eere/fuelcells/hydrogen-storage)

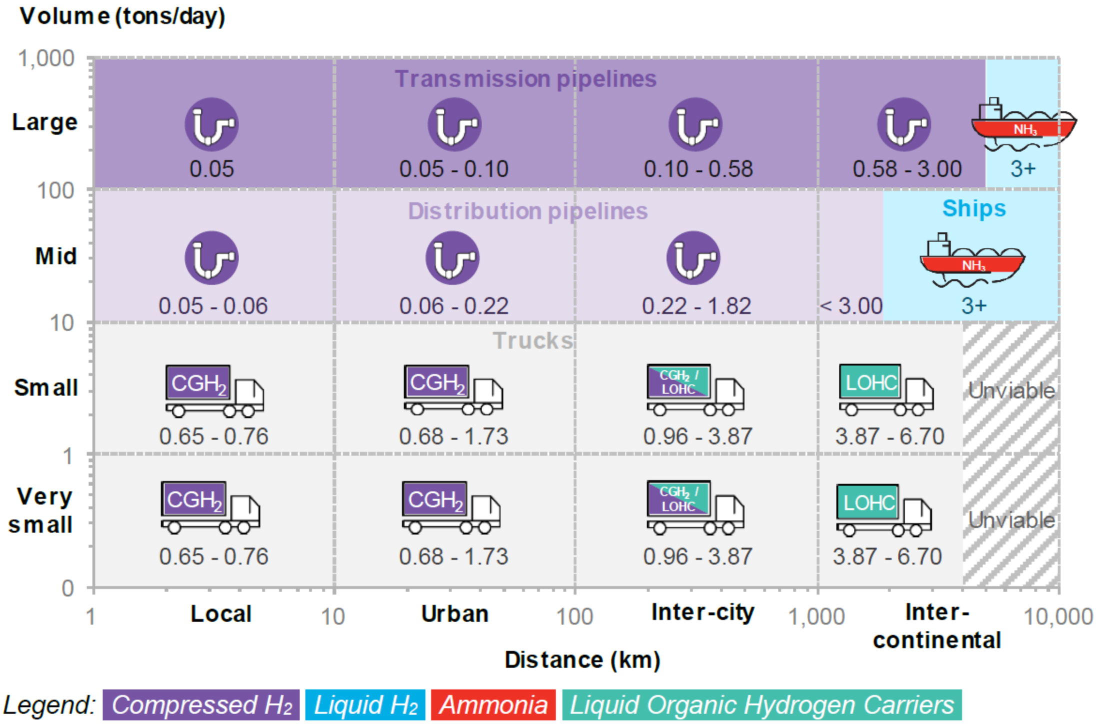

Fig 1-9 H2 transport costs based on distance and volume, $/kg, 2019 (Source: BloombergNEF)

The transportation of compressed hydrogen is carried out after compressing the hydrogen into high-pressure gas, which is suitable for the transportation to the hydrogen station of the off-site hydrogen production type. The characteristic of this method is that there is no phase change in the process of transportation, storage and consumption, and the energy loss is small, but the amount of one-time transportation is also relatively small, so it is suitable for occasions with short distances and small transportation volume. For small-scale occasions such as laboratory use, hydrogen cylinders can generally be used to transport compressed hydrogen gas, while hydrogen refueling stations require large-scale transportation methods. For this purpose, a tractor that transfers large high-pressure containers has been developed. For tractor transportation, what is important is the amount that can be transported at one time, but the size of the tractor driving on ordinary roads is subject to the restrictions of the Road Traffic Law, especially the quality and size control. Since the steel container is too heavy to increase the loading capacity, efforts are being made to achieve lighter weight and higher pressure to increase the hydrogen loading capacity.

The principle of liquid hydrogen transportation is similar to compressed hydrogen. The main difference is that the storage tank is filled with liquid hydrogen, which requires higher thermal insulation performance. Because the liquefaction efficiency during the production of liquid hydrogen is low, the energy efficiency of the overall delivery will be reduced. In addition, when transferring liquid hydrogen from the liquid hydrogen tank to the hydrogen storage tank of the hydrogen refueling station, the evaporation loss when cooling the piping to the liquid hydrogen temperature cannot be ignored. In addition, it is also important to prevent the entry of water vapor, nitrogen, oxygen, and other substances that may accumulate in the liquid hydrogen tank. It can be seen that when the scale of transportation is large, it is beneficial to improve energy efficiency and reduce transportation costs.

Hydrogen storage medium transportation is a method that uses hydrogen storage technology to absorb hydrogen in a carrier for transportation. However, the percentage of hydrogen storage mass of the above-mentioned hydrogen storage carriers is low, which means that the total mass of this method is greater when transporting the same quality of hydrogen. It can be seen that in order to reduce transportation costs during transportation, quality is more important than volume, so this is the main disadvantage of this method. Taking organic hydride as an example to introduce this method. Hydrogen and cyclohexane are reacted under certain conditions to produce liquid benzene, then the benzene is stored in an oil tank, and then transported to the destination by tank truck, and then dehydrogenated and separated by a certain chemical reaction Get hydrogen.

Pipeline transportation will be a very advantageous method in terms of cost and energy consumption. In large industrial complexes, the pipeline transportation of hydrogen has been put into practical use. People are studying new combinations that take advantage of the characteristics of pipelines. For example, the idea of using existing city gas pipelines to transport a mixture of natural gas and hydrogen, and extracting purified hydrogen in hydrogen refueling stations as needed is under discussion. If the pressure of the pipeline itself is increased, no compressor is needed in the hydrogen refueling station. Because the storage and transportation of hydrogen has more or less technical or economic problems, it is possible to directly transport the raw materials for hydrogen production to the hydrogenation station, and then prepare the hydrogen for direct use or storage. Common raw materials include various hydrocarbons, methanol, etc. The transportation technology of these raw materials is mature and the cost is low. However, the larger the hydrogen refueling station, the better the benefit.

1.2.2.3 The main ways of using hydrogen energy

(1) Fuel cell

Fuel cells are one of the most widely used methods of hydrogen energy. The scope of application includes: fuel cell vehicles, small household fuel cell water heaters and large fuel cell cogeneration. The working principle of the fuel cell is: when working, the fuel (hydrogen) is fed into the negative electrode, and the oxidant (air or oxygen) is fed into the positive electrode. Pt is usually used as a catalyst to accelerate the entire electrochemical reaction. Among them, the electrolyte and electrode parts are not consumed during the entire oxidation reaction. Generally, hydrogen is decomposed into electrons e- and positive ions H + in the negative electrode. The electrons move to the positive electrode along the external circuit, and the hydrogen ions enter the electrolyte. On the positive electrode, electrons, hydrogen ions and oxygen react to form water. The load that uses electricity is connected to the external circuit to form a current. [17] Compared with other energy systems, fuel cells have the following advantages: (1) High energy conversion efficiency. [18] (2) Modularization. (3) Short construction period and flexible start and stop. [19]

Fuel cells can be divided into the following five types: alkaline fuel cells (Alkaline Fuel Cell), proton exchange membrane fuel cells (Proton Exchange Membrane Fuel Cell), phosphoric acid fuel cells (Phosphoric Acid Fuel Cell), molten carbonate fuel cells (Molten Carbonate Fuel Cell) and Solid Oxide Fuel Cell etc. According to the gradual increase of the operating temperature from 50 ℃ to 1000 ℃, it is low, medium and high temperature. PEMFC and SOFC are considered to be the future development direction due to their special operating temperatures. At the same time, the proton exchange membrane fuel cell is also the most mature fuel cell currently developed, and has a wide range of applications in home power, mobile power, distributed power and vehicle power.

(2) Hydrogen car

Hydrogen vehicles are an important part of the new energy vehicles that are being vigorously promoted worldwide. New energy vehicles include pure electric vehicles (PEV), hybrid electric vehicles (HEV), fuel cell electric vehicles (FCV), hydrogen engine vehicles (HEV) and so on. At present, pure electric vehicles and hybrid electric vehicles have improved after many years of promotion, occupying a certain share of the automobile market. According to the statistics of the International Energy Agency, in 2017, electric vehicles accounted for 2.2% of the total sales market share of automobiles, of which Norway accounted for the highest proportion, and its sales market share of electric vehicles reached 39%.

Among them, as hydrogen energy [20] and fuel cell technology have become the major strategic direction of energy and power transformation in the world, the next stage of development in the field of new energy vehicles will focus on the technical innovation and application promotion of FCVs. Fig 1-10 shows a comparison between FCV and other types of vehicles. The number of stars varies between 1 and 5, reflecting the advantages or disadvantages of the car in this comparison. The outstanding part with red stars represents the advantages of FCV and EV, as well as the problems FCV is facing at present. The main advantage of FCV and EV is that there is no carbon dioxide emission during driving. In addition, the fuel filling of FCV is fast. The main problems FCV faces are high cost and imperfect supporting facilities.

Project	FCV	EV	PHV	HV
CO2 emission	★★★★★ (Carbon dioxide is not emitted while driving)	★★★★★ (Carbon dioxide is not emitted while driving)	★★★★	★★★
Maximum driving distance	★★★★★ (760km)	★★ (200km)	★★★★★ (Over 500km)	★★★★★ (Over 500km)
Durability	★★★★★	★★★★	★★★★★	★★★★★
Vehicle price	★★★★★ (Just beginning to popularize)	★★★	★★★	★★★★
Complementary facilities	★ (Just beginning to popularize)	★★★★ (Mass popularization)	★★★★ (Mass popularization)	★★★★★
Energy replenishment time	★★★★★ (3 minutes)	★ (Normal 8 hours Fast 20-30 minutes)	★ (Normal 4 hours)	★★★★★ (2-3 minutes)

Fig 1-10 Carbon emissions and economic chart of various vehicles [21]

1.3 Development status of hydrogen energy

1.3.1 The development and status of hydrogen energy in the world

Many developed countries abroad have formulated development goals, strategic planning, R & D investment, road maps and other related policies for the use of hydrogen energy. Among them, Japan, Europe, and the United States are leading. In addition, due to its huge basic industrial system, China has become one of the countries with the largest development of hydrogen energy.

(1) United States

The United States was the first country to adopt hydrogen energy and fuel cells as an energy strategy. As early as 1970, the concept of 'hydrogen economy' was proposed, and the "Hydrogen Research, Development and Demonstration Act of 1990" was introduced. The Bush administration proposed a blueprint for the development of the hydrogen economy. The Obama administration issued a "Comprehensive Energy Strategy". As a priority energy strategy of the United States, fuel cells and fuel cells carry out cutting-edge technology research. In 2018, the United States announced October 8 as the National Hydrogen and Fuel Cell Memorial Day. A brief description of important policies is shown in Fig 1-11 below.

The number of patents owned by the United States in the field of hydrogen energy and fuel cells is second only to Japan, especially in the number of technology patents in the three major areas of global proton exchange membrane fuel cells, fuel cell systems, and on-board hydrogen storage. 50%.

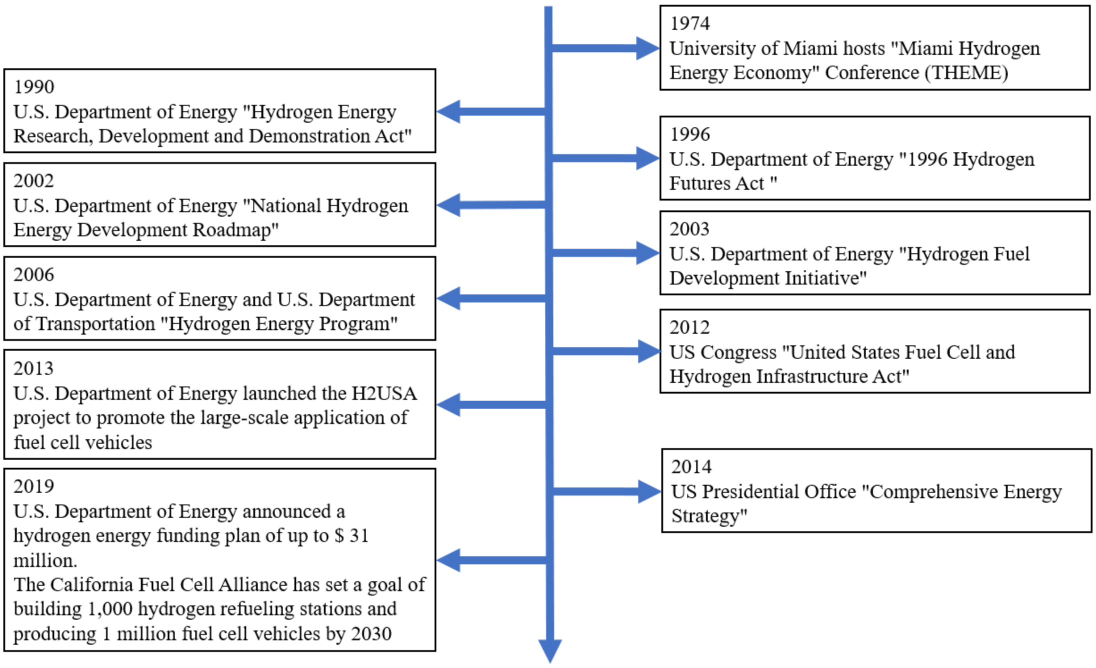

Fig 1-11 Development policy timeline of U.S. hydrogen energy

The United States has the world's largest liquid hydrogen production capacity and fuel cell passenger car ownership. In addition, warehouses and distribution centers in more than 40 states operate more than 23,000 fuel cell-powered forklifts and perform more than 6 million hydrogenation operations. Dozens of different types of fuel cell buses are used or planned in California, Ohio 7 Michigan, Illinois and Massachusetts.

On November 6, 2019, the Fuel Cell and Hydrogen Energy Association (FCHEA) released an executive summary report on the US hydrogen economic roadmap. The report shows that the US Department of Energy 's funding for hydrogen and fuel cells has been approximately US $ 100 million to US $ 280 million per year over the past decade, and approximately US $ 150 million per year since 2017.

The report said that by 2050, hydrogen will account for 14% of US energy demand. The strong hydrogen industry will strengthen the US economy. The United States plans to realize the application of hydrogen energy in the fields of small passenger cars, forklift trucks, distributed power sources, household cogeneration, and carbon capture from 2020 to 2022. The objectives are summarized in Tables 1-2below.

Table 1-2 Key objectives of the development route

	Present	2022	2025	2030
Hydrogen demand (10,000 tons)	1100	1200	1300	1700
Fuel cell vehicles for business and transportation	7600	50000	200000	5300000
Fuel cell forklift	25000	50000	125000	300000
Hydrogen refueling station	63	110	580	5600
Hydrogenation station for fuel cell forklift	120	300	600	1500
Annual investment quota (100 million US dollars)		7	13	80
New jobs		50000	120000	500000

(2) European Union

Since the 28 EU member states signed and approved the Paris Agreement to maintain global warming "far below the pre-industrial level of more than 2 degrees Celsius and strive to further limit the temperature rise below 1.5 degrees Celsius." Therefore, Europe is transitioning to a decarbonized energy system. This shift will fundamentally change how the EU produces, distributes, stores and consumes energy. It actually requires carbon-free power generation, improved energy efficiency, and deep decarbonization in transportation, construction, and industry. Stakeholders must take all feasible measures to limit energy-related carbon dioxide emissions to less than 7.7 megatons (Mt) per year by 2050. The recent report of the Intergovernmental Panel on Climate Change (IPCC) emphasized the urgency of reducing emissions completely: by 2030, global warming will not exceed 1.5 degrees Celsius, and emissions must be reduced by 45% (compared to 2010 levels) It must be reduced to "zero emissions" by 2050. Otherwise, it will lead to more extreme temperatures, sea level rise and severe loss of biodiversity and other major climatic effects.

The European Intergovernmental Panel on Climate Change (IPCC) report shows that large-scale hydrogen will be needed to achieve the EU's energy transition, otherwise the EU will not be able to achieve its decarbonization goals. Fuel provides a versatile, clean and flexible energy carrier for this transformation. Although hydrogen is not the only way to decarbonize, it is an essential support in a range of other technologies. It enables large-scale access to renewable energy because it enables energy operators to convert and store energy as renewable gas. It can be used for energy distribution across sectors and regions and as a buffer for renewable energy. It provides a decarbonization method for the power, transportation, construction and industrial sectors, otherwise it is difficult to decarbonize.

Therefore, the EU regards hydrogen energy as an important guarantee for strategic safety and energy transformation. At the energy strategy level, the "2005 European Hydrogen Energy R & D and Demonstration Strategy", "2020 Climate and Energy Package Plan", "2030 Climate and Energy Framework", "2050 Low Carbon Economy Strategy" and other documents were proposed, which could not be issued at the energy transformation level "Renewable Energy Directive", "New Electricity Market Design Directives and Specifications" and other documents. The EU Joint Action Plan for Fuel Cells and Hydrogen (FCHJU) provides a large amount of financial support for the development and promotion of hydrogen energy and fuel cells in Europe. The total budget for 2014-2020 is 665 million euros.

According to the EU's hydrogen energy development plan, Europe may produce about 2,250 terawatt hours (TWh) of hydrogen by 2050, accounting for about a quarter of the EU's total energy demand. This number will fuel approximately 42 million large cars, 1.7 million trucks, approximately 250,000 buses and more than 5,500 trains. Its heat supply will exceed the equivalent of 52 million households (about 465 terawatt hours), and provide up to 10% of the building's electricity demand.

By 2030, the EU hydrogen industry can provide employment opportunities for about 1 million highly unemployed workers, reaching 5.4 million by 2050. In terms of transportation, by 2030, a scale of 3.7 million fuel cell passenger cars and 500,000 fuel cell LCVs will be formed. In addition, by 2030, about 45,000 fuel cell trucks and buses will be on the road. By 2030, fuel cell trains can also replace about 570 diesel trains. For the construction sector, by 2030, hydrogen can replace 7% of natural gas (by volume), and by 2040, hydrogen can replace 32%. In the power sector, large-scale conversion of “excess” renewable energy to hydrogen, large-scale demonstration of hydrogen power generation and renewable energy-hydrogen power plants may also be achieved by 2030.

(3) China

China is currently in the stage of low-carbon transformation and development. At present, carbon dioxide emissions caused by the burning of fossil fuels are still the most important source of greenhouse gas emissions. China's carbon emissions surpassed the European Union in 2003 and the United States in 2006, and it has become the largest carbon emitter for many years in a row. This has caused China to face increasing pressure to reduce emissions internationally. Although China has initially formed an energy supply system with comprehensive development of coal, electricity, oil, natural gas and new energy, and its consumption structure is gradually developing towards a clean and low-carbon economy, structural problems remain prominent. In terms of optimizing the energy structure and accelerating energy transformation, hydrogen energy as a secondary energy helps to improve the efficient and clean utilization of primary energy, enhance the flexibility of the power system, and help achieve the optimal allocation of multi-heterogeneous energy across regions and seasons To form a sustainable and highly flexible multi-energy complementary system. Therefore, China is highly concerned about the development of hydrogen energy and fuel cell industries. Because the hydrogen energy industry chain is long, it covers many links such as hydrogen production, storage and transportation, hydrogenation infrastructure, fuel cells and their applications. Compared with developed countries, China is still lagging behind in terms of independent research and development of hydrogen energy, equipment manufacturing and infrastructure construction. However, due to the support of a huge industrial system, China's production of hydrogen energy ranks first in the world. From the "Thirteenth Five-Year Plan" Strategic Emerging Industries Development Plan successively released in 2011, "Energy Technology Revolution Innovation Action Plan (2016-2030)", "Energy Saving and New Energy Automotive Industry Development Plan (2012-2020)" Various top-level energy plans such as "Made in China 2025" have encouraged and guided the research and development of hydrogen energy and fuel cell technology.

The "China Hydrogen Energy and Fuel Cell Industry White Paper" proposed in June 2019 shows that hydrogen energy will become an important part of China's energy system. It is estimated that by 2050, hydrogen energy will account for 10% of China's energy system, the demand for hydrogen will be close to 6,000 tons, and the annual economic output will exceed 10 trillion yuan. There are more than 10,000 hydrogen refueling stations in the world; the transportation, industry and other fields will realize the universal application of hydrogen energy; the output of fuel cell vehicles will reach 5.2 million units / year, the fixed power generation device will be 20,000 units / year, and the fuel cell system capacity will be 5.5 million /year.

The overall goals are shown in Table 1-3 below. The policy system guarantee of China's hydrogen energy are shown in Tables 1-4 below. The focus of development and assurance is large-scale university hydrogen production, distributed hydrogen production, hydrogen purification technology, key materials and technical equipment for hydrogen storage and transportation, advanced hydrogen energy and fuel cell technologies such as PEMFC and SOFC.

Table 1-3 China's overall target of hydrogen energy and fuel cell industry

Industry target		Present (2019)	Short-term target (2020-2025)	Medium-term target (2026-2035)	Long-term target (2036-2050)
Hydrogen energy ratio		2.7%	4%	5.9%	10%
Industrial output value (100 million RMB)		3000	10000	50000	120000
Equipment manufacturing scale	Hydrogenation station	23	200	1500	10000
	Fuel cell vehicles (ten thousand)	0.2	5	130	500
	Fixed power supply / power station	200	1000	5000	2000
	Fuel cell system (ten thousand)	1	6	150	550

Table 1-4 China's policy system guarantee of hydrogen energy and fuel cell industry policy system guarantee

Standard system	Standard system of hydrogen	Laws and regulations of fuel cell
Present (2019)	Lack of systematic hydrogen production, storage and transportation and filling standards	The fuel cell standard system has basically been formed and needs to be continuously refined and improved
Short-term target (2020-2025)	45Mpa gas transportation, type IV bottle group standard; hydrogen station safety, technical acceptance standard; liquid hydrogen civil standard	According to the terminal fields of transportation, industry and construction, continue to improve the standard system, timely expand and follow up the standard formulation of new application scenarios
Middle-term target (2026-2035)	Hydrogen fuel standards; solid and organic liquid storage and transportation standards; pipeline transmission and distribution standards	
Long-term target (2036-2050)		

(4) International organizations and industrial cooperation

1) International Partnership Program of Hydrogen Economy and Fuel Cell (IPHE)

The International Hydrogen Economy and Fuel Cell Partnership Program is an international government cooperation organization that was launched in Washington, DC, in November 2003. It was originally called the "International Hydrogen Energy Economic Partnership Program", and China is one of the initiators of IPHE. At present, the organization has absorbed extensive participation from 18 countries and the European Union.

2) International Energy Agency Hydrogen Cooperation Group (IEA-HCG)

The International Energy Agency's Hydrogen Energy Collaboration Group was established in April 2003 and was jointly signed by 24 member countries of the International Energy Community (IEA). It aims to promote cooperation in hydrogen R & D and fuel cell technology development and policy formulation among member countries.

3) International Association of Hydrogen Energy (IAHE)

The International Hydrogen Energy Association was established in the United States in 1974. It is committed to accelerating the promotion of hydrogen energy as the basis and guarantee for the future rich clean energy supply in the world. It is the world ’s highest level of hydrogen energy and the most influential non-profit academic organization.

4) International Hydrogen Council

The International Hydrogen Energy Commission was established at the 2017 World Economic Forum in Davos. It was the first CEO to accelerate the development and commercialization of hydrogen energy and fuel cell technology, and promote the role of hydrogen energy technology in the global energy transformation. Initiative organization. At present, the International Hydrogen Energy Commission has recruited a total of 53 leading companies in the hydrogen energy industry from Asia, Europe and North America to join, National Energy Group and other four Chinese companies are its guiding member units. In addition, the International Organization for Standardization Hydrogen Energy Technical Committee (ISO / TC197), mission innovation and other organizations and initiatives continue to play a role in the global hydrogen energy and fuel cell standard formulation, technological innovation and other fields.

5) Hydrogenation Infrastructure Alliance

Germany has established a joint venture H2Mobility, led by the National Hydrogen and Fuel Cell Technology Organization, with the participation of multinational companies such as Air Liquide, Daimler, Linde, OMV, Shell and Total, aiming to create convenient hydrogenation within Germany Station network to promote fuel cell vehicles on a large scale. It is planned to build and operate 100 hydrogen refueling stations in major metropolitan areas such as Hamburg, Berlin, Rhine-Ruhr, Frankfurt, Nuremberg, Scogart and Munich, as well as major roads and highways by 2019; Construct 400 hydrogen refueling stations in Germany and establish a nationwide supply network to promote the development of the hydrogen energy industry.

6) Alliance of fuel cell vehicle manufacturers

In the promotion of fuel cell vehicles, Japan and South Korea took the lead in large-scale mass production, successfully launched mass-produced models such as Toyota Mirai, Honda Clarity, and Hyundai Nexo. In recent years, four major automobile group alliances have gradually formed in the market: Daimler, Ford and Renault-Nissan, GM and Honda, BMW and Toyota, Audi and Hyundai. Through the alliance, all parties are committed to jointly developing a fuel cell system platform to accelerate the commercialization process.

1.3.2 Development and current status of hydrogen energy in Japan

1.3.2.1 Historical process

Japan attaches great importance to the development of the hydrogen energy industry and proposes to "become the first country in the world to realize a hydrogen society". The government has failed to issue policies such as the "Japan Renaissance Strategy", "Energy Strategy Plan", "Hydrogen Energy Basic Strategy", "Hydrogen Energy and Fuel Cell Strategic Roadmap", etc., and has planned a technical route to realize a hydrogen energy society. In 2018, Japan held the world ’s first hydrogen ministerial meeting, and energy ministerial government officials from more than 20 countries and the European Union participated in the meeting; and took the opportunity of the Tokyo Olympics to promote fuel cell vehicles and build a hydrogen energy town. The following table1-5 shows the development history of hydrogen energy in Japan over the years.

Table 1-5 Development history of hydrogen energy in Japan

Year	Event
1973	The "Hydrogen Energy Association" was established to carry out hydrogen energy technology research and development centered on university researchers.
1981	The Ministry of International Trade and Industry initiated the development of fuel cells in the "Long-term Research Plan for Energy Saving Technologies".
1990s	Toyota, Nissan and Honda automobile manufacturers start the development of fuel cell vehicles, Sanyo Electric, Matsushita Electric and Toshiba start the development of home fuel cells.
1993	Leaded by NEDO, a 10-year comprehensive project of "Hydrogen Energy System Technology Research and Development" was established.
2002	1) The government activates the fuel cell demonstration vehicles of Toyota and Honda. 2) Practical application of hydrogen fuel cell and fuel cell demonstration project (JHFC) to start fuel cell vehicles and hydrogen refueling stations
2005	NEDO started large-scale practical application research on fixed fuel cells.
2008	The Fuel Cell Commercialization Association (FCCJ) developed a plan to promote fuel cell vehicles to ordinary users from 2015.
2013	1) The "Renewal Strategy for Japan" launched by the Ampere government promotes the development of hydrogen energy as a national policy and starts the preliminary work of the construction of hydrogen refueling stations. 2) The Ministry of Economy, Trade and Industry has established the "Hydrogen and Fuel Cell Strategic Agreement" with wide participation of industry, research institutions and government representatives.
2014	1) The Cabinet revised the "Japan Revival Strategy" and issued a call for the construction of a "hydrogen energy society". 2) The fourth "Energy Basic Plan", positioning hydrogen energy as the core secondary energy in parallel with electricity and heat, and proposing to build a "hydrogen energy society" 3) Announcement of "Japan's Hydrogen and Fuel Cell Strategic Roadmap"
2015	1) In his policy address speech, Ampere expressed his determination to realize a "hydrogen society", aiming to continue to build fuel cell hydrogen refueling stations and increase the circulation of hydrogen energy and reduce prices through the commercial operation of hydrogen power plants. 2) NEDO issued a hydrogen energy white paper, positioning hydrogen energy as the third pillar of domestic power generation.

The NEDO mentioned in the table 1-5 is called The New Energy and Industrial Technology Development Organization in Japan. It is the largest public research and development management organization in Japan. Its main goal is to solve energy and environmental problems and promote the transformation of scientific and technological products. According to statistics, from 2010 to 2015, NEDO received a total of 52.98 billion yen from government investment, mainly for hydrogen and fuel cell technology development support. NEDO's research on fuel cells began in 1981, mainly including phosphoric acid fuel cells (PAFC), solid oxide fuel cells (SOFC) and solid polymer fuel cells (PEFC). In addition to fuel cells, NEDO also develops technologies related to the use of hydrogen energy, and has built approximately 100 hydrogen refueling stations in 2015 centered on Tokyo, Nagoya, Osaka, and Fukuoka. In addition, NEDO also conducts research and development on hydrogen power generation technology and new technologies related to the entire hydrogen industry chain such as hydrogen production, hydrogen storage, and hydrogen transportation.

1.3.2.2 Development strategy

(1) National strategy

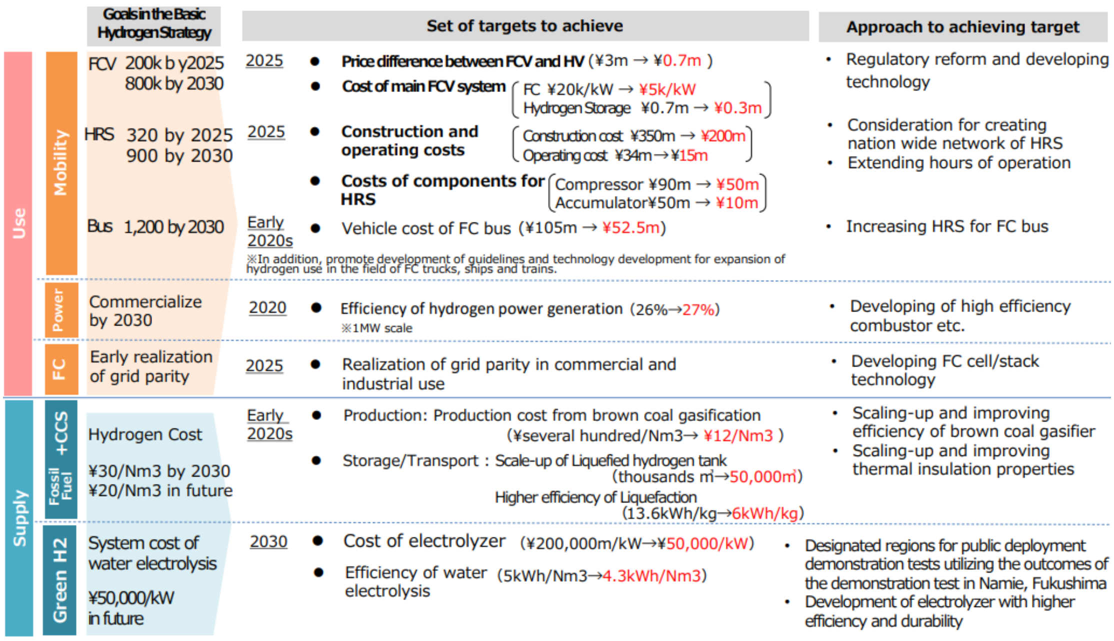

Fig1-12 Japan's strategic road map for hydrogen and fuel cells (Source: Ministry of Economy, Trade and Industry (METI))

In December 2017, the Japanese government released the "Basic Strategy for Hydrogen Energy" (Fig. 1-12), proposing strategic steps and goals for the application of hydrogen energy. "Basic Hydrogen Energy Strategy" aims to achieve hydrogen energy parity production, establish the entire supply chain covering production to downstream market applications, in addition to fuel cell vehicles, it also includes hydrogen energy power generation, fuel cell shipping, chemical production industry, hydrogen replacement of natural gas and other applications . The strategy also clarifies the reasons for Japan's vigorous development of hydrogen energy, which comes down to energy security, environmental protection, energy conservation, and promotion of related industries. There are two main points below, one is energy security considering diversified energy supply and improving energy self-sufficiency rate; the second is to build a deep decarbonized energy system to achieve emission reduction goals.

1) Guarantee national energy security

Japan's primary energy is extremely scarce, and energy for industrial production and daily life depends heavily on imports. At present, about 94% of primary energy in Japan depends on fossil fuels imported from overseas, and about 87% of oil is mainly imported from the Middle East. Coupled with the impact of the Fukushima nuclear power plant accident in Japan, the role of nuclear energy in the energy structure is weakening, and Japan ’s energy self-sufficiency rate is only 6% -7% [22]. To achieve energy security and enhance industrial competitiveness, Japan has accelerated the pace of development of alternative energy sources. Hydrogen energy has become one of Japan's alternative energy sources due to its energy efficiency, cleanliness, and diversity of manufacturing sources and manufacturing methods.

2) Help to achieve carbon emission reduction goals

In the Paris Agreement, Japan set a goal of reducing carbon emissions by 26% by 2030 (compared to 2013 emissions). Among them, the electricity sector accounts for 40% of the total emissions. However, based on the fact that Japan ’s current power generation relies on coal, LNG and nuclear power, and the relatively low proportion of renewable energy power generation, achieving this goal is more challenging. Regarding the hydrogen production route, Japan is currently mainly producing hydrogen from fossil fuels. The "Basic Hydrogen Energy Strategy" proposes to establish domestic renewable energy hydrogen production technology by 2030 and build an international hydrogen energy supply chain. CCS) technology realizes the decarbonization of cheap fossil fuels (such as lignite) to produce hydrogen and renewable energy to produce hydrogen. Therefore, combining carbon capture technology and renewable energy hydrogen production technology, hydrogen energy has become an important way for Japan to achieve carbon emission reduction targets.

(2) Industry strategy

In addition to the government, Japanese companies are also very active in the construction of fuel cells. On October 15, 2015, Toyota Motor announced "Toyota Environmental Challenge

2050". Toyota plans to have Toyota fuel cell vehicles (FCV) with annual global sales of more than 30,000 vehicles after 2020; in terms of fuel cell buses (FCB), FCB will be introduced around Tokyo in 2016, which will be the 2020 Tokyo Olympics At the Paralympic Games, more than 100 FCBs will be prepared. In addition, the average CO2 emissions of new global vehicles in 2050 will be reduced by 90% compared to 2010.

1.3.2.3 Development status

At present, fuel cells in Japan are the world leader in commercial applications, mainly including household fuel cell combined heat and power fixed power stations, business / industrial fuel cells, and fuel cell vehicles.

1) Household cogeneration system ENE-FARM

The Japanese household cogeneration system ENE-FARM is an energy system that uses fuel cells efficiently in the home. It produces hydrogen by reforming natural gas, and then injects hydrogen into the fuel cell to generate electricity. At the same time, it uses the heat generated during power generation to supply heating and hot water. The overall energy efficiency can reach 90%.

Compared with traditional power generation systems, ENE-FARM can effectively use waste heat that is difficult to use in large thermal power plants, thereby greatly improving energy efficiency; compared with renewable energy (solar, wind, etc.) power generation systems, ENE-FARM is not restricted by weather and can generate electricity at any time. In addition, ENE-FARM is installed at home, does not depend on the existing power grid, and can be used in an emergency during a large-scale power outage, and there is almost no transmission loss.

Japanese household fuel cell cogeneration systems (ENE-FARM) manufacturers mainly include Aisin Seiki, Panasonic and Toshiba. The power generation efficiency of the products of the three companies is up to 40%, the total efficiency is up to more than 90%, the durability time is more than 80,000 hours, the startup time is only 1-2 minutes, and can be used on-grid according to demand. It is reported that users can save about 60,000 yuan in lighting and heating costs each year using the ENE-FARM system.

In terms of sales volume, ENE-FARM sold 110,000 units worldwide in 2014, priced at 1.49 million yen (approximately 87,000 yuan). In May 2017, ENE-FARM global sales exceeded 200,000 units. In response, the Japanese government proposed to achieve a sales target of 5.3 million units equivalent to 10% of Japanese households by 2030.

2) Business / industrial fuel cells

Business / industrial fuel cells work similarly to household fuel cells. They all generate electricity through the chemical reaction of hydrogen and oxygen in fuel cells. The difference is that business fuel cells are mostly made from city gas as fuel. hydrogen.

The output power of business fuel cells ranges from several kilowatts to several megawatts. The types of fuel cells commonly used are phosphoric acid fuel cells (PAFC), molten carbonate batteries (MCFC), solid oxide fuel cells (SOFC), etc.

3) Fuel cell vehicle

The successful commercialization of fuel cell vehicles in Japan are mainly Toyota and Honda.

The Toyota FCV fuel cell four-seater commercial vehicle MIRAI was launched in Japan in December 2014. The car's acceleration time is about 10 seconds per 100 kilometers, the maximum cruising range is more than 482 miles (about 700 kilometers), and hydrogen fuel is added for 3 minutes. It produced 700 vehicles in 2015 and 2000 vehicles in 2016. It is expected to reach 30,000 vehicles in 2020. Toyota plans to reduce the price of fuel cell vehicles to about $ 20,000 by 2025.

The Honda FCV fuel cell five-seater commercial vehicle Clarity was launched in Japan in March 2016. Its maximum power is 100kW (136PS), the maximum cruising range will reach 700 kilometers, and it takes only 3 minutes to replenish hydrogen fuel.

Compared with traditional cars, hydrogen fuel cell vehicles are more expensive. In order to promote the popularization of hydrogen energy, the Japanese government provides subsidies to every consumer who purchases fuel cell vehicles. In view of the market situation in 2016, Toyota's Mirai car is priced at 6.7 million yen / unit, with a subsidy of 2.02 million yen / unit; Honda Clarity Fuel Cell is priced at 7.09 million yen / unit, and a subsidy of 2.08 million yen / Cars.

In terms of sales volume and construction of hydrogen refueling stations, in 2016, 1,000 hydrogen fuel cell vehicles were sold in Japan, and 100 hydrogen refueling stations have been built. In 2026, the government plans to complete the sales target of 2 million hydrogen fuel cell vehicles and the construction target of 1,000 hydrogen refueling stations.

1.4 Research structure and logical framework

1.4.1 Research purpose and core content

The research logic of the article is shown in Figure 4-13 below. Based on the demand for wisdom and cleanliness in the transformation of global energy system, this research proposes provide help for the development of hydrogen energy through analysis of environmental and economy. Carbon tax is introduced to convert the environmental advantages of hydrogen energy into economic benefits, and the development of hydrogen energy will be forecasted based on comparison with conventional systems.

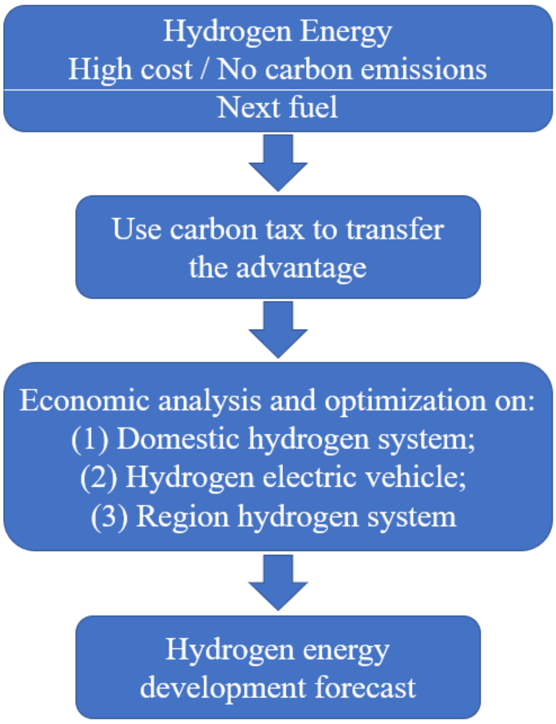

Fig 4-13 Research logic of the article

1.4.2 Chapter content overview and related instructions

The chapter names and basic structure of the article are shown in Fig 1-14. The brief chapters are shown in Fig 1-15.

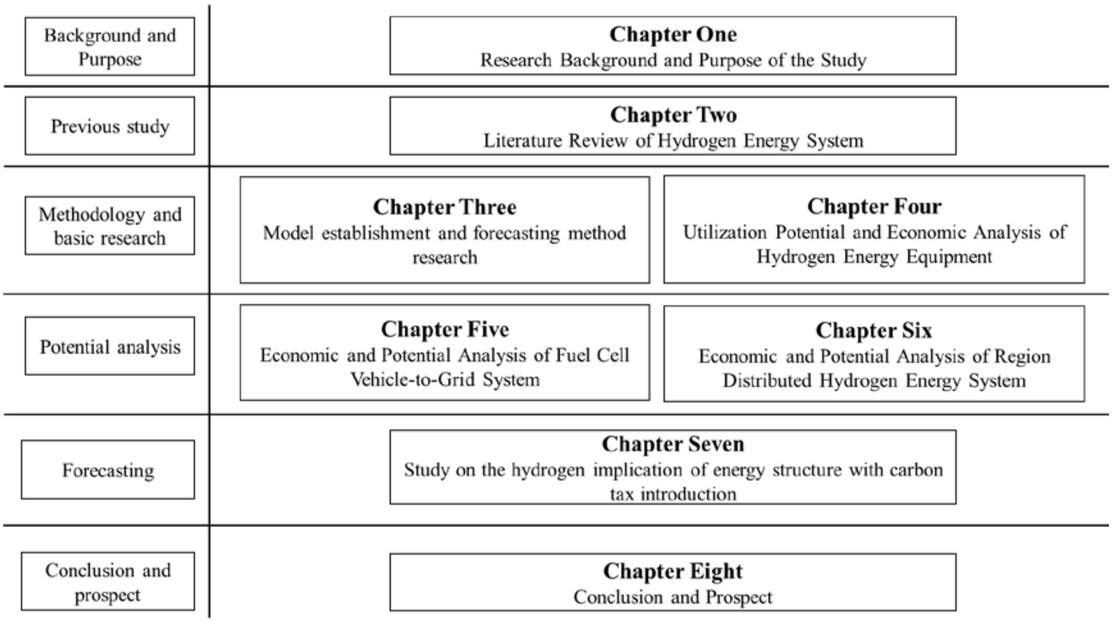

Fig 1-14 Chapter name and basic structure

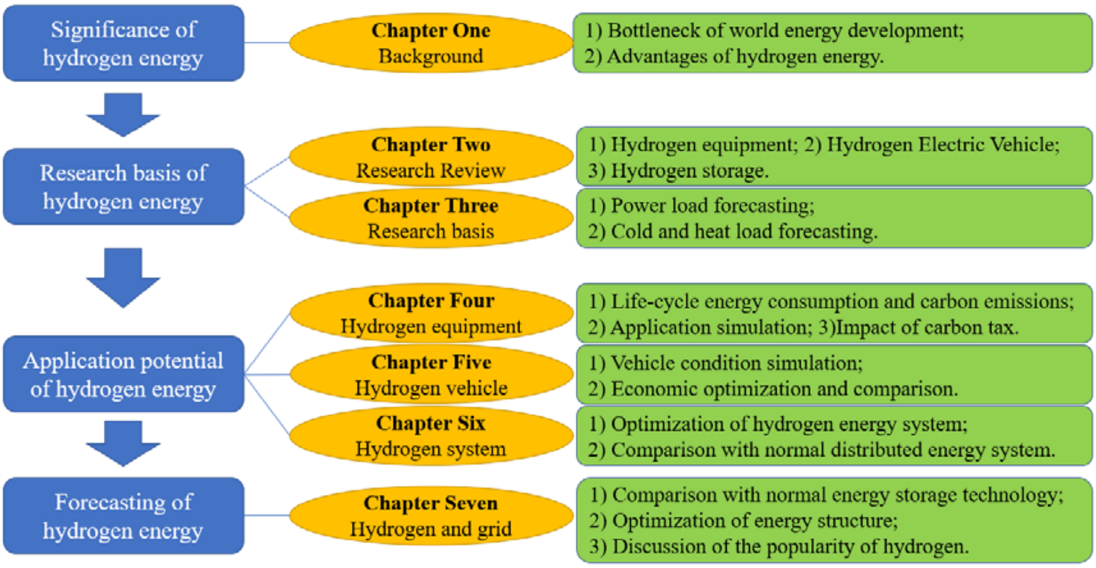

Fig 1-15 Brief chapter introduction

In Chapter 1, Research Background and Purpose of the Study:

Renewable energy is the focus of today's global energy development. However, due to the instability of renewable energy, the current development is already in a bottleneck stage. The development of hydrogen energy can solve this problem well. This part analyzed the significance of hydrogen energy for renewable energy and global deep decarbonization. Then through the analysis of the characteristics of hydrogen energy, it shown the high safety of hydrogen energy. After that, the process of producing, storing, transporting and using hydrogen energy was explained.

Then, through the elaboration of the hydrogen energy development process and goals of the United States, the European Union, China and Japan, the importance of hydrogen energy in the energy strategies of various countries was highlighted. Finally, the research logic and content of the article were expounded.

In Chapter 2, Literature Review of Hydrogen Energy System:

This part is mainly to sort out the research status of hydrogen energy. First of all, through the review of the research on the development of hydrogen energy by the policies of various countries, the current status and trends of the cost reduction of hydrogen energy systems were explained. Then it shown that the current research focus on hydrogen energy is the production of hydrogen energy and the performance improvement of fuel cells, and the latest research results were described. Next, since the core of development based on hydrogen energy is to combine with renewable energy, the literature and compares the characteristics of hydrogen storage and other energy storage technologies was reviewed. Finally, according to the research object of this article, the research and combing of the application of fuel cell, fuel cell vehicle and hydrogen energy in regional energy system were carried out.

In Chapter 3, Model establishment and forecasting method research:

This part is about methodological research and model building. Firstly, the research motivation and main research methods of the article were expounded. Then the general load and equipment model to be used in the follow-up study were established. At the same time, different operating strategies based on regional energy systems were explained. Next, it was believed that load forecasting is the basis of follow-up research, so a new forecasting method of cold and hot load based on transfer learning was proposed and verified.

In Chapter 4, Utilization Potential and Economic Analysis of Hydrogen Energy Equipment:

In this part, the energy utilization and economic potential of fuel cells were analyzed. TRNSYS software was used to simulate the system based on large amounts of data running under different power by a 5kW methanol reforming PEMFC system experimental platform. The residual heat of the system is analyzed, and the residual heat recovery module is added to the simulation system to simulate the residual heat utilization of the whole system and calculate the recovery of residual heat and the promotion of comprehensive utilization of system energy. Finally, fuel cells and fuel cell vehicles were used to compare with conventional energy systems under different carbon taxes.

In Chapter 5, Economic and Potential Analysis of Fuel Cell Vehicle-to-Grid System:

The popularization of fuel cell electric vehicles (FCV) is an important measure for solving the global carbon emission reduction problem. However, the overall cost of FCV and the production cost of fuel hydrogen are relatively high, so FCV promotion is slow. Considering that FCV has the characteristics of near-zero carbon emission and high endurance, which is suitable for the vehicle-to-grid (V2G) system, this part hoped to provide a boost for the promotion of FCV by analyzing the economic potential of the FCV2G system.

Firstly, a large-scale commercial building in Japan was selected as the research target and the agent of vehicles to provide a V2G service for the power grid. Then the Monte Carlo simulation method was used to simulate the visiting time and condition of the vehicles. Secondly, the discharge model was established. Combined with the carbon emission price and self-elasticity coefficient of the discharge price, the overall economic optimization model was established. Then, the genetic algorithm was used to optimize the model. With continuous importing of FCVs, the overall economic benefit was improved. Finally, a sensitivity analysis was carried out on the six parameters of daily electricity price, battery cost, fuel cell cost, carbon emission price, power grid carbon emission and hydrogen cost. It was concluded that FCV2G has good economic benefits and high development potential, and the economic benefits of FCV2G will continue to increase with the passage of time.

In Chapter 6, Economic and Potential Analysis of Region Distributed Hydrogen Energy System:

The development of hydrogen energy system is one of the important measures to help renewable energy break through the bottleneck and accelerate the decarbonization of the world. However, due to the high cost of the equipment, the overall system economic efficiency is poor, which hinders the commercialization of the hydrogen energy system. In order to give suggestions for improving the economic benefits of hydrogen energy systems, based on the characteristics of efficient and clean, this part considers the introduction of carbon taxes into the calculation of economic benefits and studies the economic benefits of the application of hydrogen energy in regional distributed energy systems (RDES).

This part took buildings rely on hydrogen energy supply line in a demonstration area of hydrogen energy application in Kitakyushu, Japan as an example. First, five different types of buildings were selected, and the electric load was converted into cooling and heating load through load forecasting. After that, the total cost model of the RDES was established, and the conventional RDES, including combined cooling heating and power (CCHP) and photovoltaic-energy storage system, was used as a comparative item to study the economic benefits of regional distributed hydrogen energy system (RDHES) in different carbon taxes conditions. Finally, the adaptability analysis of different building types as well as the sensitivity analysis of different photovoltaic penetration rates, equipment investment costs and energy consumption carbon emissions were obtained to study the future application potential of hydrogen energy in RDESs.

In Chapter 7, Study on the Hydrogen Implication of Energy Structure with Carbon Tax Introduction:

The development of hydrogen energy is one of the important ways to solve the current energy shortage and environmental pollution, but at present, the development of hydrogen energy system is relatively slow, mainly due to high equipment investment and imperfect supporting system. In this paper, according to the characteristics of no carbon dioxide emission when hydrogen energy system is used, the strategic planning and price prediction of hydrogen energy system and carbon tax in Japan and the United States are sorted out.

First, a comparison between hydrogen storage and different energy storage technologies under different renewable energy environments was conducted. Then, using data from ten Japanese power companies, after importing carbon taxes and hydrogen storage technologies, the impact on the share of energy structure was studied. Next, according to the research results in the field of power generation, the impact of the promotion of hydrogen energy on the primary energy consumption structure and CO2 emissions was explored.

In Chapter 8, Conclusion and Prospect:

This part summarized the research of previous chapters. And based on the conclusions, the future development of hydrogen energy system and the prospect of further research are put forward.

Reference

[1] Economics, BP Energy. "BP energy outlook." (2019). https://www.bp.com/content/dam/bp/business-sites/en/global/corporate/pdfs/energy-economics/energy-outlook/bp-energy-outlook-2019.pdf

[2] D.H. Zhang, J.Q. Wang, Y.G. Lin, Y.L. Si,C. Huang, J. Yang, B. Huang. Present situation and future prospect of renewable energy in China. Renewable and Sustainable Energy Reviews 76 (2017) 865-871.

[3] K. Liu, B.R. Lin. Research on influencing factors of environmental pollution in China: A spatial econometric analysis. Journal of Cleaner Production 206 (2019) 356-364

[4] Q. Wang, M.P. Kwan, J. Fan, K. Zhou, Y.F. Wang. A study on the spatial distribution of the renewable energy industries in China and their driving factors. Renewable Energy 139 (2019) 161-175.

[5] Robert, Fabien Chidanand , G. S. Sisodia , and S. Gopalan . "A Critical Review on the Utilization of Storage and Demand Response for the Implementation of Renewable Energy Microgrids." Sustainable Cities and Society (2018):S2210670717307084.

[6] Murdock, Hannah E., et al. "Renewables 2019 Global Status Report." (2019).

[7] Dudley, Bob. "BP statistical review of world energy." BP Statistical Review, London, UK, accessed Aug 6 (2018): 2018.

[8] Y.C. Chang, N.N. Wang. Legal system for the development of marine renewable energy in China. Renewable and Sustainable Energy Reviews 75(2017) 192-196

[9] D. Zhang, P.Y. You, F. Liu, Y.H. Zhang, Y.T. Zhang, C. Feng. Regulating cost for renewable energy integration in power grids. Global Energy Interconnection 1 (2018) 544-551.

[10] A.R. Dehghani-Sanij, E. Tharumalingam, M.B. Dusseault, R. Fraser. Study of energy storage systems and environmental challenges of batteries. Renewable and Sustainable Energy Reviews 104 (2019) 192-208

[11] Glenk, Gunther, and Stefan Reichelstein. "Economics of converting renewable power to hydrogen." *Nature Energy* 4.3 (2019): 216-222.

[12] D ′Agostino D. Assessment of the progress towards the establishment of definitions of nearly zero energy buildings (nZEBs) in European member States. J Build Eng 2015;1:20–32.

[13] Swain, Michael R. "Fuel leak simulation." Proceedings of the 2001 DOE Hydrogen Program Review, NREL/CP-570-30535. 2001.

2017;42(19):13357e67.

[14] Staffell I, Dodds PE, editors. The role of hydrogen and fuel cells in future energy systems. London, UK: H2FC SUPERGEN; 2017.

[15] Office of Energy Efficiency & Renewable Energy, US Department of Energy, Fuel Cell Technologies Office. Fuel cell technologies office multi-year research, development, and demonstration plan: chapter 3.1 hydrogen production. 2015. https://energy.gov/eere/fuelcells/downloads/fuel-celltechnologies-office-multi-year-research-development-and-22.

[16] Midilli A, Dincer I. Hydrogen as a renewable and sustainable solution in reducing global fossil fuel consumption. Int J Hydrogen Energy 2008;33(16):4209e22.

[17] Yi Baolian. "Fuel Cells-Principles, Technology, Applications." (2003). (in Chinese)

[18] Rodi, W., et al. "Status of large eddy simulation: results of a workshop." Transactions-American Society of Mechanical Engineers Journal of Fluids Engineering 119 (1997): 248-262.

[19] Liu, Shewen, Charles Meneveau, and Joseph Katz. "On the properties of similarity subgrid-scale models as deduced from measurements in a turbulent jet." Journal of Fluid Mechanics 275 (1994): 83-119.

[20] Acar, Canan, and Ibrahim Dincer. "Energy and Exergy Analyses of a Zero Emission Power Plant for Coproduction of Electricity and Methanol." Progress in Exergy, Energy, and the Environment. Springer, Cham, 2014. 145-156.

[21] Fuel Cell Promotion Office of Japan Agency for Natural Resources and Energy, ‘About Fuel cell automatic vehicles’, 2014: 13-14. https://www.meti.go.jp/committee/kenkyukai/energy/suiso_nenryodenchi/suiso_nenryodenchi_wg/pdf/003_02_00.pdf

[22] Japan Agency for Natural Source and Energy Annual report on energy in 2019 (Energy White Book 2019)

Chapter 2

LITERATURE REVIEW OF HYDROGEN ENERGY SYSTEM

CHAPTER TWO: LITERATURE REVIEW OF HYDROGEN ENERGY SYSTEM

2.1 Review of Research on Policy Promotion

The development of hydrogen energy is currently undergoing an unprecedented political and industrial rapid development stage, and the number of hydrogen energy policies and projects around the world is rapidly increasing. At the same time, the cost of equipment related to the hydrogen energy system is also steadily decreasing. [1] With sufficient policy support and reduced hydrogen energy costs, clean hydrogen energy can reduce global greenhouse gas emissions by up to 34% from fossil fuels and industrial sectors in the future. [2,3] The relationship between hydrogen energy technology and current maturity shown in the 2015 International Energy Agency (IEA) report is shown in Figure 2-1 below.

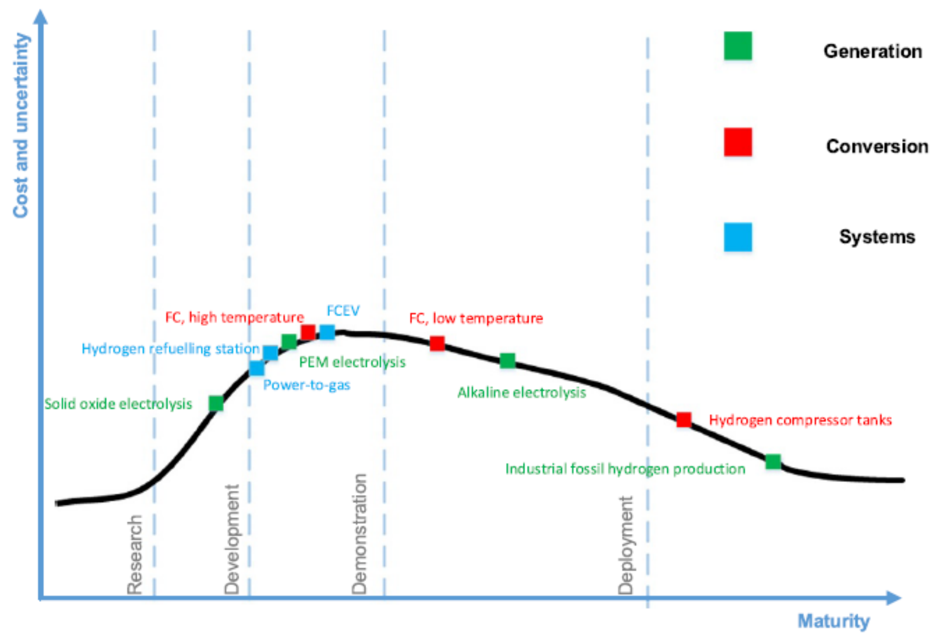

Fig 2-1 The relationship between hydrogen technology and current maturity

At present, the scale of the hydrogen energy industry is still small, and the cost is also extremely high, which hinders the deployment of hydrogen energy production, storage and transportation infrastructure. [4] Although the potential for cost reduction of hydrogen energy systems is great (Fig 2-2,2-3), the premise is that hydrogen energy can be used in large-scale production and at the same time establish a complete infrastructure network. To this end, countries around the world have successively made relevant technical route development plans and policy subsidies, [5] mainly concentrated in the fields of fuel cell manufacturing, storage, and hydrogen fuel cell vehicles. [6-7] Based on these measures, in the past five years, in Europe and North America, the cost of producing hydrogen from renewable energy by electrolysis technology has dropped by 40%. [3] However, the current cost level of the existing hydrogen energy system still has a gap with the mainstream energy system, and the use of hydrogen energy is still at the initial stage of commercialization. The main commercial development areas are hydrogen fuel cell electric vehicles and household fuel cells, with research focused on large-scale production of hydrogen from renewable energy sources. [8,9]

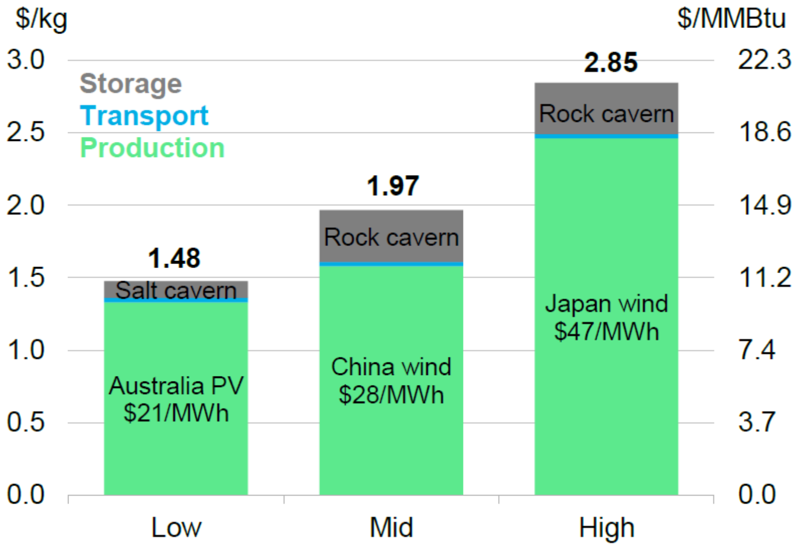

Fig 2-2 Estimated delivered hydrogen costs to large-scale industrial users, 2030 [2]

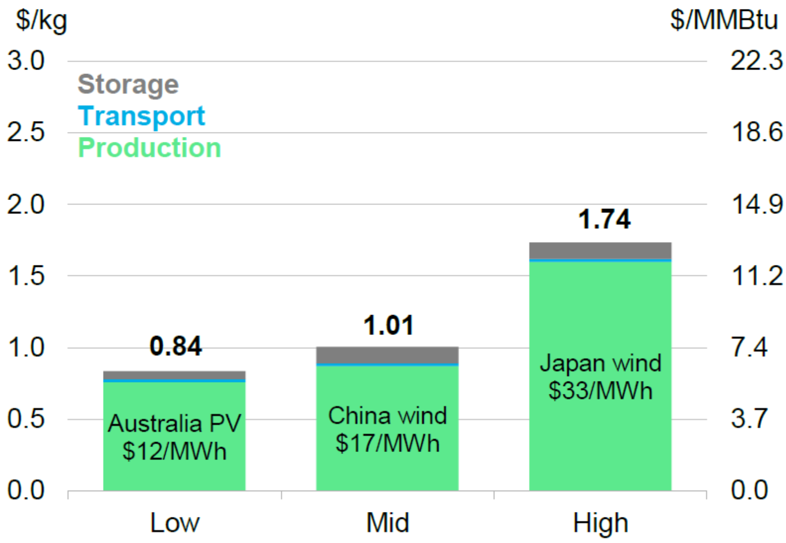

Fig 2-3 Estimated delivered hydrogen costs to large-scale industrial users, 2050 [2]

2.2 Review of hydrogen energy Manufacturing

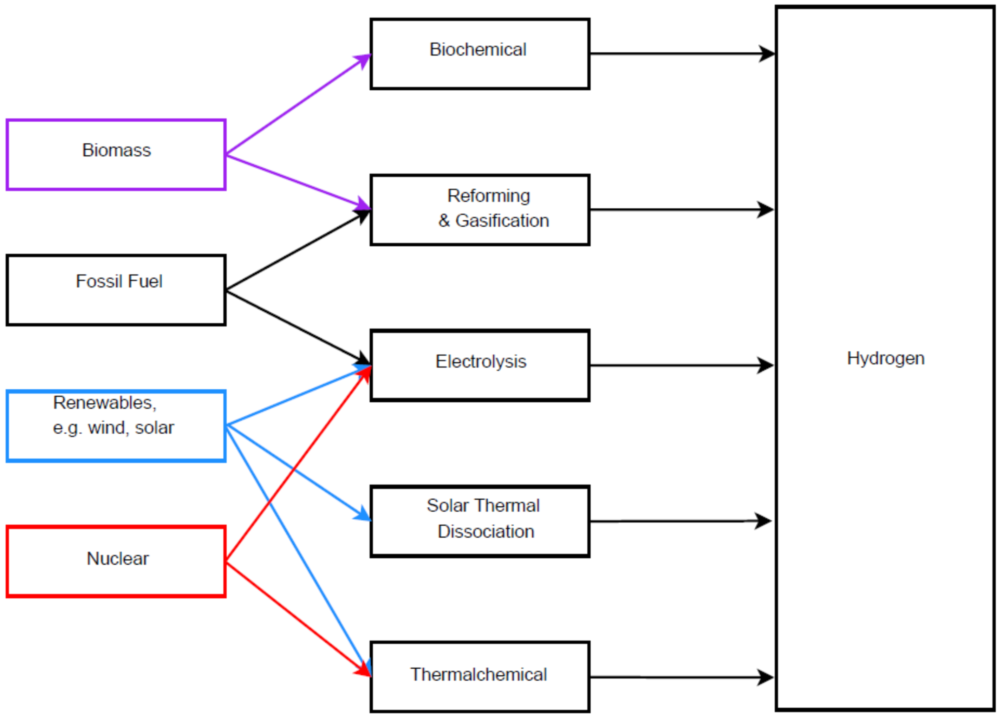

Fig 2-4 The proposed hydrogen production pathways [14]

In the new technology of hydrogen energy production. Hydrogen production systems can be classified by the use of primary energy type; biological, electrical, electrochemical, electrothermal, photochemical, photo-electrochemical, photonic, thermal, and thermochemical are some of the most commonly used alternatives in the literature [10], and the source of hydrogen is shown in Fig 2-4. Many researchers have carried out research on efficient hydrogen production, especially hydrogen production from electricity or renewable energy [11-13].

The National Institute of Materials Science and Technology (NIMS), in collaboration with the University of Tokyo and Hiroshima University, conducted a technical and economic evaluation of a "hydrogen production system" that combines solar power and storage batteries, and published "cheap hydrogen energy" with international competitiveness standard. [15] Prof. Shigeru Mori of Osaka Prefecture University and the research team of the American Academy of Materials Science jointly developed a new water decomposition catalyst. [16] The Quantum Science and Technology Research and Development Agency of Japan, in April 2020, jointly published with Shibaura University of Technology and the Japan Atomic Energy Agency, a hydrogen production method that can effectively reduce the main reaction energy consumption in the process of thermochemical hydrogen production, and expressed the use of this method Hydrogen production will save 70%

energy compared to previous manufacturing. [17] This method refers to the use of water to thermally decompose compounds of "iodine" (I) and "sulfur" (S). Use solar energy to increase the temperature of the water for thermal decomposition to produce hydrogen. The "IS" hydrogen production method is a manufacturing method that is expected to become the next generation of main energy "hydrogen energy". This method is one of the stable hydrogen production methods.

But for now, the focus of research is still on the relatively mature aspect of hydrogen production by electrolysis. [18] Although commercial PEM water electrolysis devices have been introduced, the cost of proton exchange membranes and precious metal electrocatalysts used in the acidic electrolyte environment of PEM water electrolysis cells is too high, which is not conducive to the large-scale promotion of PEM water electrolysis cells. [19] Therefore, while reducing the energy consumption of electrolysis, the need to develop new low-cost electrolysis systems is more urgent.

Under alkaline conditions, the low-cost non-precious metal catalyst can be used, which greatly reduces the cost of the electrolytic cell. Combining the two characteristics of solid electrolyte and alkaline system, alkaline solid electrolyte is used instead of proton exchange membrane to conduct hydrogen Oxygen ions, insulating the gas on both sides of the electrode, the anode and cathode of the electrolytic cell are in close contact with the solid polymer anion exchange membrane, thereby reducing the voltage drop between the two electrodes, combining the advantages of traditional alkaline liquid electrolyte water electrolysis and PEM water electrolysis As a result, alkaline solid anion exchange membrane (AEM) water electrolysis technology came into being. [20]

From the perspective of improving energy efficiency, the solid oxide electrolyte solid oxide water electrolysis technology (SOEC) uses solid oxide as the electrolyte material, can work at a high temperature of 400 ~ 1000 ℃, can use heat for electrical hydrogen conversion, with energy conversion High efficiency and no need to use precious metal catalysts and other advantages. [21]

The US Idaho National Laboratory, BloomEnergy, Danish Topsoe Fuel Cell Company, Korea Energy Research Institute and EU Relhy High Temperature Electrolysis Technology Development Project have also carried out research on SOEC technology, and the research direction has gradually shifted from electrolytic cell material research to electrolytic cell stacks. And system integration [22]. The SOEC stack power of the Idaho National Laboratory project in the United States reached 15kW, and CO2 + H2O co-electrolysis was used to prepare syngas. [23] The Idaho National Laboratory of the United States cooperated with Ceramatec to realize the quantitative control of the product CO and H2 in the operating temperature range of 650 ~ 800 ℃. They also directly passed the electrolytic product into the 300 ℃ methanation reactor containing Ni catalyst. Obtained 40% to 50% (vol) of methane fuel, confirming the feasibility of CO2 / H2O co-electrolysis to prepare hydrocarbon fuel. [24]

The GenHyPEM project funded by the European Commission plans to invest 2.6 million euros to specialize in PEM water electrolysis technology. Its members include 11 universities and research institutes in Germany, France, the United States, Russia and other countries. The goal is to develop high current density (> 1A / cm), high working pressure (> 5MPa) and high electrolysis efficiency PEM water electrolysis cell. The GenHy® series of products developed by it can achieve an electrolytic efficiency of 90% and a system efficiency of 70% to 80%. [25] The NEXPEL project jointly carried out by companies and universities such as Sintef, University of Reading, Statoil and Mumatech, with a total investment of 3.35 million euros, is dedicated to the research of new PEM water electrolysis cell hydrogen production technology, and aims to reduce the cost of hydrogen production (5000 euros / Nm3), The life of the electrolysis device reaches 40,000h. [26] The levelized cost forecasting of hydrogen production from large projects are shown in Fig 2-5. Comparing with nature gas and coal with CCS, it is forecasted that the cost of hydrogen produced by renewable energy will be more lower since 2030.

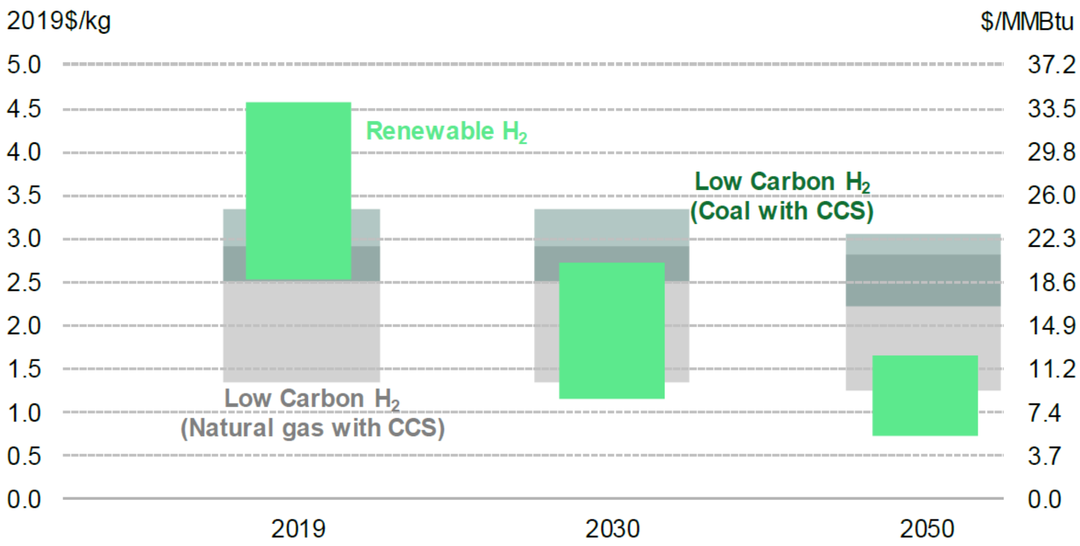

Fig 2-5 Forecast global range of levelized cost of hydrogen production from large projects [2]

2.3 The research on hydrogen production from renewable energy

The renewable energy represented by solar energy and wind energy has the advantages of inexhaustible, inexhaustible and widely distributed resources, which is regarded as the main method to solve the energy crisis [27,28]. Therefore, all countries in the world have issued relevant laws and regulations to promote the promotion and use of renewable energy [29,30]. Especially in the photovoltaic [31] and wind [32] industries, high subsidies ensure the sustained and rapid development of these two industries [33].

Even so, after a period of development, the share of renewable energy still reaches the bottleneck, unable to make further breakthroughs. It is mainly the low-grade and intermittent characteristics of renewable energy [34]. Solar energy only produces energy when the irradiance is high, and wind energy changes with the change of outdoor wind speed; such highly volatile renewable energy, in the process of power generation and grid connection, has great impact on the power grid, and it is difficult to ensure the stability of the power grid, making it more difficult to quickly match with the urban power grid [35]. In addition to planning and distribution of renewable energy plant locations to improve grid stability [36], the second solution to the utilization of renewable energy is energy storage integration [37]. However, the low energy storage efficiency and high initial investment of traditional batteries slow the progress of this technology [38]. Hydrogen energy has the characteristics of high energy storage, convenient storage and transportation, and zero pollution. It is considered to be the most promising energy storage option in the future.[39] Table 2−1 shows the comparison between several common energy storage technologies and hydrogen energy storage. Although the application of hydrogen energy in the global energy system is relatively low at present, as an important energy storage link in the efficient utilization of renewable energy, it has attracted much attention and made in-depth research and achieved fruitful results.

Table 2−1 Comparison of hydrogen energy storage and conventional energy storage [40]

Technology	Advantage	Disadvantage
Battery	Convenient for modular operation	Not suitable for large-scale energy storage
Pumped storage	(1) Higher efficiency (2) Lower cost (3) Suitable for large-scale energy storage	Strict requirements for geographical environment
Hydrogen energy storage [41]	(1) High energy density (2) Long energy storage time (3) Hydrogen energy is widely used (4) Suitable for large-scale energy storage	High cost

First of all, in terms of the dynamic prediction model of hydrogen production potential of renewable energy, literature [42-46] respectively analyzed the potential of hydrogen production from renewable energy in Venezuela, Algeria, South Africa, Ecuador and Pakistan, and believed that hydrogen production from renewable energy is a good way to solve the current energy dilemma, but low-efficiency hydrogen production and high investment make hydrogen production from renewable energy At a price disadvantage [44], however, the sharp decrease of fossil energy, the increase of energy demand, the increasingly serious pollution problem, the improvement of hydrogen production efficiency and other phenomena will gradually become prominent, and the economic and environmental benefits of hydrogen production from renewable energy will become increasingly prominent.

Secondly, in the research of efficient hydrogen production technology of renewable energy, renewable energy power generation and electrolytic water hydrogen production are the most stable way at present, and also the only way to produce hydrogen for mechanical energy renewable energy such as wind energy and tidal energy [47]. Some studies have improved the efficiency of hydrogen production through the improvement of catalysts [48,49]. At the same time, some studies show that hydrogen production from electrolyzed wastewater can improve the wastewater treatment effect [50]. On the other hand, some scholars try to optimize hydrogen production by electrolysis using numerical simulation method [51]. It can be seen that there are many researches on the production of hydrogen from electrolyzed water, but even so, there are still many deficiencies for the production of hydrogen from electrolyzed water due to the characteristics of various influencing factors, complex combination and mutual restriction; on the other hand, the production of hydrogen from electrolyzed water from renewable energy is far from enough to only study the production of hydrogen from electrolyzed water, so it is necessary to consider the generation efficiency of renewable energy and combine the characteristics of renewable energy to generate electricity In order to improve the efficiency of hydrogen production by electrolyzing water from renewable energy, there is a serious lack of research in this area.

In addition, in the production of hydrogen energy, in addition to electrolytic hydrogen production from renewable energy, some scholars also study the use of solar energy in renewable energy to produce hydrogen through photocatalysis [52] and photochemical conversion [53-55]. The technology of combined hydrogen production can utilize solar energy in high efficiency and full spectrum, but it is still in the exploration stage for solar energy photothermal, photoelectric and photocatalytic multi-element collaborative hydrogen production, and the multi-element priority and interaction mechanism are still pending.

2.4 The research on hydrogen energy equipment application

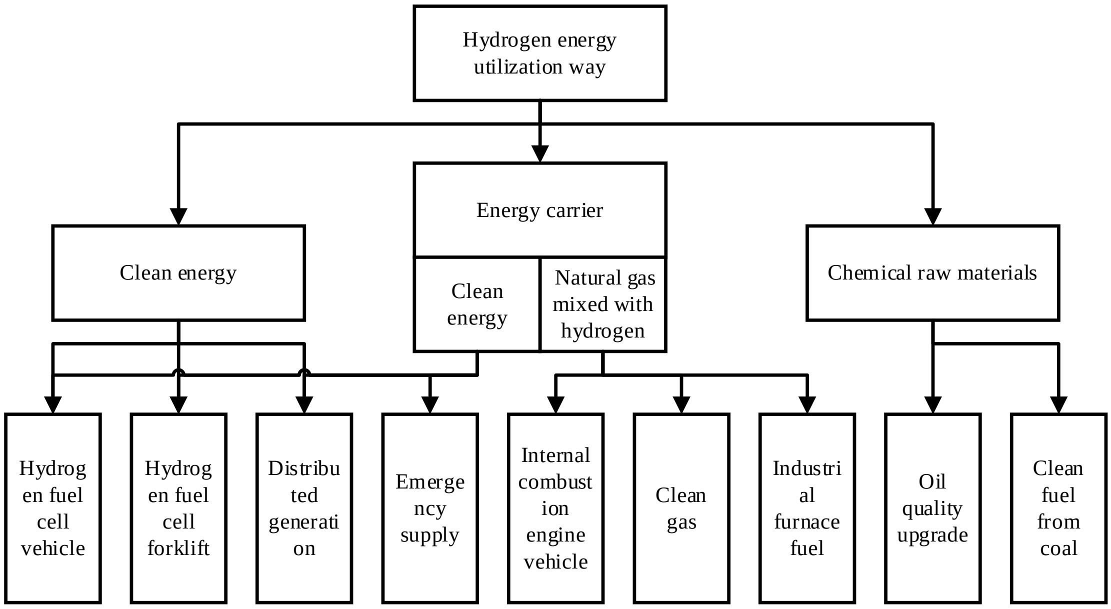

Fig 2-6 Hydrogen energy utilization way

Hydrogen energy is widely used in many fields, such as electric power, industry and transportation (Fig 2-6). In the traditional application, the industry with the largest consumption is the petrochemical industry [56], which is used for the production of synthetic ammonia, methanol and hydrogenation in the process of petroleum refining. In addition to traditional applications, hydrogen can be used as energy. Hydrogen energy and fuel cell technology are the major strategic direction of energy transformation and power transformation in the world. Hydrogen fuel cell technology has always been considered as the ultimate solution to solve the future energy crisis of mankind by using hydrogen energy.[57] However, due to the high cost and the slow development of infrastructure [58], the application of hydrogen energy is currently still in its infancy.

2.3.1 Fuel cell

The current focus of fuel cell research is on PEMFC, SOFC and MCFC. Their current main characteristics are shown in Figure 2-7 below.

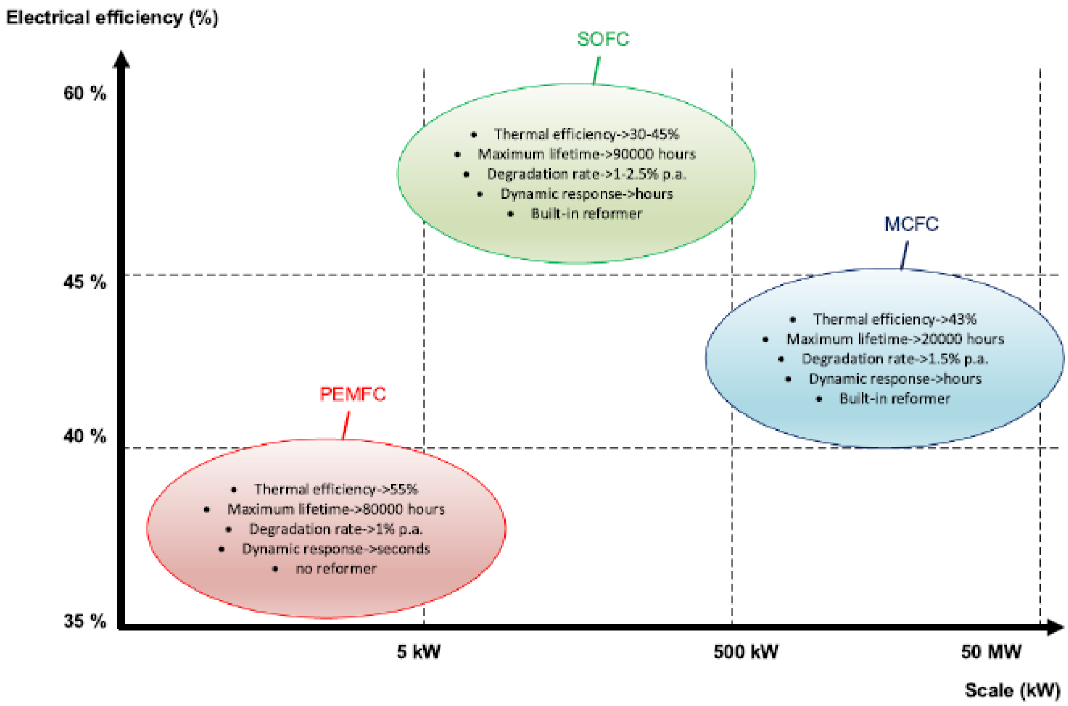

Fig 2-7 Schematic comparison of the key characteristics of PEMFCs, SOFCs and MCFCs as a function of the scale [59]

In the current fuel cell research, the research on the chemical reaction mechanism and catalyst is the main field [60,61]. In the energy field, most of the research on fuel cells focuses on the simulation of internal heat flow, water management, flow path design, and heat dissipation of the fuel cell system. This is based on the fuel cell's own heat and water volume management in order to achieve its power generation efficiency optimization. At the same time, there is also an applied research on cogeneration of heat and power after the waste heat of various parts of the fuel cell. Based on the thermal model and electrochemical model, Khan [62] used simulation software to establish a dynamic model of the lumped parameters of the stack, and analyzed the dynamic changes of temperature and stack voltage when the power of the fuel cell stack changed. Tu Shuguang [63] used the PEM module in the computational fluid software Fluent to simulate and analyze the influence of various system parameters on the steady-state performance of the fuel cell. Shao Qinglong [64] established the dynamic heat transfer model of the stack and analyzed the influencing factors affecting the stack heat transfer from various aspects.

In the technical research of hydrogen fuel cell, except for large-scale fuel cell, because the working temperature of small-scale fuel cell is low and the safety is strong, a large number of scholars have carried out analysis and Research on its thermoelectric characteristics, and discussed its research potential in building and household energy supply system. Aralis [65] took the kW level PEMFC cogeneration system with natural gas as raw material as the research object, studied and simulated the system with EES software, and obtained that the maximum total efficiency of PEMFC cogeneration system is 83.08%, of which the power generation efficiency is 27.62% and the thermal efficiency is 55.46%. Torchio [66] tested the steady-state operation performance and dynamic response performance of 2kW proton exchange membrane fuel cell cogeneration system under different thermal loads according to the experimental equipment. Korsgaard [67] established a model of high temperature proton exchange membrane fuel cell cogeneration system based on PBI membrane on MATLAB platform, and studied the dynamic characteristics of the system. The total efficiency of the system is more than 90%.

Since there are few actual cases of fuel cell waste heat utilization system, most researches also focus on the simulation of the overall system. Zhang Xingmei [68] used 60kW-level PEMFC as the building power and heat supply system. Through regular analysis of users 'electricity and hot water loads, they simulated the supply and demand relationship and operation mode, and analyzed the seasonal and daily time changes. The impact of system efficiency and the satisfaction of user load, and calculated the carbon dioxide and nitrogen oxide emission reduction of the system under the design conditions. Chu [69] conducted a comprehensive simulation and analysis of each process of the fuel cell system. Barelli [70] compared the kW-level SOFC and low-temperature PEMFC cogeneration system with the simulation software ASPEN, and concluded that under normal pressure and low-temperature working environment, the PEMFC cogeneration system has high efficiency. Has a higher economic benefit. Arsalis [71] analyzed and studied the cogeneration system of household kW natural gas high-temperature PEMFC through the simulation software EES, and obtained a comprehensive energy utilization rate of 83.08%. The simulation results show that the high-temperature PEMFC cogeneration system has higher energy utilization efficiency, and because its operating temperature is higher than that of the general PEMFC, it can eliminate the deep removal step in the natural gas processing process, greatly reduce operating costs, and improve the overall system. Economic benefits. But at the same time, how to maintain the good effect of the proton exchange membrane at a higher working temperature is still one of the important issues in the development of the high-temperature PEMFC industry. Borja [72] made economic, thermodynamic and geometric models of proton exchange membrane fuel cells suitable for the supply of cold and heat electricity in multiple units. Through the cost analysis of the fuel and processing subsystems, it is concluded that the economically applicable objects of PEMFC are large-scale settlements. At the same time, the combined heat and power efficiency of most systems is calculated to be about 72%. Huang Yuewu [73] modeled and analyzed the hybrid system of proton exchange membrane fuel cell-four-temperature absorption chiller, studied the overall characteristics of the hybrid system and the different regular changes of the system under different working conditions, and analyzed the system Optimized workspace for important parameters such as efficiency, power, current density, etc. Jie Weiping [74] and others comprehensively considered the characteristics of PEMFC and thermoelectric heat engine, and organically matched the two. Through specific experiments, the feasibility and effectiveness of the joint operation of the two were verified. The experimental results show that the PEMFC stack produces The waste heat can drive the thermodynamic heat engine to work, and the overall energy utilization efficiency of the overall system can reach 58.5%.

2.3.2 Hydrogen fuel cell electric vehicle

(1) Research on Related Technologies of FCV

The research on fuel cells not only combines with that on electric vehicles but also has its own characteristics [75-77] and application modes [78-80]. These studies also provide a reference for the performance improvement of FCV.[81]

FCV has attracted more and more attention because of its low emission, fast refueling and quiet driving. However, the resistance to its promotion is also huge, including the safe storage and transportation of hydrogen energy, the number of hydrogenation stations being too small, and the price being high [82]. Therefore, the research on FCV mainly focuses on these aspects. S Ahmadi [83] designed the powertrain elements of an FCHEV, and proved by simulation that fuel economy, vehicle performance and battery charging maintenance ability were improved to a certain extent. Y Kojima [84] studied many kinds of hydrogen storage materials, which are hydrogen storage alloys, inorganic chemical hydrides, carbon materials and liquid hydrides, and found NH3 is burnable without emission of CO2 and has advantages as hydrogen and energy carriers. JO Abe [85] gave a brief review of hydrogen as an ideal sustainable energy carrier for the future economy, its storage as the stumbling block as well as the current position of solid-state hydrogen storage in metal hydrides and makes a recommendation based on the most promising novel discoveries made in the field in recent times which suggests a prospective breakthrough towards a hydrogen economy. H Li [86] presented an online adaptive equivalent consumption minimum strategy (AECMS) for a fuel cell hybrid electric vehicle powered by a fuel cell, battery, and a supercapacitor.

(2) Research on the Application of FCV2G

Many countries in the world have formulated the development goals, strategic planning, R&D investment, road map and other related policies for hydrogen energy utilization and fuel cells, among which are Japan, Germany, the United States and other leading countries. Taking Japan as an example, a demonstration of a hydrogen gas pipeline network was set up in Kitakyushu City from 2011 to 2014, including verified research on hydrogen fuel cell vehicles. As a part of the smart community demonstration project in Kitakyushu City, the FCV2H power supply from the FCV to the housing was verified by the external power supply function in emergencies and the peak cut effect in the power supply and demand tightening. The current concept of FCV2G is shown in Fig 2-8 below. FCV forms an energy aggregator through buildings with large parking lots to participate in V2G services with the grid.

At present, the research on FCV2G is still relatively small, but there is much V2G and V2H research with pure electric vehicles and hybrid electric vehicles, which have great reference value. Nathaniel S [87] provided a comprehensive and current review of concepts, recently published studies, and demonstration projects/deployments of V2X technology from around the world. Triviño-Cabrera [88] studied dynamic pricing and V2G market-driven models for driving habits and revenue of electric vehicle fleets. P H Hashemi-Dezaki [89] proposed a comprehensive method to evaluate the system's reliability based on PHEV Monte Carlo simulations. M Alirezaei [90] aimed to investigate the role of vehicle-to-home technology in satisfying the energy requirements for a net-zero energy building and indicated that, this system can not only reduce the monetary value of the required grid electricity but also earn money to compensate for the installation costs of other technologies.

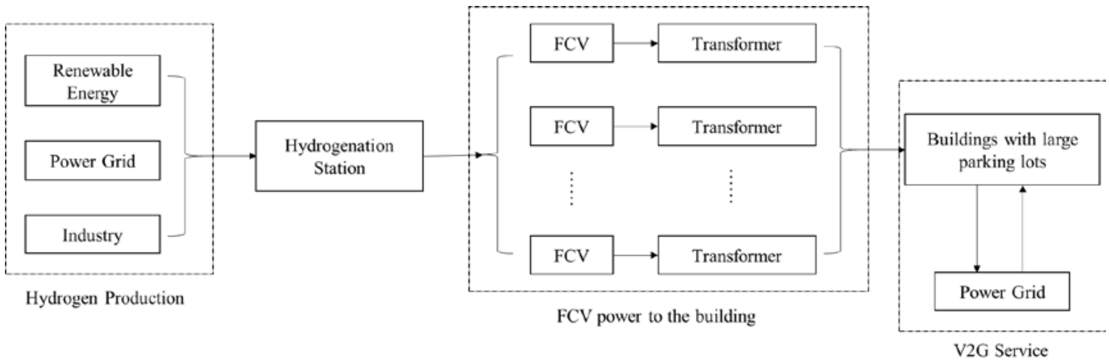

Fig 2-8 The current concept of FCV2G

2.5 Research on hydrogen energy participating in hybrid energy system

The compound system of hydrogen energy and other energy sources, especially the application of hydrogen energy in regional distributed energy systems (RDES), is still in the theoretical research stage. The RDES refers to the establishment of an energy system on the user's side, and at the same time generating electricity, it will also provide users with multiple composite energy sources such as cold and heat. [91] At present, the core areas of conventional RDES s are mainly: gas-fired combined heat and power [92], photovoltaic and energy storage integration [93], etc. The equipment involved mainly includes: internal combustion engines, absorption lithium bromide , Heat pump, photovoltaic and battery etc. At present, the research and application promotion of these devices and core fields are relatively mature, and many more mature theoretical systems have been derived. Including cross-research in different directions or cross-domains with electric vehicles V2G [94], electricity price incentive mechanism [95] and urban spatial structure [96]. Due to large-scale production, the cost of related energy equipment has also been greatly reduced. [97] At present, the RDES has become a high-quality investment project receiving high attention in the capital market. [98]

There are few studies on the combination of hydrogen energy systems and regional distributed energy sources, and more attention is focused on fuel cells [99,100], hydrogen fuel cell electric vehicles [101] and large-scale hydrogen storage [102,103], And the interaction between these areas. [104,105] At present, there are three main ways to combine hydrogen energy systems with regional distributed energy sources. One is to replace equipment with similar functions, that is, use fuel cells to replace internal combustion engines and gas turbines as the core equipment for combined heat and power. Kang [106] studied the operating characteristics and optimization models of the SOFC-engine composite system applied to distributed energy sources, and confirmed the reliability of the proposed model through comparison with experimental data. Yang [107] proposed a distributed energy system based on the new utilization of LNG cold energy combined with SOFC. Through modeling, it was verified that the system can achieve higher thermoelectric efficiency, and the sensitivity of parameters such as fuel cell utilization rate and fuel supply capacity was conducted.

The second is based on the ability of hydrogen energy to be stored across seasons, and uses the hydrogen storage system as a backup storage system for RDES s [108]. The Fig 2-9 below shows the practical application concept of hydrogen energy as a storage medium for photovoltaic power. Mehrjerdi [110] proposed a photovoltaic-hydrogen storage P2P model for distributed energy systems in homes and buildings, and proved that this model can effectively improve the system's revenue. Hemmati [111] proposed the improvement of the hybrid energy storage of hydrogen storage and storage battery. The optimization analysis after combining with photovoltaic proved that it can increase the overall income by 28%.

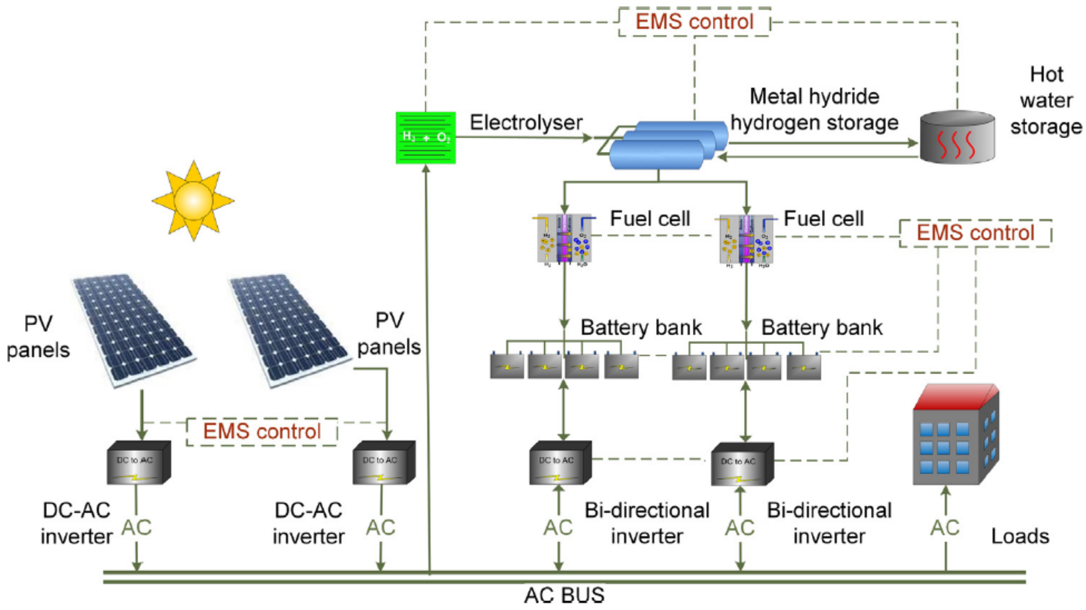

Fig 2-9 Example of a real hydrogen fuel-cell system design. The main electrical components are duplicated in the interest of redundancy and reliability [109]

The third is the design of RDESs [112] and operation optimization analysis [113] using hydrogen energy equipment as the main core. Virji [114] analyzed the economic benefits of combining the hydrogen energy system with wind power and photovoltaic when the island is off-grid based on the actual data of an island in Hawaii. Martin [115] introduced user evaluation into the design of the hydrogen energy system and studied the improvement space of the hydrogen energy system design.

Reference

[1] International Energy Agency IEA, The Future of Hydrogen, June 2019. https://www.iea.org/reports/the-future-of-hydrogen

[2] BloombergNEF, Hydrogen Economy Outlook, March 30, 2020. https://data.bloomberglp.com/professional/sites/24/BNEF-Hydrogen-Economy-Outlook-Key-Messages-30-Mar-2020.pdf

[3] Robert, Fabien Chidanand , G. S. Sisodia , and S. Gopalan . "A Critical Review on the Utilization of Storage and Demand Response for the Implementation of Renewable Energy Microgrids." Sustainable Cities and Society (2018):S2210670717307084.

[4] Apostolou, Dimitrios, and George Xydis. "A literature review on hydrogen refuelling stations and infrastructure. Current status and future prospects." Renewable and Sustainable Energy Reviews 113 (2019): 109292.

[5] Rodríguez, María Liliana Ávalos, et al. "The legal regulation of the H2 as a strategy for public policy in Mexico from the consolidation of the National Council of the hydrogen." International Journal of Hydrogen Energy 44.24 (2019): 12303-12308.

[6] Jones, J., A. Genovese, and A. Tob-Ogu. "Hydrogen vehicles in urban logistics: A total cost of ownership analysis and some policy implications." Renewable and Sustainable Energy Reviews 119 (2020): 109595.

[7] Ahmed, Adeel, et al. "Hydrogen fuel and transport system: A sustainable and environmental future." International journal of hydrogen energy 41.3 (2016): 1369-1380.

[8] Li, Yanxue, Weijun Gao, and Yingjun Ruan. "Potential and sensitivity analysis of long-term hydrogen production in resolving surplus RES generation—a case study in Japan." Energy 171 (2019): 1164-1172.

[9] Thomas, John Meurig, et al. "Decarbonising energy: The developing international activity in hydrogen technologies and fuel cells." Journal of Energy Chemistry (2020).

[10] Dincer, Ibrahim, and Canan Acar. "Review and evaluation of hydrogen production methods for better sustainability." International journal of hydrogen energy 40.34 (2015): 11094-11111.

[11] M.Hassen, S. K.Loudiyi. Electrolytes behavior during hydrogen production by solar energy. Renewable and Sustainable Energy Reviews 70(2017)1331-1335.

[12] Li, Yanxue, Weijun Gao, and Yingjun Ruan. "Potential and sensitivity analysis of long-term

hydrogen production in resolving surplus RES generation—a case study in Japan." Energy 171 (2019): 1164-1172.

[13] K. Petrov, S.Z. Baykara, D. Ebrasu, M. Gulin, A. Veziroglu. An assessment of electrolytic hydrogen production from H2S in Black Sea waters. International Journal of Hydrogen Energy44 (2019) 5303-5313

[14] Dawood, Furat, Martin Anda, and G. M. Shafiullah. "Hydrogen production for energy: An overview." International Journal of Hydrogen Energy (2020).

[15] Kikuchi, Yasunori, et al. "Battery-assisted low-cost hydrogen production from solar energy: Rational target setting for future technology systems." International Journal of Hydrogen Energy 44.3 (2019): 1451-1465.

[16] Yagi, Shunsuke, et al. "Covalency-reinforced oxygen evolution reaction catalyst." Nature communications 6 (2015): 8249.

[17] Myagmarjav, Odtsetseg, et al. "Research and development on membrane IS process for hydrogen production using solar heat." International Journal of Hydrogen Energy 44.35 (2019): 19141-19152.

[18] Yu, Yunsong, et al. "Non-neutral catalyst and reaction energy recovery to minimize the energy consumption for hydrogen production by recyclably indirect H2O electrolysis and CO2 capture." Energy conversion and management 180 (2019): 1203-1216.

[19] Tong, Wenming, et al. "Electrolysis of low-grade and saline surface water." Nature Energy (2020): 1-11.

[20] Hu, Congling, Lei Zhang, and Jinlong Gong. "Recent progress made in the mechanism comprehension and design of electrocatalysts for alkaline water splitting." Energy & Environmental Science 12.9 (2019): 2620-2645.

[21] Zhao, Chenhuan, et al. "Heterointerface engineering for enhancing the electrochemical performance of solid oxide cells." Energy & Environmental Science (2020).

[22] Zhang, Xiaomin, et al. "Co-electrolysis of CO2 and H2O in high-temperature solid oxide electrolysis cells: Recent advance in cathodes." Journal of energy chemistry 26.5 (2017): 839-853.

[23] Stoots, Carl, James O'Brien, and Joseph Hartvigsen. "Results of recent high temperature coelectrolysis studies at the Idaho National Laboratory." International Journal of Hydrogen Energy 34.9 (2009): 4208-4215.

[24] Stoots, Carl M., et al. "High-temperature electrolysis for large-scale hydrogen production from nuclear energy–experimental investigations." International Journal of Hydrogen Energy 35.10 (2010): 4861-4870.

[25] Millet, Pierre, et al. "GenHyPEM: A research program on PEM water electrolysis supported by the European Commission." International Journal of Hydrogen Energy 34.11 (2009): 4974-4982.

[26] Sheridan, Edel, Magnus Thomassen, and Nicolas Guillet CEA. "NEXPEL Project» Next-generation PEM electrolyzer for sustainable hydrogen production WP3 “New binary/ternary catalyst systems” Ex-situ electrocatalyst tests."

[27] Chu, Steven, and Arun Majumdar. "Opportunities and challenges for a sustainable energy future." nature 488.7411 (2012): 294-303.

[28] Wang, Qiang, et al. "A study on the spatial distribution of the renewable energy industries in China and their driving factors." Renewable energy 139 (2019): 161-175.

[29] Carley, Sanya, et al. "Empirical evaluation of the stringency and design of renewable portfolio standards." Nature Energy 3.9 (2018): 754-763.

[30] Robert, Fabien Chidanand, Gyanendra Singh Sisodia, and Sundararaman Gopalan. "A critical review on the utilization of storage and demand response for the implementation of renewable energy microgrids." Sustainable cities and society 40 (2018): 735-745.

[31] Jewell, Jessica, et al. "Limited emission reductions from fuel subsidy removal except in energy-exporting regions." Nature 554.7691 (2018): 229-233.

[32] Wiser, Ryan, et al. "Expert elicitation survey on future wind energy costs." Nature Energy 1.10 (2016): 1-8.

[33] Best, Rohan, and Paul J. Burke. "Adoption of solar and wind energy: The roles of carbon pricing and aggregate policy support." Energy Policy 118 (2018): 404-417.

[34] Chang, Yen-Chiang, and Nannan Wang. "Legal system for the development of marine renewable energy in China." Renewable and Sustainable Energy Reviews 75 (2017): 192-196.

[35] Zhang, Dong, et al. "Regulating cost for renewable energy integration in power grids." Global Energy Interconnection 1.5 (2018): 544-551.

[36] Drechsler, Martin, et al. "Efficient and equitable spatial allocation of renewable power plants at the country scale." Nature Energy 2.9 (2017): 17124.

[37] Zhao, Evan Wenbo, et al. "In situ NMR metrology reveals reaction mechanisms in redox flow

batteries." Nature (2020): 1-5.

[38] Dehghani-Sanij, A. R., et al. "Study of energy storage systems and environmental challenges of batteries." Renewable and Sustainable Energy Reviews 104 (2019): 192-208.

[39] Glenk, Gunther, and Stefan Reichelstein. "Economics of converting renewable power to hydrogen." Nature Energy 4.3 (2019): 216-222.

[40] Zakeri, Behnam, and Sanna Syri. "Electrical energy storage systems: A comparative life cycle cost analysis." Renewable and sustainable energy reviews 42 (2015): 569-596.

[41] Tong, Wenming, et al. "Electrolysis of low-grade and saline surface water." Nature Energy (2020): 1-11.

[42] Posso, F., and J. Zambrano. "Estimation of electrolytic hydrogen production potential in Venezuela from renewable energies." International journal of hydrogen energy 39.23 (2014): 11846-11853.

[43] Rahmouni, Soumia, et al. "Prospects of hydrogen production potential from renewable resources in Algeria." International Journal of Hydrogen Energy 42.2 (2017): 1383-1395.

[44] Hoffmann, J. E. "On the outlook for solar thermal hydrogen production in South Africa." International Journal of Hydrogen Energy 44.2 (2019): 629-640.

[45] Posso, F., et al. "Preliminary estimation of electrolytic hydrogen production potential from renewable energies in Ecuador." international journal of hydrogen energy 41.4 (2016): 2326-2344.

[46] Gondal, Irfan Ahmad, Syed Athar Masood, and Rafiullah Khan. "Green hydrogen production potential for developing a hydrogen economy in Pakistan." International Journal of Hydrogen Energy 43.12 (2018): 6011-6039.

[47] Acar, Canan, and Ibrahim Dincer. "Review and evaluation of hydrogen production options for better environment." Journal of cleaner production (2019).

[48] Sellami, M. Hassen, and K. Loudiyi. "Electrolytes behavior during hydrogen production by solar energy." Renewable and Sustainable Energy Reviews 70 (2017): 1331-1335.

[49] Petrov, K., et al. "An assessment of electrolytic hydrogen production from H2S in Black Sea waters." international journal of hydrogen energy 36.15 (2011): 8936-8942.

[50] Mraoui, A., B. Benyoucef, and L. Hassaine. "Experiment and simulation of electrolytic hydrogen production: Case study of photovoltaic-electrolyzer direct connection." International Journal of Hydrogen Energy 43.6 (2018): 3441-3450.

[51] Rahim, AH Abdol, et al. "An overview of polymer electrolyte membrane electrolyzer for hydrogen production: Modeling and mass transport." Journal of Power Sources 309 (2016): 56-65.

[52] Ismail, Adel A., and Detlef W. Bahnemann. "Photochemical splitting of water for hydrogen production by photocatalysis: a review." Solar Energy Materials and Solar Cells 128 (2014): 85-101.

[53] Dincer, Ibrahim, and Canan Acar. "Review and evaluation of hydrogen production methods for better sustainability." International journal of hydrogen energy 40.34 (2015): 11094-11111.

[54] Yuan, Dandan, et al. "Solar STEP organic decomposition plus hydrogen: A novel approach to efficient degradation of organic pollutants exemplified by acrylonitrile." International Journal of Hydrogen Energy 41.39 (2016): 17199-17207.

[55] Yuan, Dandan, et al. "Three-field synergy of solar energy for induced the enhancement of the oxidation of acrylonitrile in coordination with the production of hydrogen." International Journal of Hydrogen Energy 44.11 (2019): 5303-5313.

[56] Malerød-Fjeld, Harald, et al. "Thermo-electrochemical production of compressed hydrogen from methane with near-zero energy loss." Nature Energy 2.12 (2017): 923-931.

[57] Cano, Zachary P., et al. "Batteries and fuel cells for emerging electric vehicle markets." Nature Energy 3.4 (2018): 279-289.

[58] Hydrogen on the rise. Nature. Energy (2016): 1, 16127.

[59] Parra, David, et al. "A review on the role, cost and value of hydrogen energy systems for deep decarbonisation." Renewable and Sustainable Energy Reviews 101 (2019): 279-294.

[60] Steele, Brian CH, and Angelika Heinzel. "Materials for fuel-cell technologies." Materials For Sustainable Energy: A Collection of Peer-Reviewed Research and Review Articles from Nature Publishing Group. 2011. 224-231.

[61] Irvine, John TS, et al. "Evolution of the electrochemical interface in high-temperature fuel cells and electrolysers." Nature Energy 1.1 (2016): 15014.

[62] Khan, M. J., and M. T. Iqbal. "Modelling and analysis of electro‐chemical, thermal, and reactant flow dynamics for a PEM fuel cell system." Fuel cells 5.4 (2005): 463-475.

[63] Tu Shuguang. Research on the dynamic characteristics of proton exchange membrane fuel cells for vehicles. Diss. Wuhan University of Technology, 2007. (in Chinese)

[64] Shao Qinglong, Cao Guangyi, and Zhu Xinjian. "Dynamic heat transfer model of proton

exchange membrane fuel cell stack." Journal of Shanghai Jiaotong University 08 (2004): 76-79. (in Chinese)

[65] A. Arsalis, Mads P. Nielsen, Søren K. Kær. Modeling and parametric study of a 1kWe HT-PEMFC-based residential micro-CHP system [J]. International Journal of Hydrogen Energy, 2011, 36(8): 5010-20.

[66] M. F. Torchio, M. G. Santarelli, A. Nicali. Experimental analysis of the CHP performance of a PEMFC stack by a 24 factorial design [J]. Journal of Power Sources, 2005, 149(33-43.

[67] Anders R. Korsgaard, Mads P. Nielsen, Søren K. Kær. Part one: A novel model of HTPEM-based micro-combined heat and power fuel cell system [J]. International Journal of Hydrogen Energy, 2008, 33(7): 1909-20.

[68] Zhang Xingmei, Zhao Xiling, and Duan Changgui. "Study on the Cogeneration System of Proton Exchange Membrane Fuel Cell Building." Gas and Heat 01 (2011): 58-63. (in Chinese)

[69] Chu, Hsin-Sen, et al. "The development of a small PEMFC combined heat and power system." Journal of Power Sources 176.2 (2008): 499-514.

[70] Barelli, L., et al. "An energetic–exergetic comparison between PEMFC and SOFC-based micro-CHP systems." International Journal of Hydrogen Energy 36.4 (2011): 3206-3214.

[71] Arsalis, Alexandros, Mads P. Nielsen, and Søren K. Kær. "Modeling and parametric study of a 1 kWe HT-PEMFC-based residential micro-CHP system." International Journal of Hydrogen Energy 36.8 (2011): 5010-5020.

[72] Oyarza´ bal, Borja, Michael W. Ellis, and Michael R. von Spakovsky. "Development of thermodynamic, geometric, and economic models for use in the optimal synthesis/design of a PEM fuel cell cogeneration system for multi-unit residential applications." J. Energy Resour. Technol. 126.1 (2004): 21-29.

[73] Huang Yuewu, Wei Feifei, and Chen Peng. "Performance Analysis of Proton Exchange Membrane Fuel Cell-Four Temperature Absorption Refrigerator Hybrid System." Journal of Mechanical Engineering 24 (2013): 159-164. (in Chinese)

[74] Jie Weiping. Experimental study of PEMFC stack electrical efficiency and PEMFC-thermoelectric thermoelectric cogeneration. Diss. Tianjin University, 2007. (in Chinese)

[75] Zeng, Hongyu, et al. "Micro-tubular solid oxide fuel cell stack operated with catalytically enhanced porous media fuel-rich combustor." Energy 179 (2019): 154-162.

[76] Kim, Tae-Hyun, et al. "Influence of the Nafion agglomerate morphology on the water-uptake behavior and fuel cell performance in the proton exchange membrane fuel cells." Applied Surface Science (2019).

[77] Chen, Bin, et al. "Thermal modelling of ethanol-fuelled Solid Oxide Fuel Cells." Applied Energy 237 (2019): 476-486.

[78] Forysinski, Piotr, et al. "Development and use of a mixed-reactant fuel cell." Journal of Power Sources 414 (2019): 366-376.

[79] Boait, Peter John, and R. Greenough. "Can fuel cell micro-CHP justify the hydrogen gas grid? Operating experience from a UK domestic retrofit." Energy and Buildings 194 (2019): 75-84.

[80] Napoli, R., et al. "Techno-economic analysis of PEMFC and SOFC micro-CHP fuel cell systems for the residential sector." Energy and Buildings 103 (2015): 131-146.

[81] Cano, Zachary P., et al. "Batteries and fuel cells for emerging electric vehicle markets." Nature Energy 3.4 (2018): 279-289.

[82] Tanç, Bahattin, et al. "Overview of the next quarter century vision of hydrogen fuel cell electric vehicles." International Journal of Hydrogen Energy 44.20 (2019): 10120-10128.

[83] Ahmadi, Saman, S. M. T. Bathaee, and Amir H. Hosseinpour. "Improving fuel economy and performance of a fuel-cell hybrid electric vehicle (fuel-cell, battery, and ultra-capacitor) using optimized energy management strategy." Energy conversion and management 160 (2018): 74-84.

[84] Kojima, Yoshitsugu. "Hydrogen storage materials for hydrogen and energy carriers." International Journal of Hydrogen Energy (2019).

[85] Abe, J. O., E. Ajenifuja, and O. M. Popoola. "Hydrogen energy, economy and storage: Review and recommendation." International Journal of Hydrogen Energy (2019).

[86] Li, Huan, et al. "Online adaptive equivalent consumption minimization strategy for fuel cell hybrid electric vehicle considering power sources degradation." Energy Conversion and Management 192 (2019): 133-149.

[87] Pearre, Nathaniel S., and Hajo Ribberink. "Review of research on V2X technologies, strategies, and operations." Renewable and Sustainable Energy Reviews 105 (2019): 61-70.

[88] Triviño-Cabrera, Alicia, José A. Aguado, and Sebastián de la Torre. "Joint routing and scheduling for electric vehicles in smart grids with V2G." Energy 175 (2019): 113-122.

[89] Hashemi-Dezaki, Hamed, et al. "Risk management of smart grids based on managed charging

of PHEVs and vehicle-to-grid strategy using Monte Carlo simulation." Energy conversion and management 100 (2015): 262-276.

[90] Alirezaei, Mehdi, Mehdi Noori, and Omer Tatari. "Getting to net zero energy building: Investigating the role of vehicle to home technology." Energy and Buildings 130 (2016): 465-476.

[91 Mahmud, Khizir, et al. "An internet of energy framework with distributed energy resources, prosumers and small-scale virtual power plants: An overview." Renewable and Sustainable Energy Reviews 127 (2020): 109840.

[92] Wu, Qiong, et al. "Multi-objective optimization of a distributed energy network integrated with heating interchange." Energy 109 (2016): 353-364.

[93] Kumar, Abhishek, et al. "Strategic integration of battery energy storage systems with the provision of distributed ancillary services in active distribution systems." Applied Energy 253 (2019): 113503.

[94] Li, Cuiping, et al. "Economic dispatching strategy of distributed energy storage for deferring substation expansion in the distribution network with distributed generation and electric vehicle." Journal of Cleaner Production (2020): 119862.

[95] Varghese, Sushant, and Ramteen Sioshansi. "The price is right? How pricing and incentive mechanisms in California incentivize building distributed hybrid solar and energy-storage systems." Energy Policy 138 (2020): 111242.

[96] Wu, Qiong, et al. "Coupling optimization of urban spatial structure and neighborhood-scale distributed energy systems." Energy 144 (2018): 472-481.

[97] Bustos, Cristian, David Watts, and Daniel Olivares. "The evolution over time of Distributed Energy Resource’s penetration: A robust framework to assess the future impact of prosumage under different tariff designs." Applied Energy 256 (2019): 113903.

[98] Ren, Hongbo, et al. "Cost–benefit analysis of distributed energy systems considering multi-benefits and multi-stakeholders." Energy 189 (2019): 116382.

[99] Vijay, Avinash, and Adam Hawkes. "Impact of dynamic aspects on economics of fuel cell based micro co-generation in low carbon futures." Energy 155 (2018): 874-886.

[100] Qiu, Diankai, et al. "Numerical Analysis of Air-cooled Proton Exchange Membrane Fuel Cells With Various Cathode Flow Channels." Energy (2020): 117334.

[101] Qian, Fanyue, et al. "Economic optimization and potential analysis of fuel cell vehicle-to-grid

(FCV2G) system with large-scale buildings." Energy Conversion and Management 205 (2020): 112463.

[102] Seo, Seung-Kwon, Dong-Yeol Yun, and Chul-Jin Lee. "Design and optimization of a hydrogen supply chain using a centralized storage model." Applied Energy 262 (2020): 114452.

[103] Samsatli, Sheila, and Nouri J. Samsatli. "The role of renewable hydrogen and inter-seasonal storage in decarbonising heat–Comprehensive optimisation of future renewable energy value chains." Applied Energy 233 (2019): 854-893.

[104] Corgnale, Claudio, et al. "Hydrogen storage in a two-liter adsorbent prototype tank for fuel cell driven vehicles." Applied Energy 250 (2019): 333-343.

[105] Zhou, Yang, Alexandre Ravey, and Marie-Cecile Péra. "Multi-mode predictive energy management for fuel cell hybrid electric vehicles using Markov driving pattern recognizer." Applied Energy 258 (2020): 114057.

[106] Kang, Sanggyu, and Kook-Young Ahn. "Dynamic modeling of solid oxide fuel cell and engine hybrid system for distributed power generation." Applied Energy 195 (2017): 1086-1099.

[107] Yang, Xiaoyu, and Hongbin Zhao. "Thermodynamic performance study of the SOFC-STIG distributed energy system fueled by LNG with CO2 recovery." Energy 186 (2019): 115860.

[108] Reuß, Markus, et al. "Seasonal storage and alternative carriers: A flexible hydrogen supply chain model." Applied energy 200 (2017): 290-302.

[109] Eriksson, E. L. V., and E. MacA Gray. "Optimization and integration of hybrid renewable energy hydrogen fuel cell energy systems–A critical review." Applied energy 202 (2017): 348-364.

[110] Mehrjerdi, Hasan. "Peer-to-peer home energy management incorporating hydrogen storage system and solar generating units." Renewable Energy (2020).

[111] Hemmati, Reza, Hasan Mehrjerdi, and Mosayeb Bornapour. "Hybrid hydrogen-battery storage to smooth solar energy volatility and energy arbitrage considering uncertain electrical-thermal loads." Renewable Energy (2020).

[112] Fonseca, Juan D., et al. "Trends in design of distributed energy systems using hydrogen as energy vector: a systematic literature review." International journal of hydrogen energy 44.19 (2019): 9486-9504.

[113] Maghami, Mohammad Reza, et al. "Hybrid energy management with respect to a hydrogen energy system and demand response." International Journal of Hydrogen Energy 45.3 (2020): 1499-

1509.

[114] Virji, M., et al. "Analyses of hydrogen energy system as a grid management tool for the Hawaiian Isles." International Journal of Hydrogen Energy 45.15 (2020): 8052-8066.

[115] Martin, Antoine, Marie-France Agnoletti, and Eric Brangier. "Users in the design of Hydrogen Energy Systems: A systematic review." International Journal of Hydrogen Energy (2020).

Chapter 3

MODEL ESTABLISHMENT AND FORECASTING METHOD RESEARCH

CHAPTER THREE: MODEL ESTABLISHMENT AND FORECASTING METHOD RESEARCH

3.1 Motivation and main method

3.1.1 Motivation

Through the combing of the second chapter on the research of hydrogen energy, it is found that although the cost of hydrogen energy equipment and supporting systems has dropped to a large extent, and there is still a large room for decline in the future. However, the current price of hydrogen energy is still insufficient to obtain economic advantages under the existing energy system, and it still needs to rely on policy support for a long period of time afterwards. Therefore, based on the characteristic that hydrogen energy does not produce carbon emissions when it is used, this study proposes to convert the environmental advantages of hydrogen energy into economic benefits through carbon tax. Although the large-scale popularization of hydrogen energy is bound to come according to the development plans of various countries, most of the current research is still based on the current energy supply and demand relationship and the demand for the environment. Considering the carbon tax will help to understand the application and development potential of hydrogen energy more clearly under more restrictive environmental conditions. This study will conduct research on the economic potential, impact analysis and development forecast of hydrogen energy based on carbon tax limitation from the three levels of equipment, system and region. It is hoped that it can provide new ideas for the promotion of hydrogen energy and provide theoretical reference for the research on the practical application of hydrogen energy.

3.1.2 Introduction of carbon tax

As an important measure of global energy saving and emission reduction, carbon emission price is one of the research hotspots nowadays. Carbon emissions are currently commonly used for comparative technology or building life cycle analysis [1]. A Ozawa [2] analyzed the life cycle carbon emissions of different hydrogen carriers based on the analysis of the whole supply chain and the Japanese life cycle inventory database. The results show that the life cycle carbon emission of liquid hydrogen (LH2) and ammonia (NH3) is still 52% and 36% lower than that of conventional natural gas-combined power generation. At present, the impact analysis of carbon emission price on technology is less, and the research mainly focuses on the impact on countries or regions. B Lin [3] analyzed the impact of different ETS price levels by applying a dynamic recursive computable general equilibrium mode. They argued that ETS prices in China's ETS pilot cities are too low, and would provide little emission reduction, and suggested increasing carbon prices to $20 and focusing on the appropriate subsidies for new energy generation. J Chevallier [4] investigated the presence of outliers in the volatility of carbon prices. Three different measures of volatility for European Union allowances were computed based on daily data (EGARCH model), option prices (implied volatility), and intraday data (realized volatility).

3.2 Model establish and energy system design strategies

3.2.1 Energy Equipment

(1) Fuel cell (FC)

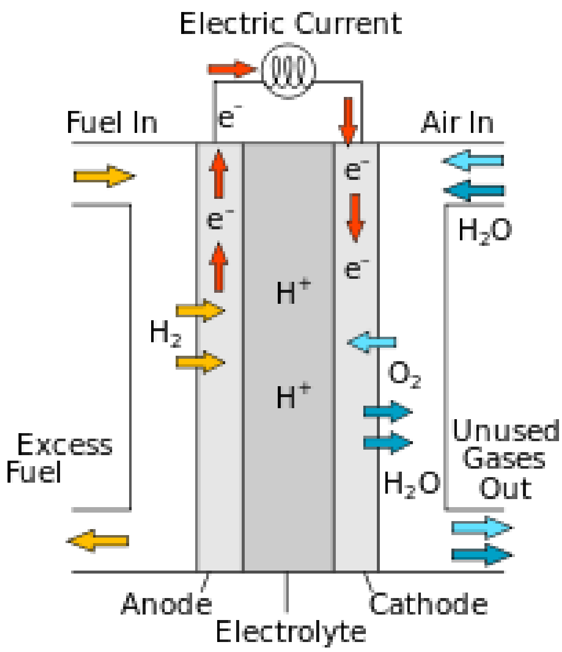

Fig 3-1 Schematic diagram of fuel cell power generation process

The principle of a fuel cell is an electrochemical device, and its composition is the same as that of a general battery. The single cell is composed of positive and negative electrodes (negative electrode is fuel electrode and positive electrode is oxidant electrode) and electrolyte. The difference is that the active material of a general battery is stored inside the battery, therefore, the battery capacity is limited. The positive and negative electrodes of the fuel cell itself do not contain active materials, but only a catalytic conversion element. Therefore, fuel cells are literally energy conversion machines that convert chemical energy into electrical energy. When the battery is in operation, fuel and oxidant are supplied from outside to react. In principle, as long as the reactants are continuously input and the reaction products are continuously eliminated, the fuel cell can continuously generate electricity.

The fuel cell power generation model can be expressed as:

$$P_{FC} = f_{FC} \times L_h \times \delta_{FC} \tag{3-1}$$

Where, P_{FC} is the power generation power of the fuel cell; f_{FC} is the hydrogen consumption of the fuel cell; L_h is the low calorific value of hydrogen; δ_{FC} is the power generation efficiency of the fuel cell. The output thermal power model of the fuel cell can be expressed as:

$$Q_{FC} = P_{FC} \times \delta_{FC,heat} \quad (3\text{-}2)$$

Where, Q_{FC} is the output thermal power of the fuel cell; $\delta_{FC,heat}$ is the thermoelectric ratio of the fuel cell

(2) Internal combustion engine (ICE)

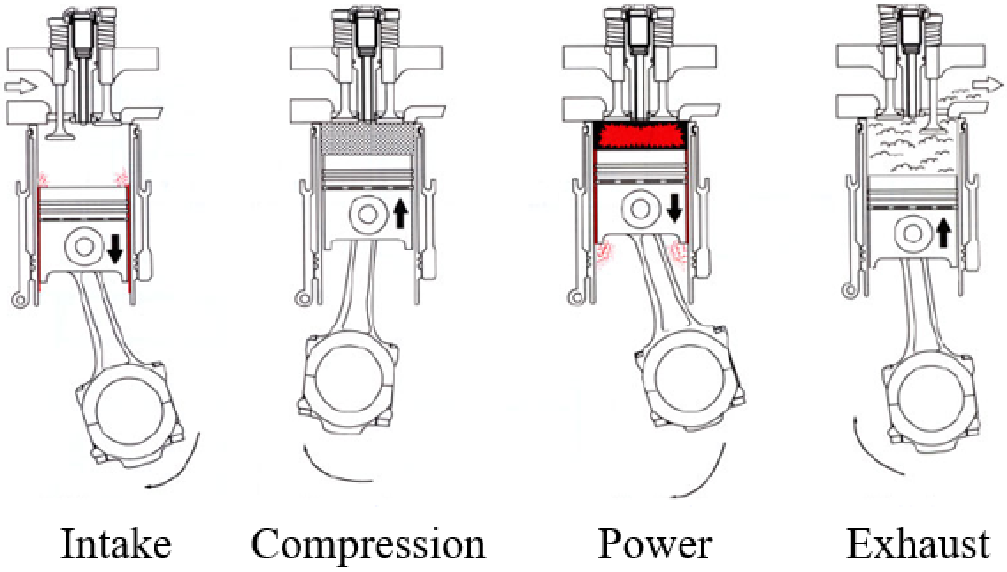

Fig 3-2 Schematic diagram of the working principle of a gas internal combustion engine

Working principle of gas internal combustion engine: First, the engine mixes natural gas with air and then pressurizes it through a turbocharger and enters the cylinder to burn and do work. At the same time, the piston pushes the connecting rod to rotate the crankshaft. In this process, the engine undergoes four strokes of intake, compression, work, and exhaust to convert chemical energy into mechanical energy. Secondly, the engine drives the rotor of the generator through elastic couplings and generates electrical energy. Due to the high temperature of the exhaust gas of the gas internal combustion engine and the high-temperature cylinder liner water, it can be used through the waste heat utilization equipment to provide users with cooling and heating loads. (Fig 3-2)

The technology of gas-fired internal combustion generators is very mature, and there are many famous manufacturers in the world. Such as American Cummins, American Caterpillar, American Waukesha, German MWM, Finnish Wärtsilä, and American GE (Yanbach). The power generation model of the internal combustion engine can be expressed as:

$$P_{ICE} = f_{ICE} \times L_g \times \delta_{ICE} \tag{3-3}$$

Where, P_{ICE} is the power generation power of the internal combustion engine; f_{ICE} is the natural gas consumption of the internal combustion engine; L_g is the low calorific value of natural gas; δ_{ICE} is the power generation efficiency of the internal combustion engine. The output thermal power model of the internal combustion engine can be expressed as:

$$Q_{ICE} = P_{ICE} \times \delta_{ICE,heat} \tag{3-4}$$

Where, Q_{ICE} is the output thermal power of the internal combustion engine; $\delta_{ICE,heat}$ is the thermoelectric ratio of the internal combustion engine

(3) Absorption chiller-heater (AC)

Absorption chiller-heater uses lithium bromide solution as absorbent and water as refrigerant, using water to evaporate and absorb heat under high vacuum to achieve the purpose of refrigeration. In order to allow the refrigeration process to continue continuously, the evaporated refrigerant water vapor is absorbed by the lithium bromide solution, and the solution becomes thinner. This process occurs in the absorber, and then the thermal energy is used as the power to heat the dilute solution. The water is separated and the solution becomes concentrated. This process is carried out in the generator. The steam obtained from the generator is condensed into water in the condenser, and after throttling, it is sent to the evaporator for evaporation. This cycle achieves the purpose of continuous refrigeration. (Fig 3-3)

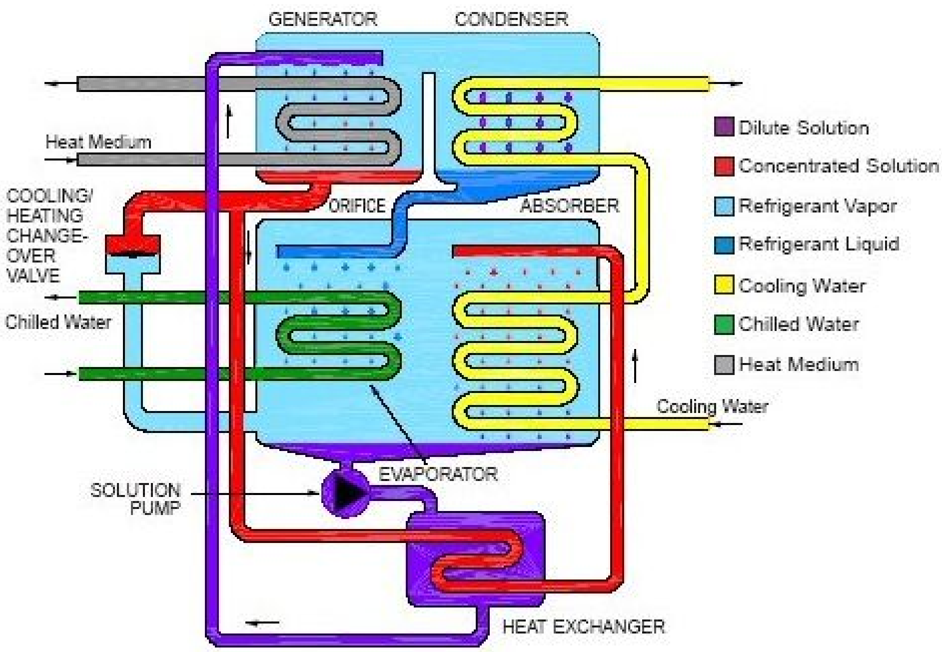

Fig3-3 Schematic diagram of the working principle of Absorption chiller-heater

Absorption chiller-heater s are equipment that uses heat to provide heating and cooling. At present, there are many manufacturing plants in the world that can manufacture absorption chiller-heater units. Larger companies are Carrier, Trane, York and other companies in the United States, Sanyo Electric, Mitsubishi Heavy Industries, Hitachi, Ebara, Kawasaki Heavy Industries and other companies in Japan, LG Machinery Century Heavy Industries and other companies.The COP of absorption chiller-heater is expressed as follow. (cold mode as an example)

$$COP_{AC,cold} = \frac{Q_{AC}}{R_{AC,cold}} \tag{3-5}$$

Where Q_{AC} is the energy supplied by absorption chiller-heater and $R_{AC,cold}$ is the capacity of absorption chiller-heater.

(4) Heat pump (HP)

The heat pump uses electricity to generate cold or heat using compression refrigeration. It has a high COP and high energy efficiency. The cooling capacity of the heat pump is expressed as follows. (Take cooling as an example)

$$Q_{HP,cold} = P_e \times COP_{HP,cold} \tag{3-6}$$

Where, $Q_{HP,cold}$ is the cooling capacity of the heat pump, P_e is the power consumption of the heat pump; $COP_{HP,cold}$ is the energy conversion efficiency of the heat pump.

(5) Cold and heat storage

The principle of the energy storage device is to use the excess valley charge of the power grid at night to continue to operate cooling and heating, and store the cooling and heat through the medium, and release the cooling and heat during the peak electricity consumption during the day to provide air conditioning services, thereby alleviating air conditioning Conflicts over peak power. There are currently three popular cold storage methods, namely water cold storage, ice cold storage, and excellent salt cold storage. The heat storage methods mainly include water heat storage and solid heat storage. Among them, the method of water storage can be used as heat storage in winter, and can partially replace the fire water tank of the building, so it is the most widely used.The energy supply method of the water storage tank is relatively simple, and the basic performance parameters are shown in the following table 3-1. (Taking 2500 m^3 of cold storage tank as an example, the temperature difference is 7°C.)

Table 3-1 Characteristics of water storage tank

No.	Parameter name	Data	No.	Parameter name	Data
1	Total effective water storage (m^3)	2500	5	Main tank service life	Not less than 20 years
2	Maximum cold storage flow (m^3/h)	417(6 hours full)	6	Storage tank volume utilization	Not less than 90%
3	Effective cold storage and release capacity (kWh)	20000kWh	7	Reynolds number Re	Re≦850
4	Inclined temperature layer thickness (mm)	≤1500	8	Froude number Fr	Fr≦1
9	Insulation performance	(1) The surface of the tank does not condense on the outer surface under the conditions of ambient temperature 40 ℃ and relative humidity 85%. (2) The 24-hour cold loss is no more than 2% of the total effective cold release.			

(6) Photovoltaic (PV)

Photovoltaic is defined as the direct conversion of ray energy. In practical applications, it usually refers to the conversion of solar energy to electrical energy, that is, solar photovoltaic. Its implementation is mainly through the use of solar panels made of semiconductor materials such as silicon, using light to generate direct current. Photovoltaic cell is an important component of photovoltaic power generation system, its probability density function is shown below, and its output power is closely related to the temperature and light intensity of the device.

$$f\left(G_t\right)=\frac{\Gamma\left(\alpha+\beta\right)}{\Gamma\left(\alpha\right)+\Gamma\left(\beta\right)}\left(\frac{G_t}{G_{max}}\right)\left(1-\frac{G_t}{G_{max}}\right)^{\beta-1} \tag{3-7}$$

Where, α and β are the shape parameters of Beta distribution, Γ is the Gamma function, and G_t is the light intensity (W/ m^2). After obtaining the average value μ and the standard deviation σ of light intensity according to statistics, the values of α and β can be obtained by the following formula:

$$\begin{cases} \alpha=\mu\left[\frac{\mu(1-\mu)}{\sigma^2}-1\right], \\ \beta=(1-\mu)\left[\frac{\mu(1-\mu)}{\sigma^2}-1\right]. \end{cases} \tag{3-8}$$

Where, the temperature of the photovoltaic cell cannot be obtained by direct measurement, so it is estimated from the ambient temperature and light intensity:

$$T_{c,t} = T_{amd,t} + 30\frac{G_t}{1000} \tag{3-9}$$

Where, $T_{c,t}$ is the temperature of the photovoltaic cell, $T_{amd,t}$ is the ambient temperature. Knowing the temperature and light intensity, the output power of the photovoltaic cell can be expressed as follows:

$$P_{pv,t} = P_{STC}\frac{G_t}{G_{STC}}\left[1+k\left(T_{c,t} - T_{STC}\right)\right] \tag{3-10}$$

Where, $P_{pv,t}$ is the output power of the photovoltaic cell.

(7) Battery

The meaning of the state of charge of the battery SOC (t) is:

$$\mathrm{SOC}(t) = \frac{Q_B(t)}{Q_{B,max}} \tag{3-11}$$

Where, $Q_B(t)$ is the remaining capacity of the battery at time t, and $Q_{B,max}$ is the maximum capacity of the battery.

3.2.2 HVAC load model

According to the law of conservation of energy, taking cooling load demand as an example, in each time interval, the load demand Q_c of the HVAC system is equal to the sum of the following five loads [5]: Q_e caused by heat dissipation of electrical equipment, Q_n required by fresh air, Q_s required to achieve the set temperature, energy loss Q_i caused by different fencing structures, and Q_p brought about by personnel flow:

$$Q_c = Q_e + Q_n + Q_s + Q_i + Q_p \tag{3-12}$$

(1) Heat dissipation of electrical equipment Q_e

In electrical equipment, the heat dissipation of equipment can usually be measured by the load density per square meter:

$$Q_e = \sum_n A \times e \tag{3-13}$$

N denotes different floors or functional areas; A denotes the area of floors or functional areas, m^2; e denotes the load density of electrical equipment such as lighting, pumps, and office equipment, W/m^2.

(2) Fresh air cooling load demand Q_n

The calculation of fresh air load is complicated. Generally, fresh air cooling load can be calculated by the size of fresh air volume:

$$Q_n = V \times p \times Cp \times (T_i - T_0) \tag{3-14}$$

V denotes fresh air volume, m^3; P denotes air density, kg/m^3; Cp denotes specific heat of air, J/(℃*kg); T_i denotes outflow temperature of fresh air, ℃; T_0 denotes inflow temperature of fresh air, ℃.

(3) Cooling load requirement to achieve set temperatureQ_s

The formula of the cooling load requirement to achieve the set temperature is similar to fresh air load. The fresh air volume in equations (3-14) is replaced by the air volume in the target area, and the inlet and outlet temperature of the fresh air is replaced by the initial temperature in the target area and the set temperature.

(4) Fencing structures cooling load Q_i

The cooling load demand of fence structure includes the loss of cooling load, i.e. the heat imported through the roof, window and wall, as well as the solar radiation heat irradiated into the room:

$$Q_i = \sum(K \times A_w \times \Delta T) + A_s \times (q_i + q_w) \tag{3-15}$$

K denotes the thermal conductivity of the roof and exterior wall, W/(m^2*°C); A_w denotes the area of exterior wall and roof, m^2; ΔT denotes the temperature difference between the interior and exterior; A_s denotes the area of window, m^2; q_i denotes the heat transfer of glass per unit area to the room after obtaining solar radiation heat, W/m^2; q_w denotes the radiation heat transferred into the room through unit area glass of window, W/m^2:

$$q_w = I \times \gamma \times \mu \tag{3-16}$$

I denotes the irradiation intensity of the sun, W/m^2; γ denotes the transmittance of glass; μ denotes the correction factor, mainly considering the effect of window frames, balconies, and internal and external shading measures.

(5) Personnel flow cooling load demandQ_p

The cooling load of personnel flow is calculated using empirical formula, and there are certain differences in the simulation software of different energy consumption, usually calculated by using the empirical value of each person's cold load demand.

In load forecasting, the main uncertainties come from Q_p of personnel flow and Q_i of heat loss caused by changes in the meteorological environment. Among them, because the fence structure of the building itself will not change, this part of the error will be smaller, and through the combination of meteorological prediction, the prediction accuracy can be further improved. However, in the part of Q_p, improving the learning ability of the prediction model itself is the only way to reduce error. Once there is a small amount of data, the errors caused by Q_p will increase substantially.

3.2.3 Operational mode of combined cooling heating and power (CCHP) energy system

(1) Heat setting mode

In this mode, the heat (cold capacity) to be provided by the joint supply system will first match the user's cooling and heating load requirements, and the power generation may be redundant or insufficient. At a certain moment, when the generated power is higher than the user's electrical load demand, the excess power can be used to drive the electric refrigeration, air conditioning, refrigeration or sold to the grid; when the generated power is lower than the user's electrical load demand, the insufficient power is replenished from the grid . This mode is suitable for the bidirectional grid-connected heat, power and cooling combined supply system, which is the most widely used.

(2) Electric setting mode

In this mode, the power provided by the joint supply system is preferentially matched to the user's electrical load demand, and the heat (cooling) generated may be redundant or insufficient. At a certain moment, when the available heat (cold capacity) is lower than the heat (cold) load demand, the insufficient heat (cold capacity) is replenished by the gas boiler (electric refrigeration and air conditioning). When the available heat (cold capacity) is higher than the heat (cold) load demand, the excess heat is discharged to the external environment. This mode is suitable for places that preferentially match electrical loads and have low requirements on heating and cooling loads.

(3) Mixed operation mode

In this mode, certain time periods are based on heat and electricity, and some periods are based on electricity and heat. The method used is based on parameters such as real-time heating and cooling loads and electrical prices in specific time periods. This mode is flexible, Strong adaptability, suitable for places that require the full play of the economy, energy saving and environmental protection of the joint supply system.

(4) Island operation mode

In this mode, the joint supply system operates completely in a closed manner, and the joint supply system provides the heat, electricity and cooling load required by the user. The system is isolated from the external network and cannot buy electricity from the grid or heat from the external heat network. This mode requires additional power generation equipment and heating equipment in case of unexpected needs. However, this model has the largest initial investment. This mode is suitable for systems that require independence from external networks, such as remote mountain villages, islands, and areas with high demand for energy supply reliability.

3.3 Load forecasting method research

As a result of the increasing demand for energy and the improvement of carbon emission policies, the world energy system is now in the stage of transition [6]. In this stage, it is particularly important to improve energy efficiency. According to British Petroleum's (BP) report 'World Energy Outlook 2019', industry and buildings have the largest energy consumption and growth demand among all areas. Therefore, it has become one of the hotspots to study the efficient utilization of energy in these fields, combining the advantages of intelligent technology, such as big data analysis and machine learning.

In building energy consumption, the HVAC system occupies a large proportion and has great energy-saving potential. For example, in the United States, this part of energy consumption accounts for about 50% of building energy consumption [7]. In commercial buildings, this part of energy consumption accounts for about 15-30% [8].

To reduce this part of consumption, various kinds of technology and energy system optimization emerge endlessly, including:

1) Research on new energy systems, such as the performance and economic optimization of residential photovoltaic systems [9], the optimization design of fuel cell systems [10], and the collaborative optimization of biomass energy and user needs [11];

2) Research on distributed energy systems, such as thermoelectric coupling multi-objective planning [12] and method study on user participation in demand-side management [13];

3) Other energy-saving technologies, such as the correlation between energy storage and photovoltaic [14], and research on the combination of Organic Rankine Cycle and distributed energy system [15].

In these studies, accurate load forecasting is necessary for the realization of various control systems or optimal design, so efficient and accurate forecasting methods are particularly important and worth studying [16].

Load forecasting is the basis of model optimization. The premise of the optimization model in Chapter 5 and Chapter 7 is to ensure efficient load forecasting. The sixth chapter involves the practical application of cold and heat load forecasting. Therefore, this paper summarizes the methods of load forecasting and proposes a new application of cold and hot load forecasting based on transfer learning.

3.3.1 Difficulties in HVAC load forecasting

Load forecasting of building HVAC systems can be divided into the design stage and the operation stage. Load forecasting in the design stage is mainly for the selection of energy supply equipment and the determination of pipeline size, so as to ensure the system runs comfortably and economically. In the operation stage, load forecasting is mainly to cooperate with other energy-saving technologies, such as cold and heat storage systems, chillers, and VAV air conditioning systems. These optimization processes need to determine the optimal operating conditions and setting points based on load analysis.

For load forecasting in the design stage, the main influencing factors are building physical parameters, outdoor meteorological parameters, indoor environmental parameters, and room usage. In this stage, the common load forecasting method is simulation modeling, but on the one hand, it is difficult to obtain the influencing factors in the design stage. On the other hand, there must be different degrees of assumptions and simplification in the process of building the model, resulting in significant differences between the forecasting results and the actual situation [17].

For load forecasting in the operation stage, besides those in the design stage, the main influencing factors are heat capacity, time delay, operation regulation, and actual use of the air conditioning system. The common methods of load forecasting in the operation stage are the artificial neural network (ANN), support vector machine (SVM), fuzzy regression model (FRM), and the combination method [18]. However, in operation, there will always be a permanent increase or decrease in the load caused by human factors, such as the expansion of the energy consumption area caused by the investment behavior of commercial buildings or the idle space caused by personnel adjustment in office buildings, etc. Or, in the initial stage of operation, the prediction accuracy is reduced because of the small amount of historical data.

3.3.2 Existing forecasting methodologies

Load forecasting simulation in the design stage mainly uses building energy consumption simulation software such as Designbuilder, OpenStudio, and DeST. In the operation stage, the research directions of ANN, SVM, and other commonly used load forecasting methods are different.

(1) Artificial Neural Network (ANN)

As a result of the strong learning and generalization ability of artificial neural networks, the related load forecasting methods have become a hot research topic [19]. Most of the latest research results are based on different neural network structures or training algorithms combined with classical load forecasting methods or statistical theory [20,21]. Deb [22] presents a methodology to forecast diurnal cooling load energy consumption for institutional buildings using data-driven techniques. Ahmad [23] depicted the novel data mining-based methods that consist of six models (tree bagger, Gaussian process regression, multiple linear regression, bagged tree, boosted tree and ANN) for forecasting accurate future heating and cooling load demand of water source heat pumps. Koschwitz, D [24] compared the performance of radial basis function (RBF), polynomial kernel-based e-SVM regression (e-SVM-R) and two non-linear autoregressive exogenous recurrent neural networks (NARX RNNs) with different depths in heat load forecasting.

(2) Support Vector Machine (SVM)

The support vector machine (SVM) is a supervised learning model that has many advantages in solving small samples and high-dimensional pattern recognition. It is also one of the hotspots of current research. J Zhao [25] proposes a load forecasting method for office buildings based on artificial intelligence and regression analysis, including wavelet transform, SVM, and partial least squares regression. Ma, Zhitong [26] used SVM to forecast building energy consumption in China. To improve the reliability of SVM in building energy consumption prediction, a variety of parameters including annual average outdoor dry-bulb temperature, relative humidity, GDP and other economic factors were proposed.

(3) Fuzzy Regression Model (FRM)

The fuzzy logic system imitates the reasoning thinking mode of the human brain to uncertain concepts and has the function of fitting any dynamic system. It can be used in short-term load forecasting combined with regression analysis [27]. Sivaneasan, B [28] proposed an improved algorithm for solar prediction based on the ANN model and fuzzy logic preprocessing. Through a fuzzy pretreatment toolbox, the correlation between cloud amount, temperature, wind speed, wind direction and irradiance were determined.

(4) Combination method

The combination method refers to the combination of various models weighted into a total system for prediction. This combination can be based on the same training data set and different structural models, or different training sets cooperating with the same model. This method can make full use of the advantages of various models and is a simple and effective means of improving the prediction accuracy [29]. Marmaras [30] describes a model-based approach to forecast triad periods for commercial buildings, using a multi-staged analysis that takes several different data sources into account, with each stage adding more accuracy to the model.

It can be seen that various load forecasting methods have good results in terms of data nonlinearity. However, in dealing with small-scale data, only SVM has advantages. Moreover, they are unable to provide help in dealing with the inaccuracy of simulation in the design stage. This is because in traditional machine learning, to ensure the accuracy and reliability of the training model, there are two basic assumptions: 1) the training data for learning and the new test data satisfy the same distribution independently; 2) enough training samples must be available to learn a good model.

However, in many real-world applications, this assumption may not hold. For example, as mentioned above, in HVAC load forecasting, the amount of data available is small because of load mutation. In this case, if we can transfer the available experience from a large number of previously unavailable historical data, we can greatly improve the prediction accuracy [31]. For example, when a person learns to ride a bicycle, he learns faster when he learns to ride a motorcycle. The experience of balance mastery has transferred from learning to ride a bicycle to learning to ride a motorcycle.

Transfer learning addresses the problem of how to utilize plenty of labeled data in a source domain to solve related but different problems in a target domain, even when the training and testing problems have different distributions or features [32]. It relaxes two basic assumptions in traditional machine learning.

As a new research field, transfer learning mainly focuses on the research of algorithms; its practical applications are mostly focused on image recognition, artificial intelligence, and other fields [33]. In recent years, some application research on the combination of energy and transfer learning has gradually emerged, including the application of migration learning in smart grids [34], power systems [35], and indoor environments [36]. At the same time, the study proves that transfer learning can be well combined with other load forecasting methods. Cen [37] extended the training data set through transfer learning, combined with deep learning, established the forecasting method of crude oil price fluctuation, and verified the superiority of the method through actual data. Ribeiro [38] proposed Hephaestus, a novel transfer learning method for cross-building energy forecasting based on time series multi-feature regression with seasonal and trend adjustment. It improves the energy prediction accuracy for a new building with limited data by using datasets from other similar buildings.

Load forecasting can be divided into ultra-short-term, short-term, medium-term and long-term according to different purposes [39]:

1) Ultra-short-term load forecasting refers to load forecasting within the next one hour, which is mainly used for safety monitoring and preventive control.

2) Short-term load forecasting refers to daily load forecasting and weekly load forecasting, which are used to arrange daily and weekly dispatching plans respectively.

3) Medium-term load forecasting refers to the monthly to annual load forecasting, mainly to determine the unit operation mode and equipment overhaul plan.

4) Long-term load forecasting refers to the load forecasting in the next 3-5 years or even longer. It is mainly the long-term plan of the power grid reconstruction and expansion made by the power grid planning department according to the development of the national economy and the demand for power load.

The research objective of this part is to forecast the short-term and medium-term heating and cooling load with a small amount of actual data. In this paper, ANN is used to forecast the cold and heat load of Kitakyushu Science and Research Park’s (KSRP) energy center. Short-term and medium-term load forecasting is carried out. Then a small amount of data is used to forecast the whole cooling season of the next year and a forecasting method based on simulation software and the transfer learning algorithm is proposed. The target cooling and heating load is forecasted by simulation software, which is used as auxiliary training data, combined with a small amount of actual data as training and validation data, and the next year's cooling season load is forecasted by the transfer learning algorithm TrAdaboost (SVR). Finally, through sensitivity analysis, the influence of simulation data and actual training data selection on this method is studied.

3.3.3 TrAdaBoost (SVR) model

Academic research on transfer learning focuses on the following points: (1) reducing the dependence on labeled data through semi-supervised learning, coping with the asymmetry of labeled data; (2) using transfer learning to improve the stability and generalization of the model; (3) using transfer learning to achieve continuous learning, retaining the skills learned in old tasks. Thus, integrated learning, such as the mechanism behind AdaBoost, can also be another form of transfer learning, which uses training samples many times and gives different weights to different samples. On this basis, there is a typical transfer learning algorithm, TrAdaboost.

The flow chart (Fig 3-4) and main steps of the TrAdaboost algorithm are as follows:

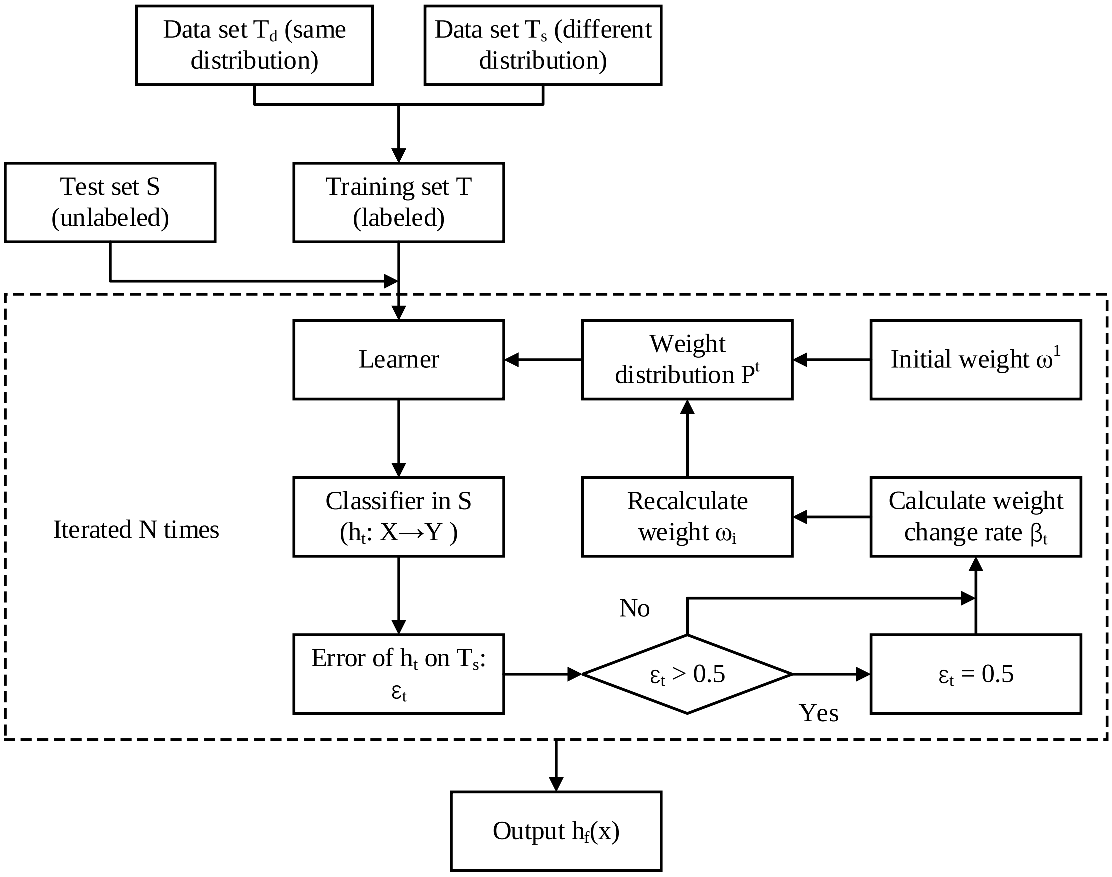

Fig 3-4 Flow chart of TrAdaboost

(1) Input the two labeled data sets Td (data with different distributions) and Ts (data with the same distribution), the unlabeled data set S, a base learning algorithm Learner, and the maximum number of iterations N. The weight is set as $w^1 = (w_1^1, \dots \dots, w_{n+m)}^1$. Normalize the weight of each data and make it a distribution, set the distribution as:

$$p^t = \frac{w^t}{\sum_{i=1}^{n+m} w_i^t}, (t = 1, \dots \dots, N) \quad (3\text{-}17)$$

(2) Taking the data of Td and Ts as training data, the process is the same as that of AdaBoost. This step is where old data works on the model. Get a classifier $h_t: X \to Y$ in S.

(3) Calculating the error of h_t on Ts. Only the data extracted from Ts is calculated. When calculating the error rate, it is necessary to normalize the weight of extracted data in Ts. Set the error rate as:

$$\epsilon_t = \sum_{i=n+1}^{n+m} \frac{\omega_i^t \cdot |h_t(x_i) - c(x_i)|}{\sum_{i=n+1}^{n+m} \omega_i^t} \quad (3\text{-}18)$$

(4) Calculate the rate of weight adjustment of Ts and Td. Each iteration, the weight adjustment rate of T_s is different, and Td is the same.

$$\beta_t = \epsilon_t/(1-\epsilon_t) \tag{3-19}$$

$$\beta = 1/(1+\sqrt{2\ln n/N}) \tag{3-20}$$

(5) Update data weight. If the data in Ts is misclassified, the weight value will be increased, which is consistent with the traditional AdaBoost algorithm. The data in Td, on the contrary, reduce the weight value if the classification error occurs, because the classification error considers that the difference between old data and new data is too large.

$$\omega_i^{t+1} = \begin{cases} \omega_i^t \beta^{|h_t(x_i)-c(x_i)|}, & 1 \le \mathrm{i} \le \mathrm{n} \\ \omega_i^t \beta^{-|h_t(x_i)-c(x_i)|}, & \mathrm{n}+1 \le \mathrm{i} \le \mathrm{n}+\mathrm{m} \end{cases} \tag{3-21}$$

(6) Output. The voting of the last half of the weak classifiers (N/2~N) is used to determine whether the output result is correct.

$$h_f(\mathrm{x}) = \begin{cases} 1, & \prod_{t=[N/2]}^{N} \beta_t^{-h_t(\mathrm{x})} \ge \prod_{t=[N/2]}^{N} \beta_t^{-\frac{1}{2}} \\ 0, & \text{otherwise} \end{cases} \tag{3-22}$$

In this paper, Td represents simulation data different from actual load distribution that needs to be predicted, and Ts represents a small amount of actual load that has the same distribution as the actual load that needs to be predicted. First, give them initial weights. Then the model is trained to learn the correlation between temperature, time and load changes brought by Td and Ts. Next, a small amount of actual data Ts used for training is used for checking. If the accuracy is not satisfactory, the weight is adjusted according to the error of equation (7) and the model training is carried out again. Equation (10) ensures that most of the Ts of the actual data participating in the training can be accurately classified after the weight adjustment. Finally, a satisfactory prediction model is obtained.

At present, the main application is TrAdaBoost (SVM) in classification [40]. In this article, TrAdaBoost (SVR) will be used. The simulation data of heat and cold load will be used as auxiliary training data to enhance the accuracy of the training model.

3.4 Case study of load forecasting application

3.4.1 Conventional forecasting methods——ANN

(1) Case introduction and Data preprocessing

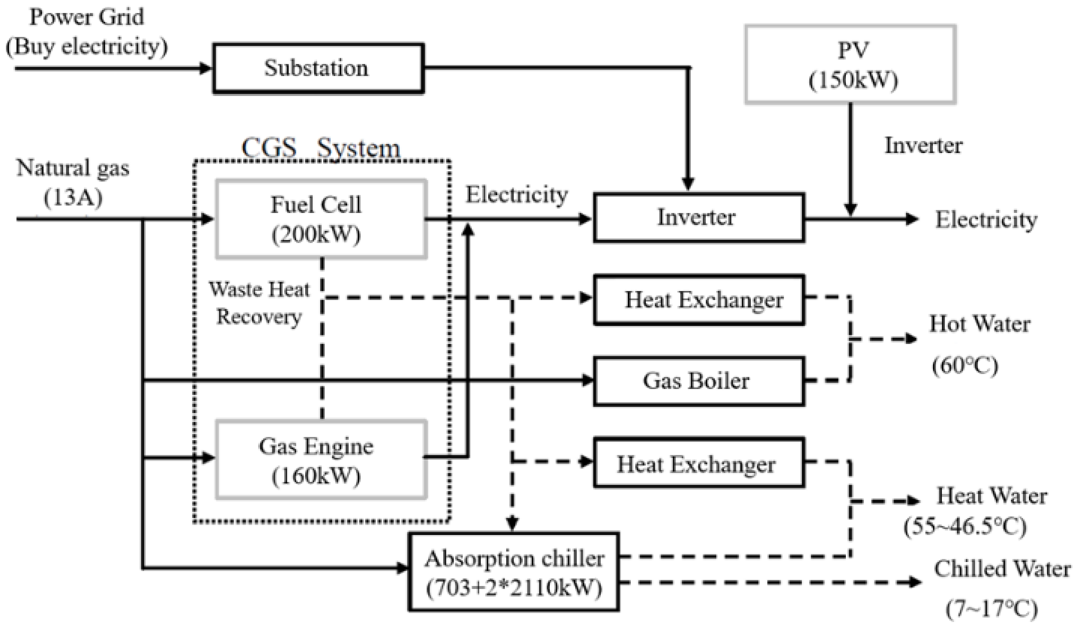

Fig 3-5 The basic schematic diagram of the distributed energy system

The target building studied in this paper is in Kitakyushu, Japan. All the cold and heat supply comes from a distributed energy system. In the distributed energy system, the electricity is met by a gas engine (the capacity is 160kW) and fuel cell (the capacity is 200 kW), solar cell and the grid utilities of Kyushu. Gas boiler and waste heat from the gas engine and fuel cell meet part of the heating load. The waste heat from the gas engine and fuel cell meet part of the cooling load through the hot water absorption chiller. The remaining heat and cold load are supplied by the gas absorption chiller. The basic schematic diagram of the system is as follows (Fig 3-5).

The energy system has a very sophisticated data acquisition system, which can record in detail the system including the main equipment: internal combustion engine, fuel cell, gas absorption chiller, and auxiliary equipment: water pumps, cooling towers and other detailed operating data, and real-time record of the temperature and humidity of the user in various regions. Relevant heat and cold load demand data of the target building are also recorded in the energy center, including the objective conditions such as temperature and humidity around the building, as well as the cold and hot water flow and temperature data supplied to the building. Through these, the hourly cooling and heating load demand of the building can be obtained. This system has been established since 2001.

The research database was established by selecting the data from 2002 to 2011 when the system equipment was relatively new and stable. The temperature and flow rate of cold and warm water supply and return collected by the gas distributed energy center are used to calculate the cooling and heat load demand of users. At the same time, in order to verify the reliability of the data, the cooling and heating output of the equipment are calculated through the natural gas consumption of the equipment and the annual average COP (refrigeration 1.00, heating 0.85). Finally, 78816 reliable data sets were obtained by comparing the demand and supply of heat and cooling enerngy. Examples of these data are shown in Table 3-2. Each set of data includes the time of the day, the day of the week, temperature, humidity, and the heat and cold load requirements. Among them, temperature and humidity mainly reflect the objective environment, time and day mainly reflect the impact of human action.

Compare the temperature with the load and distinguish the colors according to the different time of the day, as shown in Figure 3-6. A large part of the year is in the state of no-load demand. From the color distribution point of view, the higher load demand occurs in the 10-14 points of the day. At the same time, there are still load demands in the early mornings of winter, but less in summer.

Table 3-2 Examples of database (2010.12.31)

Time	Week	Temperature (°C)	Humidity (%)	Load (kWh)
1	1	26.2	98	0
2	1	25.9	98	0
3	1	25.7	99	0
4	1	25.5	100	0
5	1	25.3	100	0
6	1	25.5	100	0
7	1	27.3	95	-158.382
8	1	29.1	88	-312.83
9	1	31.6	77	-468.442
10	1	32.7	69	-455.081

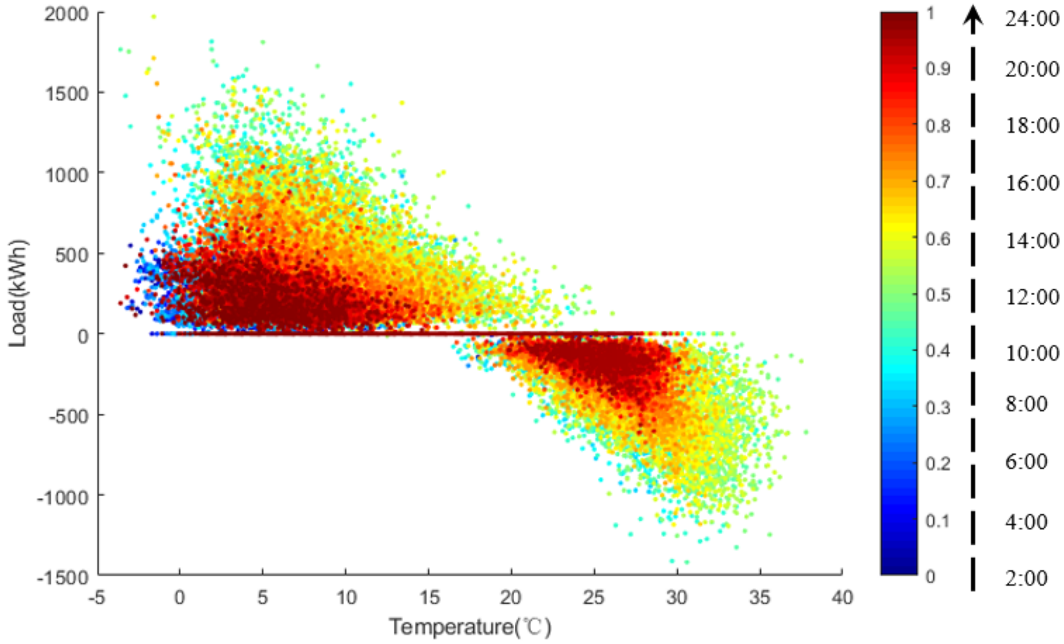

Fig 3-6 Diagram of temperature and load distinguished by time

(2) Ordinary short and medium-term load forecasting with ANN

Firstly, ANN will be used to forecast the cooling and heating load. Four sets of data from 2002-2010, 2006-2010, 2008-2010 and 2009-2010 are used as training, validation, and test data. The ratio between them is 3:1:1. Then the summer data are selected from each group of data for forecasting. The results are shown in Table 3-3. Among them, the fitting chart of test and forecast data in 2009-2010 is shown in Fig. 3-7. Besides the fitting degree, the root mean square error (RMSE) and the mean absolute error (MAE) are also calculated. With the increase in the amount of data, the fitting degree increases gradually. However, from 2002-2010, this group of fitting, as a result of excessive data, led to the occurrence of over-fitting.

Table 3-3 Results of load forecasting (yearly and seasonally)

Data	Fitting Degree	Data	Fitting Degree
2009-2010	88.42	Summer in 2009-2010	84.68
2008-2010	89.39	Summer in 2008-2010	85.85
2006-2010	90.43	Summer in 2006-2010	86.61
2002-2010	87.83	Summer in 2002-2010	84.93

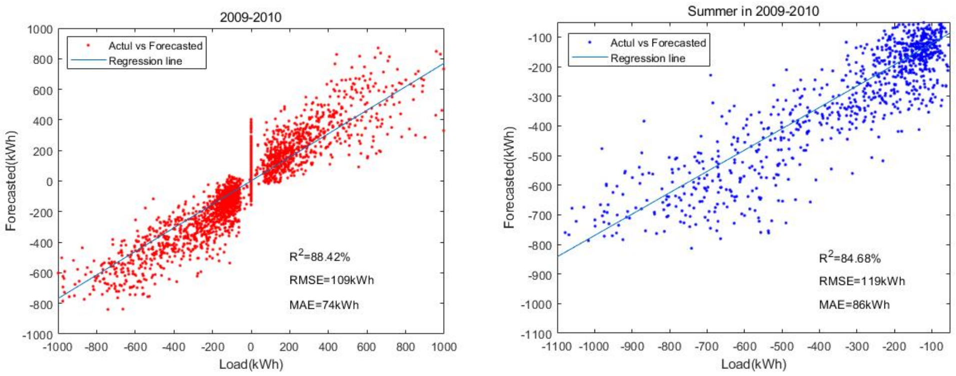

Fig 3-7 Fitting chart of test and forecast data from 2009-2010

At the same time, the corresponding seasons of 2010 are forecasted by using the four seasons of spring, summer, autumn and winter in 2009. The data of 2009 were used as training data, and the data of 2010 were used as validation and test data. The results are shown in Table 3-4. The results of seasonal forecasting are basically the same as those of annual and seasonally forecasting, but there are still differences between different seasons.

From the previous medium-term forecast, the regularity of the results of different years' data is obvious, and the fitness gap is basically less than 2%. Therefore, the month and week data of July, and July 15- 21 in 2009 are selected as training data, and the data of 2010 are taken as target and test data. The results are shown in Table 3-5 below.

The forecast results of ANN are at a high level in both medium-term and short-term load forecasting. At present, the focus of the research is to carry out in-depth research on such a high forecasting accuracy. However, in practical applications, there is usually only a small amount of data, but it is necessary to forecast the load changes for a long time afterwards.

Table 3-4 Results of load forecasting (different season)

Training Data	Test & validation Data	Fitting Degree of test data
Spring in 2009	Spring in 2010	83.71
Summer in 2009	Summer in 2010	85.72
Autumn in 2009	Autumn in 2010	84.32
Winter in 2009	Winter in 2010	84.56

Table 3-5 Results of load forecasting (monthly and weekly)

Training Data	Test Data & validation Data	Fitting Degree of test data
July, 2009	July, 2010	89.23
July 15- 21, 2009	July 15- 21, 2010	92.72

(3) Load forecasting using a small amount of data with ANN

Table 3-6 Results of load forecasting (using a small amount of data)

Training & validation Data	Test Data	Fitting Degree of test data
July,2009	May-Oct, 2010	78.93
July15-21,2009	May-Oct, 2010	65.33

The following will use the data of July and July15-21 of 2009 to forecast the whole cooling season of 2010 (choose May-October). The forecast results are shown in Table 3-6 below. The forecasting accuracy has decreased significantly, especially when using weekly data for forecasting. The results can hardly be used.The main reason for the poor forecasting results is that the amount of data is small, so the simulation data is used instead of more actual data when it is impossible to obtain more actual data.

3.4.2 Application of load forecasting based on transfer learning

(1) Building of simulation model

To simulate the cooling and heating load demand of the building, the simulation software is first selected. DesignBuilder is a commonly used software for building load simulation. It is an integrated user graphical interface simulation software developed for EnergyPlus. By establishing the framework of the building, and then setting up the behavior of the residents, building materials, window-wall ratio, fence structure and HVAC system, the energy demand of the building, such as cold, hot, electricity, water and so on can be accurately simulated. To build the overall framework of the building more accurately, the Revit software which is compatible with DesignBuilder and AutoCAD is selected to build the 3D model, and then imported into DesignBuilder for parameter setting and simulation.

The total area of the target building is about 20,000 m^2, and the volume ratio is 1.5. The main body of the building is a prefabricated and assembled concrete frame structure, and the foundation and some floor slabs are poured on site. The climate zoning of the project is hot summer and cold winter. According to the school building drawings, build a 3D model and import it into the DesignBuilder as shown in Fig 3-8.

The building is divided into four floors, first is the student center, conference room and classroom. The second to fourth floors are the teacher's office and the student's research lab. By dividing energy use areas with different characteristics through rooms, six different functional areas are finally obtained, and their areas and functions are shown in Table 3-7. These energy demand areas will be differentiated according to different personnel density, working hours and other settings.

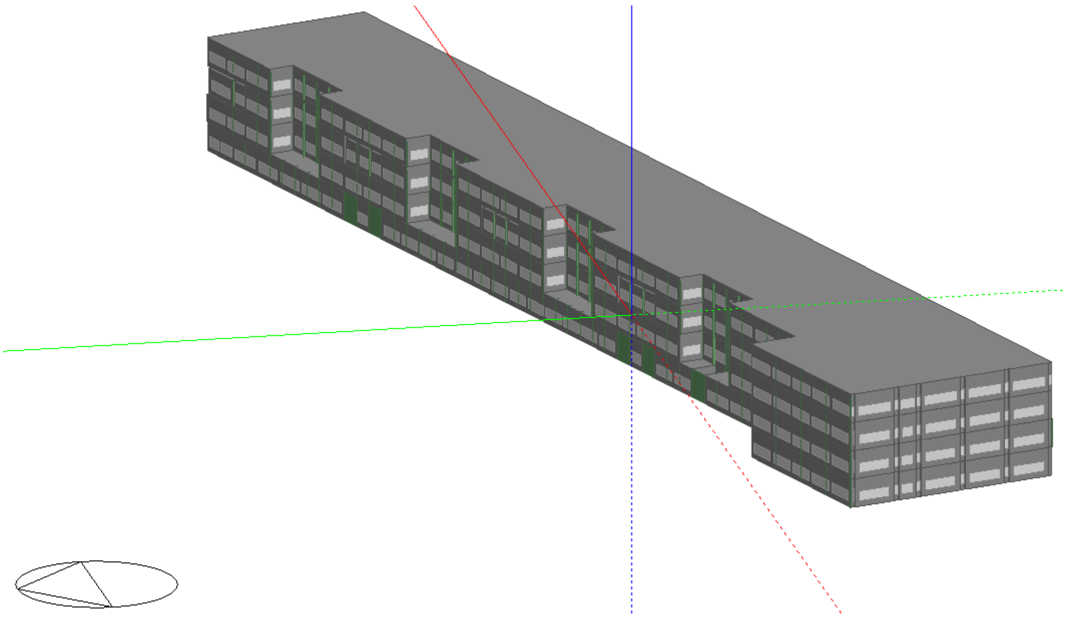

Fig 3-8 Simulation drawing of the building in DesignBuilder

Table 3-7 Regional Function Division

Function	Area (m^2)	Function	Area (m^2)
Students Center	276	Research Lab	4304
Conference Room	1149	Office	2892
Classroom	964	Corridors and others	6483

(2) Parameter setting

The overall layout of the building is mainly to set building materials, window-wall ratio, window height, fence structure and HVAC system, as shown in Table 3-8. For different functional areas, according to different uses, it is necessary to set the personnel density, working hours, heat dissipation of equipment, start-up of air conditioning and setting temperature, as shown in Table 3-9.

Table 3-8 Integral parameter setting

Content	Settings	Content	Settings
Building materials	Conventional reinforced concrete	Shape coefficient	0.157
Roof heat transfer coefficient	0.37W/(m^2*K)	External wall heat transfer coefficient	0.75 W/(m^2*K)
Heat Transfer Coefficient of Extended Components Contacting with Air	0.58 W/(m^2*K)	External sunshade	1.0m
Window-wall ratio	45%	Heating system seasonal COP	0.85
Window height	0.8m	Cooling system seasonal COP	1.00

Table 3-9 Function area parameter setting

Function	Persons per unit area (Person/m2)	Daily working time	Start-up temperature (Heat/Cold,℃)	Setting temperature (Heat/Cold,℃)
Students Center	0.2	7:00-19:00	10/30	22/26
Classroom	0.7	7:00-19:00	10/30	22/26
Conference Room	0.7	7:00-23:00	10/30	22/26
Research Lab	0.2	7:00-23:00	10/30	22/26
Office	0.1	7:00-23:00	10/30	22/26
Corridors and others	0.01	7:00-23:00	10/30	22/28

At the same time, it is necessary to set the corresponding percentage of load demand in different working hours. Among them, although the personnel density, equipment heat dissipation and other settings are different, the first floor of the classroom, student activity center, conference rooms and corridors in working hours corresponding to the load demand percentage is roughly the same. Similarly, the load requirements of student research rooms, teachers' offices and corridors on the second to fourth floors are set the same. For the second to fourth floor areas, there is still a demand for load on rest days and holidays because of research needs. Its cooling season is mainly in 5.15-10.15 per year, which is divided into two different load rate distributions: working day and rest day. The heating season is 10.16-5.14. Because the first floor is a teaching area, there will be no load demand in March, August, September and all rest days according to the holidays. The date of load demand for each floor is shown in Table 3-10, and all daily load rate changes are shown in Table 3-11.

Table 3-10 Date of load demand

Area	Cooling season	Heating season
Frist floor	5.15-7.31, 10.1-10.15	3.31-5.14, 10.16-2.28
Second to fourth floor	5.15-10.15	10.16-5.14

Table 3-11 Daily load rate changes

Workday load rate changes						
Time	9	10	12	14	17	20
Load rate	0.5	0.75	1	0.75	1	0.5
Rest day load rate changes						
Time	10	11	12	14	17	19
Load rate	0.5	0.75	1	0.75	1	0.5

3.4.3 Simulation results and application of transfer learning

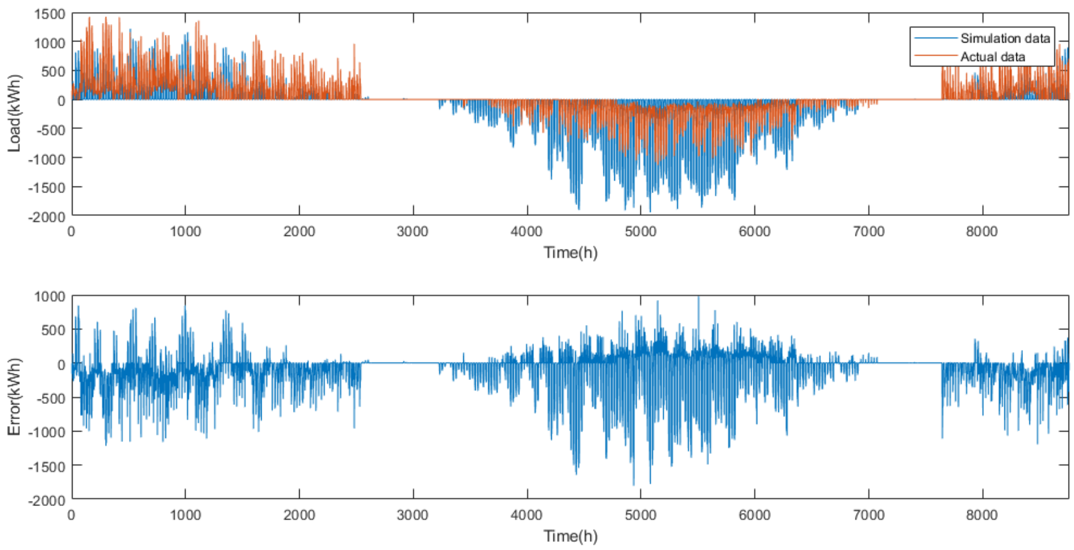

Fig 3-9 Error between the simulation data and the actual data

After setting the parameters, the simulation of annual energy consumption per hour is conducted. The error between the simulation data and the actual data in 2010 is shown in Figure 3-9 below. Although the trend of change is similar, there is a huge gap between the values.

The main reason for the errors in Fig 4-2 is the uncertainty of the use of air conditioning. The 2-4 floors of the building are the working areas of graduate students, doctors and professors. Because of the investigation and experiment, the regularity of room use is poor. Therefore, even if the simulation process is carried out in the case of holidays and other detailed settings used in the rooms, it can't be similar to the actual load. This is also the reason why transfer learning and simulation software need to be combined.

The simulation data is used as auxiliary training data, July and July 15-21, 2009 as training and target data, and the cooling season of 2010 as test data. The Gaussian kernel is chosen as the kernel function. After testing, the appropriate width is 30-40. The results through regression fitting with TrAdaboost (SVR) algorithm are shown in Table 3-12 below.

Table 3-12 Results of load forecasting (TrAdaboost (SVR))

Auxiliary training data	Training & validation data	Test data	Fitting degree of test data
Year	July, 2009	May-Oct, 2010	78.15
Summer	July, 2009	May-Oct, 2010	76.22
July	July, 2009	May-Oct, 2010	77.49
July 15-21	July, 2009	May-Oct, 2010	78.93
year	July 15-21, 2009	May-Oct, 2010	78.70
Summer	July 15-21, 2009	May-Oct, 2010	78.45
July	July 15-21, 2009	May-Oct, 2010	74.30
July 15-21	July 15-21, 2009	May-Oct, 2010	71.22

In the monthly forecast, the forecast results are similar to those of ANN. However, in the week's forecast, the forecast results improved significantly. At the same time, different simulation data selection has a greater impact on the forecasting results. Therefore, in the next chapter, we will discuss the impact of different simulation data, actual training data, and the setting of simulation software itself on the forecasting results.

3.4.4 Sensitivity analysis

(1) Auxiliary training data

Choose the data with the worst results (monthly data) in the previous forecast as the sensitive item and use the data from May to October as the auxiliary training data for load forecasting. The results are shown in Table 3-13 below. The change of auxiliary data has an influence on the fitting degree, and the change of fitting degree is about 4%.

Table 3-13 Results of load forecasting (change the auxiliary training data)

Auxiliary training data	Training & validation data	Test data	Fitting degree of test data
May	July, 2009	May-Oct, 2010	79.00
June	July, 2009	May-Oct, 2010	79.02
July	July, 2009	May-Oct, 2010	77.63
August	July, 2009	May-Oct, 2010	76.17
September	July, 2009	May-Oct, 2010	79.17
October	July, 2009	May-Oct, 2010	78.60
May	July 15-21, 2009	May-Oct, 2010	78.86
June	July 15-21, 2009	May-Oct, 2010	75.79
July	July 15-21, 2009	May-Oct, 2010	74.30
August	July 15-21, 2009	May-Oct, 2010	77.49
September	July 15-21, 2009	May-Oct, 2010	76.65
October	July 15-21, 2009	May-Oct, 2010	78.20

(2) Training & validation data

Similarly, different months and weeks of the cooling season are selected for load forecasting. The results are shown in Table 3-14 below. It can be seen that the change of auxiliary data has an influence on the fitting degree, and the change of fitting degree is about 3%.

From the two tables above, the choice of data has a certain impact on load forecasting, but the results change only a little, because the distribution of the overall data and the test data have a high level of similarity. At the same time, the regularity of the impact of data changes on the forecasting results is not obvious. The main reason is that the distribution of data and test data does not change regularly when the selection of months and weeks changes. Next, we will analyze the influence of distribution changes on the forecasting results by changing the parameters of simulation data.

Table 3-14 Results of load forecasting (change the training & validation data)

Auxiliary training data	Training & validation data	Test data	Fitting degree of test data
July	May, 2009	May-Oct, 2010	76.98
July	June, 2009	May-Oct, 2010	74.66
July	July, 2009	May-Oct, 2010	77.63
July	August, 2009	May-Oct, 2010	77.97
July	September, 2009	May-Oct, 2010	77.27
July	October, 2009	May-Oct, 2010	78.19
July	May 15-21, 2009	May-Oct, 2010	77.54
July	Jun 15-21, 2009	May-Oct, 2010	76.73
July	Jul 15-21, 2009	May-Oct, 2010	74.30
July	Aug 15-21, 2009	May-Oct, 2010	77.04
July	Sep 15-21, 2009	May-Oct, 2010	76.75
July	Oct 15-21, 2009	May-Oct, 2010	78.12

(3) Simulation accuracy and parameter selection

In fact, the sensitivity analysis of simulation accuracy and parameter setting is the study of the universality of this algorithm. Under most practical conditions, the setting of simulation parameters cannot be specific. Therefore, the refrigeration time during the 7.20-9.20 period is extended to 12 p.m., the window-wall ratio is set to 30 as the default value, and start-up temperature of air conditioning in summer is set to 28 C, which is more common. Load forecasting is carried out after re-simulation. The extending of refrigeration time can make the simulation data closer to the actual data, while the other two adjustments have the opposite effect. The results of load forecasting are shown in Table 3-15 below. There are some differences between the data obtained by the three adjustment measures and the original data, and the errors are shown in Fig. 3-10 below.

Table 3-15 Results of load forecasting (three adjustment measures)

Adjustment	Training & validation data	Test data	Fitting degree of test data
Original	Jul 15-21, 2009	May-Oct, 2010	74.30
Adjust the window-wall ratio	Jul 15-21, 2009	May-Oct, 2010	74.28
Extend refrigeration time	Jul 15-21, 2009	May-Oct, 2010	75.59
Adjust Start-up temperature	Jul 15-21, 2009	May-Oct, 2010	77.11

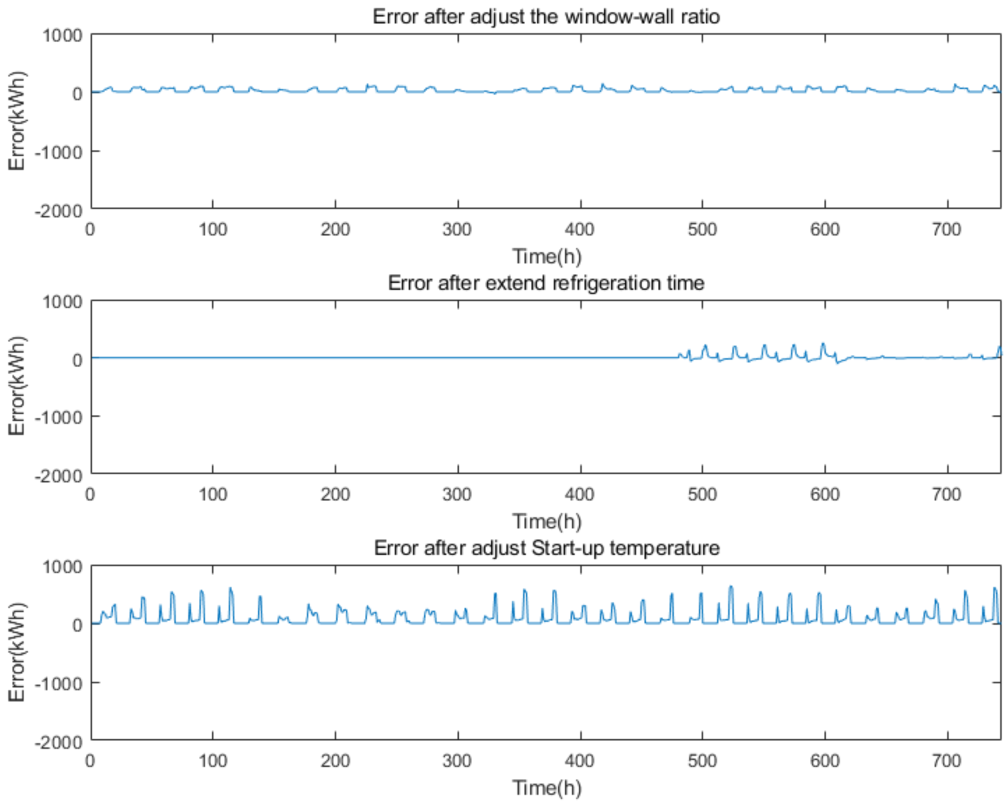

Fig 3-10 Error between three adjustment and original data

Extending the refrigeration time and adjusting the opening temperature of air conditioning will make the distribution of simulation data much different from the original data distribution. After adjusting the window-wall ratio, although there are errors in the original data, the change of data distribution is small. The performance of this result in load forecasting is that the simulation data after adjusting the window-to-wall ratio are very close to the forecasting fit of the original data. The forecasting results of the other two adjustment measures differ greatly from those of the original data, and the greater the difference in distribution, the greater the difference in forecasting results.

3.4.5 Summary

In this part, firstly, based on the 10-year actual operation data of the energy center of KSRP, the short-term and medium-term cold and heat load forecasting are carried out by using ANN. The results show the forecasting results are at a high level. Whether annual or seasonal prediction, the accuracy is more than 85%, and with the increase of data, the accuracy is increasing. Then it is pointed out that in practice, enough training data cannot be achieved smoothly in many cases. Therefore, the short-term month and week data are used as training and validation data to forecast the whole cooling season, and the forecasting accuracy has decreases significantly. When the training data is reduced to one month, the accuracy decreases by 6%. When it is reduced to one week, the accuracy decreases by nearly 20%, and the results can hardly be used.

Therefore, this paper presents a method of combining load simulation with transfer learning, using REVIT and Design Builder simulation software to forecast the cooling and heat load of buildings throughout the year, and combining the forecasting results as auxiliary training data with a small amount of actual data. The load of the 2010 cooling season was forecasted using the TrAdaboost(SVR) algorithm. When the training data was one month, the accuracy was the same as the ANN. When it was reduced to one week, the accuracy increased by more than 10%. The improvement effect of the new method is obvious. The results show that this method can effectively improve the forecasting accuracy.

Finally, the sensitivity analysis of data selection and simulation parameters setting was carried out. Different months were selected as auxiliary data, and different months and weeks were selected as training and validation data. The forecasting accuracy fluctuated between 74% and 79%, with little effect, but it was obvious that the distribution of data had influence on the forecasted results. Then, in the process of adjusting the simulation parameters, three adjusting measures were adopted to get different simulation data distribution with the original simulation data. The results show that the greater the difference in distribution, the greater the impact on the forecasting results.

In summary, in view of the invalidation of historical data as a result of changes in external environment and energy use habits and new buildings, the combined method of simulation and transfer learning proposed in this paper can effectively improve the forecasting accuracy of heat and cold load and has high practical application value for the operation and design optimization of energy systems. However, the distribution of training data will have a certain impact on the results, and its in-depth impact mechanism needs further analysis. At the same time, the forecasting results with nearly 80% accuracy can be used in some energy system optimization, but there is still much room for improvement.

The goal of this paper is to solve the problem of HVAC load forecasting with only a small amount of available data. In reality, this problem is caused by the permanent increase of the load caused by the new occupants of commercial buildings, or the inability to obtain a large number of valid data at the initial stage of construction. However, load forecasting is still needed to ensure the setting of the HVAC control system. The combination of simulation software and the transfer learning method proposed in this paper have been proven to be 10% more accurate than the conventional load forecasting method in this scenario, which has high practical value and popularization significance.

Reference

[1] Zhang, Xiaocun, and Fenglai Wang. "Analysis of embodied carbon in the building life cycle considering the temporal perspectives of emissions: a case study in China." Energy and Buildings 155 (2017): 404-413.

[2] Ozawa, Akito, et al. "Life cycle CO2 emissions from power generation using hydrogen energy carriers." International Journal of Hydrogen Energy (2019).

[3] Lin, Boqiang, and Zhijie Jia. "Impacts of carbon price level in carbon emission trading market." Applied Energy 239 (2019): 157-170.

[4] Chevallier, Julien. "Detecting instability in the volatility of carbon prices." Energy Economics 33.1 (2011): 99-110.

[5] Wang, Lan, Eric WM Lee, and Richard KK Yuen. "Novel dynamic forecasting model for building cooling loads combining an artificial neural network and an ensemble approach." Applied energy 228 (2018): 1740-1753.

[6] Singh, Harsh Vijay, et al. "The energy transitions index: An analytic framework for understanding the evolving global energy system." Energy Strategy Reviews 26 (2019): 100382.

[7] Pérez-Lombard, Luis, José Ortiz, and Christine Pout. "A review on buildings energy consumption information." Energy and buildings 40.3 (2008): 394-398.

[8] Li, Xiwang, and Jin Wen. "Review of building energy modeling for control and operation." Renewable and Sustainable Energy Reviews 37 (2014): 517-537.

[9] Li, Yanxue, Weijun Gao, and Yingjun Ruan. "Performance investigation of grid-connected residential PV-battery system focusing on enhancing self-consumption and peak shaving in Kyushu, Japan." Renewable Energy 127 (2018): 514-523.

[10] Kim, Kihyung, et al. "A hybrid multi-level optimization approach for the dynamic synthesis/design and operation/control under uncertainty of a fuel cell system." Energy 36.6 (2011): 3933-3943.

[11] Ren, Hongbo, et al. "Integrated design and evaluation of biomass energy system taking into consideration demand side characteristics." Energy 35.5 (2010): 2210-2222.

[12] Wu, Qiong, et al. "Multi-objective optimization of a distributed energy network integrated with heating interchange." Energy 109 (2016): 353-364.

[13] Wu, Qiong, et al. "Benefit allocation for distributed energy network participants applying game

theory based solutions." Energy 119 (2017): 384-391.

[14] Li, Yanxue, et al. "The performance investigation of increasing share of photovoltaic generation in the public grid with pump hydro storage dispatch system, a case study in Japan." Energy 164 (2018): 811-821.

[15] Wu, Qiong, et al. "Design and operation optimization of organic Rankine cycle coupled trigeneration systems." Energy 142 (2018): 666-677.

[16] Cao, Xiaodong, Xilei Dai, and Junjie Liu. "Building energy-consumption status worldwide and the state-of-the-art technologies for zero-energy buildings during the past decade." Energy and buildings 128 (2016): 198-213.

[17] Ma, Weiwu, et al. "Modeling of district load forecasting for distributed energy system." Applied Energy 204 (2017): 181-205.

[18] Nihuan, L. I. A. O., et al. "Review of the short-term load forecasting methods of electric power system." Power system protection and control 39.1 (2011): 147-152.

[19] Ahmad, A. S., et al. "A review on applications of ANN and SVM for building electrical energy consumption forecasting." Renewable and Sustainable Energy Reviews 33.1 (2014): 102-109.

[20] Doucoure, Boubacar, Kodjo Agbossou, and Alben Cardenas. "Time series prediction using artificial wavelet neural network and multi-resolution analysis: Application to wind speed data." Renewable Energy 92 (2016): 202-211.

[21] Rahman, Aowabin, Vivek Srikumar, and Amanda D. Smith. "Predicting electricity consumption for commercial and residential buildings using deep recurrent neural networks." Applied Energy 212 (2018): 372-385.

[22] Deb, Chirag, et al. "Forecasting diurnal cooling energy load for institutional buildings using Artificial Neural Networks." Energy and Buildings 121 (2016): 284-297.

[23] Ahmad, Tanveer, and Huanxin Chen. "Short and medium-term forecasting of cooling and heating load demand in building environment with data-mining based approaches." Energy and Buildings 166 (2018): 460-476.

[24] Koschwitz, D., J. Frisch, and C. van Treeck. "Data-driven heating and cooling load predictions for non-residential buildings based on support vector machine regression and NARX Recurrent Neural Network: A comparative study on district scale." Energy 165 (2018): 134-142.

[25] Zhao, Jing, and Xiaojuan Liu. "A hybrid method of dynamic cooling and heating load

forecasting for office buildings based on artificial intelligence and regression analysis." Energy and Buildings 174 (2018): 293-308.

[26] Ma, Zhitong, et al. "Applying support vector machines to predict building energy consumption in China." Energy Procedia 152 (2018): 780-786.

[27] Pombeiro, Henrique, et al. "Comparative assessment of low-complexity models to predict electricity consumption in an institutional building: Linear regression vs. fuzzy modeling vs. neural networks." Energy and Buildings 146 (2017): 141-151.

[28] Sivaneasan, B., C. Y. Yu, and K. P. Goh. "Solar Forecasting using ANN with Fuzzy Logic Pre-processing." Energy Procedia 143 (2017): 727-732.

[29] Hibon, Michele, and Theodoros Evgeniou. "To combine or not to combine: selecting among forecasts and their combinations." International Journal of Forecasting 21.1 (2005): 15-24.

[30] Marmaras, Charalampos, et al. "Predicting the energy demand of buildings during triad peaks in GB." Energy and Buildings 141 (2017): 262-273.

[31] Pan, Sinno Jialin, and Qiang Yang. "A survey on transfer learning." IEEE Transactions on knowledge and data engineering 22.10 (2010): 1345-1359.

[32] Pan, Sinno Jialin, James T. Kwok, and Qiang Yang. "Transfer Learning via Dimensionality Reduction." AAAI. Vol. 8. 2008.

[33] Zhang, Shiwei, et al. "Irony detection via sentiment-based transfer learning." Information Processing & Management 56.5 (2019): 1633-1644.

[34] Zhang, Xiaoshun, et al. "Deep transfer Q-learning with virtual leader-follower for supply-demand Stackelberg game of smart grid." Energy 133 (2017): 348-365.

[35] Zhang, Xiaoshun, et al. "Equilibrium-inspired multiagent optimizer with extreme transfer learning for decentralized optimal carbon-energy combined-flow of large-scale power systems." Applied energy 189 (2017): 157-176.

[36] Grubinger, Thomas, Georgios C. Chasparis, and Thomas Natschläger. "Generalized online transfer learning for climate control in residential buildings." Energy and Buildings 139 (2017): 63-71.

[37] Cen, Zhongpei, and Jun Wang. "Crude oil price prediction model with long short term memory deep learning based on prior knowledge data transfer." Energy 169 (2019): 160-171.

[38] Ribeiro, Mauro, et al. "Transfer learning with seasonal and trend adjustment for cross-building

energy forecasting." Energy and Buildings 165 (2018): 352-363.

[39] Guo, Zhifeng, et al. "A deep learning model for short-term power load and probability density forecasting." Energy 160 (2018): 1186-1200.

[40] W. Dai, Q. Yang, G. Xue, and Y. Yu, “Boosting for Transfer Learning,” Proc. 24th Int’l Conf. Machine Learning, pp. 193-200, June 2007.

Chapter 4

UTILIZATION POTENTIAL AND ECONOMIC ANALYSIS OF HYDROGEN ENERGY EQUIPMENT

CHAPTER FOUR: UTILIZATION POTENTIAL AND ECONOMIC ANALYSIS OF HYDROGEN ENERGY EQUIPMENT

4.1 Content

Fuel cell are known as the new generation of power generation technology following the water, fire, nuclear power, solar, natural gas because of its high energy conversion efficiency, environmentally friendly and other advantages. Among them, the proton exchange membrane fuel cell (PEMFC) is currently most mature in commerce and considered to be the main development direction of the automotive power, portable power, spare power supply for important building and other fields. PEMFC reactor needs to maintain a temperature of about 80 to 60 degrees Celsius at runtime, so it is necessary to cool the fuel cell, and using the residual heat while cooling can greatly enhance the efficiency of the overall system.

In this part, a 5kW methanol reforming PEMFC will be simulated based on a simulation software called TRNSYS to analyze the situation of the residual heat. Then, through the simulation models of the two waste heat recovery methods of refrigeration and hot water production, the comprehensive energy utilization potential of the fuel cell was studied. After introducing carbon tax restrictions, the economic comparison of fuel cells and fuel cell vehicles with conventional energy systems was explored.

4.2 Introduction to the experimental platform

Proton exchange membrane fuel cell (PEMFC) is the most mature fuel cell which has a wide range of applications in the field of vehicle power, mobile power, distributed generation and home power supply [1]. Methanol reforming hydrogen production has received extensive attention and research because of its good economic performance, low energy consumption, easy storage and transportation, low temperature, convenient and safe feeding, and so on [2]. In addition to the analysis of a large number of operational data, the simulation method has been widely used in the study of fuel cell.

As shown in Fig 4-1 is the methanol reforming hydrogen PEMFC system experimental platform which store the power output by external storage battery. The experimental platform can monitor the temperature, pressure, voltage, current and other parameters of the methanol fuel cell, and can also output the numerical and analog control signals.

Fig 4-1 Methanol reforming hydrogen production PEMFC experimental platform

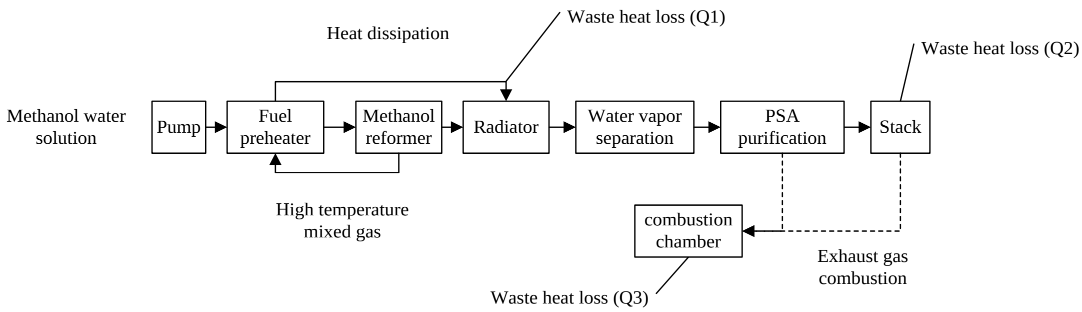

Fig. 4-2 Flow chart of PEMFC system

As shown in Fig 4-2 is the flow chart of PEMFC system. The system mainly has three heat residual, first of all is the residual heat Q1 by reformed gas in radiator, then the residual heat Q2 produced in the course of operation by the reactor, finally is the residual heat Q3 generated by the combustion chamber.

Among them, the common part of Q1 and Q3 is the heat exchange of the fuel preheater, so resetting Q1 is only a loss of the radiator, and part of the flue gas needs to increase the heat of the reformer, so reset Q3 to flue gas The residual heat minus the heat absorbed by the reformer, the total available residual heat Q_{R} of the system is:

$$Q_{\mathrm{R}} = Q_1 + Q_2 + Q_3 - Q_{\mathrm{reformer}} \tag{4-1}$$

4.3 Theoretical calculation of fuel cell residual heat

By setting the output power of the system, it is maintained at 1 ~ 5kW, and it runs steadily every 0.5kW for a period of time, and records the methanol fuel flow, voltage, stack current, temperature difference between the inlet and outlet of the radiator under the corresponding working conditions, etc. Relevant data, because the measurement points of the experimental platform itself cannot fully calculate the residual heat of each part, so in addition to processing the data, a part of the theoretical calculation is also required.

4.3.1 Radiator residual heat Q1

Table 4-1 Experimentally measured temperature at the inlet and outlet of the reformer radiator

Setting power W	Actual power W	Methanol aqueous solution flow kg/h	Radiator inlet temperature ℃	Radiator outlet temperature ℃
1000	1280	1.8	80	27
1500	1700	2.4	85	22
2000	2130	2.4	87	21
2500	2560	2.7	95	26
3000	3100	3.1	104	26
3500	3680	3.5	112	28
4000	3780	3.6	115	28
4500	4310	4.2	116	31
5000	5350	5.3	126	30

As shown in Table 4-1, the temperature of the radiator inlet and outlet is measured by the thermocouple temperature sensor when the experimental platform is operated at different powers.

The flow rate and temperature difference of the high-temperature mixed gas are measured, but since the specific heat of the high-temperature mixed gas cannot be determined, it is necessary to derive the residual heat of the Q1 part from the principle of high-temperature mixed gas generation. First, Q1 is equal to the difference in internal energy flowing into and out of the radiator:

$$Q_1 = E_{out} - E_{in} \tag{4-2}$$

The internal energy of the high-temperature mixed gas can be expressed as:

$$\mathrm{E} = \mathrm{m_{CO2}} \times \mathrm{e_{CO2}} + \mathrm{m_{H2}} \times \mathrm{e_{H2}} + \mathrm{m_{H2O}} \times \mathrm{e_{H2O}} \tag{4-3}$$

In the methanol steam reforming reaction, the molar ratio of methanol, water, hydrogen, and carbon dioxide is 1: 1: 3: 1, and 49.4 kJ of heat needs to be absorbed. After the reaction, the ratio of hydrogen, carbon dioxide and water in the high-temperature mixed gas is 3:1:0.5.

Main reaction: $CH_3OH + H_2O \rightarrow 3H_2 + CO_2$ $\triangle H_{298}$=49.4 kJ/mol (4-4)

Side reaction: $CH_3OH \rightarrow CO + 2H_2$ $\triangle H_{298}$=90.7kJ/mol (4-5)

$2CH_3OH \rightarrow CH_3OCH_3 + H_2O$ $\triangle H_{298}$=-24.9kJ/mol (4-6)

$CO + 3H_2 \rightarrow CH_4 + H_2O$ $\triangle H_{298}$=-206.3kJ/mol (4-7)

The internal energy of hydrogen, carbon dioxide, and water can be obtained through inquiries. The final Q1 calculation results are shown in Table 4-2 below.

Table 4-2 Residual heat Q1 at the radiator under different stack output power

Actual power W	Radiator residual heat $Q1/kJ\cdot h^{-1}$	Actual power W	Radiator residual heat $Q1/kJ\cdot h^{-1}$
1282	213	3684	653
1698	329	3781	697
2126	341	4315	797
2556	409	5350	1126
3100	526		

4.3.2 Fuel cell stack residual heat Q2

Due to the lack of coolant flow rate and inlet and outlet temperatures, Q2 carried by the stack coolant needs to be calculated according to the difference between the theoretical voltage and the actual voltage of the stack, as shown in equation (4-8).

$$Q_2 = (V_{ocv} - V_{cell}) \times I \times n_{cell} \times 3.6 \quad (4\text{-}8)$$

Among them, V_{cell} and I are the output voltage and output current of each battery, and n_{cell} is the number of batteries. In this article, V_{ocv} takes 1.23V, n_{cell} = 80. As shown in Table 4-3, the output current, output voltage and other parameters of the stack under different actual powers.

Import the current, voltage and actual voltage of the single cell in the above table into the formula (4-8), then the residual heat of the Q2 part is shown in Table 4-4.

Table 4-3 The stack condition under different output power measured by experiment

Actual power W	Average output current of stack A	Average output voltage of the stack V	Monolithic battery voltage V
1282	20	64	0.80
1698	27	63	0.79
2126	35	60	0.76
2556	43	60	0.75
3100	52	59	0.74
3684	62	60	0.75
3781	63	60	0.75
4315	75	57	0.72
5350	94	57	0.71

Table 4-4 Residual heat Q2 of the stack under different output powers

Actual power W	Stack residual heat $Q_2/(kJ\cdot h^{-1})$	Actual power W	Stack residual heat $Q_2/(kJ\cdot h^{-1})$
1282	2484	3684	8629
1698	3437	3781	8837
2126	4808	4315	11055
2556	5908	5350	13963
3100	7336		

4.3.3 Residual gas combustion residual heat Q3

The residual heat of part Q3 is the heat of combustion of the remaining part of hydrogen minus the heat absorbed by the reformer. The combustion of hydrogen takes its status calorific value 241.83 kJ / mol. The current data that needs to be obtained is the remaining amount of hydrogen, that is, the amount of hydrogen reformed by methanol minus the amount of hydrogen consumed by power generation, then:

$$n_{H_2} = \frac{I}{2F} \quad (4\text{-}9)$$

Among them, n_{H_2} is the supply of hydrogen per unit time, the unit is mol / h, I is the output current of the stack, and F is the Faraday constant, which is characterized by the electrical energy of 1 mol of electrons, taking F = 96485.3365 C/mol.

Therefore, the residual heat Q3 of the fuel cell stack at the actual average output power can be calculated separately, as shown in Table 4-5. So far, the waste heat of the three parts Q1, Q2 and Q3 has been calculated, and the three are summarized in a table 4-6.

Table 4-5 Residual gas combustion residual heat Q3 at different output powers

Actual power W	Methanol flow rate (mol·h)	Methanol hydrogen production ($mol·h^{-1}$)	Stack hydrogen consumption ($mol·h^{-1}$)	Residual gas combustion residual heat Q_3/kJ
1282	31	92	30	13490
1698	40	121	40	17574
2126	40	119	53	14202
2556	45	135	64	15138
3100	52	156	78	16378
3684	59	178	92	17780
3781	61	184	95	18640
4315	71	214	112	21190
5350	90	269	140	26819

Table 4-6 Three kinds of waste heat summary table under actual power

Stack actual output power W	Q_1 kJ	Q_2 kJ	Q_3 kJ	$Q_{余}$ kJ	Total energy entering the system kJ	Power efficiency η_{sys} %	Heat efficiency $\eta_{residual}$ %
1282	213	2484	13490	16187	22213	20.7	72.9
1698	329	3437	17574	21340	29266	20.8	72.9
2126	341	4808	14202	19351	28832	26.5	67.1
2556	409	5908	15138	21455	32729	28.1	65.6
3100	526	7336	16378	24240	37754	29.4	64.2
3684	653	8629	17780	27062	42970	30.8	63.0
3781	697	8837	18640	28175	44498	30.5	63.3
4315	797	11055	21190	33042	51747	29.9	63.9
5350	1126	13963	26819	41908	65038	29.5	64.4

Fig 4-3 shows the relationship between output power and power generation efficiency and waste heat efficiency. From the figure, it can be seen that when the output power starts to rise, the power generation efficiency is the highest at 3.5kW, which can reach 30%. The trend is due to the fact that with the increase of power, the heat dissipation of the stack increases, and the cooling fluid cannot cool this part of heat in time, which causes a decrease in power generation efficiency. It can be seen that the heat management and waste heat utilization of the fuel cell can not only improve its primary energy utilization efficiency by using excess heat, but also that the fuel cell itself is in the best operating state, reaching the peak of power generation efficiency.

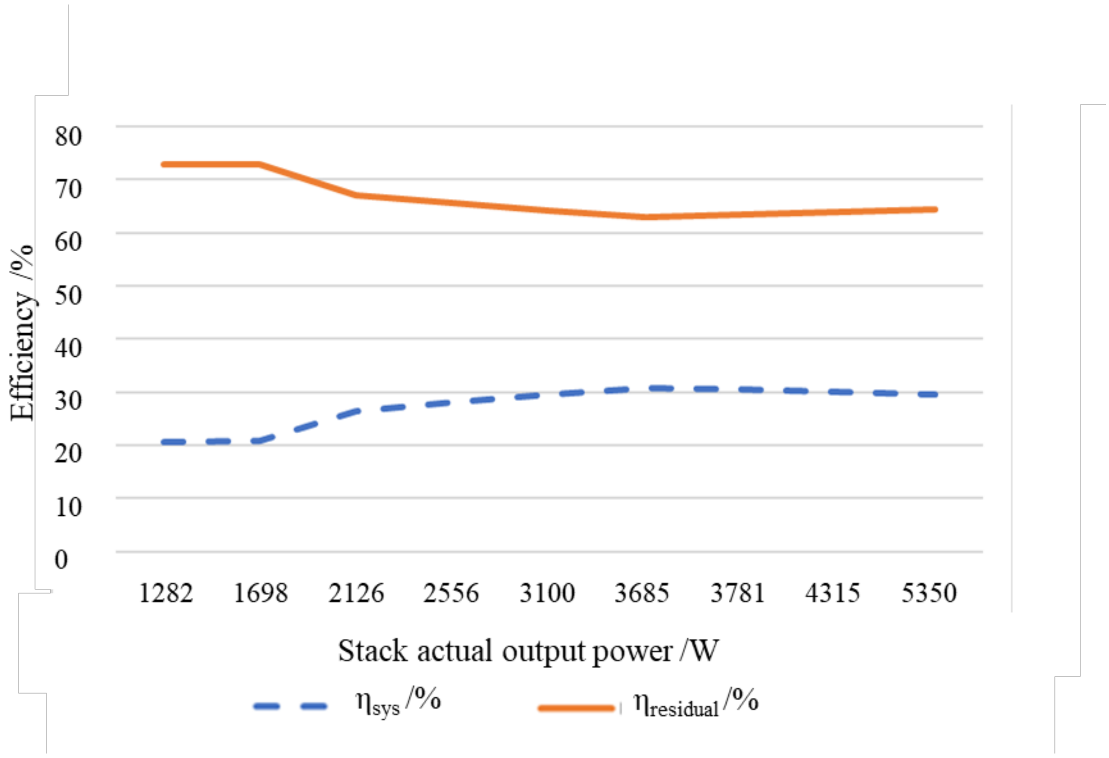

Fig 4-3 Relationship between output power and power generation efficiency and waste heat efficiency

4.4 System model building

TRNSYS which used in this paper is a transient systems simulation program with a modular structure. The modular nature of TRNSYS gives the program tremendous flexibility, and facilitates the addition to the program of mathematical models not included in the standard TRNSYS library. Main applications of TRNSYS include: solar systems(solar thermal and photovoltaic systems), low energy buildings and HVAC systems, renewable energy systems, cogeneration, fuel cells.

4.4.1 Simplifying assumptions and building of system model

Simplifying assumptions for the system model are shown below:

1) The system is under standard atmospheric pressure.

2) The methanol water solution, cooling water and air temperature of the system are all equal to the ambient temperature.

3) Methanol reforming reaction is complete, and the outlet temperature of reformer is 290℃ which is a fixed value.

4) According to the operating data of the experimental bench, there are shown in Figures 4-4 and 4-5.

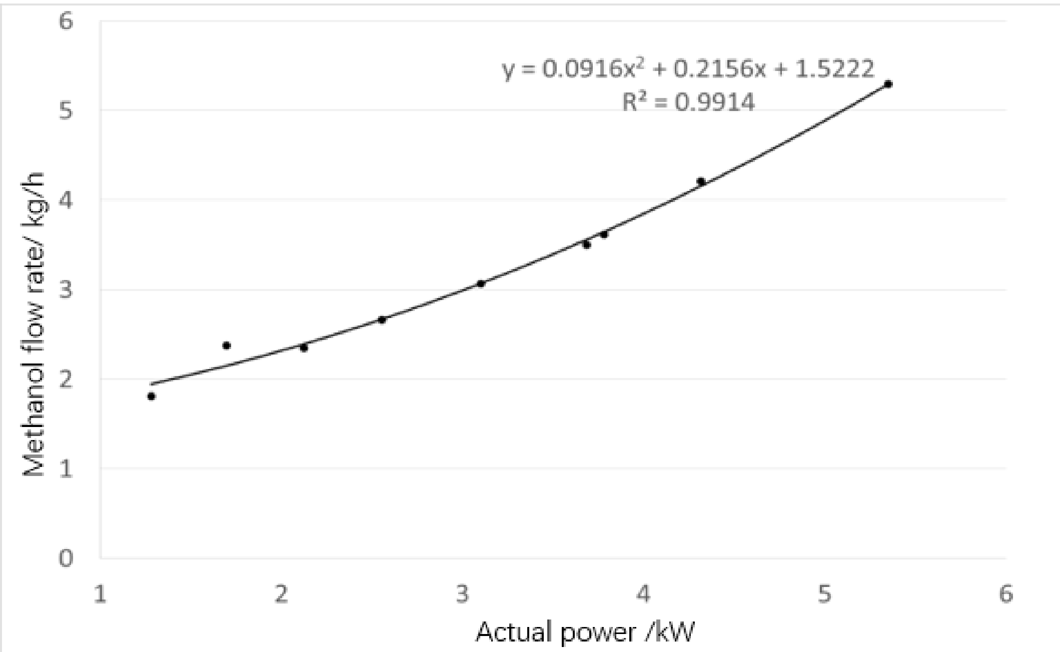

Fig 4-4 Trend of methanol flow and actual power

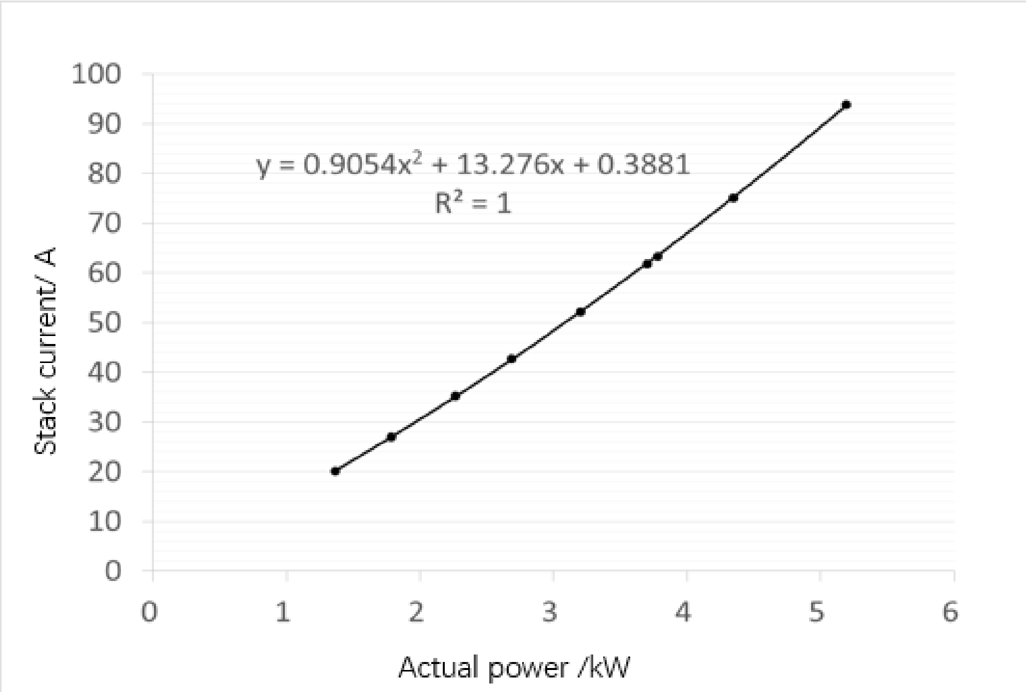

Fig4-5 Trend of stack current and power

Because the PEMFC module needs to input the stack current, and the methanol flow is related to the simulation results of Q1 and Q3 later, according to the trend lines shown in Figures 4-4 and 4-5, the output current P can be changed to change the stack current and The methanol flow is linked to achieve overall control of the system.

5) The internal reaction of the reformer is complicated. At the same time, this part of the content is not the focus of this study, so it is simplified. According to the characteristics of TRNSYS modularization, the relevant data of the reformer is distributed to each module, for example, the outlet temperature of the reformer is directly input into the fuel preheater, so as to achieve the purpose of simplifying the model.

As shown in Fig4-6, the TRNSYS simulation model is built according to the existing methanol reforming proton exchange membrane fuel cell experimental platform system. The simulation model of the system consists of six basic parts, including: Time dependent forcing function (Type14h), pump (Type3d), cross flow heat exchanger (Type5e), output file on line drawing device (Type65a), and proton exchange membrane fuel cell (Type170e). Module Type 170 made the following hypothesis: there is air at the cathode side, the temperature of the reactor is calculated internally and to calculate the R_t and C_t two input parameters in detail.

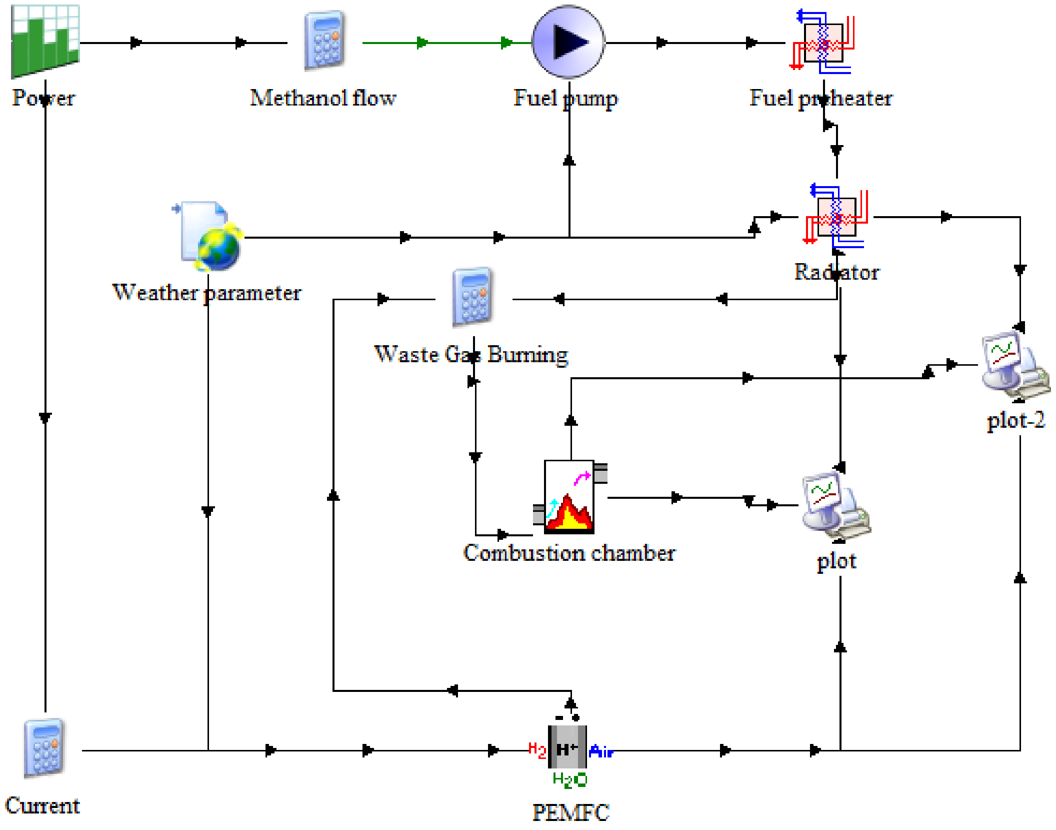

Fig4-6 Simulation system

The power is set to linear change from 0 to 5 within 5 hours. The output signal is changed into the methanol solution flow input fuel pump, and changed into the electric current input fuel cell module. Heat of the radiator, the reactor and the combustion chamber and the temperature of cooling water and flue gas can be collected by the On-line drawing device.

The model includes various TRNSYS modules, and the parameters of each module are set as follows:

1) Output power of the stack (Type14h)

This module can set its output value to change with time. Through this module, it can achieve the temporal change of the output power of the stack, and the power increases uniformly between 0 and 5 kW within 5 hours.

2) Input of calculation formula for stack current (system calculator)

This module is a system calculator module that connects input and output values to each other through input formulas. At the same time, due to its pure numerical nature, it is often used for the conversion of data units.

3) Input of methanol flow calculation formula (system calculator)

Similarly, by entering the formula, the stack power is related to the methanol flow. The formula for calculating the mass flow of methanol is set to m = 0.0916 * P ^ 2 + 0.2156 * P + 1.5222.

4) Input of calculation formula of exhaust gas combustion heat (system calculator)

The system calculator module can perform complex input and output calculations. This component calculates the remaining mass flow rate of hydrogen through the formula, where mH2 is the mass flow rate of the high-temperature mixed gas, and vH2 is the hydrogen consumption rate of the stack. In the calculation in the previous section, the mass fraction of hydrogen at the outlet of the reformer is 10.17%, and the hydrogen consumption rate of the stack is similarly calculated, and the difference can be calculated, that is, the mass flow of exhaust gas into the combustion chamber. Multiplied by the low heat of hydrogen is the residual heat generated by its combustion.

6) Fuel cell combustion chamber (HVAC)

This module needs to set two basic parameters, one is the humidity mode, which is the relative air humidity; the other is the surface area used to calculate the heat loss of the module, which is set to 1 square meter.

7) Fuel pump module

This module needs to set basic parameters: the maximum mass flow rate is 10kg / h, the specific heat capacity of methanol is 3.26kJ / kg · k; the input parameters of methanol aqueous solution flow rate and temperature are output by the methanol aqueous solution mass flow formula calculator and the weather parameter module; its output Flow rate and temperature of methanol aqueous solution to the fuel preheater module.

8) Fuel preheater module

This module needs to set the specific heat capacity of the two fluids that need to be exchanged, which are 3.26kJ / kg · k of methanol aqueous solution and 2.68kJ / kg · k of high temperature mixed gas; it needs to enter the outlet temperature of the reformer at 290 degrees Celsius, Heat exchange capacity 29kJ / h · K; output high temperature mixed gas temperature and flow rate to radiator.

9) Radiator module

One module needs to set the specific heat capacity of the two fluids that need to be exchanged, which are 2.68kJ / kg · k for high-temperature mixed gas and 4.19kJ / kg · k for water; the cold end flow rate of 100kg / h and heat exchange capacity of 20kJ / h · K; output hydrogen mass flow rate to the exhaust gas combustion heat calculation formula input device.

10) Proton exchange membrane fuel cell (Type 170e)

The basic parameters of this model are set according to the fuel cell test bench.

4.4.2 Analysis of the residual heat of each module

Running the model get the following data: the residual heat Q1 by reformed gas in radiator, the residual heat Q2 produced in the course of operation by the reactor, the residual heat Q3 generated by the Combustion chamber, the temperature of cooling water and flue gas of the radiator and the reactor T1, T2, T3. As shown in Fig4-7, 4-8, 4-9, 4-10.

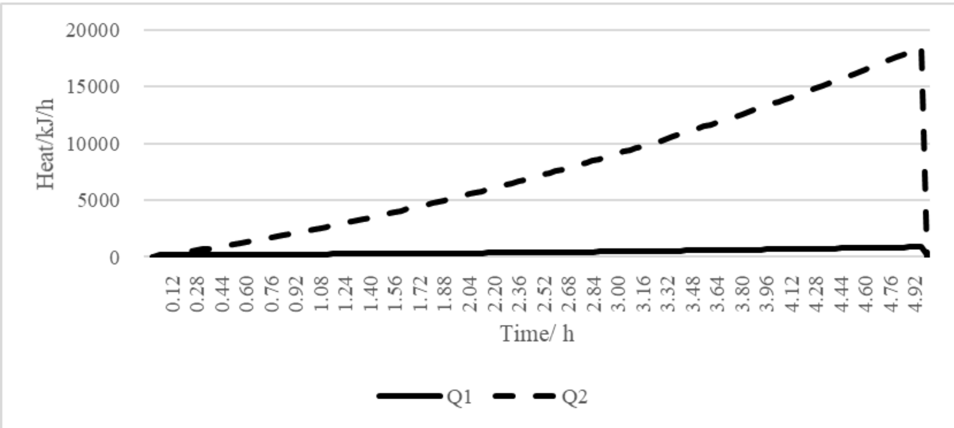

Fig. 4-7 Simulation results of Q1 and Q2

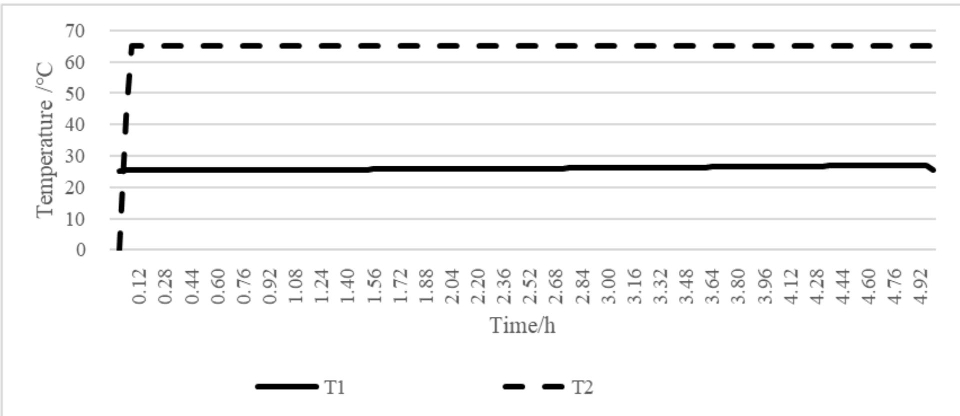

Fig. 4-8 Simulation results of T1 and T2

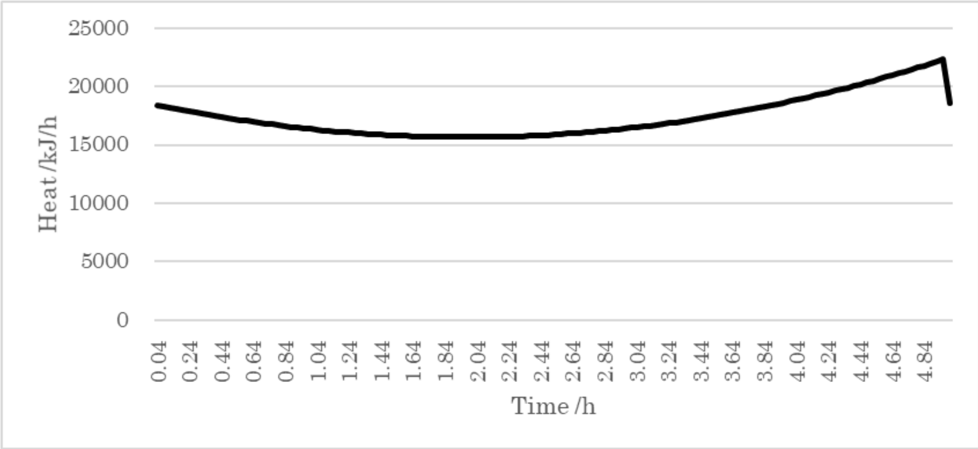

Fig. 4-9 Simulation results of Q3

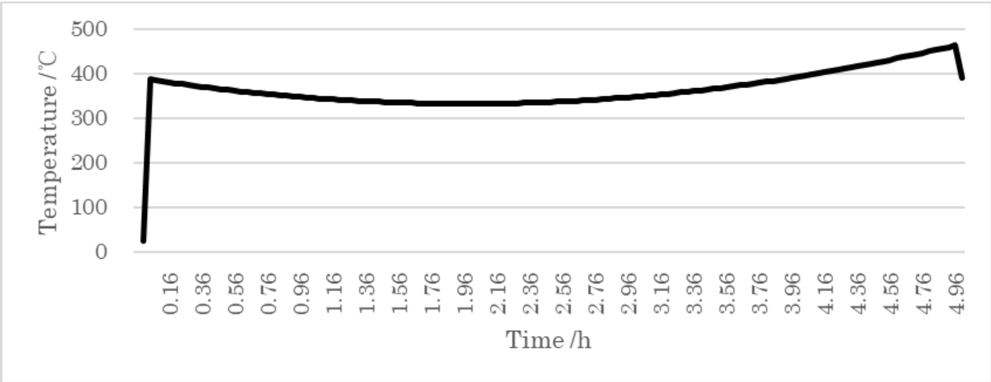

Fig. 4-10 Simulation results of T3

As shown in above Figures, in addition to the Q3 is relatively constant, the other parameters are changed follow the power. The residual heat is lower and the outlet temperature of the cooling water is lower in the part of Q1, which is difficult to use. The residual heat is high but the outlet temperature of the cooling water is lower in the part of Q2, which can be used as the preheating or as the heat medium water. the residual heat is high and the temperature of flue gas can reach 360 degrees in the part of Q3, which has a wide range of uses. As shown in Table 4-7 is the power generation efficiency, available residual heat efficiency, the comprehensive utilization efficiency of energy after the transformation of residual heat recovery of the system, (including Q1, Q2, Q3) calculated based on the simulation results.

Table 4-7 System efficiency

Output power/kW	Available residual heat efficiency/kJ	chemical energy input the system/kJ	Power generation efficiency	Residual heat efficiency	Comprehensive utilization efficiency
1	16729.85	22562.86	16.25%	74.15%	90.39%
2	18252.51	28476.64	25.25%	64.10%	89.35%
3	21623.46	36777.88	29.37%	58.79%	88.17%
4	26871.58	47491.86	30.45%	56.58%	87.03%
5	33723.04	59820.26	29.98%	56.37%	86.36%

4.5 The establishment and analysis of residual heat recovery model

After the simulation results are obtained and the preliminary analysis is carried out, the residual heat recovery simulation of the system is to be carried out. Due to the presence of high temperature flue gas, so choose the following two recovery mode: residual heat absorption refrigeration chiller and direct production of hot water.

4.5.1 The establishment of residual heat recovery model

(1) Residual heat absorption refrigeration chiller

Adding the lithium bromide absorption refrigeration module (Type677) into the system to obtain the model as shown in Fig4-11.

In order to make the lithium bromide module and actual equipment line, external call file need to be used. Part of the external file as shown in Table 4-8.

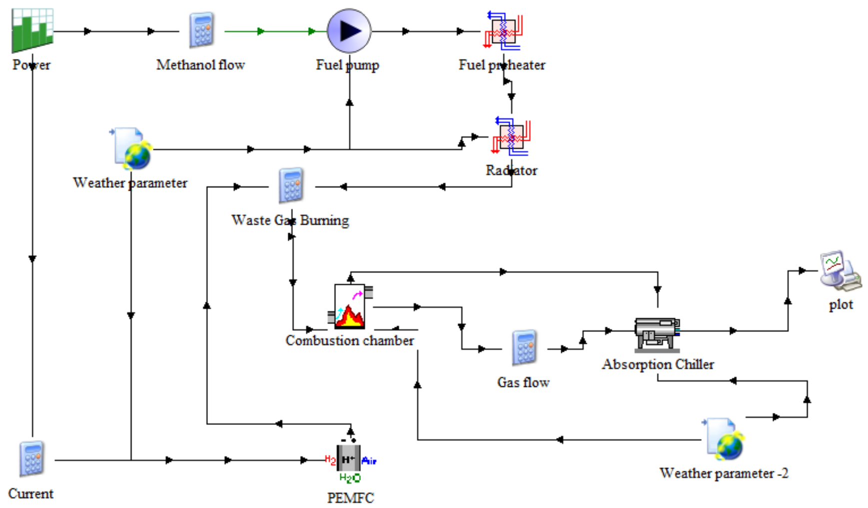

Fig4-11 Model of residual heat recovery (refrigeration)

Table 4-8 Relationship between the partial load rate and the inlet flue gas pressure

Partial load rate	Inlet flue gas pressure/kPa	Partial load rate	Inlet flue gas pressure/kPa
0.00	103.42	0.73	482.63
0.20	137.90	0.80	551.58
0.35	206.84	0.86	620.53
0.47	275.79	0.92	589.48
0.58	344.74	0.98	758.42
0.65	413.69	1.00	792.90

In addition to relationship between the partial load rate and the inlet flue gas pressure, there are 3 external call files that define the COP value of equipment, the output energy, the temperature of the outlet gas temperature and pressure.

The refrigerant water inlet flow rate is set to 1000kg/h, the temperature is set to 15℃. The cooling water flow rate is set to 2000kg/h, and the temperature is set to room temperature. Running the system, the cold water outlet temperature can be get as shown in Fig 4-12.

From figure 4-12, Because the heat supply of the flue gas is stable, the outlet temperature of the refrigerant water also keeps stable. Each hour 1 tons of refrigerant water is cooled from 15℃ to about 10℃. This process produces energy transfer about 20950kJ.

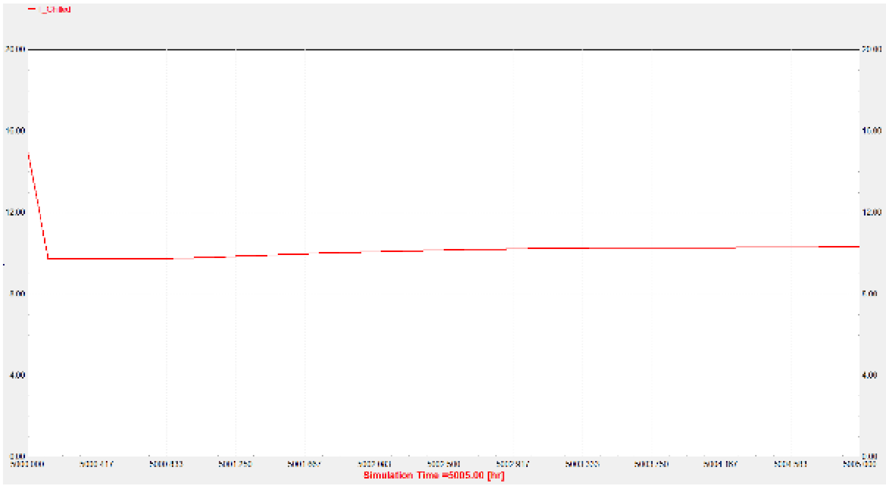

Fig 4-12 Temperature curve of refrigerant water

(2) Direct production of hot water

Similarly, adding direct production of hot water module into the system. Adding zero heat capacity explicit heat exchanger (type 91) into the model, as shown in Figure 4-13. The electric reactor coolant is used as heat medium water, and the combustion chamber outlet flue gas is used for heating. The heat exchange efficiency of the heat exchanger is set to 90%, and the temperature curve of the heat medium water is shown in Fig 4-14.

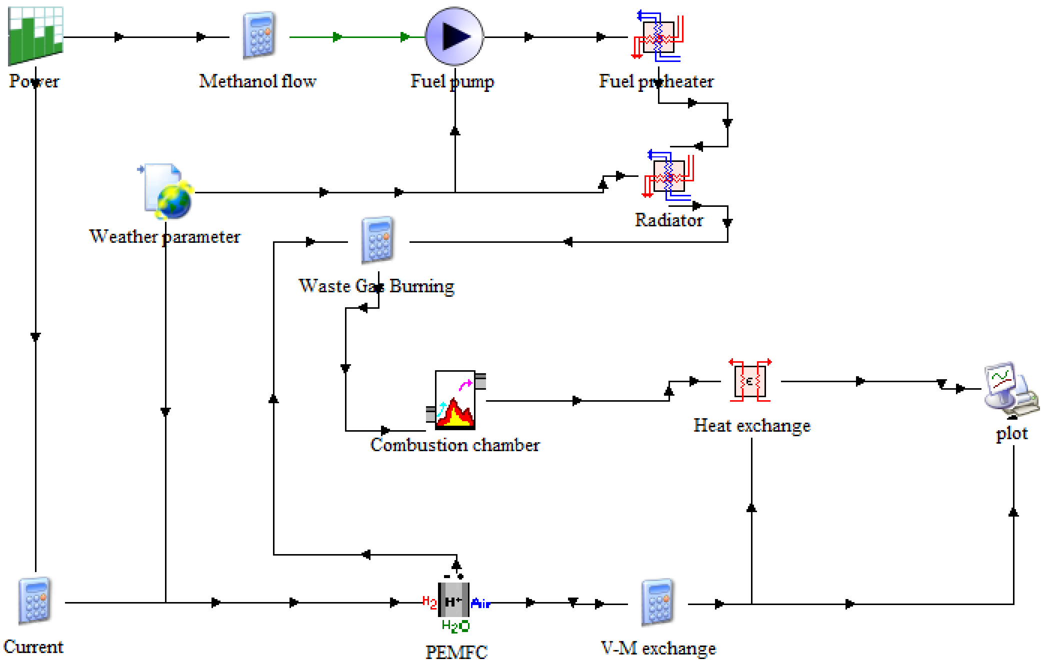

Figure4-13 Residual heat recovery model (direct production of hot water)

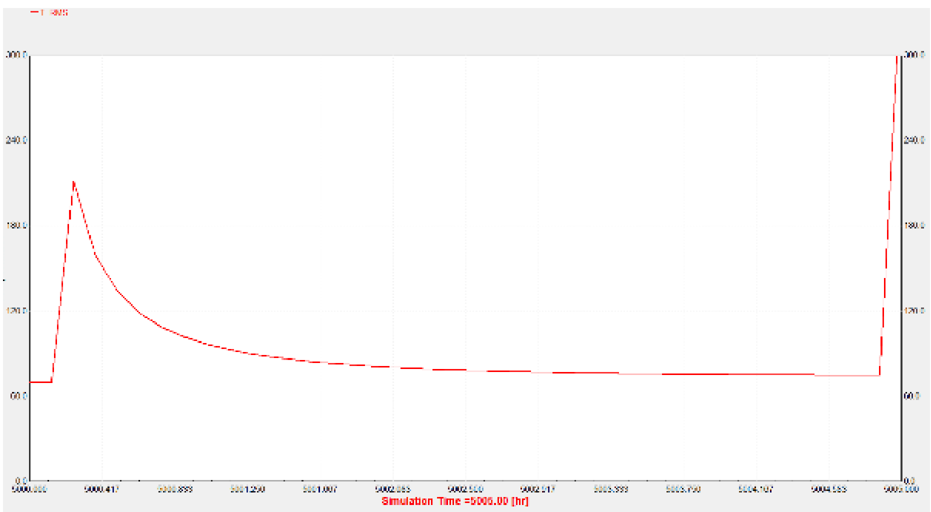

Fig4-14 Temperature of heat medium water

As shown in Figure 10, when the fuel cell power is low, due to the low waste heat generated, the reactor only needs less cooling water for cooling, however, due to the high heat supplied by the flue gas, the heat medium water temperature is higher than 100℃. Then when the system reaches the rated power 5KW, the temperature of heat medium water is stable at about 75 ℃. Each hour 0.85 tons of heat medium water is heated from 65℃ to about 75℃. This process produces energy transfer about 35615kJ.

4.5.2 System energy saving analysis

Table 4-9 Comparison of the efficiency of the system before and after the recovery of residual heat

	Residual heat absorption refrigeration chiller	Direct production of hot water	No residual heat recovery
Medium water flow	1t/h	0.85t/h	/
Medium water temperature	15/10℃	65/75℃	/
Recycling Energy	38950kJ/h	53615kJ/h	18000kJ/h
Residual heat efficiency	35.01%	59.53%	/
Comprehensive utilization efficiency	64.99%	89.51%	29.98%
System equipment	Fuel cell, LiBr absorption chiller	Fuel cell, Heat exchanger	Fuel cell

According to the simulation data, the energy saving table 4-9 can be obtain as shown above. As shown in table 4-9, the temperature of direct production of hot water is lower by 75 degrees, but its efficiency is higher, reaching 89.51%. The efficiency of refrigerant water which product by residual heat absorption refrigeration chiller is only 64.99%.

4.6. Comparison between fuel cell and conventional energy system

Table 4-10 Annual energy utilization and cost of fuel cells

Project	Value	Unit
Hot water demand	20.10	GJ
Gas consumption	979.5322	Nm3
Electricity produce	2938.60	kWh
Electricity cost reduce	75169.3	Yen
Gas cost	14584	Yen
Total energy cost	60585.3	Yen

According to Japan's statistics on the use of domestic fuel cells in 2009, the average annual carbon dioxide emission reduction of each 700W fuel cell is 1330kg. According to the trial calculation and relevant gas price policies of Tokyo Gas Company for fuel cells, the annual energy utilization and cost of fuel cells are as follows (table 4-10).

It can be seen that the energy cost reduction after using fuel cells is about 60000 yen. Using the same hot water demand, according to the heat pump trial model of Tokyo Gas Company, the energy cost reduction is about 50000 yen. According to the carbon dioxide emission coefficient of 0.418kg/kWh for electricity and 2.2455Nm3/kWh for gas (Statistics publicity of Japan's Ministry of economy and industry in 2018), the carbon dioxide emission after using the heat pump increased by about 155kg. Although the energy cost of using fuel cells is reduced more than that of heat pumps, and it helps to reduce carbon dioxide emissions. However, due to the high purchase cost of fuel cells, this part of the revenue cannot be recovered within the service life of fuel cells. Therefore, the concept of carbon tax should be introduced to re measure the economic benefits of domestic fuel cells by converting carbon dioxide emission reduction into economic benefits.

According to the ‘World Energy Outlook’ put forward by the International Energy Agency (IEA) in 2014, it is expected that by 2020, the carbon emission prices of all countries will be around 2.17 Yen/kg-CO2, and will reach 15.22 Yen/kgCO2 by 2040.(6.52 Yen/kgCO2 by 2025,10.87 Yen/kgCO2 by 2030) On the one hand, the introduction of carbon tax will increase the cost of electricity and hydrogen, on the other hand, because the equipment manufacturing stage will also produce carbon dioxide emissions, it will cause the price of equipment to rise. The carbon dioxide emissions during the production of 1kW fuel cell are 275kg [3], and the carbon emissions during the heat pump production process account for 2-3% of the carbon emissions throughout the life cycle [4]. Table 4-11 shows the CO2 emissions of different power generation types and Japan's carbon emissions per kilowatt-hour. The fuel cells and heat pumps used in the study are natural gas and electricity respectively. The CO2 emissions of different power generation types in the table are all conversions of carbon emissions from production, use, scrapping and recycling throughout the life cycle. According to the statistics of Tokyo Gas Company, the CO2 emission coefficient of natural gas is 2.245kgCO2/Nm3.

According to Japan's fuel cell development strategy, the cost of fuel cells will be gradually reduced from 1400000 yen to 600000 yen. The development of heat pump technology is relatively mature, but there is still room for further decline. With reference to the prices of different brands of heat pump, the price fluctuation of heat pump is set at 600000-800000 yen. The dynamic payback period of domestic fuel cell and heat pump shown in Table 4-12 and table 4-13 is calculated. The benchmark yield is 4.5%.

Table 4-11 CO2 emissions of different power generation types and carbon emissions per kilowatt-hour of electricity in Japan [5]

Type	CO2 emission (g/kWh)
Photovoltaic	10
Wind-onshore	9
Hydroelectric	17
Natural gas	405
Coal	935
Japan [6]	418-769（Kansai- Okinawa）

Table 4-12 Payback period of domestic fuel cell

	Carbon tax (Yen / kg-CO2)				
Price (Yen)	0	2.17	6.52	10.87	15.22
1000000	15+	15+	15+	15.05	13.58
800000	13.58	12.75	11.37	10.27	9.36
600000	8.10	7.66	6.92	6.31	5.81

Table 4-13 Payback period of heat pump

	Carbon tax (Yen / kg-CO2)				
Price (Yen)	0	2.17	6.52	10.87	15.22
750000	15.78	15+	15+	15+	15+
700000	13.58	13.72	14.02	14.32	14.64
650000	11.79	11.91	12.16	12.42	12.68
600000	10.14	10.24	10.44	10.66	10.88

In the above table, cases with recoveries greater than 15 years under all carbon taxes are not shown in the table. The dynamic payback period of more than 15 years is displayed as' 15+ ', indicating that the service life of the equipment is exceeded. It can be seen that the revenue of fuel cell will rise with the increase of carbon tax, while that of heat pump is the opposite. Fuel cells need to be reduced to 1000000 Yen to recover costs, while heat pumps cost 750000 Yen.

At the same time, it can be seen that when the cost of fuel cell is reduced to 800000 Yen, its economic benefit is the same as that of heat pump in the period of carbon tax of 10.87Yen/kg-CO2. When the cost of fuel cell reaches the target of 600000 Yen, or when the cost is 800000 Yen and carbon tax is 15.22Yen/kg-CO2, the economic benefit of fuel cell will exceed that of heat pump.

In the aspect of hydrogen fuel cell vehicles and electric vehicles, the same method is used to calculate the dynamic payback period of them. If it is assumed that the hydrogen used by the fuel cell is produced from renewable energy sources, the CO2 emissions of 1kW of hydrogen are 10-24g (conversion efficiency is 0.7[7]).

The price of hydrogen fuel cell vehicles is expected to fall to 5300000 Yen from the current 7600000 Yen. The price range of electric vehicles is set at 3700000-3300000 Yen with reference to different automobile brands. The calculation parameters are shown in table 4-14, and the calculation results are shown in table 4-15 and table 4-16.

Table 4-14 Parameters of hydrogen fuel cell vehicle and electric vehicle

	Hydrogen fuel cell vehicle	Electric vehicle
100 km energy consumption	0.99kg	15.7kWh
Unit Price	1011Yen/kg	23Yen/kWh
Cost (Yen)	1000	361
Vehicle selling price (10^4 Yen)	760	570
100 km CO2 emission(kgCO2)	0.4-0.96 (Wind- Hydroelectric)	9.53
CO2 emissions during the manufacturing stage (gCO2/km) [8]	45-55	55-100

Table 4-15 Payback period of hydrogen fuel cell vehicle

	Carbon tax (Yen / kg-CO2)				
Price (Yen)	0	2.17	6.52	10.87	15.22
5700000	15+	15+	14.91	13.20	11.85
5500000	11.54	10.80	9.56	8.58	7.79
5300000	6.20	5.85	5.24	4.75	4.35

Table 4-16 Payback period of electric vehicle

	Carbon tax (Yen / kg-CO2)				
Price (Yen)	0	2.17	6.52	10.87	15.22
3600000	15+	15.26	14.49	13.80	13.17
3500000	12.19	11.89	11.34	10.83	10.37
3400000	9.174	8.97	8.57	8.21	7.88
3300000	6.51	6.37	6.11	5.86	5.64

Because hydrogen fuel cell vehicles and electric vehicles can reduce carbon dioxide emissions when they are used, their income increases with the rise of carbon tax, but the rise of hydrogen fuel cell vehicles is higher. At the same time, when the cost of hydrogen fuel cell vehicles is reduced to 5700000 yen, which is the medium level of current vehicles, it begins to have economic competitiveness. When the target of jpy5300000 is reached, its economic benefits will exceed that of electric vehicles.

It can be seen that the introduction of carbon tax will promote the promotion of fuel cell due to the reduction effect of carbon dioxide emission of fuel cell. At the same time, it is predicted that by 2030, when the price of fuel cell has been reduced to a certain extent and the price of carbon tax has been stabilized at a higher level, fuel cell will realize the same or even higher economic benefits as the existing conventional energy system and have market competitiveness.

4.7. Summary

In this part, the experimental data are obtained by the experiment table, and the regression equation can be made on the output current of the reactor and the flow of Methanol water according to the obtained data. Then the simulation model is built according to the equation, and the residual heat of the experiment table is simulated and analyzed.

After that, through the analysis of the residual heat of each part, respectively, make two kinds of residual heat transformation program. One way is to use the absorption chiller to recover the residual heat by flue gas residual heat Q3 produced by combustion chamber. The other way is using residual heat Q2 and Q3 directly to product hot medium water. The module is added in the original model, and the simulation results are obtained at last.

Then, the efficiency of the system is analyzed and calculated. The efficiency of the refrigeration system was found to increase from 30% to 65%, and the efficiency of the hot water system increased from 30% to 89.5%. It shows that the combined heat and power transformation of methanol reforming PEMFC has great potential.

Finally, through the comparison of fuel cells, fuel cell vehicles and conventional systems under carbon tax restrictions, it can be seen that hydrogen energy equipment does not have economic advantages under the existing price system. With the cost reduction, by 2030 the price system and carbon tax level, hydrogen energy equipment does not require policy support to enter the mainstream energy market.

Reference

[1] Yi BaoLian. Fuel cell: principle, technology and application [M]. Beijing: Chemical Industry Press, 2003:23-24.

[2] George A. Olah, Alain Goeppert, G.K. Surya Prakash. Beyond Oil and Gas: The Methanol Economy[M]. Publisher: Wiley-VCH, 2006-03-23.

[3] Dhanushkodi, S. R., et al. "Life cycle analysis of fuel cell technology." Journal of Environmental Informatics 11.1 (2008): 36-44.

[4] Johnson, Eric P. "Air-source heat pump carbon footprints: HFC impacts and comparison to other heat sources." Energy Policy 39.3 (2011): 1369-1381.

[5] Jacobson, Mark Z. "Evaluation of coal and natural gas with carbon capture as proposed solutions to global warming, air pollution, and energy security." (2020).

[6] Compare electric power companies by CO2 emissions. https://power-hikaku.info/choice/eco/co2.php

[7] Japan Ministry of Economy, Trade and Industry, ‘Hydrogen/fuel cell strategy roadmap’. https://www.meti.go.jp/press/2018/03/20190312001/20190312001.html

[8] Up, Hydrogen Scaling. "A sustainable pathway for the global energy transition." Hydrogen Council, November (2017). https://hydrogencouncil.com/wp-content/uploads/2017/11/Hydrogen-scaling-up-Hydrogen-Council.pdf

Chapter 5

ECONOMIC AND POTENTIAL ANALYSIS OF FUEL CELL VEHICLE-TO-GRID SYSTEM

CHAPTER FIVE: ECONOMIC AND POTENTIAL ANALYSIS OF FUEL CELL VEHICLE-TO-GRID SYSTEM

5.1 Contents

FCV will occupy an important position in the field of new energy vehicles in the future. Compared with other new energy vehicles, FCV has lower carbon emissions, larger capacity and higher discharge power, which is consistent with the V2G service. Firstly, this paper chooses a large shopping mall in Japan as the research scenario, after obtaining its annual electricity consumption. The Monte Carlo simulation method is used to simulate the basic parameters such as vehicle visiting time, running kilometers and departure time, and to analyze the impact of FCV discharging on building energy consumption. Then, replacing part of the FCVs with EVs is considered, as well as the discharges of vehicles to buildings and power grids, using buildings as agents for all vehicles to provide V2G services for power grids. A genetic algorithm (GA) is used to find the best discharge price, the choice of vehicle discharging under the condition of the highest economic benefit, and to analyze the change of building income under different FCV ratios and EV charging demand. Through sensitivity analysis, the influence of six parameters on economic benefit is analyzed, including daily electricity price for buildings, battery cost, fuel cell cost, carbon emission price, electricity grid carbon emission and hydrogen cost.

5.2. Methodology and model

5.2.1 Charge-discharge model

(1) Visiting vehicle model

The residual energy of the vehicle when it visits SOC_t^i is：

$$SOC_t^i = SOC_{max}^i - E_{use}^i \tag{5-1}$$

Among them, I is the serial number of the visiting vehicles in the same time period; t is the different time period.； SOC_{max}^i is the maximum energy of the vehicle, kWh； E_{use}^i is the used energy, kWh：

$$E_{use}^i = P_{use}^i \times D_t^i \tag{5-2}$$

Among them,P_{use}^i is energy consumption per kilometer, kWh/km;D_t^i is the number of miles traveled, km. According to statistics from the Ministry of Land, Infrastructure, Transport, and Tourism in Japan, from 2010 to 2014, the average annual mileage of household cars was 8-9 thousand kilometers, averaging 22-25 km/day [28]. According to the National Household Travel Survey (NHTS) conducted by the U.S. Department of Transportation in 50 states, the average vehicle runs 24.65 kilometers per day, similar to Japan. Among them, 43.5% of vehicles travel less than 36 km per day and 83.7% of vehicles travel less than 100 km per day, and, on average, 14% of private passenger cars are idle. According to the statistical data of the survey report, the daily driving distance D of electric vehicles is approximated to a lognormal distribution, and its probability density function can be expressed as follows: [29,30]

$$f_D = \frac{1}{x\sigma_D\sqrt{2\pi}} e^{-\frac{(InD-\mu_D)^2}{2\sigma_D}} \tag{5-3}$$

Among them, μ_D is the expected value of logarithmic InD of daily driving distance D_t^i, μ_D=3.20; σ_D is the standard deviation of logarithmic InD of daily driving distance D_t^i, σ_D=0.88.

(2) Charge and discharge model

$$SOC_{t+1}^i = SOC_t^i + \left(P_{ch}^i \times ich_t^i - P_{dis}^i \times idis_t^i\right)\Delta t \tag{5-4}$$

Among them, P_{ch}^i is charging capacity, kWh/h; P_{dis}^i is discharging capacity, kWh/h; ich_t^i is the charging signal; $idis_t^i$ is the discharging signal.

For FCVs, there is only discharge, but it still needs to be limited according to capacity. According to the charging and discharging situation of each vehicle, the total charging amount Ech_t, discharging amount $Edis_t$ and the capacity to participate Cp_t in the scheduling can be obtained at each moment.

$$Ech_t = \sum_{i=1}^{n}(ich_t^i \times P_{ch}^i) \tag{5-5}$$

$$Edis_t = \sum_{i=1}^{n}(idis_t^i \times P_{dis}^i) \tag{5-6}$$

$$Cp_t = \sum_{i=1}^{n}(SOC_t^i - limit_{cp}) \tag{5-7}$$

Among them, $limit_{cp}$ is the limit of the maximum discharge capacity, kWh.

5.2.2 Establishment of Profit Model

(1) Economic Income Model

The building with its large parking lot will be regarded as an agent, on the one hand, to provide reasonable discharge prices for vehicles, on the other hand, to provide V2G services for the grid. In this case, the gains of the building are:

$$Income_{total} = Income_{PR} + Income_{V2G} - Spend_S - Spend_E \tag{5-8}$$

$Income_{PR}$, income by reducing peak demand for electricity, Yen; $Income_{V2G}$, V2G service income, Yen. The spending to pay are: $Spend_S$, the discharging electricity price, Yen; $Spend_E$, V2G equipment cost, Yen. Their formulas are shown below:

$$Income_{PR} = Price_{basic} \times \Delta Load_{peak} \tag{5-9}$$

$Price_{basic}$ is the price of the basic capacity of the building for one month, Yen/kW. $\Delta Load_{peak}$ is reduced peak demand for electricity, kW.

$$Income_{V2G} = Price_{V2G} \times Cp_t \tag{5-10}$$

$Price_{V2G}$ is the income from participation in V2G, including basic capacity income and ancillary services income, Yen/kW.

$$Spend_S = (Price_{dis}^j - Price_{co2}^j - Price_{normal}) \times Edis_t \tag{5-11}$$

$Price_{dis}^j$ is discharge price obtained by vehicles, Yen/kWh. j denotes the discharged vehicle as an EV or FCV. $Price_{co2}^j$ is the price of reducing carbon emissions by using electricity generated from clean energy sources, Yen/kWh. As the electricity of EV comes from the power grid, it is considered the discharge of EV will not result in the reduction of carbon emissions, $Price_{co2}^{EV}$=0. $Price_{normal}$ is price of building electricity purchased from the power grid.

EV and FCV have different discharge prices as a result of different discharge losses, fuel costs and carbon content:

$$Price_{dis}^{EV} = Price_{add}^{EV} + \frac{Cost_{battle}}{k \times Number_{cycle} \times SOC_{max}^{i} \times \mathrm{DoD}} \tag{5-12}$$

$Price_{add}^{EV}$ is the additional discharge price for EV, Yen/kWh. $Cost_{battle}$ is the total cost of the battery, Yen. $Number_{cycle}$ is the number of cycles, 2000. k is the cyclic multiple, 3. DoD is the depth of discharge.

$$Price_{dis}^{FCV} = Price_{add}^{FCV} + \frac{Cost_{FC} \times \mathrm{Eco}_{FC}}{365 \times \delta_{FC}} \tag{5-13}$$

$Price_{dis}^{FCV}$ is the additional discharge price for FCV. $Cost_{FC}$ is the total cost of the fuel cell. Eco_{FC} is the capital recovery coefficient of the fuel cell. δ_{FC} is the conversion coefficient between daily fuel use and electricity.

$$Spend_{E} = \frac{Cost_{dis}^{j} \times Eco_{dis}^{j}}{365} \tag{5-14}$$

$Cost_{dis}^{j}$ is the cost of discharge equipment, Yen. Eco_{dis}^{j} is the capital recovery coefficient of the discharge equipment.

(2) Optimization model

The objective of this study is to consider the effect of price on user behavior guidance, and to maximize the benefits of large-scale buildings as V2G agents. Therefore, the price self-elasticity coefficient is introduced:

$$\varepsilon = \frac{(Edis_t - \Delta Edis_t)/Edis_t}{(Price_{fuel}^{j} - Price_{dis}^{j})/Price_{fuel}^{j}} \tag{5-15}$$

$\Delta Edis_t$ is the rate of change of discharge, kWh. $Price_{fuel}^{j}$ is the fuel price of EV and FCV, Yen/kWh. After importing the coefficient of self-elasticity, the target model comes to:

$$\max\ Income_{total} = Income_{PR} + Income_{V2G} + Cost_{S} + Cost_{E} \tag{5-16}$$

The variables of the function are: $Price_{dis}^{j}$, $idis_{t}^{i}$, and their limiting conditions are:

$$SOC_{min}^{i} \leq SOC_{t}^{i} \leq SOC_{max}^{i} \tag{5-17}$$

$$ich_{t}^{i} = \begin{cases} 1 & Charge \\ 0 & Non\ Charge \end{cases} \tag{5-18}$$

$$idis_{t}^{i} = \begin{cases} 1 & Discharge \\ 0 & Non\ Discharge \end{cases} \tag{5-19}$$

$$ich_t^i + idis_t^i \leq 1 \tag{5-20}$$

$$\Delta Edis_t = Edis_t - \varepsilon \frac{Price_{fuel}^j \times Edis_t}{(Price_{fuel}^j - Price_{dis}^j)} \geq 0 \tag{5-21}$$

5.2.3 Simulation and optimization methods

(1) Monte Carlo simulation

Firstly, many basic parameters such as vehicle driving distance, parking time, and residence time need to be determined. Therefore, the Monte Carlo method is considered for stochastic simulation. The Monte Carlo method is based on the principle of mathematical statistics, also known as the stochastic simulation method. It is a unique numerical method that can’t be developed with the development of computers [1].

The advantage of the Monte Carlo method is that it avoids the mathematical difficulties in structural reliability analysis, does not need to consider the complexity of the limit state surface of the structure, and only needs to get the response of the structure. The disadvantage is that the calculation is too large. Therefore, it is only suitable for some complicated structures. Because of its relatively high accuracy, it is often used for checking the accuracy of various approximate methods of structural reliability and checking the calculation results.[2] The basic parameters in this paper need to be obtained through an empirical probability density function and website statistics, so the Monte Carlo method can effectively integrate data with different probability distribution structures.

(2) Genetic Algorithm (GA)

The optimization algorithm in this paper is a genetic algorithm (GA). It’s a computational model to simulate the natural selection and genetic mechanism of Darwin's biological evolution theory. It is a method to search for the optimal solution by simulating the natural evolution process. The GA takes the target fitness function as the evaluation basis, replaces the parameter set in the problem by coding, selects and mutates some bit-string genes of individuals in the population, and establishes an iterative mechanism to simulate the genetic process. After generations of continuous evolution of individuals and even groups, the optimal solution of the problem is obtained by the end of iteration.[3] Its operation flow is shown in Fig 5-1.

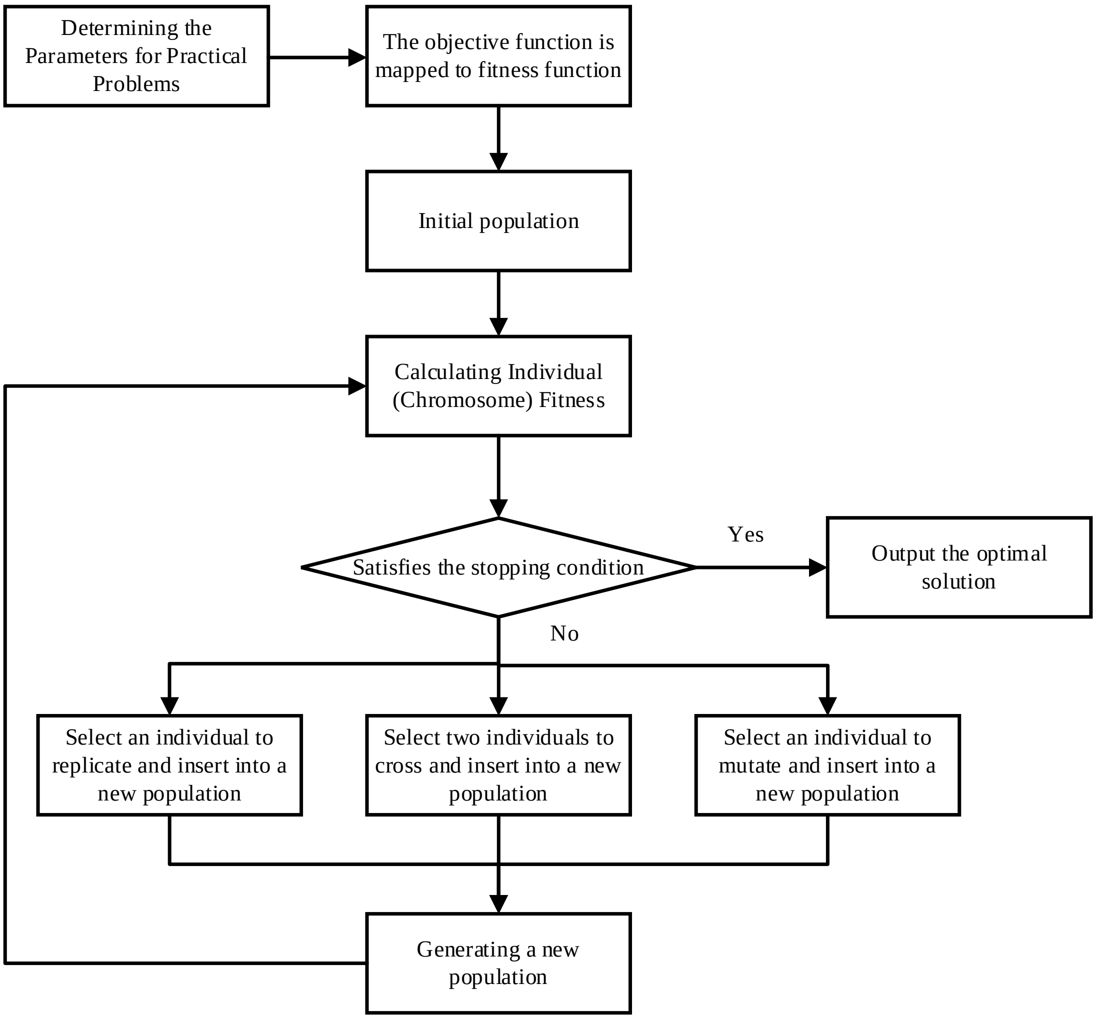

Fig 5-1 Operation flow of GA

5.3. Demand load and visiting vehicle condition simulation

5.3.1 Base load data processing

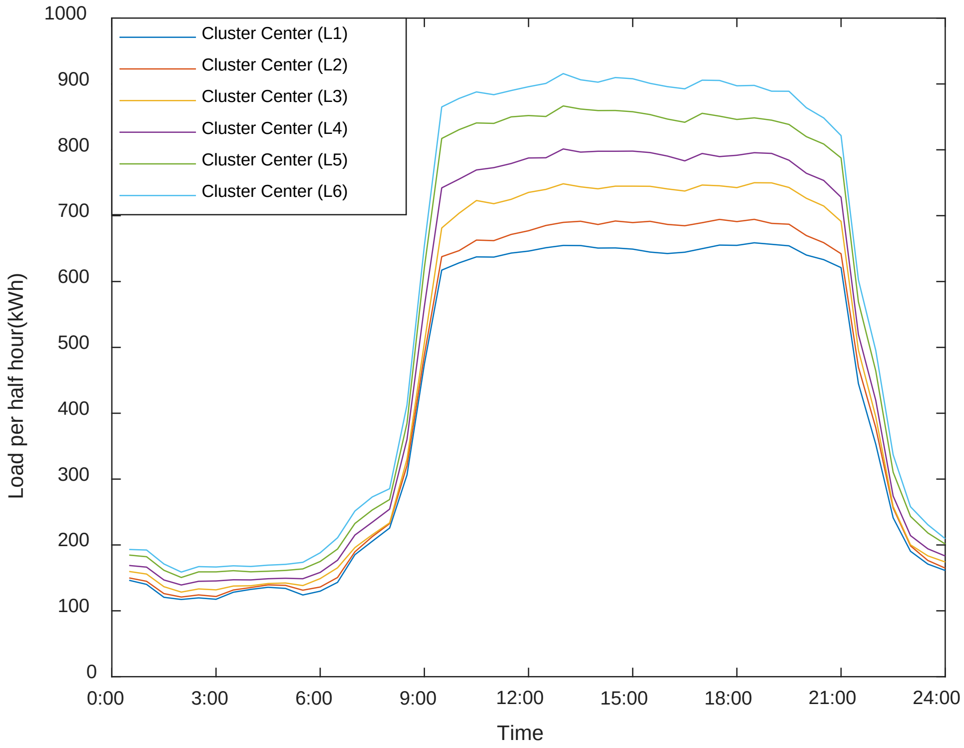

Fig 5-2 Clustering centers of daily half-hour change curve

The research objective of this paper is a large shopping mall in Kitakyushu, Japan. Its daily half-hour change curve for the whole year is shown in Appendix Fig A-1 below. Through correlation analysis, it shows that the trend of energy consumption is similar every day. The Pearson correlation coefficient is above 0.99.(Appendix table A-1) Therefore, through K-means clustering analysis, it is concluded that when the clustering center is 6, the differences among the clustering centers are most obvious. Six load change curves representing the load change are obtained (Fig 5-2). The clustering centers are arranged from large to small as L1-L6.

5.3.2 Monte Carlo simulation of visiting vehicle condition

The average daily vehicle visit rate (proportion of visiting vehicles to maximum in a year) for the target area is shown in Fig5-3 below. As the changes in visiting vehicles from Monday to Friday are close, in subsequent simulations, Monday will represent the other weekdays.

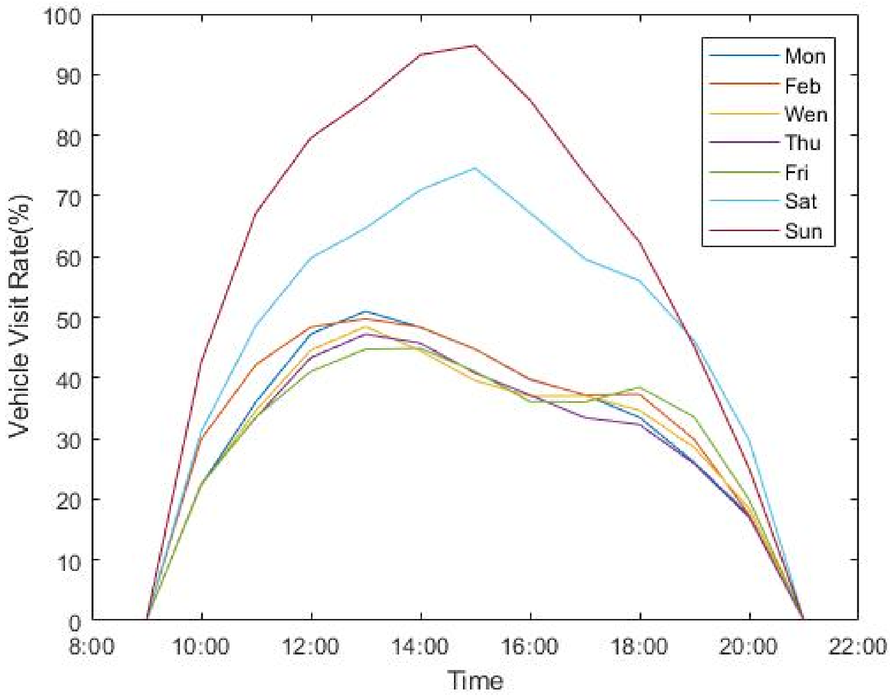

Fig 5-3 Vehicle visit rate in one week

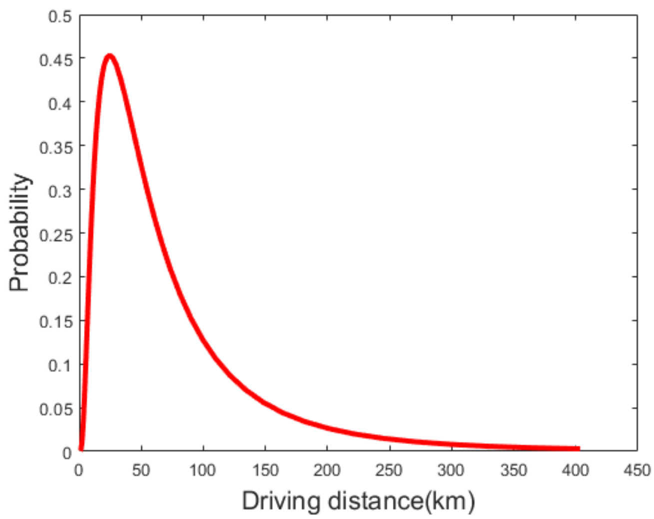

Fig 5-4 Probability density curve of driving distance

According to the density function of InD, a probability density curve of driving distance D_t^i is drawn. (Figure 5-4). At the same time, the vehicle residence time in the target area is mostly 1-2.25 hours. Using the expected value of 1.625, in order to ensure there is no negative standard deviation of 0.5163, the probability density curve of vehicle residence time is obtained (Figure 5-5).

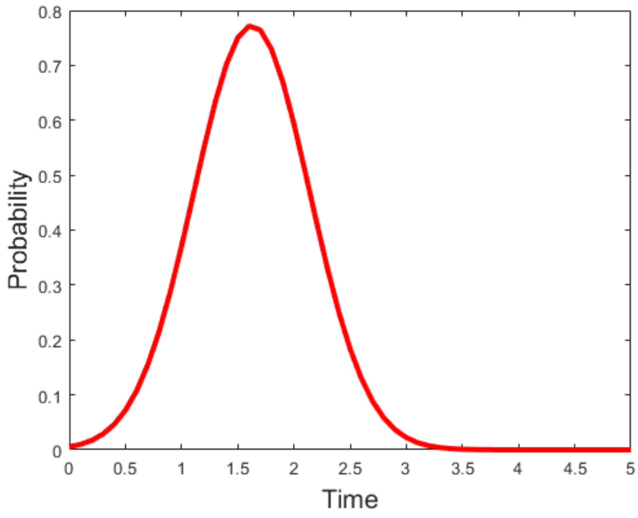

Fig 5-5 Probability density curve of residence time

Firstly, assuming all vehicles are FCVs, the load curve is calculated by the maximum clustering center (L6) and the number of vehicles visited (Sunday). Monte Carlo method is used to simulate the charging start time and driving distance of each FCV. Based on the Monte Carlo simulation statistical model, the charging load of FCVs is studied. The simulation process is as follows:

1) Input basic data. Energy consumption per 100 km of FCV is converted to power consumption, about 15 kWh. The maximum number of kilometers of FCV is about 650 km. Set the total number of FCVs N as the size of random numbers, etc.

2) Start by initializing i, set i=1. i is the number of FCVs that is currently calculating the discharging load, i = 1, 2, ..., N. According to the number of vehicles in different time periods, the simulation is carried out in different time periods.

3) The FCV start discharging time t and daily travel distance data D are generated. By using the Monte Carlo simulation method, the probability density function of the satisfaction formula (3-1) is obtained as the starting discharging time data of FCVs. Similarly, the logarithmic normal distribution of the satisfaction formula (3-2) is obtained as the daily driving distance data of FCVs.

4) Calculat**ed** the allowed discharging time. After calculating the start discharging time and the daily driving distance of FCVs, the allowed discharging time of the FCV can be calculated according to the power consumption and discharging power per 100 km from the basic data input. The maximum discharge depth of each FCV is 50%.

5) Calculate the discharging load of FCV s. The discharging load of each vehicle is calculated, and the load is added to the total load.

5.3.3 Discussion of the simulation results

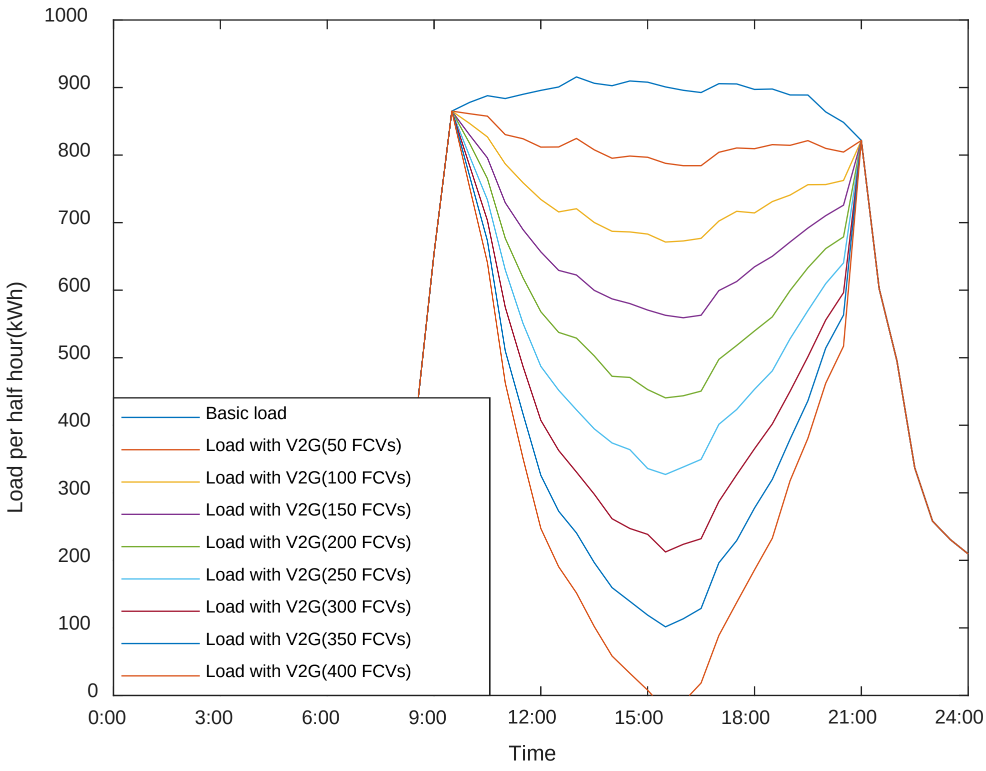

Fig 5-6 Basic load and load with FCV2G (with 50-400 FCVs)

The comparison with the original load is obtained as shown in Figure 5-6. The maximum visiting FCVs is accumulated every 50. When 400 FCVs are found, the discharge exceeds the building's power demand.

Considering that the excess discharges can be stored, the total discharges provided by different maximum visiting FCVs on Monday, Saturday and Sunday are calculated and compared with the total power consumption of the six cluster centers (Fig 5-7).

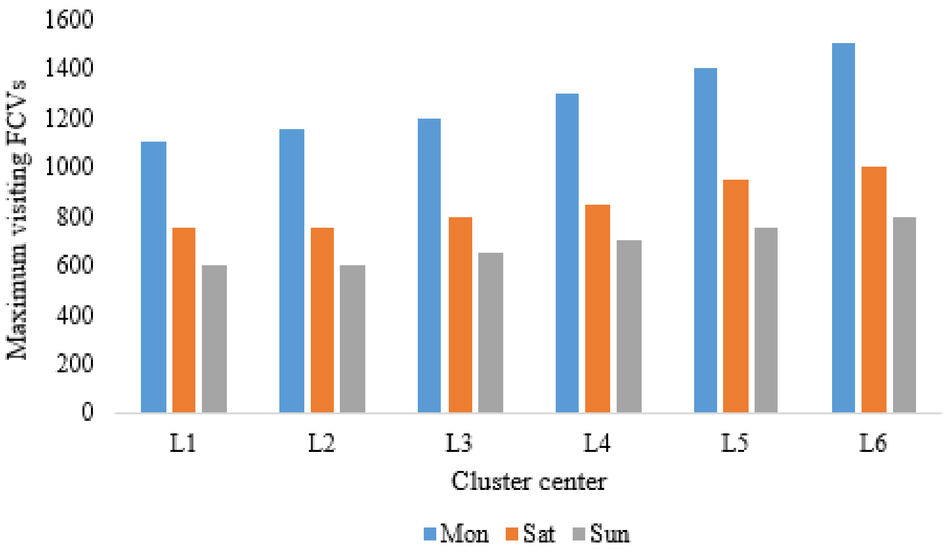

Fig 5-7 Maximum visiting FCVs when cumulative discharge exceeds daily electricity consumption

As a result of the low rate of visits, a larger maximum visit to FCVs is needed on Monday to meet the demand for electricity throughout the day. On Sunday (the highest vehicle visit rate), the maximum visiting FCVs needed are 500-800. If it is necessary to establish discharge devices for the visiting vehicles, from the economic considerations, the smallest number of Sunday data should be selected to avoid the situation where the partial discharge device is stopped because of excessive discharge. Therefore, in the subsequent calculation, the maximum number of visiting vehicles is set at 500-800. The target building has two parking lots, which can accommodate 2000 and 500 vehicles respectively. Therefore, 500 is more reasonable from the actual situation.

5.4. Solution of the profit model

5.4.1 Profit type setting for electricity and carbon emissions

(1) Electricity Price Selection

The target shopping mall is located in Kitakyushu City, Japan, which is within the scope of the Kyushu power grid. Therefore, the price we choose comes from the official website of Kyushu Electric Power. The electricity price model of households in the selected area is divided into ladder price and hourly price. Because the charging demand of electric vehicles accounts for a large proportion compared with the conventional household energy consumption, the time-sharing price is selected, and it is considered that the electric vehicles will be charged when the price is low at night. The specific price is: spring and autumn season, daytime price 23.51 Yen/kWh, night price 12.97 Yen/kWh; summer and winter season, daytime price 26.35 Yen/kWh, night price 12.97 Yen/kWh.

The commercial electricity price model is divided into hourly, seasonal price and special price on rest day. Because of the business model and visitor situation of the shopping mall, the special price model on rest day is chosen. Specific prices are: working day price 20.62 Yen/kWh, weekend and holiday price 12.64 Yen/kWh, and basic capacity fee 1296 Yen/kWh.

(2) Carbon Emission Price

In 2010, Japan began promoting the application of the carbon emission price. The first stage was from 2010-2014 and the second stage was from 2015-2019. Users need to refer to the original carbon emissions and reduce emissions according to the fixed target year by year. If they fail to meet the target, they will be fined. According to the calculation of fines, the price of carbon emissions varies from 2500-4500 Yen/t-CO2. According to the ‘World Energy Outlook’ put forward by the International Energy Agency (IEA) in 2014, it is expected that by 2020, the CO2 emission prices of all countries will be around 20 $/t-CO2, and will reach 140 $/t-CO2 by 2040. It can be seen that the current carbon emission pricing in Japan has exceeded the forecast value of IEA in 2014. At the same time, the application scenario of the FCV2G system proposed in this paper is after the commercial promotion of FCV in the future. Therefore, 4320 Yen/t-CO2 (about 40$/t-CO2, close to the highest value of Japan's current CO2 emission price) is chosen as the initial carbon emission pricing, and its sensitivity analysis will be carried out in the follow-up. At present, the CO2 emission of 1kWh in the Kyushu region of Japan is 0.463kg/kWh, so the carbon price of 1kWh is about 2 Yen/kWh.

5.4.2 Solution of the model by GA

(1) Parameter setting

Considering that EVs will still dominate the new energy vehicles for a long time, all the V2G vehicles will be divided into six situations: 100% FCV, 80% FCV + 20% EV, 60% FCV + 40% EV, 40% FCV + 60% EV, 20% FCV + 80% EV, and 100% EV. Next, the main parameters in the optimization process will be introduced.

1) Discharge loss

Fuel cells are currently expensive. It is expected that when large-scale production is formed, the price will be reduced to 157,000 yen [4]and the service life will be about 10,000 hours. The discharge loss of fuel cells is calculated to be 4.8 Yen/kWh. At present, the cost of batteries has formed large-scale production, but it is decreasing. According to the battery unit price of 27000 Yen/kWh and the number of cycles of 2000, the discharge loss of batteries is 6.1 Yen/kWh.

2) Discharge equipment

The cost of electric vehicle discharge equipment is 94000 yen, and that of FCV discharge equipment is 63000 yen.[5] Through calculation, unit investment cost is 20.6 yen and 13.6 yen, respectively.

3) Price self-elasticity coefficient

As it is impossible to judge whether the user will choose V2G to discharge, referring to papers on the charging behavior of users, it is considered that not all users will be attracted by more favorable prices and participate in V2G, and the situation of residence time and residual energy of the vehicle will affect the users' behavior. Referring to the EV Project Electric Vehicle Charging Infrastructure Summary Report, this data shows the behavior of electric vehicle owners varies with the price. Through analysis, the self-elasticity coefficient is -1.66[5].

(2) Optimization without charging demand

Firstly, the optimization results on Sunday are obtained without considering the charging demand of EV (Table 5-1). According to the calculation of basic load, the full-time electricity cost is 570 848 Yen, and the total income after optimization can reduce 6% of the electricity cost, which has high practical application value.

Table 5-1 The results of optimization on Sunday without EV charging demand

Monday ($Price_{dis}^{EV}$=25.18Yen/kWh, $Price_{dis}^{FCV}$=31.81Yen/kW)						
Proportion of FCV	100%	80%	60%	40%	20%	0%
Proportion of EV	0%	20%	40%	60%	80%	100%
Peak-cutting income (Yen)	2186	2186	2186	2186	2186	2186
V2G income (Yen)	78513	70848	63191	54547	46674	38792
Total spending (Yen)	-47828	-42534	-37244	-31214	-25733	-20250
Total income (Yen)	32871	30499	28133	25519	23127	20728

If the charging demand of EV is not considered, the peak-valley gap during V2G discharge is small, so the peak-cutting effect is the same in all cases. As the proportion of FCV decreases, the discharge of the V2G service will be reduced. Although the total discharge cost will be reduced, the income of the V2G service will also be reduced, and the final total income will be reduced. Therefore, it is believed that FCV can bring higher benefits than EV in V2G services. Fig 5-8 shows the optimization results with 80%FCV+20%EV and 20%FCV+80%EV.

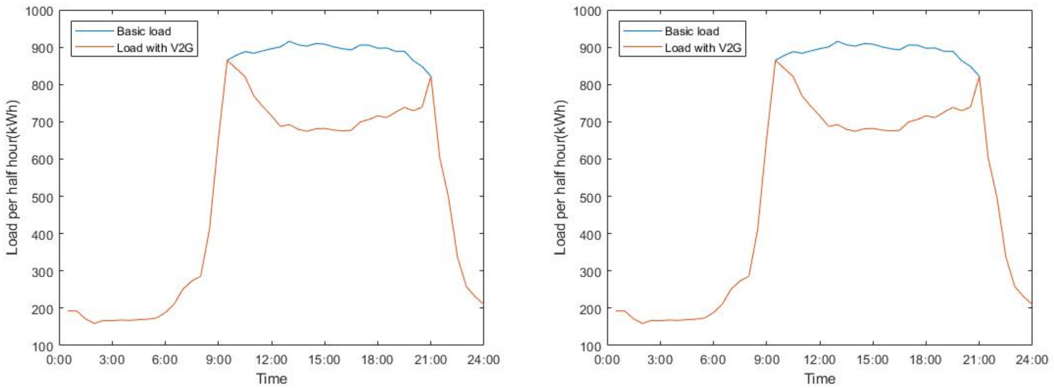

Fig 5-8 Basic load and load with V2G (Monday without EV charging demand, 80%FCV+20%EV and 20%FCV+80%EV)

(3) Optimization with charging demand

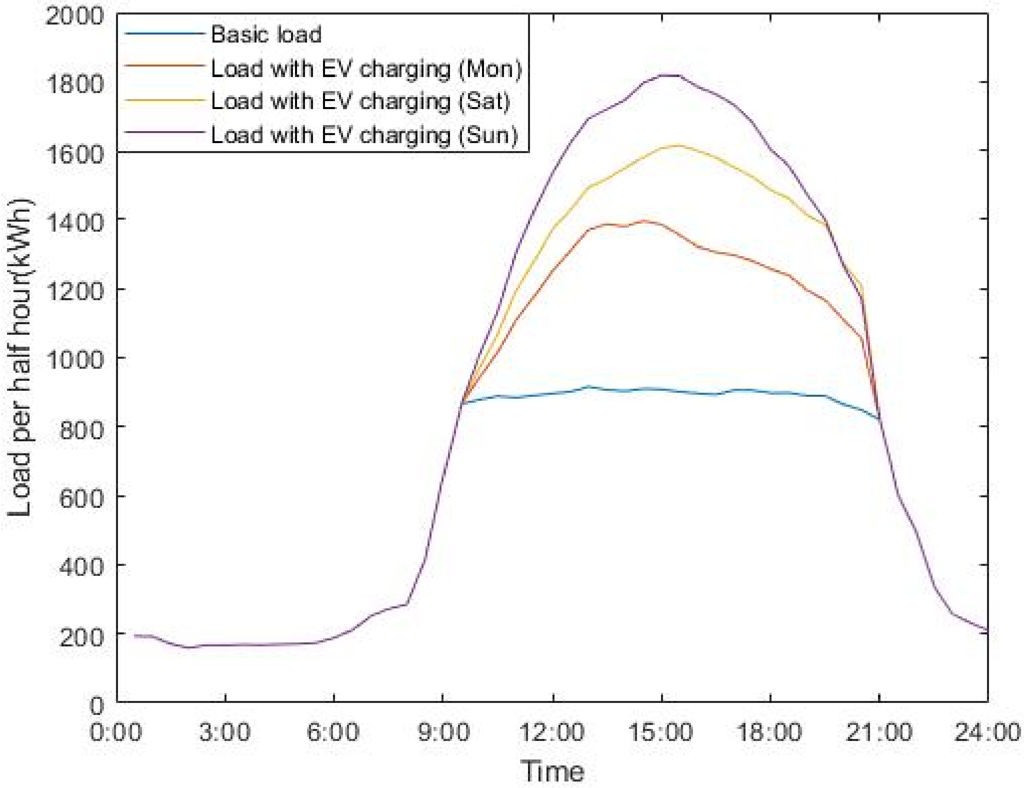

Fig 5-9 Basic load and load with EV charging (Monday, Saturday, Sunday)

If the charging demand of EV is considered, it is assumed that there are some EVs that don't participate in the V2G but need to be charged. Through Monte Carlo simulation, the different situation on Monday, Saturday and Sunday is shown in Figure 5-9. As a result of the difference in the number of vehicles visited, there are also differences in the charging demand on Monday, Saturday and Sunday, with Monday being the smallest and Sunday the largest. The results of optimization on Monday, Saturday and Sunday are shown in Table 5-2.

Table 5-2 The results of optimization on Monday, Saturday and Sunday with EV charging demand

Monday ($Price_{dis}^{EV}$=25.85Yen/kWh, $Price_{dis}^{FCV}$=32.57Yen/kW)						
Proportion of FCV	100%	80%	60%	40%	20%	0%
Proportion of EV	0%	20%	40%	60%	80%	100%
Peak-cutting income (Yen)	2206	6123	10320	13427	13133	12678
V2G income (Yen)	78601	70940	63098	66345	58036	49136
Total spending (Yen)	-47894	-42606	-37152	-43895	-37958	-31389
Total income (Yen)	32913	34458	36266	35877	33210	30425
Saturday ($Price_{dis}^{EV}$=22.90Yen/kWh, $Price_{dis}^{FCV}$=28.92Yen/kW)						
Proportion of FCV	100%	80%	60%	40%	20%	0%
Proportion of EV	0%	20.0%	40.0%	60.0%	80.0%	100.0%
Peak-cutting income (Yen)	2211	7769	9972	9101	9428	1123
V2G income (Yen)	17408	49328	53941	46303	40184	630
Total spending (Yen)	-15799	-47096	-53989	-47336	-43255	-1187
Total income (Yen)	3820	10001	9925	8068	6357	567
Sunday ($Price_{dis}^{EV}$=22.95Yen/kWh, $Price_{dis}^{FCV}$=28.89Yen/kW)						
Proportion of FCV	100%	80%	60%	40%	20%	0%
Proportion of EV	0%	20.0%	40.0%	60.0%	80.0%	100.0%
Peak-cutting income (Yen)	2220	9710	13329	12454	11164	1416
V2G income (Yen)	18170	61700	70762	61336	47869	884
Total spending (Yen)	-16116	-58626	-70764	-62882	-51057	-1600
Total income (Yen)	4274	12785	13328	10908	7977	699

As can be seen from Table 4-2, because of the addition of EV charging demand, the gap between the peak and the valley during the V2G period has been widened, thus increasing peak-cutting income. On Monday, because of the higher electricity price for buildings, the total income of the introduction of FCV has been improved, but the effect on peak reduction is smaller than that of V2G. The increase of total income mainly comes from the smaller discharge loss of FCV, the benefits of carbon emission reduction, and income from providing V2G services. To get a clearer comparison, the results with 80%FCV+20%EV and 20%FCV+80%EV are shown in Figure 5-10.

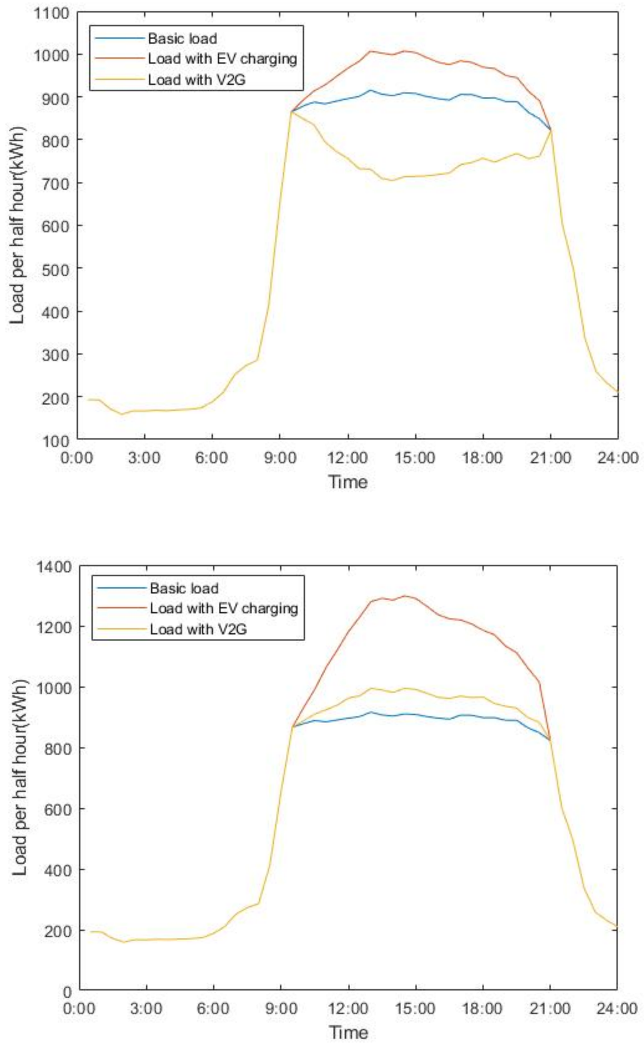

Fig 5-10 Load with EV charging and load with V2G (Monday, 80%FCV+20%EV and 20%FCV+80%EV)

In the case of 80%FCV, the overall benefit is about 3.8% higher than that of 20%FCV, of which 53.4% is lower than that of peak cutting and 22.2% is higher than that of V2G. V2G service income occupies the dominant position, so the optimization goal tends to make more vehicles participate in V2G services. At the same time, due to the reduction of EV charging demand, the peak cutting income is reduced, resulting in the situation of maximum revenue at 60%FCV+40%EV. It can be seen that EV and FCV are not completely in conflict, and EV charging demand can bring the benefit of FCV.

When building electricity prices were low on Saturday and Sunday, the overall benefit suddenly drops to only 10% of that on Monday. This is because the benefit of V2G is less than the discharge spending, so the peak-cutting income has become the main determinant of the overall benefit.

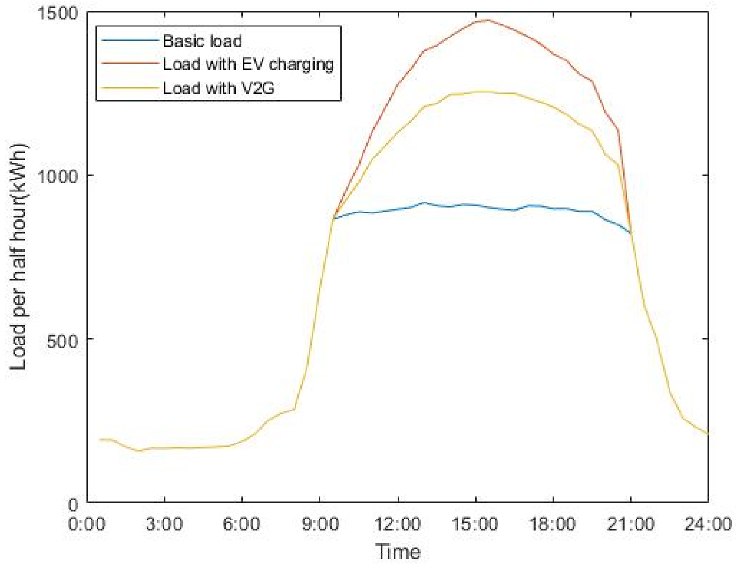

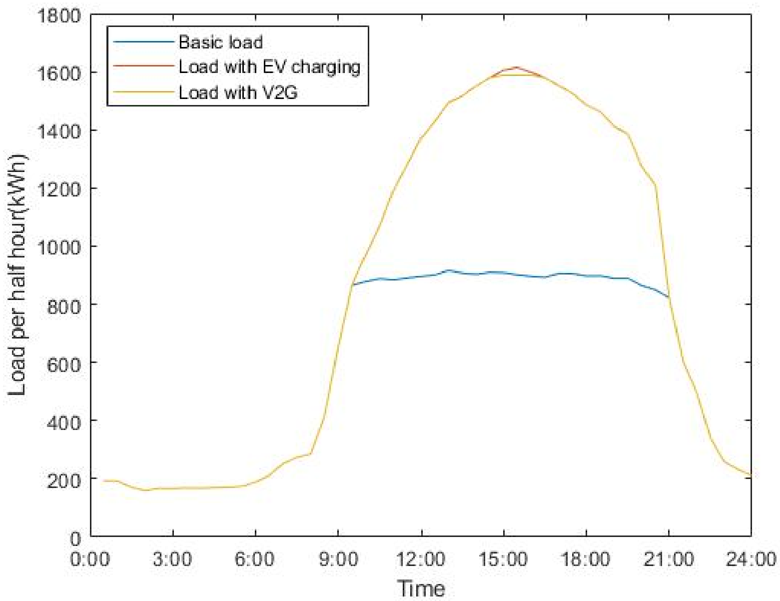

Fig 5-11 Original load and load with V2G (Saturday 20%FCV+80%EV and 100%EV)

As shown in Fig5-11, in the case of 100%EV, the final optimization curve is to ensure maximum peak shaving. With the importing of FCV, because the V2G income of FCV is higher, more power can be released, and peak load can be reduced more at the same time.

5.4.3 Sensitivity analysis of parameters

According to a forecast from the International Energy Agency (IEA), before 2030, plug-in vehicles and pure electric vehicles will still dominate the global new energy vehicle market. In 2030, hydrogen fuel cell vehicles will account for about 2%-3% of world automobile sales. From 2030 to 2050, the development sequence and market structure of plug-in, pure electric and hydrogen fuel cell vehicles remain unchanged, but the proportion of hydrogen fuel cell vehicles will increase to about 15%. Therefore, the proportion of FCV will be set at 15% to analyze the economic impact with the change of proportion.

Referring to the parameter setting and results in the optimization process, a sensitivity analysis will be carried out for the following six parameters in the sensitivity analysis: daily electricity price for buildings, battery cost, fuel cell cost, carbon emission price, electricity grid carbon emission and hydrogen cost. Referring to the introduction of the parameters mentioned above and the statistics of international organizations, the parameter changes are shown in Table 5-3.

Based on the income of 0% FCV import on Sunday, we can judge the change of income of different parameters when the import of FCV is 15%:

$$\Delta\text{income} = \frac{[income(EV85\%+FCV15\%)-income(EV100\%+FCV0\%)]}{income(EV100\%+FCV0\%)} \tag{5-22}$$

The Δincome with daily electricity price for buildings change is shown in Table 5-4.

Table 5-3 Parameter changes

Project	Initial parameters	Change range	Change interval
Daily electricity price (Yen/kWh)	20.62	10.62-20.62	2
Battery cost (Yen)	806,250	322,500-806,250	161,250
Fuel cell cost (Yen)	1562,500	625,000-1562,500	312,500
Carbon emission price (Yen/kg)	4.32	4.32-10.79	2.15
Electricity grid carbon emission (kg/kWh)	0.463	0.417-0.509	0.02
Hydrogen cost (Yen/kg)	30	20-40	5

Table 5-4 Δincome with daily electricity price

Daily electricity price (Yen/kWh)	20.62	18.62	16.62	14.62	12.62	10.62
Total income (EV100%, Yen)	30425	21828	14412	580	358	247
Total income (EV85%+FCV15%, Yen)	32540	23655	15987	9497	4285	914
Δincome, %	6.95	8.37	10.92	1537.81	1095.93	269.77

Although the total income decreases with the decline in electricity price, the effect of FCV importation is gradually improving. When the price is 14.62 Yen/kWh, the overall efficiency of EV suddenly declines. This is because the optimization direction changes from putting as many vehicles as possible into the V2G service to taking peak cutting, as shown in Fig 5-12. This shift in FCV was later than that in EV and did not occur until the price changed to 10.62 Yen/kWh, as shown in Fig5-13. FCV is more stable than EV in dealing with the decline of daily electricity price.

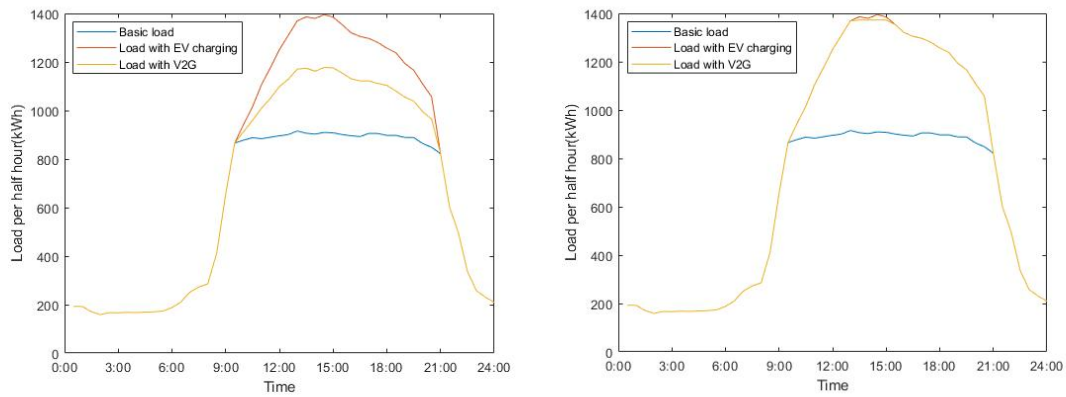

Fig 5-12 Comparisons of the impact of daily electricity price on the overall benefit (100%EV, daily electricity price 16.62 & 14.62 Yen/kWh)

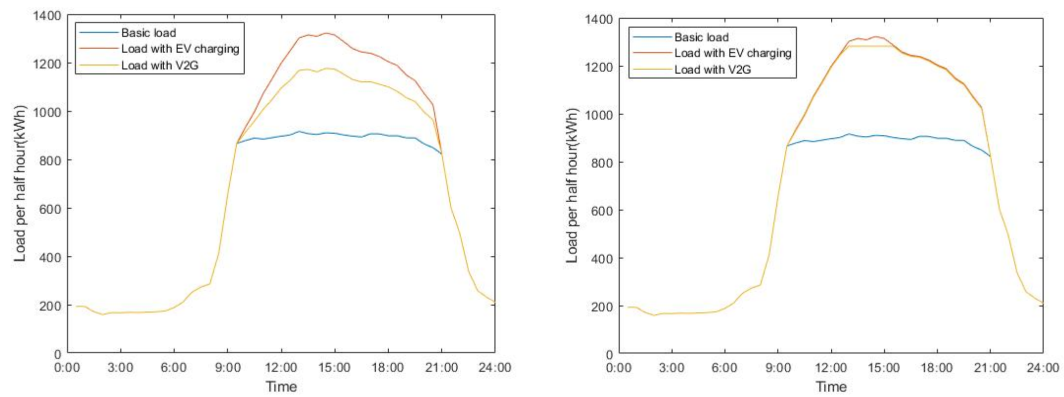

Fig 5-13 Comparisons of the impact of daily electricity price on the overall benefit (85%EV+15%FCV, daily electricity price 12.62 & 10.62 Yen/kWh)

For battery cost, fuel cell cost and carbon emission price, as there is only one direction of change and they will reach the bottleneck stage of change in 2030-2040, these three parameters are compared together. (Table 5-5) As the cost of the battery decreases, the Δincome decreases gradually. When the cost is 322,500 Yen, the overall benefit of EV exceeds. As the cost of fuel cells decreases and the price of carbon emissions increases, the result is just the opposite. The Δincome increases gradually, and the range of change is higher than that of batteries.

Table 5-5 Δincome with battery cost, fuel cell cost and carbon emission price

Battery cost (Yen)	806,250	645,000	483,750	322,500
Δincome, %	6.95	3.37	0.75	-1.14
Fuel cell cost (Yen)	1562,500	1250,000	937,500	625,000
Δincome, %	6.95	9.90	12.86	16.05
Carbon emission price (Yen/kg)	4.32	6.47	8.63	10.79
Δincome, %	6.95	13.03	19.89	27.44

Table 5-6 Δincome with electricity grid carbon emission

Electricity grid carbon emission (kg/kWh)	0.417	0.440	0.463	0.486	0.509
Δincome, %	5.81	6.43	6.95	7.48	8.20

Table 5-7 Δincome with hydrogen cost

Hydrogen cost (Yen/kg)	40	35	30	25	20
Δincome, %	-11.21	-4.52	6.95	25.72	53.47

Table 5-6,5-7 show Δincome with electricity grid carbon emission and hydrogen cost. Through the change of their parameters, we can see the overall return is positively correlated with electricity grid carbon emission, and negative correlation with hydrogen cost. However, the sensitivity of electricity grid carbon emission is low, while that of hydrogen cost is high. When the price of hydrogen is reduced to 20 Yen/kg, the overall benefit is increased by about 53.47%.

5.5. Summary

The goal of this article is to analyze the economic benefits of FCV2G and provide new ideas for FCV promotion. Firstly, the potential of FCV2G was analyzed. Based on the electricity consumption data of a large shopping mall in Japan, a Monte Carlo simulation was used to obtain the impact of large-scale FCVs on the power load of the shopping mall. It proved that the introduction of FCVs can effectively reduce the power demand of the target shopping mall, and according to the actual situation, the maximum number of discharge equipment suitable for the target mall was 500.

After that, the effects of FCV2G were specifically analyzed through comparison with EV. With the goal of maximizing the economic benefits, a genetic algorithm was used to compare and analyze the discharge electricity price and income of FCV and EV in three different situations on Monday, Saturday, and Sunday. The results showed that when the daily electricity price is high, V2G income dominates the total income, and the optimization direction is to attract as many vehicles as possible to participate in V2G services; when the daily electricity price is high and low, peak-cutting benefits dominate, and the optimization direction becomes the most economical method of reducing peak load. Through analysis, compared with EV, FCV will change the direction of optimization with lower daily electricity price, which shows that FCV is better than EV in ensuring the overall benefit under poor objective conditions.

At the same time, in the case of 80%FCV, the overall benefit is about 3.8% higher than that of 20%FCV, of which 53.4% is lower than that of peak cutting and 22.2% is higher than that of V2G. Due to the reduction of EV charging demand, the peak cutting income is reduced, resulting in the situation of maximum revenue at 60%FCV+40%EV. EV and FCV are not completely in conflict, and EV charging demand can bring the benefit of FCV.

Finally, the sensitivity analysis was performed with the FCV ratio of 15% as the benchmark. The results show that the overall benefits of FCV2G will develop in a better direction over time.

By analyzing the potential and economic benefits of the FCV2G system, we can know that FCV is more suitable for the V2G system than the current conventional EV. And the economic benefits obtained by the FCV2G system can also partially offset the economic constraints in the FCV promotion process. We hope the results we have obtained can contribute to the accelerated promotion of FCV.

Appendix

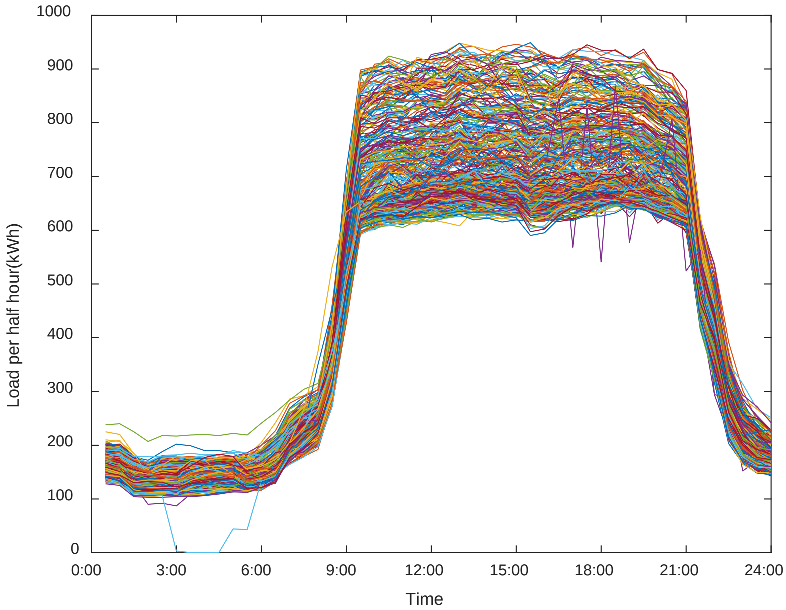

Fig A-1 Daily half-hour change curve for the whole year

Table A-1 The Pearson correlation coefficient of every day's energy consumption (Apr.1-10)

	1-Apr	**2-Apr**	**3-Apr**	**4-Apr**	**5-Apr**	**6-Apr**	**7-Apr**	**8-Apr**	**9-Apr**	**10-Apr**
1-Apr	1	.998**	.999**	.999**	.999**	.998**	.998**	.999**	.998**	.999**
2-Apr	.998**	1	.997**	.999**	.997**	.999**	.999**	.998**	.998**	.998**
3-Apr	.999**	.997**	1	.999**	.999**	.997**	.997**	.999**	.999**	.999**
4-Apr	.999**	.999**	.999**	1	.998**	.999**	.998**	.998**	.999**	.999**
5-Apr	.999**	.997**	.999**	.998**	1	.997**	.997**	.998**	.997**	.998**
6-Apr	.998**	.999**	.997**	.999**	.997**	1	.999**	.997**	.997**	.997**
7-Apr	.998**	.999**	.997**	.998**	.997**	.999**	1	.998**	.997**	.997**
8-Apr	.999**	.998**	.999**	.998**	.998**	.997**	.998**	1	.999**	.998**
9-Apr	.998**	.998**	.999**	.999**	.997**	.997**	.997**	.999**	1	.999**
10-Apr	.999**	.998**	.999**	.999**	.998**	.997**	.997**	.998**	.999**	1
**** Significant correlation at 0.01 level (double tail test)**										

Reference

[1] Gholaminezhad, Iman, et al. "Multi-scale multi-objective optimization and uncertainty analysis of methane-fed solid oxide fuel cells using Monte Carlo simulations." Energy conversion and management 153 (2017): 175-187.

[2] Urbanucci, Luca, and Daniele Testi. "Optimal integrated sizing and operation of a CHP system with Monte Carlo risk analysis for long-term uncertainty in energy demands." Energy conversion and management 157 (2018): 307-316.

[3] Yan, Z., et al. "Modeling of solid oxide fuel cell (SOFC) electrodes from fabrication to operation: Microstructure optimization via artificial neural networks and multi-objective genetic algorithms." Energy Conversion and Management 198 (2019): 111916.

[4] Hydrogen and Fuel Cell Strategy Council, 'Hydrogen and fuel cell strategy roadmap', 2019: 21-22.
https://www.meti.go.jp/shingikai/energy_environment/suiso_nenryo/roadmap_hyoka_wg/pdf/001_s02_00.pdf

[5] Tong Xin. "Electric Price Guidance and Interaction Method for Electric Vehicle Charging" [D]. North China Electric Power University (Beijing), 2017.

Chapter 6

ECONOMIC AND POTENTIAL ANALYSIS OF REGION DISTRIBUTED HYDROGEN ENERGY SYSTEM

CHAPTER SIX: ECONOMIC AND POTENTIAL ANALYSIS OF REGION DISTRIBUTED HYDROGEN ENERGY SYSTEM

6.1 Contents

Due to the addition of hydrogen energy, the energy input of the conventional RDES changed from electricity and natural gas to electricity, natural gas and hydrogen. In addition, it is also necessary to consider the hydrogen production by Valley Power, the production of hydrogen by remaining renewable energy, and the matching of hydrogen production equipment and hydrogen energy utilization equipment. These changes increase the complexity of the regional energy system and increase the difficulty of the design and operation optimization of the composite energy system. [1] At the same time, due to the high cost of existing hydrogen energy equipment, it is necessary to predict the cost reduction before comparing with the conventional RDES. [2] Based on this situation, this paper proposes the concept of introducing a carbon tax to convert the environmental advantages of the hydrogen energy system without carbon dioxide emissions into economic advantages at the same time, and at the same time reduce the cost of hydrogen equipment and the time axis of the carbon tax increase. Unified, easy to predict and analyze. This article first selects ten buildings of different building types in the Higashida area of Kitakyushu City, Japan as the research goal, the hydrogen distributed energy system is the research object, and the conventional distributed energy system is the comparative reference. Secondly, based on the actual data of building power consumption, the hourly cooling and heating load is calculated using the index method and the hourly load sharing method. After that, a RDES optimization model is established, and the genetic system is used to design and optimize the conventional system and the hydrogen energy system respectively, and the comparison of the two systems under different carbon taxes is obtained. Through the analysis of the results of different types of buildings, the adaptability of the hydrogen RDES is studied. After the lease, through the sensitivity analysis of electricity price, natural gas price, hydrogen price, and hydrogen energy equipment price, the future economic benefits of the hydrogen RDES are studied.

6.2 Methodology

6.2.1 Supply side model

In this paper, two RDESs, hydrogen and conventional, are used. Among them, conventional RDES include: Internal combustion engine (ICE), Absorption chiller-heater (AC), Heat pump (HP), Cold and heat storage (CHS), Photovoltaic (PV) and Battery. Its energy input is electricity and natural gas, and its energy output is electricity, cold and heat. As shown in Fig 6-1.

Hydrogen RDES include: Fuel cell (FC), Absorption chiller-heater (AC), Heat pump (HP), Cold and heat storage (CHS), Photovoltaic (PV) and Hydrogen storage (HS). The energy input is electricity and hydrogen, and the energy output is electricity, cold and heat. As shown in Fig 6-2.

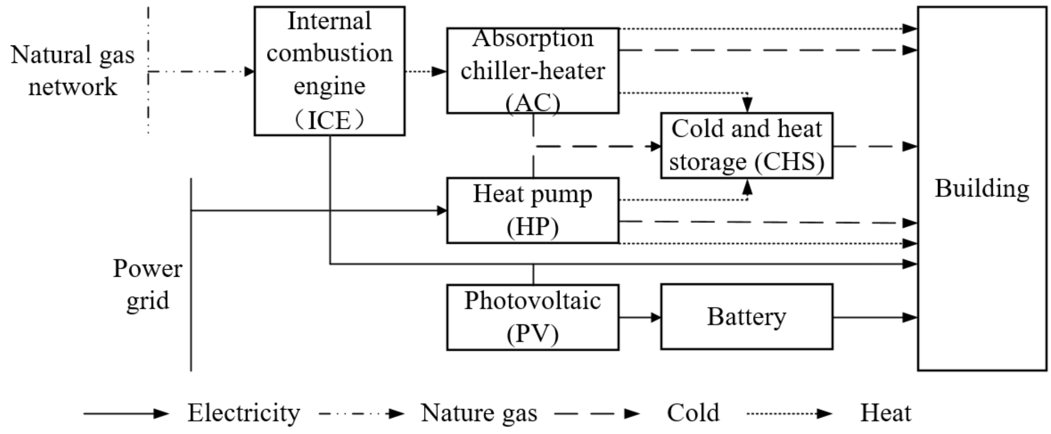

Fig 6-1 Conventional RDES

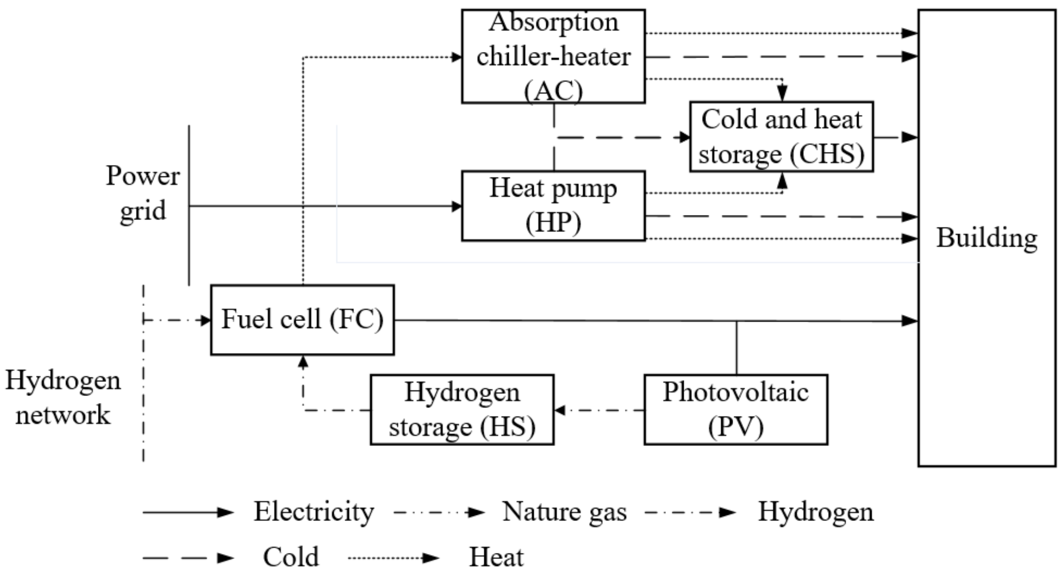

Fig 6-2 Hydrogen RDES

The balance formula of energy supply and demand of the two systems is:

$$E_{load}^{t} = E_{ICE}^{t} + E_{PV}^{t} + E_{Battery}^{t} + E_{Grid}^{t} \tag{6-1}$$

$$E_{load}^{t} = E_{FC}^{t} + E_{PV}^{t} + E_{HS}^{t} + E_{Grid}^{t} \tag{6-2}$$

E_{ICE}^{t}, E_{FC}^{t}, E_{PV}^{t} and $E_{Battery}^{t}$ are the power generation of ICE, FC, PV and battery. E_{HS}^{t} is the power storage of HS.

$$C_{load}^{t} = C_{AC}^{t} + C_{HPc}^{t} + C_{CHS}^{t} \tag{6-3}$$

$$H_{load}^{t} = H_{AC}^{t} + H_{HPh}^{t} + H_{CHS}^{t} \tag{6-4}$$

C_{AC}^{t}, C_{HPc}^{t} and C_{CHS}^{t} are cooling capacity of AC, HP and CHS. H_{AC}^{t}, H_{HPh}^{t} and H_{CHS}^{t} are heating capacity of AC, HP and CHS.

6.2.2 Economic model

The total cost of users using the two systems is as follows:

$$cost = cost_{system} + cost_{maintain} + cost_{energy} + cost_{carbon} \tag{6-5}$$

Among them, $\mathrm{cost_{system}}$ is energy system investment, $\mathrm{cost_{maintain}}$ is energy system maintenance cost, $\mathrm{cost_{energy}}$ is energy cost, and $\mathrm{cost_{carbon}}$ is carbon tax. Their detailed calculations are shown below.

$$cost_{system} = \sum cost_i \tag{6-6}$$

$$cost_{maintain} = \sum maintain_i \tag{6-7}$$

i=1,2,3,4,5,6,7, respectively represent: ICE or FC, AC, HPc, HPh, CHS, PV, Battery or HS. Among them, HPc and HPh respectively represent the cooling and heating modes of the heat pump, and are selected according to the user's cooling and heating load characteristics in actual operation. When the user's cold load is higher, HPc is used as the installed capacity of the heat pump, and HPh is 0.

Among them, ICE equipment maintenance costs can be calculated by the system power generation, as shown below. The annual maintenance cost of other equipment can be simplified to 2% of the investment cost

$$maintain_{ICE} = E_{ICE}^{t} \times price_{maitain} \tag{6-8}$$

Among them, $price_{maitain}$ electricity maintenance cost of ICE, which is 1.6Yen / kWh.

$$cost_{energy} = E_{Grid}^{t} \times price_e + gas \times price_g + hydrogen \times price_h \tag{6-9}$$

Among them, $price_e$, $price_g$, $price_h$ are the price of electricity, nature gas and hydrogen.

$$E_{Grid}^{t} = \sum_{t=1}^{8760}(load_e + P_{HP} - P_{PV} - P_{ICE} - P_{Battery} \times \varepsilon_B - P_{HS} \times \varepsilon_{HS}) \tag{6-10}$$

Among them, ε_B and ε_{HS} are the storage efficiency of battery and HS

$$gas = \sum_{t=1}^{8760}(P_{ICE}/\delta_{ICE}) \tag{6-11}$$

$$hydrogen = \sum_{t=1}^{8760}(P_{FC}/\delta_{FC} - P_{HS} \times \varepsilon_{HS}) \tag{6-12}$$

The consumption of natural gas and hydrogen comes from ICE and FC. Among them, δ_{ICE} and δ_{ICE} are the power generation efficiency of ICE and FC respectively

$$cost_{carbon} = (E_{Grid}^{t} \times carbon_e + gas \times carbon_g) \times price_{carbon} \tag{6-13}$$

$carbon_e$ and $carbon_g$are CO^2 emission coefficient of electricity and natural gas. $price_{carbon}$ is the price of CO^2 emission.

6.2.3 Objective function and constraints

The optimization goal of this article is that the total cost that users need to pay is the lowest:

$$\min(cost) = \min(cost_{system} + cost_{maintain} + cost_{energy} + cost_{carbon}) \tag{6-14}$$

The restrictions are:

1) Distributed rooftop photovoltaics are subject to site restrictions and cannot be increased indefinitely. The penetration rate is set to not exceed 30% of the total annual electricity demand in the target area.

2) The thermal balance must meet the thermal supply.

3) Considering the need to separately store heat and heat in different seasons, choose to use a natural stratified water energy storage tank that can take into account both energy storage modes as a heat storage equipment. At the same time, because the size of the tank is limited by the site, the instantaneous heat storage cannot exceed 30% of the maximum load.

6.3 Case study and basic data

6.3.1 Case study

The target area selected in this article is the Higashida area in Kitakyushu City, Japan, which serves as a key renovation and application test area for an environmentally friendly city. The target area has been selected as a new energy experimental demonstration area by the Ministry of Economy, Trade and Industry since 2010. As shown in Fig 6-3, the blue coil area is the steel plant area, and the red coil area is the smart community demonstration area, which uses heat, hydrogen, solar energy, wind power and other energy sources to achieve energy self-sufficiency. In 2011, the application demonstration of hydrogen energy in the target area began, hoping to establish a model of hydrogen energy society to promote nationwide. The white dots and yellow lines in Fig 6-3 show the core areas of the hydrogen energy demonstration project, including: 1) hydrogen production through industrial by-products of the steel plant; 2) hydrogen production through the electrolytic power plant of the steel plant; 3) Hydrogen storage, transportation and filling; 4) Application research on household fuel cells and hydrogen fuel cell electric vehicles. It can be seen that the hydrogen energy supply system is about 1.2km, almost traverses the entire Higashida area, and the scope of empirical research also involves all aspects of the use of hydrogen energy. Based on this situation, this paper selects different types of buildings on the hydrogen energy supply route as the research goal (represented by red dots in Fig 6-3) to analyze the application of hydrogen energy in the RDES.

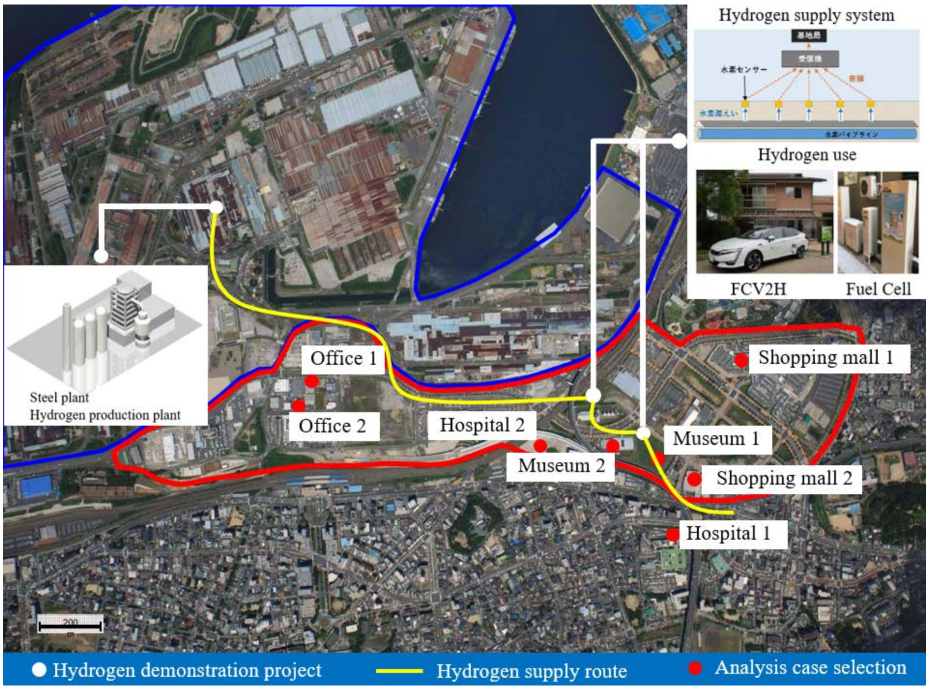

Fig 6-3 Description of hydrogen supply route and research case in Higashida area

Table 6-1 Basic information of the research target building

Building	Construction area (m^2)	Annual total electricity consumption (kWh)	Maximum electrical load (kW)
Museum 1	40111	5216559	1444
Museum 2	39690	2738580	1429
Hospital 1	55694	8149480	2005
Hospital 2	20444	2998620	736
Shopping mall 1	52417	8244028	1887
Shopping mall 2	110917	12883207	3993
Residential 1	15944	2386098	574
Residential 2	77361	8769075	2785
Office 1	30500	2883958	1098
Office 2	19833	1543671	714

This article selects five building types: museum, hospital, commercial, residential and office in the area, and selects two buildings as research objects for each type. The basic conditions of these buildings are shown in table 6-1 above.It can be seen that the selected buildings have different types of buildings with similar power consumption and maximum power load. There are also some differences between the two buildings in the same type, which is helpful for verifying the adaptability of the hydrogen energy system to different building types and different load situations.

6.3.2 Basic data pretreatment and analysis

After 0-1 standardization, the annual 8760-hour power load of the ten buildings are shown in Figure 6-4 below. It can be seen that the hospital and office buildings have similar power load changes, while the other three types of buildings have significant load characteristics.

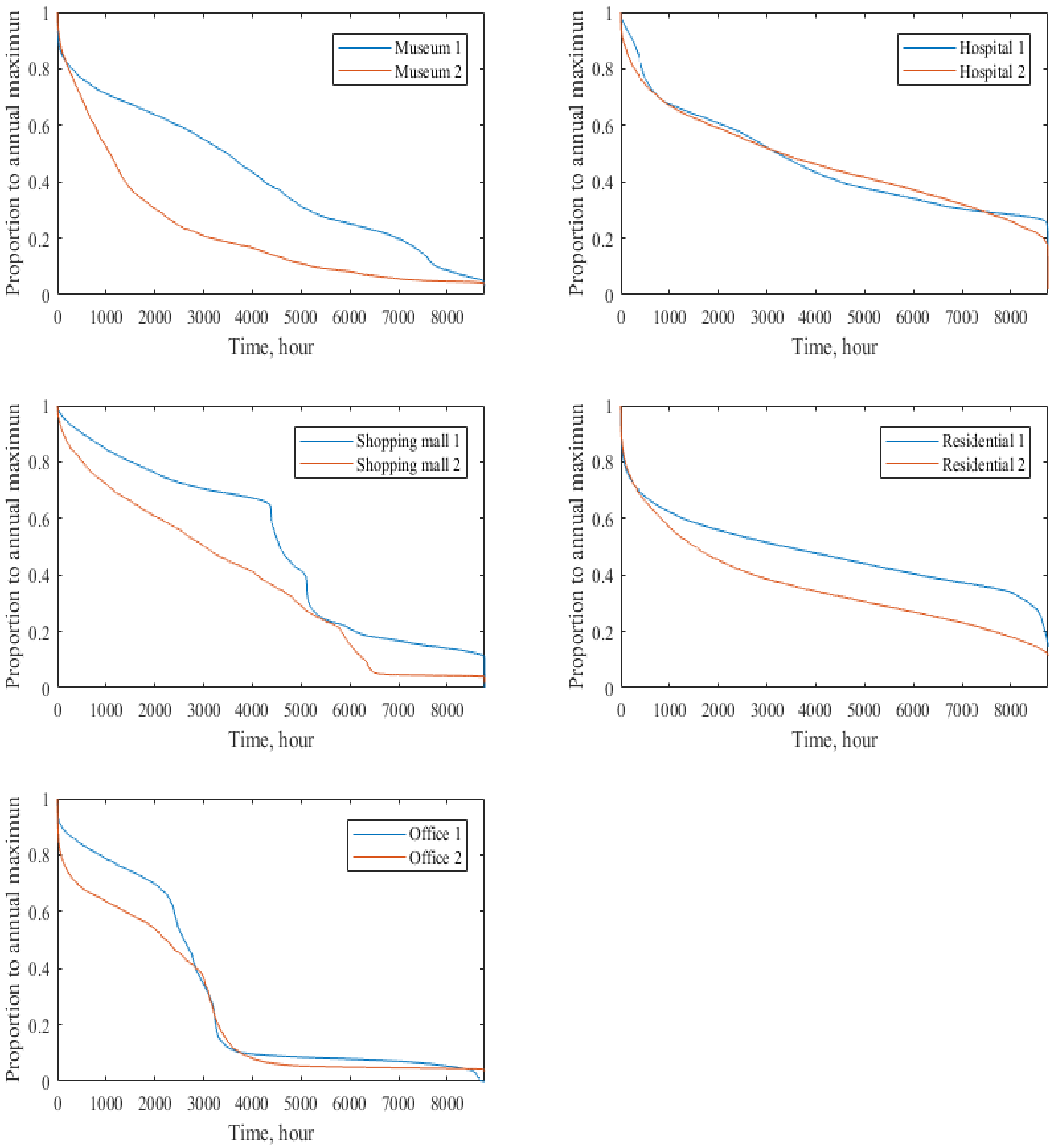

Fig 6-4 Annual 8760-hour power load of the ten buildings

In the subsequent cooling and heating load forecasting, the change of the cooling and heating load curve will be shaped according to the electric load change characteristics. Fig 6-5 (take office buildings as an example, other shows in appendix Fig A-1) show their typical daily changes in the four seasons. The electricity load of buildings showed a significant daily difference, for example, in the second office building, there was a significant drop in power load caused by the lunch break. These changing characteristics will serve as the basis for subsequent cooling and heating load curve shaping.

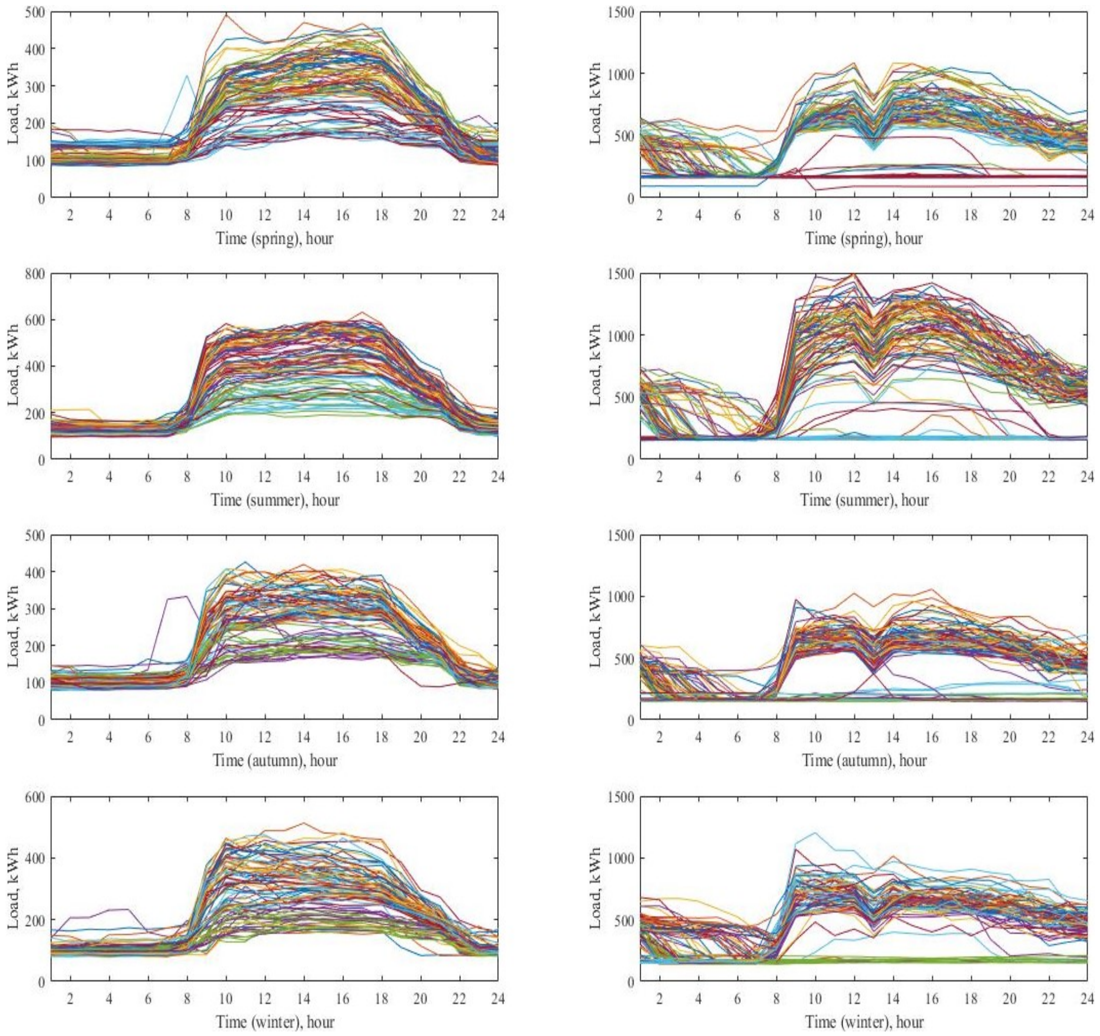

Fig 6-5 Typical daily changes in the four seasons of office buildings (electricity load)

6.3.3 Cold and heat load forecasting

In this paper, the hourly cooling and heating loads are predicted through the hourly electrical load of the building. The forecasting steps are shown in Fig6-6 below. First, through the annual maximum power load consumption, based on the conventional design redundancy of the inverter, consider that the design maximum power load is 20-30% higher than the actual value. According to the index method, the actual energy use area of the building and the theoretical maximum value of the heating and cooling load for the whole year can be obtained. According to the full-load equivalent running time method, the ratio of 8760 hours to the theoretical maximum value of the whole year is obtained, and the simultaneous utilization factor of 0.6 is considered to obtain the hourly cooling and heating load value. Finally, through the characteristics of actual power changes, such as the commuting hours of commercial buildings, lunch breaks, etc., the hourly cooling and heating load is corrected to obtain the hourly cooling and heating load used in subsequent calculations.

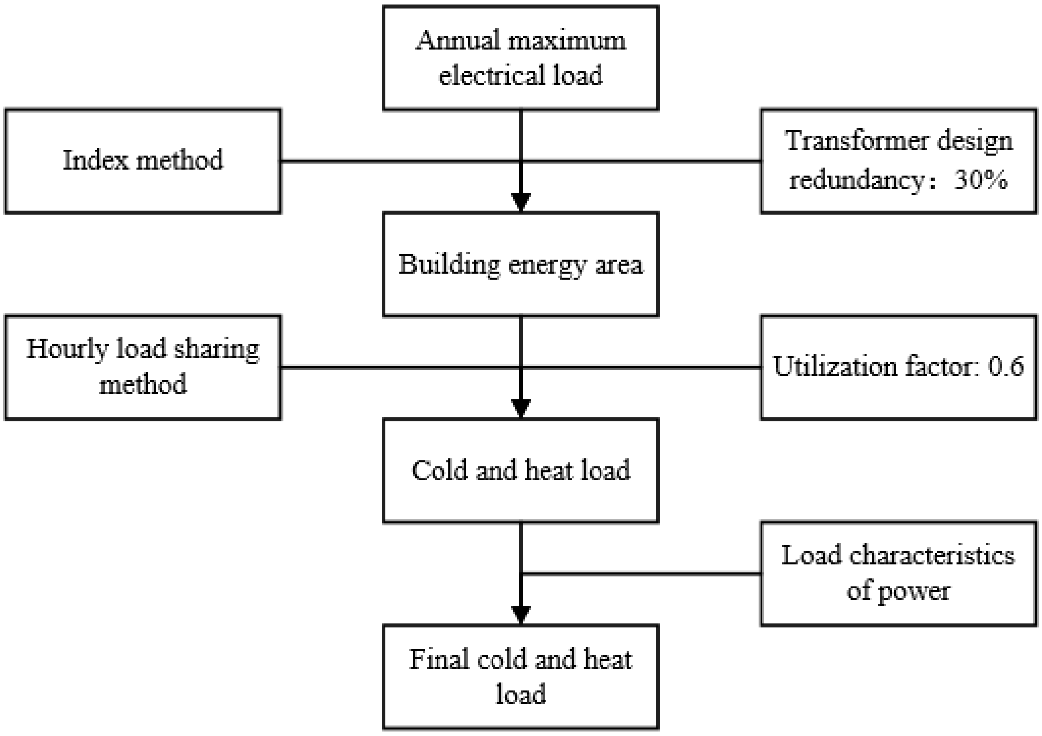

Fig 6-6 Cold and hot load forecasting process

The cooling and heating load of 10 buildings can be predicted by the method of Figure 6-7. In order to illustrate the changing characteristics of cooling and heating load, as shown in Fig 6-8 (take office buildings as an example, other shows in appendix Fig A-2), they are the annual 8760 load change curve and the typical daily change curve for the four seasons.

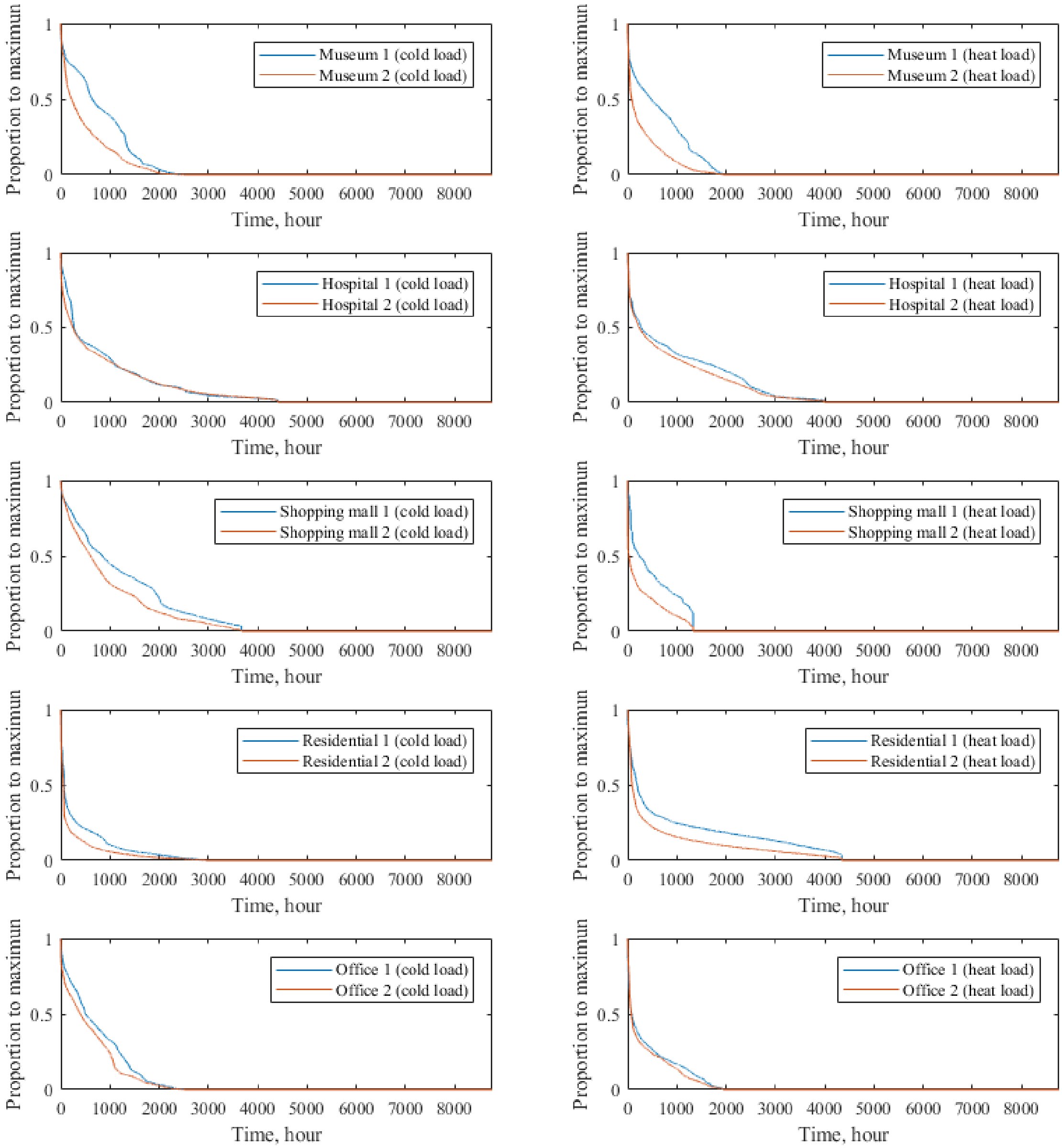

Fig 6-7 Annual 8760 load change curve of office buildings

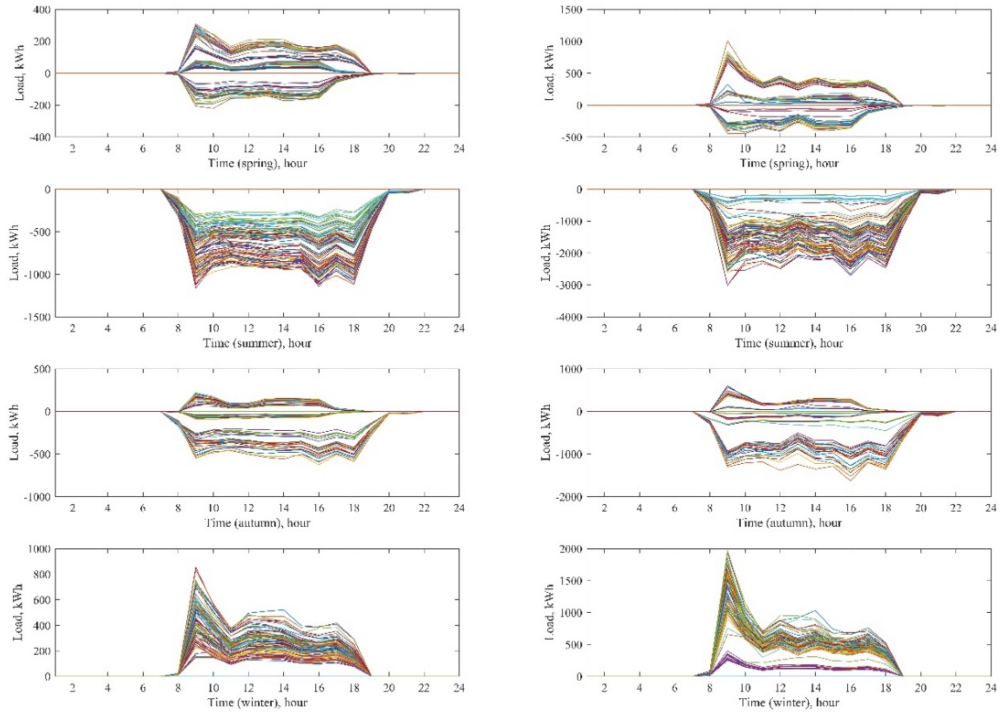

Fig 6-8 Typical daily change curve for the four seasons of office buildings (cold and heat load)

Table 6-2 Equivalent hours of cooling and heating load

	Museum		Hospital		Shopping mall		Residential		Office	
	1	2	1	2	1	2	1	2	1	2
Cold load	773	452	791	747	1164	890	328	201	703	564
Heat load	629	286	878	761	478	254	870	533	376	327

It can be seen that the demand for the heating and cooling load of the office load is relatively small, mainly affected by holidays and working hours. Table 6-2 below shows the equivalent hours of cooling and heating load calculated based on the maximum cooling and heating load demand of the ten buildings and the total annual demand. It can be seen that business, museums and hospitals have higher cooling load demands, and residences, museums and hospitals have higher heat load demands. After obtaining the basic electricity, cold and heat load data, the system design and operation optimization of the RDES based on these data will be carried out

6.4 System design and optimization after the introduction of carbon tax

6.4.1 Carbon tax

In 2010-2014 and 2015-2019, the Japanese government launched two phases of carbon price pilots. The carbon emission price is 2.5-4.5 yen / kgCO2. According to the ‘World Energy Outlook’ put forward by the International Energy Agency (IEA) in 2014, it is expected that by 2020, the carbon emission prices of Japan will be around 2.16 Yen/ kgCO2, and 15.1 Yen/ kgCO2 in 2040. It can be seen that the experimental price of carbon tax in Japan exceeds this predicted value, but the amount exceeded is not large. Since there are no cases nationwide, this forecast data is still used to illustrate the time characteristics of different carbon tax representatives.

At present, the CO2 emission of 1kWh electricity in Kyushu region of Japan is 0.463kg/kWh, and that of 1m^3 nature gas is 2.21 kg/m^3. According to the calorific value conversion of 1m3 natural gas as 10kWh, the carbon dioxide emission of natural gas per unit of 1kWh calorific value is 0.221kg / kWh.

6.4.2 Optimization model establishment

In order to make the optimization more in line with the actual situation and exclude other interference items, the following assumptions are made about the optimization:

1) It is considered that there is no split air conditioner in the target area, that is, the user load is fully supplied by the system.

2) The principle of system configuration is to determine electricity by heat, and give priority to satisfying the user's cold and heat needs. The insufficient power demand is still provided by the power grid.

3) The users in the target area all use the peak and valley electricity prices of the corresponding industries, and the gas uses a single price, while considering the basic capacity costs of electricity and gas.

4) Based on economic considerations, energy storage batteries need to be discharged according to the depth of discharge before the daily electricity price valley period.

The energy prices and equipment parameters needed for optimization calculation are shown in Tables 6-3 and 6-4 below. The energy price is sourced from the official website of Kyushu Electric Power and Kyushu Gas Company affiliated with the study area, and a more suitable energy price is selected. The energy equipment parameters and prices mainly come from the strategic planning of the hydrogen energy system in Japan [3], as well as manufacturer data.

Table 6-3 Energy price

	Electricity		Nature gas	Hydrogen
Unit energy cost	Summer peak (13:00-16:00)	16.95 Yen/kWh	67.53 Yen/m^3	40 Yen/m^3
	Summer daytime (8:00-12:00, 17:00-22:00)	14.48 Yen/kWh		
	Normal daytime (8:00-22:00)	13.53 Yen/kWh		
	Nighttime (23:00-7:00), Sunday and holiday	9.06 Yen/kWh		
Basic capacity cost		2046 Yen/kW	2365 Yen/m^3	

* Summer is from July 1st to September 30th.
* The price of natural gas is a price model suitable for larger equivalent use, and a fixed fee of 159,148 yen needs to be paid in one lump sum.
* The price of hydrogen selects the predicted target value of Japan's hydrogen energy strategic plan, without considering the cost of capacity.

The equipment cost in Table 6-4 is the average annual investment cost converted based on the service life, residual value rate, and base rate of return. The total investment of fuel cells is 1,200 USD / kWh, which is equivalent to 130,000 yen in Japanese yen. It is expected that it will reach the same level as ICE after mass production. The price of hydrogen production equipment is based on Japan's hydrogen energy related strategy in 2019, and it is planned to drop to 50000-80000Yen / kWh by 2030. In this paper, 70000Yen / kWh is selected as the total investment for calculation.

Table 6-4 Energy equipment parameters

ICE	Unit Price	3101Yen/kW
	Power efficiency	0.45
	Thermal efficiency	0.4
FC	Unit Price	13298Yen/kW
	Power efficiency	0.4
	Thermal efficiency	0.45
AC	Unit Price	3101Yen/kW
	Cold COP	1
	Heat COP	0. 9
HP	Unit Price	775 Yen/kW
	Cold COP	3. 5
	Heat COP	3. 5
CHS	Unit Price	120Yen/kWh
	Type	Water storage
	Storage loss	2% per 24hours
PV	Unit Price	5040 Yen/kW
	Type	Polysilicon
	Power efficiency	18%
Battery	Unit Price	3896Yen/kWh
	Type	Sodium-sulfur
	Storage loss	0.95
HS	Unit Price	3571Yen/kWh
	Storage loss	0.7
	Energy source	Photovoltaic

According to the above price and performance parameters, the genetic algorithm will be used to perform the optimization calculation shown in Figure 6-9 below. Because the electricity price model has strong price differences, the operation mode of the RDES is divided into two modes: Sunday and non-Sunday. The holidays refer to the Sunday mode, and in the non-Sunday mode, the summer and non-summer modes are further subdivided. Finally, the total cost is obtained through the calculation of equipment investment, energy costs and carbon tax, and the system design and optimization are aimed at the lowest total cost.

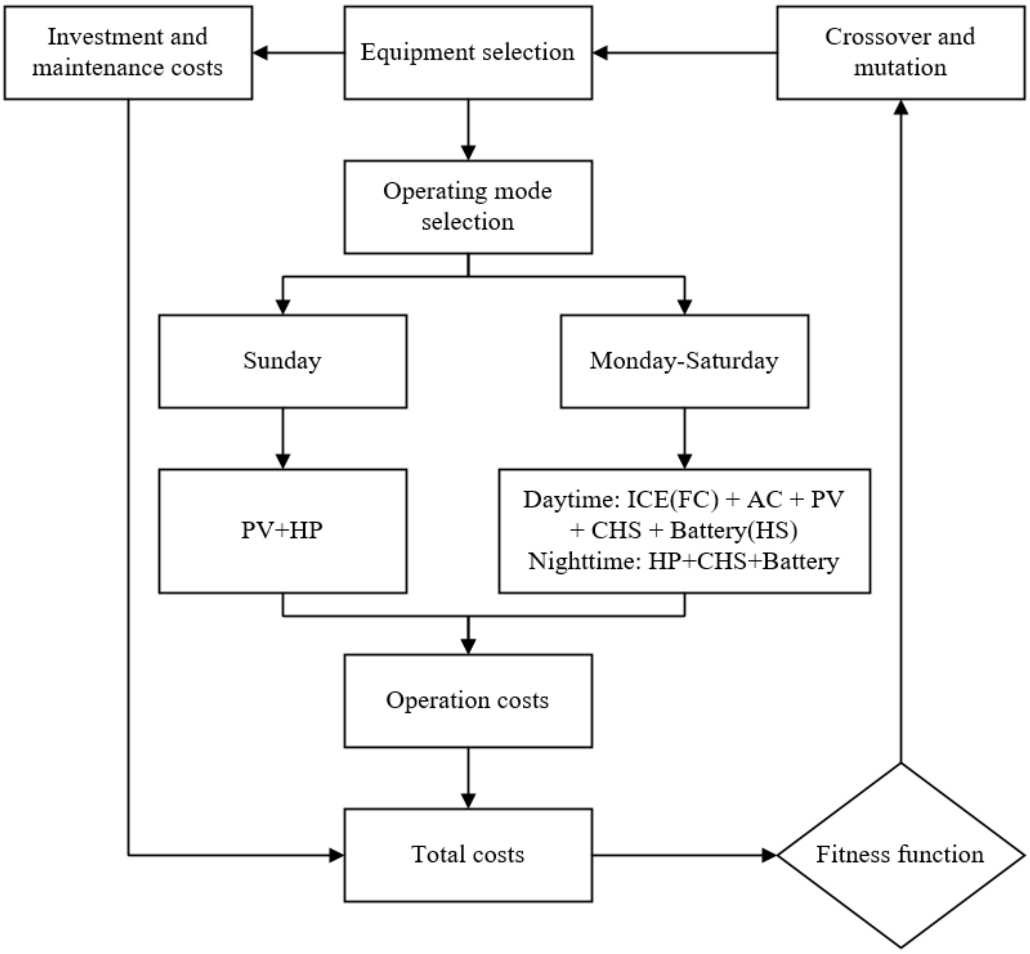

Fig 6-9 Description and optimization process of regional energy system operation mode

6.4.3 Optimization results and analysis

First, take Museum 1 as an example to explain the results. In order to highlight the comparison between ICE and FC, battery and HS, exclude the impact of PV and CHS on the overall revenue, the RDES using only HP, PV and CHS will be used as a reference value. The optimization results show that the variables fall on the boundary, the PV permeability is 40%, the installed capacity of the heat pump is 2726kW, and the total energy storage of CHS is 5454kWh. The change in carbon tax from 0 to 15 Yen / kgCO2 is shown in Fig 6-10 below.

Then calculate the total cost of hydrogen energy and conventional RDESs under different carbon taxes separately, compare with the baseline value, and calculate the total cost reduction based on the baseline value. The results are shown in Figure 6-11 below. In the case of a small carbon tax, the hydrogen energy system cannot generate revenue. The optimization results show that the values of PV, HP, and CHS fall on the boundary, and the values of FC, AC, and HS are zero. Until the carbon tax was 12 Yen / kgCO2, the total cost reduction began to occur, but the final reduction was still less than the conventional RDES. That is, under the carbon tax level of 2040, the benefit of the hydrogen RDES is still less than the conventional RDES. The carbon tax will continue to increase until 21 Yen / kgCO2, the total cost reduction will be similar to that of the conventional RDES. At this time, the installed capacity of the two systems is shown in Table 6-5. It can be seen that when the carbon tax is 21Yen / kgCO2, FC has just begun to have economic benefits. In contrast to conventional RDESs, ICE has occupied a large proportion of power generation.

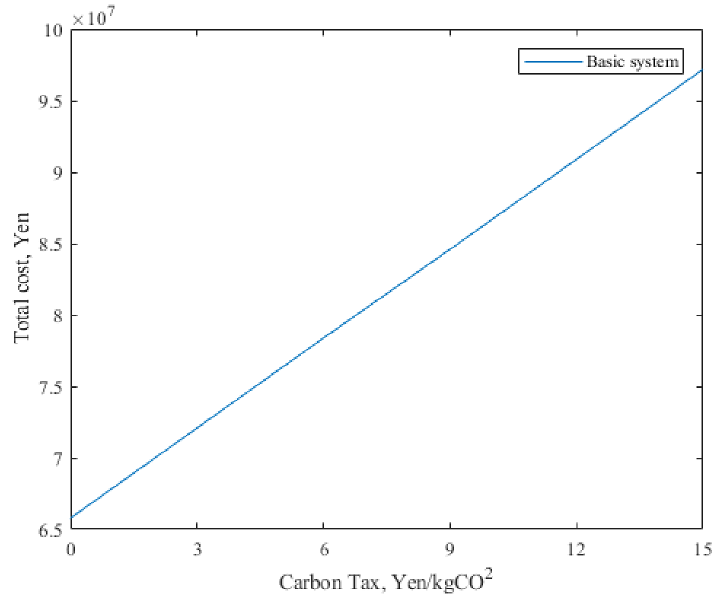

Fig 6-10 Total cost base reference value change

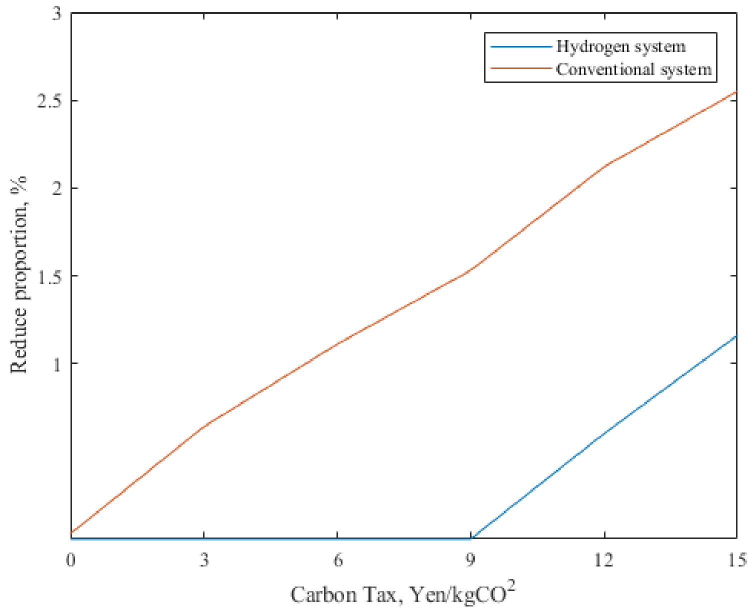

Fig 6-11 The proportion of total cost reduction under different carbon taxes

Table 6-5 Optimal results with a carbon tax of 21Yen/kgCO2

Conventional RDES					
ICE (kW)	AC (kW)	HP (kW)	CHS (kWh)	Battery (kWh)	Total cost (10^8 Yen)
397	447	2279	26	91	1.05954
Hydrogen RDES					
FC (kW)	AC (kW)	HP (kW)	CHS (kW)	HS (kW)	Total cost (10^8 Yen)
60	67	2659	657	365	1.05952

Considering future large-scale production, the price of FC will fall further, and the investment of FC will be adjusted to the same level as ICE. The optimization results of hydrogen energy and conventional regional energy system with different carbon taxes are obtained, as shown in Figure 6-12. The change of FC installed capacity with carbon tax is shown in Figure 6-13. It can be seen that the change of hydrogen energy system with carbon tax is greater than that of conventional system. When the carbon tax changes in the 12-15 stage, the hydrogen energy system has surpassed the benefits of the conventional system.

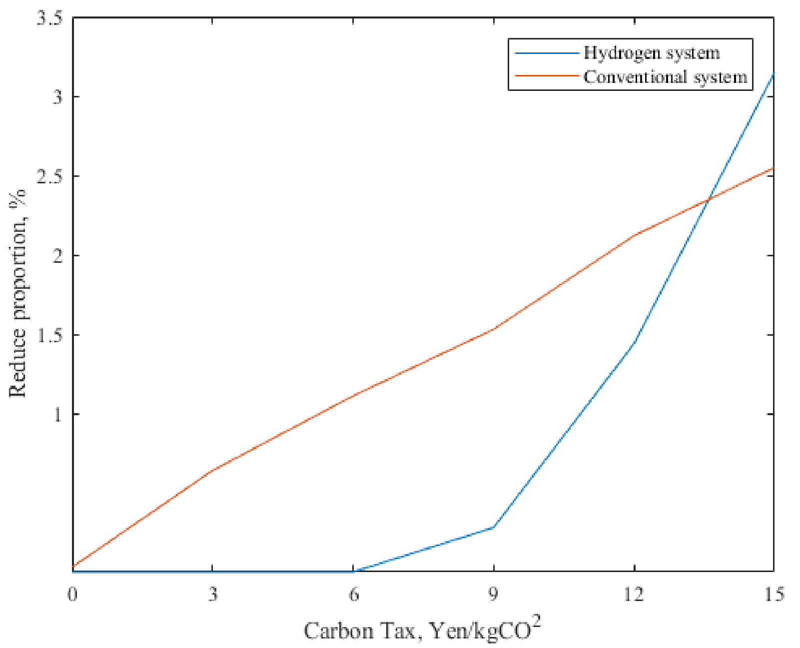

Fig 6-12 The proportion of total cost reduction under different carbon taxes

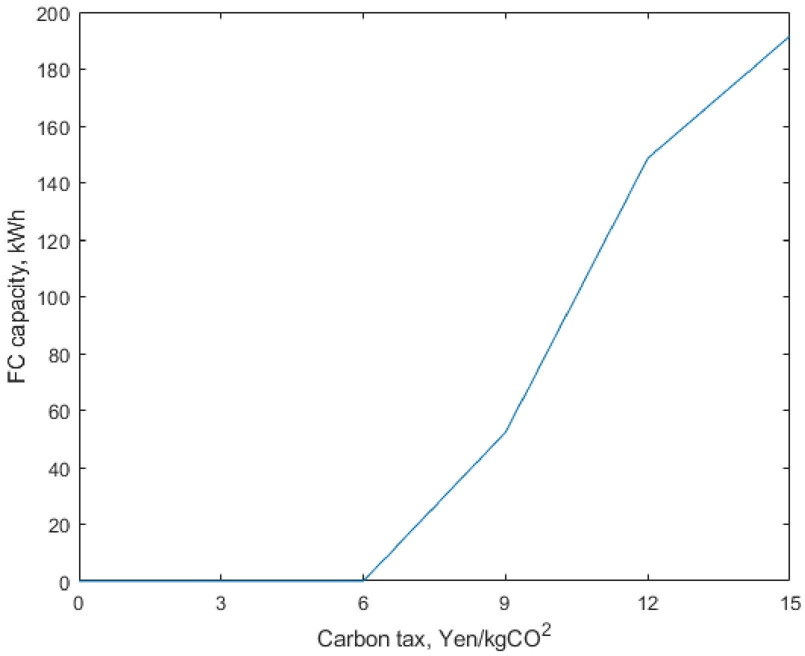

Fig 6-13 FC installed capacity under different carbon taxes

Hydrogen energy systems have a stronger carbon tax dependency than conventional systems, and the effectiveness of hydrogen energy systems depends largely on the increase in carbon taxes. At the same time, based on the cost of the current hydrogen energy system, the establishment of a carbon tax can continue to provide system benefits based on the existing PV and CHS, but the benefits provided are less than other energy systems of the same type. The cost of hydrogen energy systems still needs to be further reduced. Next, we will conduct a comparative analysis of the suitability between different buildings, as well as the sensitivity analysis of different PV penetration rates, FC costs, power and gas carbon emission coefficients, to study the future economic benefit potential of hydrogen energy systems.

6.5 Sensibility analysis and case comparison

6.5.1 Sensibility analysis

(1) FC system price

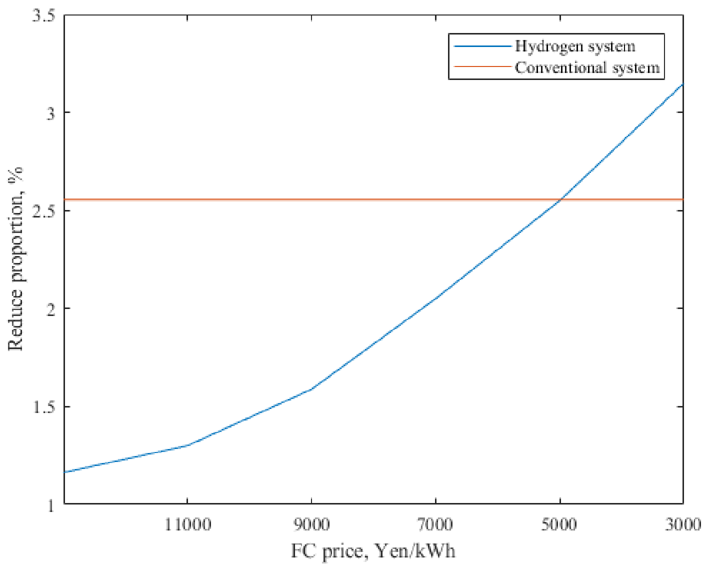

Fig 6-14 Variation curve of total cost with decreasing of FC cost

In the previous article, we calculated the current fuel cell price and when the FC price is at the same level as the ICE. It is found that the conventional RDES has better efficiency in the former case, and the hydrogen RDES has better income in the latter case. Therefore, the service life of FC will be extended to 20 years, and the price of FC will be gradually reduced from the current price to the same price level as ICE. It can be seen from Fig 6-14. When FC reaches the price of 5000Yen / kW, the two systems can achieve the same income. That is, the price of FC reaches 150% of ICE. At this time, since FC can reduce more carbon dioxide, if the government grants other related subsidies, the hydrogen RDES will be officially mainstream in the energy market.

(2) CO2 emission from electricity and natural gas

With the promotion of hydrogen energy, renewable energy will break through the bottleneck of development, and the future carbon dioxide emissions from power grids will gradually decrease. At the same time, considering the possibility of application of natural gas in the natural gas pipeline network, the carbon dioxide emissions of natural gas also have room for decline. Therefore, the carbon dioxide emissions of natural gas and electricity were reduced by 10%, 20%, and 30%, respectively. The benefits of both hydrogen energy and conventional RDESs in this case are shown in Fig 6-15,6-16.

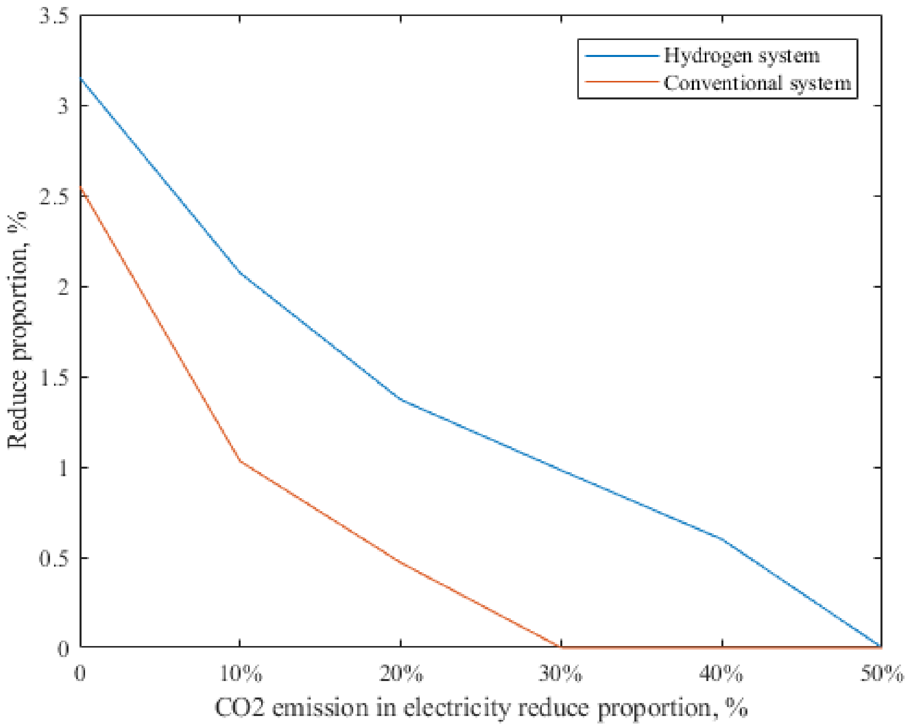

Fig 6-15 Benefits of different CO2 emission in electricity

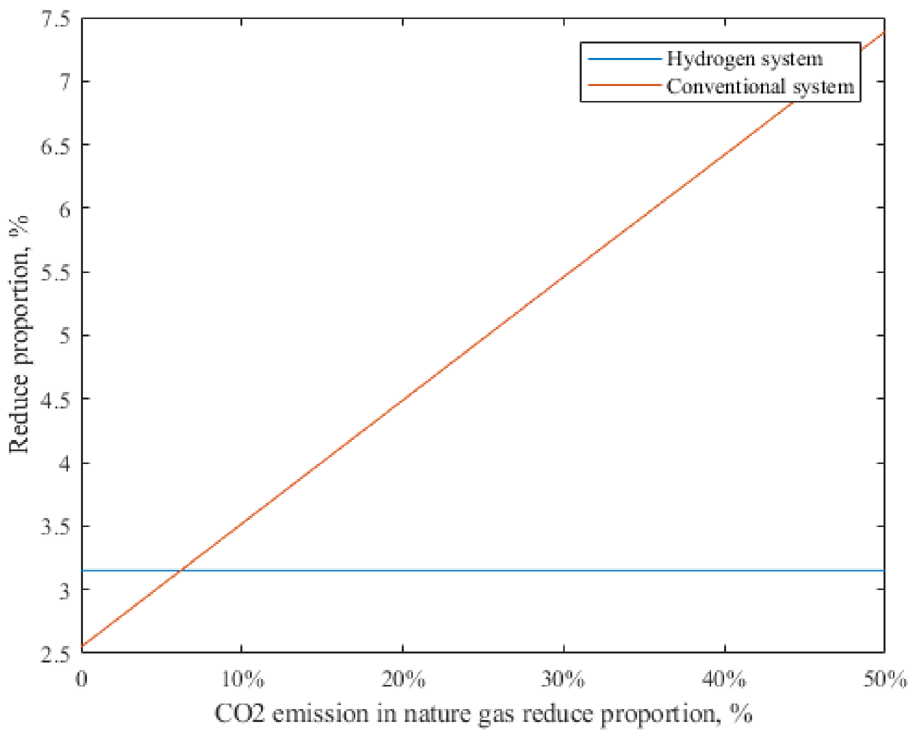

Fig 6-16 Benefits of different CO2 emission in natural gas

When the carbon dioxide emissions of electricity decrease, the benefits of both RDES will decrease. Compared with conventional RDES, the benefits of hydrogen RDES are higher, and conventional RDES appear to have no benefits earlier.

When the CO2 emissions of natural gas decrease, the benefits of conventional RDES quickly exceed that of hydrogen. Considering that the price of natural gas may increase after natural gas is doped with hydrogen, it is believed that under the condition that the proportion of natural gas doped with hydrogen does not exceed 10%, the hydrogen RDES still has a strong competitiveness

(3) PV penetration rate

FC and HS are the two cores of the distributed energy system in the hydrogen region. Among them, HS is affected by the penetration rate of photovoltaics. As the penetration rate increases, the benefit of HS in reducing hydrogen consumption will also increase. Therefore, the photovoltaic penetration rate is changed from 20% to 60%, and the total cost reduction under different penetration rates is shown in Fig 6-17.

As the phenomenon of abandoning light becomes more and more serious, the decline rate of the total cost reference value gradually becomes slow. With the increase of photovoltaic penetration rate, the hydrogen energy system has gradually increased the gap between the benefits and conventional systems.

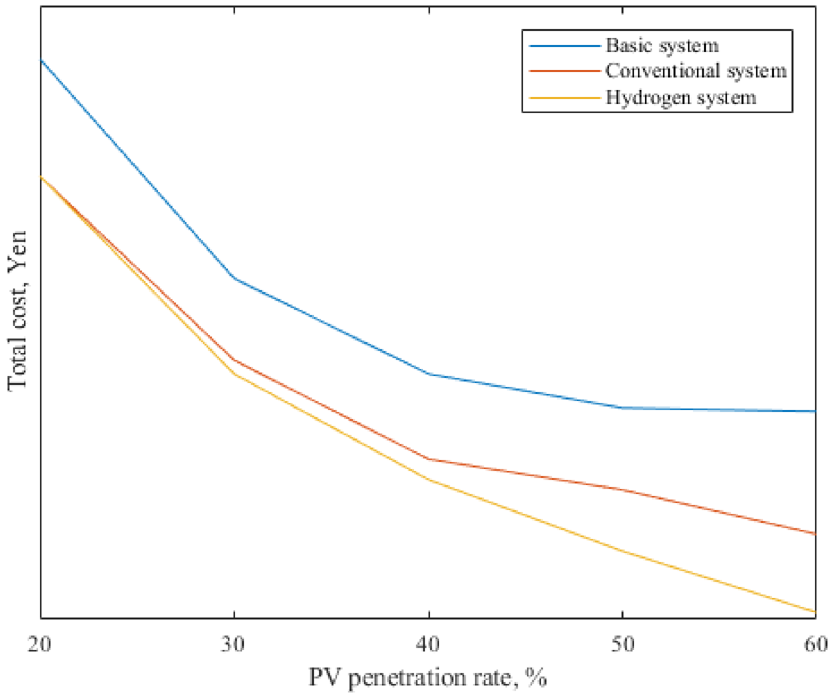

Fig 6-17 Benefits of different PV penetration rates (carbon tax: 15Yen/kgCO2)

6.5.2 Case comparison

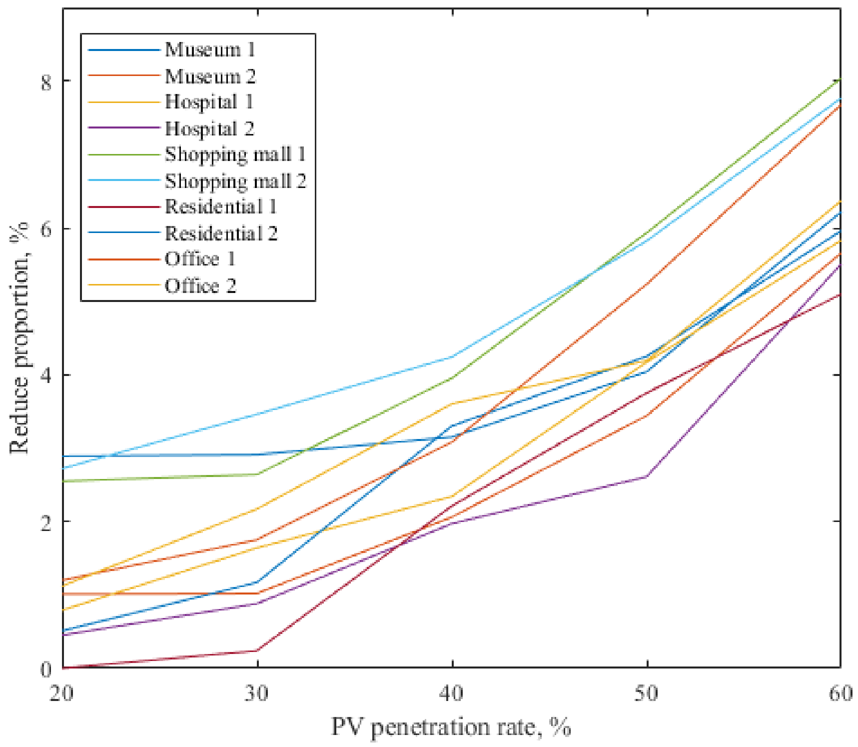

Fig 6-18 Reduce proportion of hydrogen RDES in ten buildings under different PV penetration

In order to adapt to the adaptability of different building types to hydrogen energy RDES, the optimization calculations in ten buildings under different PV penetration is carried out. (Fig 6-18)

Overall, the increase in PV permeability will bring about an increase in the economic benefits of hydrogen RDES. However, the lifting effect is different for different types of buildings. At the same time, for example, case Hospital 2 and Office 2, the improvement effect suddenly drops under a certain PV penetration rate. The reason is that the increase of PV installed capacity will affect FC's power generation revenue, so that in some types of buildings, the installed capacity of FC cannot be increased with the increase of PV. As shown in Fig 6-19 (other shows in A-3).

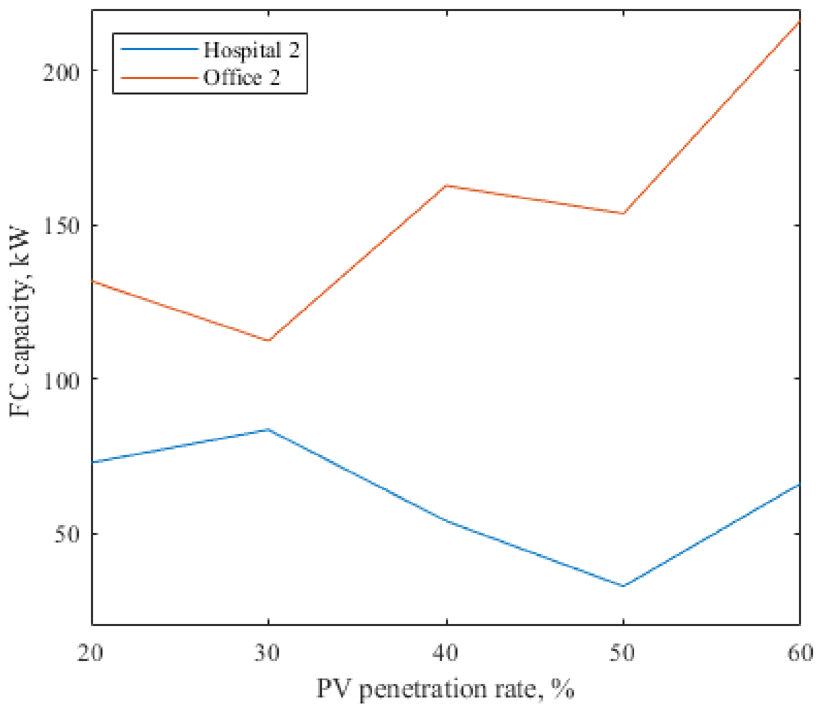

Fig 6-19 FC capacity in case Hospital 2 and Office 2 under different PV penetration

The increase in installed photovoltaic capacity will have an inhibitory effect on the increase in installed FC capacity. The increase in the amount of waste light will increase the installed capacity of HS, reduce the energy cost of hydrogen, and thus increase the installed capacity of FC. As a result, the installed capacity of FC shows periodic fluctuations with the increase of PV penetration rate. According to the power load change characteristics of Fig 6-4, 6-5 and A-1, buildings that are prone to this phenomenon have strong fluctuations in power load change. Therefore, it is considered that buildings with gentle load changes are suitable for large-scale use of hydrogen RDES, while buildings with strong changes, their hydrogen RDES can be configured according to the photovoltaic penetration limit (20-40%).

6.6 Summary

In order to analyze the economic potential of hydrogen in RDES, this paper considers introducing the concept of carbon tax to convert the environmental advantages of hydrogen energy into economic benefits. Firstly, five building types rely on hydrogen energy supply line in a demonstration area of hydrogen energy application of Kitakyushu, Japan were used as research cases, and the conventional RDES system including CCHP and PV-Battery was used as a comparative item for research and analysis. Then, the electrical load and the full-load equivalent running time method was used to forecast cooling and heating loads and curve shaping. After that, a total cost model including carbon tax was established for optimization. According to the analysis of optimization results, the price of FC had a greater impact on the benefits of RDHES. When FC was at the current cost level, RDHES can produce economic benefits, but it was less than that of conventional RDES. When the cost of FC reached the same price level as ICE, RDHES will exceeded conventional RDES under the carbon tax of 12-15Yen / kgCO2.

After that, the sensitivity analysis of FC price, PV penetration rate, and CO2 emissions of electricity and natural gas were conducted respectively. The results obtained showed that in the situation of 15Yen / kgCO2 carbon tax, when the FC price drops to about 1.5 times that of ICE, hydrogen achieves the same economic benefits as conventional RDES. At the same time, with the reduction of CO2 emissions from electricity, the benefit of hydrogen RDES decreased less and the stability was better. However, once the natural gas was mixed with hydrogen, the hydrogen RDES lost its economic advantage when the CO2 emissions of natural gas reduced more than 10%.

Finally, through the comparative analysis of different building types and buildings with varying load characteristics, it was found that with the increase of photovoltaic penetration rate, compared with conventional RDES, the economic benefit of hydrogen RDES is better and more obvious, that is, the fit with the photovoltaic system is higher. At the same time, it was found that the strong changes in the building load will inhibit the increase in the efficiency of hydrogen RDES, leading to a situation where the profitability is maximized within the photovoltaic penetration rate range of 20-40%. Therefore, it was considered that buildings with relatively gentle load changes are more suitable for large-scale introduction of hydrogen RDES systems. This result is consistent with the current demand-side management and energy consumption peak-shaving and valley-filling, which can achieve mutually beneficial effects.

This paper studied RDHES through case analysis and comparison, and obtained the carbon tax and price level that this system needs to reach the mainstream market, explored the applicability in different buildings. The result of this paper can provide a reference for the promotion of RDHES. Since the supply of hydrogen energy can be guaranteed by relying on the actual hydrogen energy supply line, the system application research in this paper has strong practical significance. However, the article only considered a price system of peak and valley electricity prices, and did not compare different price systems. At the same time, only the electrolysis of hydrogen from abandoned electricity is used, and no consideration is given to the production of hydrogen from valley electricity or other renewable energy sources. The article still has room for further research.

Appendix

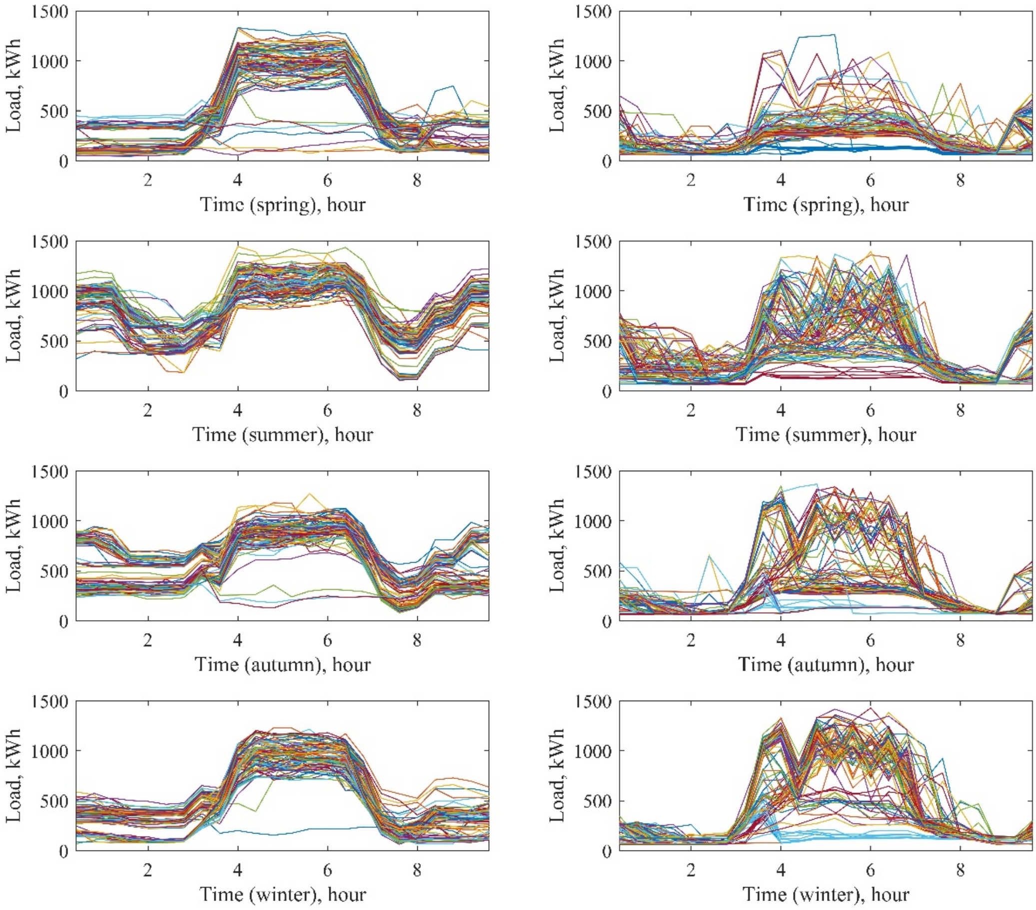

(a) Museum 1& Museum 2

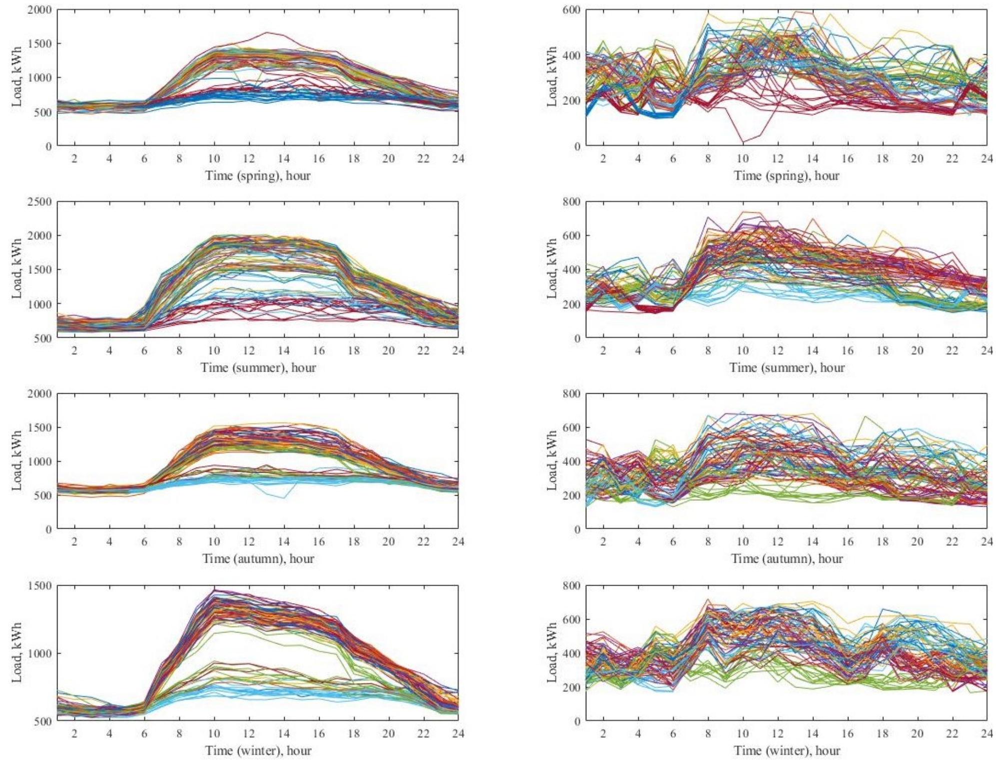

(b) Hospital 1& Hospital 2

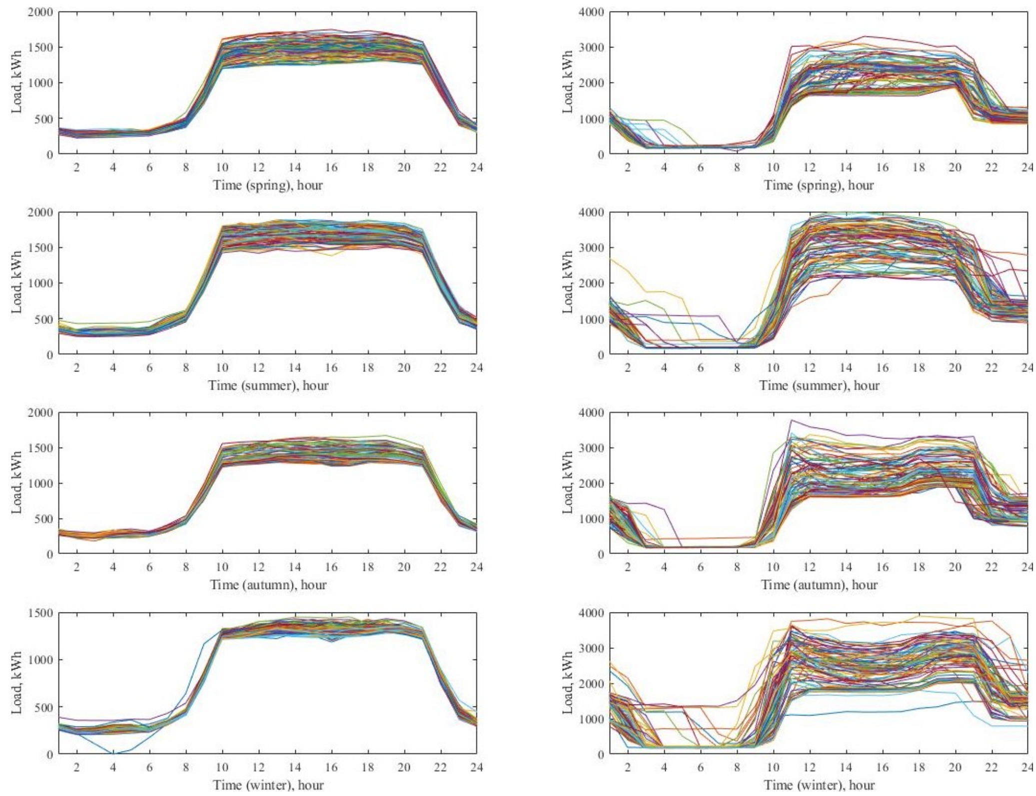

(c) Shopping mall 1& Shopping mall 2

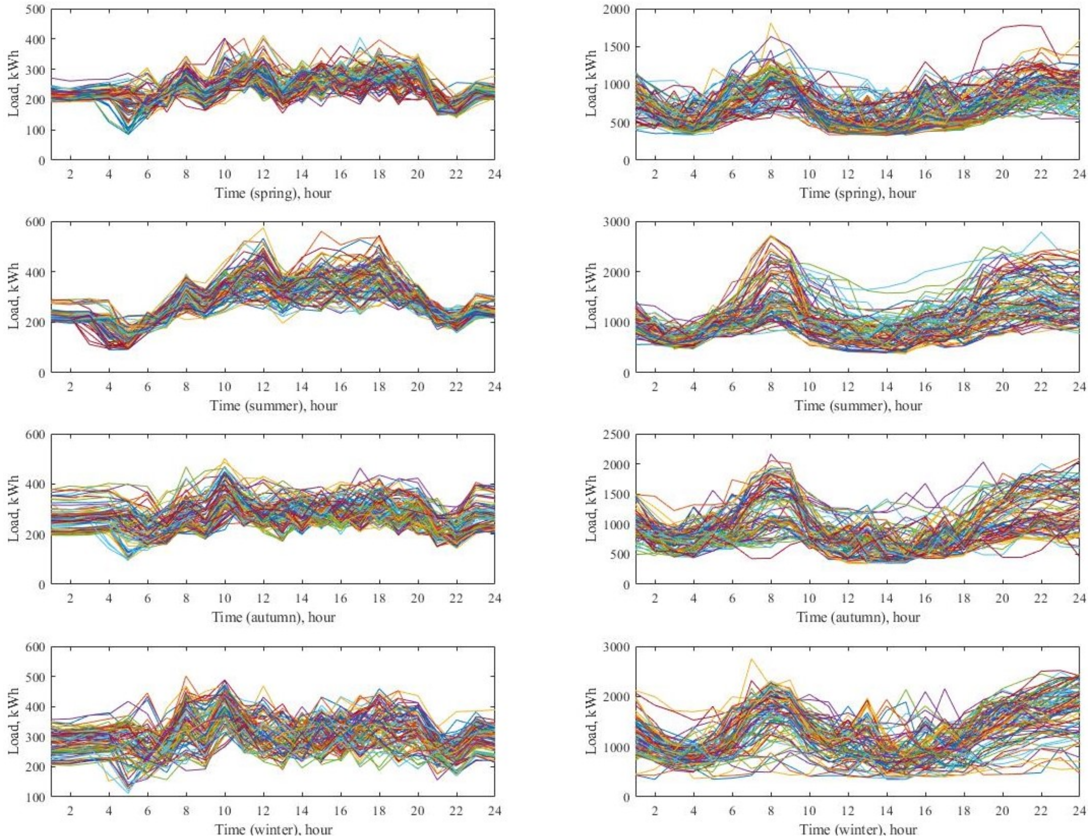

(d) Residential 1& Residential 2

Fig A-1 Typical daily changes in the four seasons of museum, hospital, shopping mall and residential buildings (electricity load)

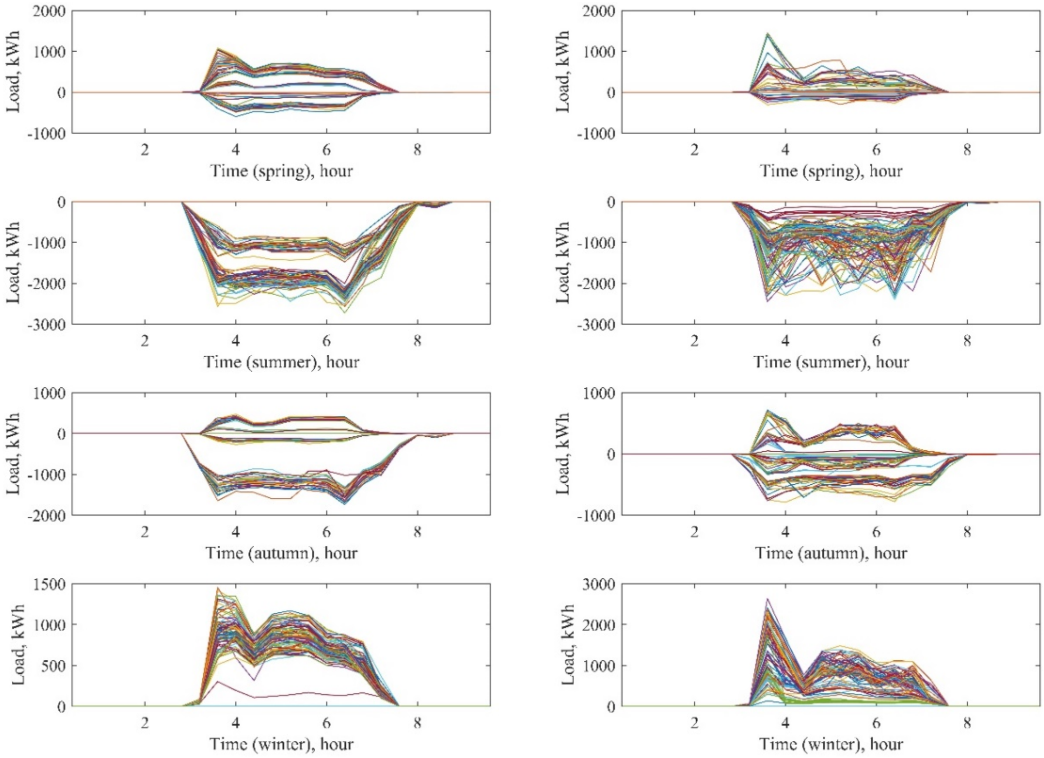

(a) Museum 1& Museum 2

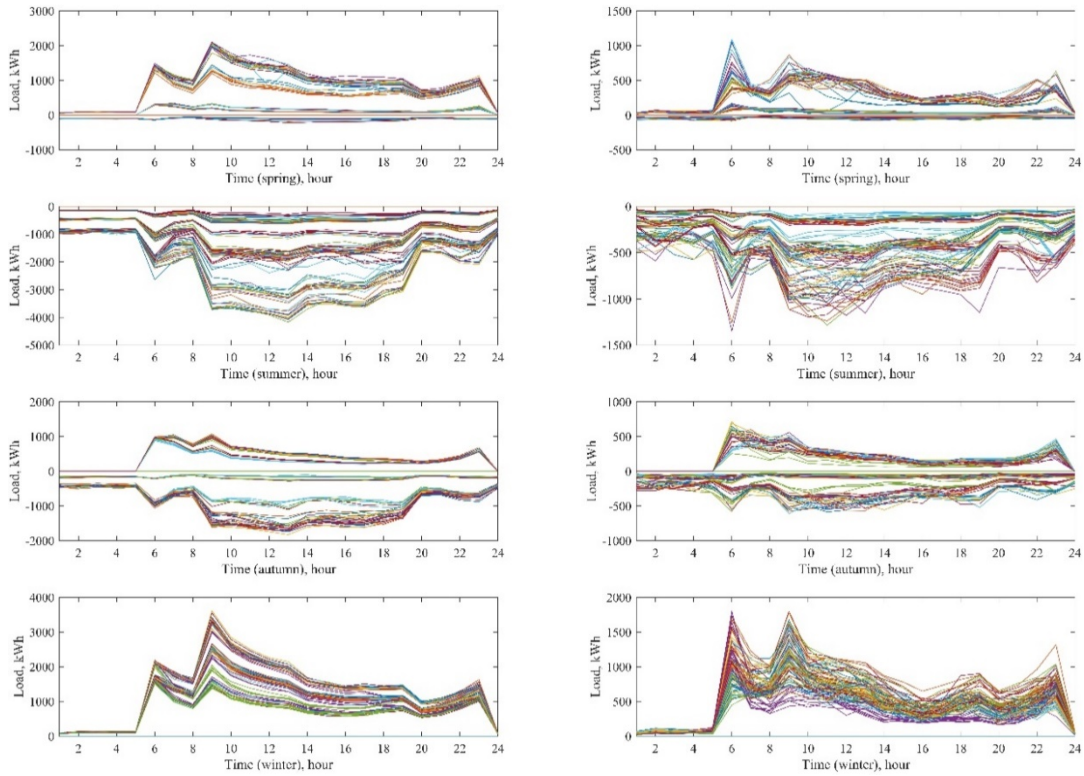

(b) Hospital 1& Hospital 2

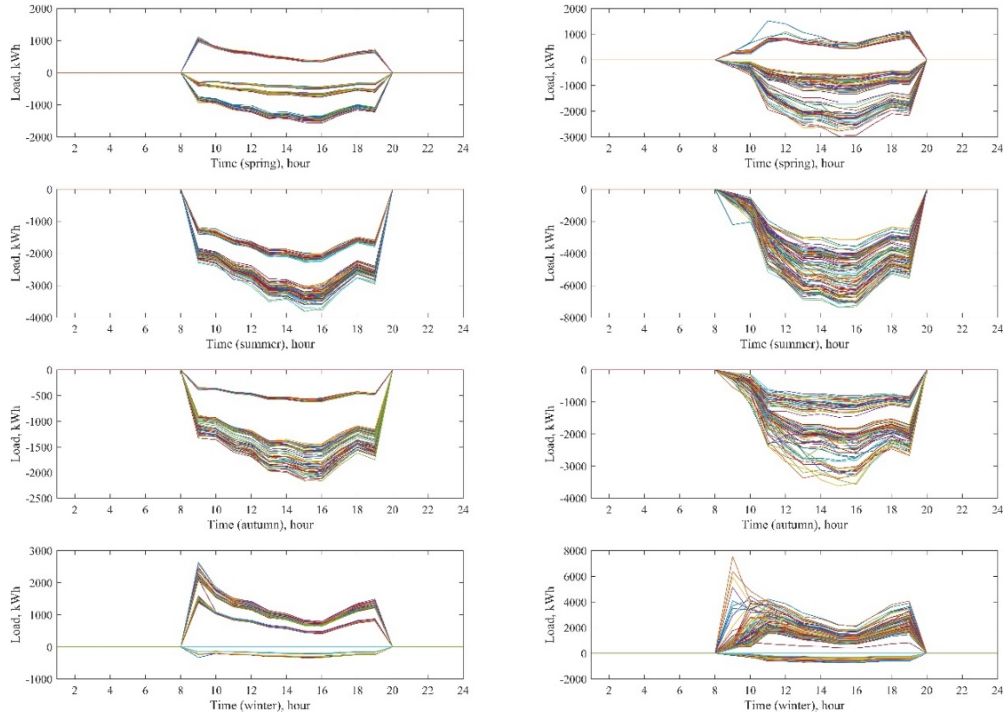

(c) Shopping mall 1& Shopping mall 2

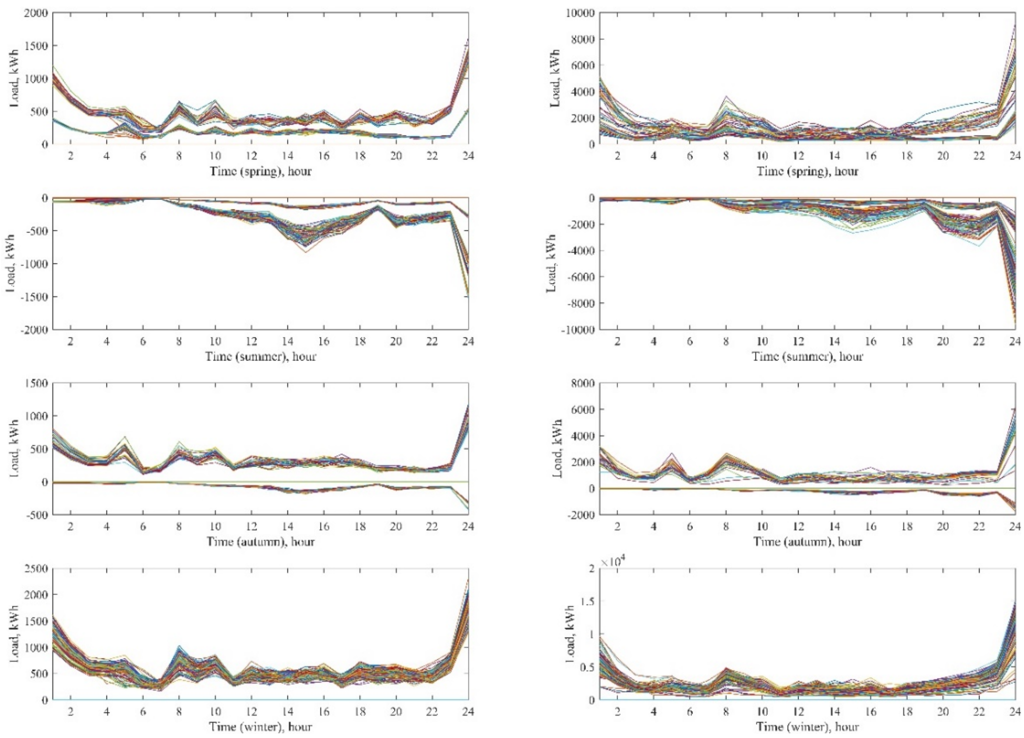

(d) Residential 1& Residential 2

Fig A-2 Typical daily changes in the four seasons of museum, hospital, shopping mall and

residential buildings (cold and heat load)

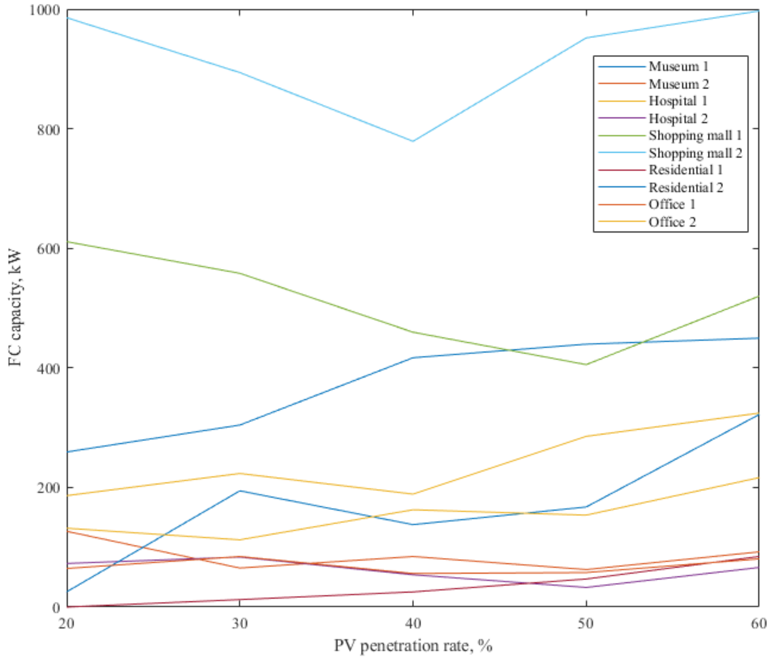

Fig A-3 FC capacity in ten buildings under different PV penetration

Reference

[1] van der Roest, Els, et al. "Introducing Power-to-H3: Combining renewable electricity with heat, water and hydrogen production and storage in a neighbourhood." Applied Energy 257 (2020): 114024.

[2] Abdin, Z., and W. Merida. "Hybrid energy systems for off-grid power supply and hydrogen production based on renewable energy: A techno-economic analysis." *Energy Conversion and Management* 196 (2019): 1068-1079.

[3] Agency for Natural Resources and Energy, Hydrogen / fuel cell strategy roadmap, March 12, 2019. https://www.meti.go.jp/press/2018/03/20190312001/20190312001.html

Chapter 7

STUDY ON THE HYDROGEN IMPLICATION OF ENERGY STRUCTURE WITH CARBON TAX INTRODUCTION

CHAPTER SVEN: STUDY ON THE HYDROGEN IMPLICATION OF ENERGY STRUCTURE WITH CARBON TAX INTRODUCTION

7.1 Contents

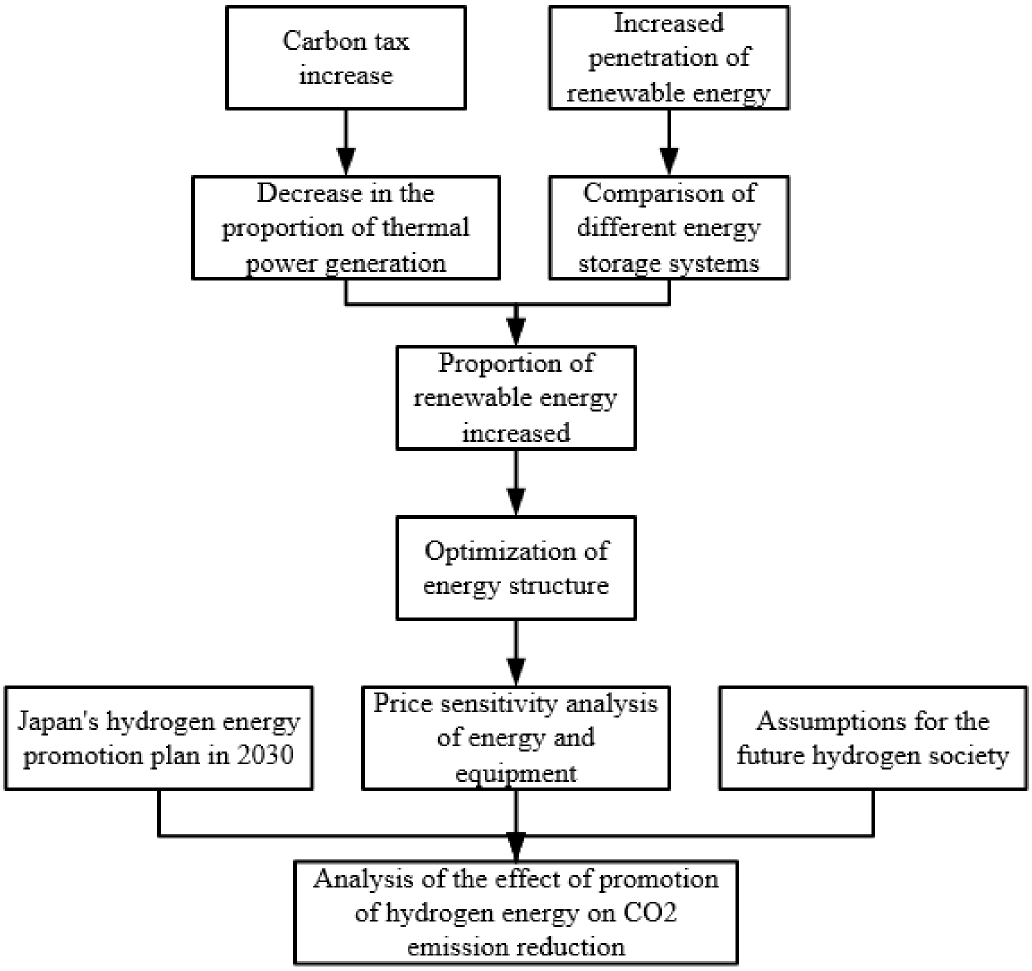

Fig 7-1 Research logic of the influence of hydrogen energy on energy structure and carbon emissions

In this part, according to the characteristics of no carbon dioxide emission when hydrogen energy system is used, the strategic planning and price prediction of hydrogen energy system and carbon tax in Japan and the United States are sorted out.

The overall logic of the article is shown in Fig 7-1 below. Firstly, the three energy storage technologies of battery, pumped storage and hydrogen storage were compared with the application in different renewable energy sources. Then ten power companies in Japan was selected and the weighted on-grid electricity price was used as the objective function to study the energy structure changes under different carbon taxes. According to the characteristics of long-distance and inter-seasonal storage, the effect of renewable energy coordination and scheduling in Japan was studied. Then through sensitivity analysis, the impact of price fluctuations of coal, LNG, photovoltaic equipment, wind power generation equipment and hydrogen energy production equipment on the research results was obtained. Finally, from the power generation field to the overall primary energy consumption, the effects of three kinds of hydrogen energy promotion measures for household fuel cells, fuel cell vehicles and natural gas dropped with hydrogen on CO2 emission reduction was carried out to explore the introduction of hydrogen energy to help Japan achieve its CO2 reduction goals.

7.2 Methodology

The logic diagram of optimization is shown in Figure 7−2. Due to the limitation of carbon tax, the economic benefits of thermal power plants have declined. Through the way of weight distribution, the reduction of thermal power plants will be filled by renewable energy. Combined with the energy storage system, the minimum feed-in tariff of different renewable energy is calculated. On the one hand, it is compared with the thermal power plant, on the other hand, it is compared internally. If the lowest weighted feed in tariff obtained by each weight distribution does not decrease significantly compared with the last time, the optimization output will be finished, otherwise, the weight will be redistributed until it reaches the limit of the set adaptive function.

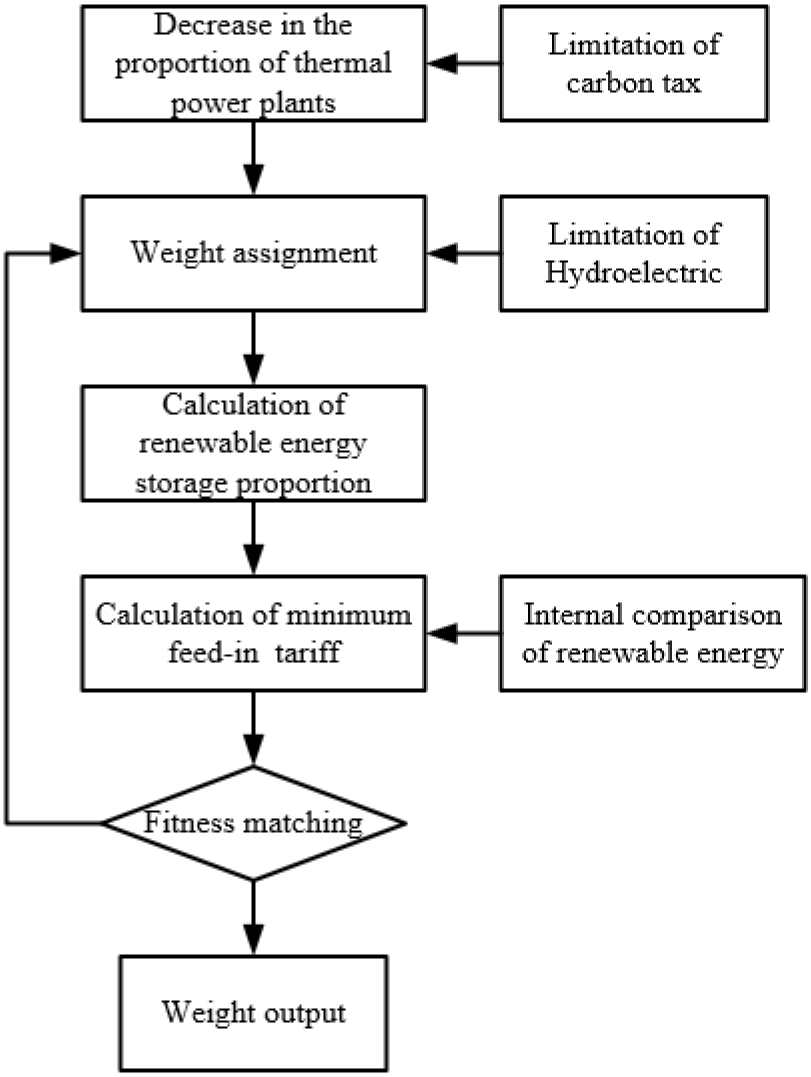

Fig 7−2 Optimization logic diagram

7.3 Comparison between hydrogen storage and conventional energy storage technology

Table 7−1 Parameters of energy storage technology and renewable energy [1]

	Hydrogen energy storage	Pumped storage	Battery
Investment cost (10^4Yen)	40	20	15
Energy storage loss	0.3	0.2775	0.23

Table 7−2 Parameters of renewable energy [2]

	Photovoltaic	Hydroelectric	Onshore wind	Offshore wind
Investment cost (10^4Yen)	22.2	40	28.4	51.5
Generation cost (Yen)	4.6	2.5	8.3	17.5
Equipment utilization	0.1-0.2	0.4-0.5	0.2-0.3	0.25-0.35
Equipment life (Year)	30	40	20	20

From the perspective of hydrogen production from renewable energy, the following three energy storage technologies will be compared economically: hydrogen storage, pumped storage and battery. The difference between the calculation of investment payback period and the calculation of investment payback period is that the renewable energy feed in tariff can be recovered within the service life after the calculation is introduced into different levels of energy storage technology. The basic parameters of energy storage technology and renewable energy are shown in table 7−1, table 7-2 above.

Whenever there is a surplus of renewable power generation, the surplus power will be stored, such as energy storage system, and used when necessary. As shown in Fig 7−3, 7−4, 7−5, 7−6 below, the minimum feed-in tariff of three kinds of energy storage technologies after they are used in case of surplus of different renewable energy. The minimum feed-in tariff is defined as the feed-in tariff that can make the renewable energy system and energy storage system recover within the service life.

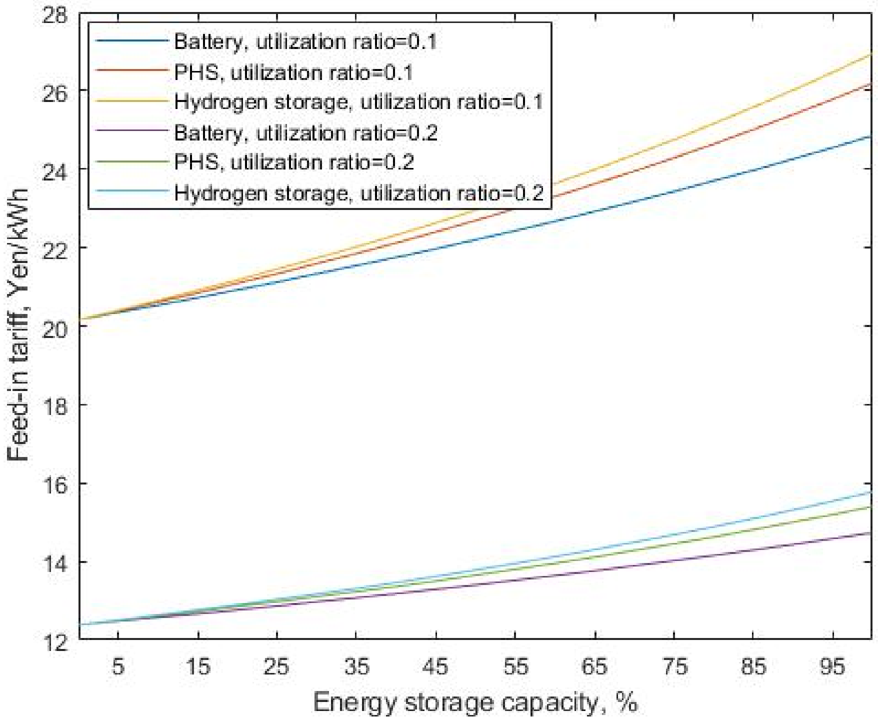

Fig 7−3 The minimum feed-in tariff with photovoltaic

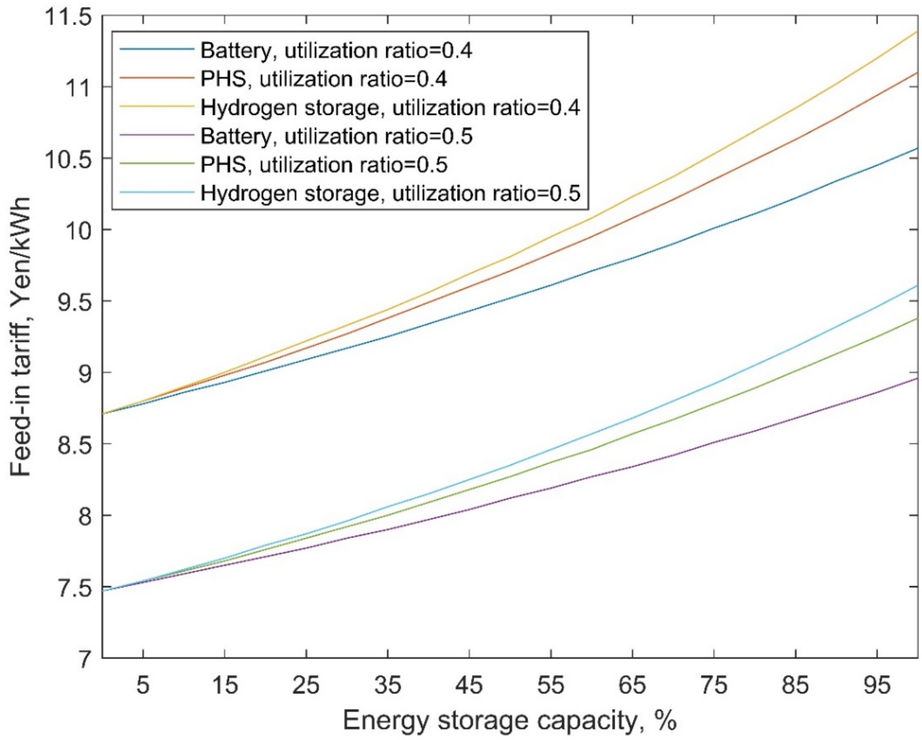

Fig 7−4 The minimum feed-in tariff with Hydroelectric

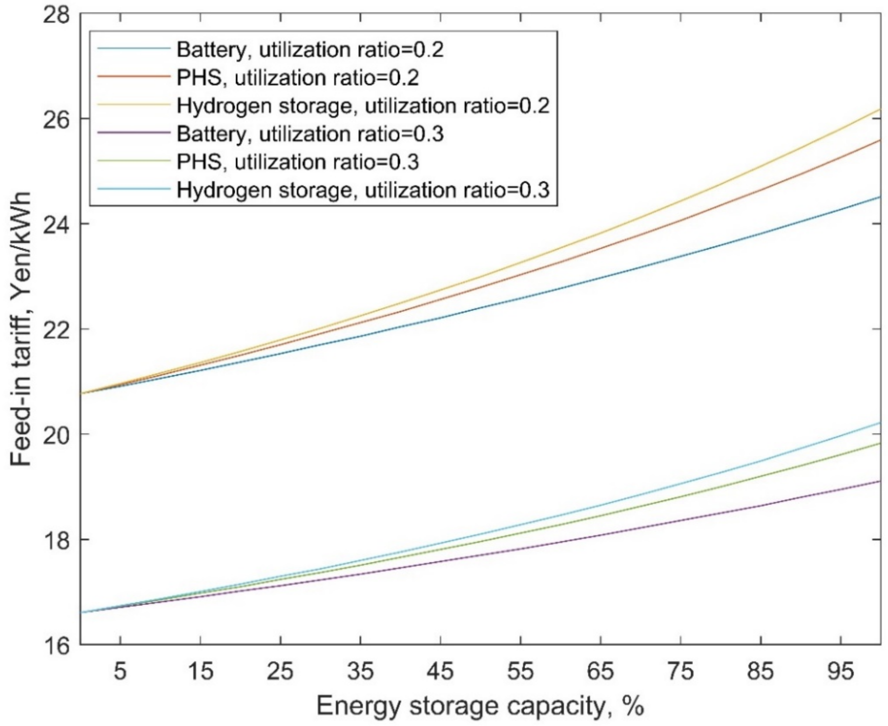

Fig 7-5 The minimum feed-in tariff with On-shore wind

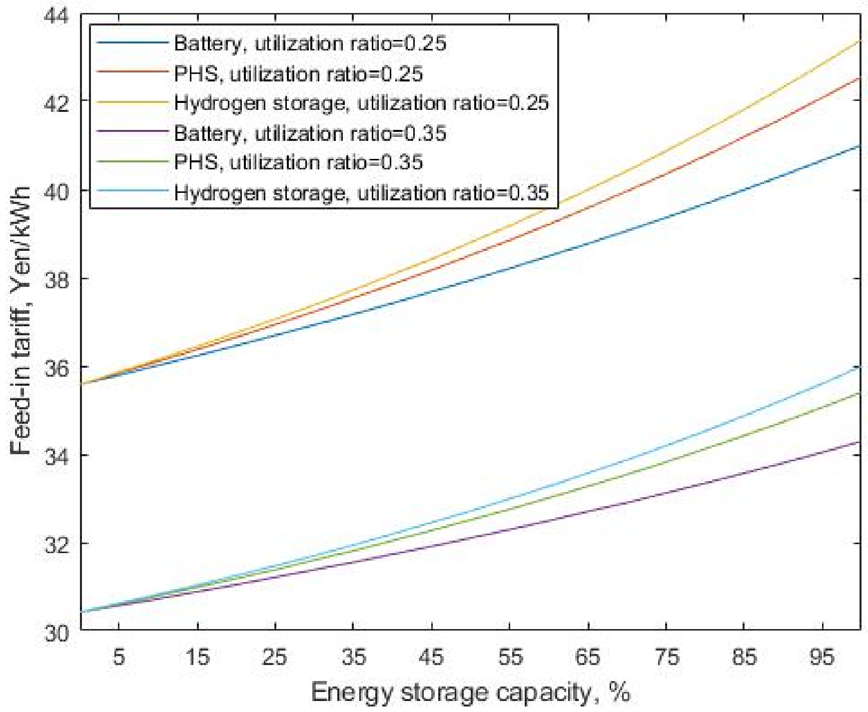

Fig 7-6 The minimum feed-in tariff with Off-shore wind

It can be seen that in terms of renewable energy, the lowest feed-in tariff of hydropower is the lowest of the four energy types. Although the investment cost of hydropower is high, its maintenance cost is low and the equipment utilization rate is the highest, so the economic benefit is the best. Compared with land-based wind power generation, offshore wind power generation has a higher utilization rate of equipment, but its investment and maintenance costs are too high, so its minimum feed-in tariff is the highest of the four energy types. The minimum feed-in tariff of photovoltaic has a great impact on the utilization rate of equipment. When the utilization rate of equipment is high, its minimum feed-in tariff is lower than that of wind power generation. When the utilization rate of the equipment is low, its minimum feed-in tariff is basically the same as that of onshore wind power generation.

In terms of energy storage technology, the economic benefit of battery is the best, and the economic benefit of hydrogen storage is the worst, because the equipment investment of fuel cell is higher than that of battery and pumped storage. However, the storage battery cannot be used in large-scale storage, and pumped storage is also limited by objective conditions. Therefore, hydrogen storage in the initial stage of development can be used as a supplement to pumped storage. After the equipment cost is reduced, hydrogen storage is not limited by objective conditions, and the characteristics of long storage time can be fully demonstrated.

7.4 Optimization of energy structure for the purpose of feed in tariff

This chapter will discuss the change of economic benefits of conventional thermal power plants after the introduction of carbon tax. The previous analysis of renewable energy storage technology will be combined to study the optimal change of energy structure with the lowest feed-in tariff as the goal.

7.4.1 Economic benefit analysis of coal-fired and gas-fired power station

(1) Excluding carbon tax

In conventional thermal power generation, coal-fired power plants and gas-fired power plants account for the largest proportion. This paper also chooses these two kinds of power plants as representatives to analyze the economic benefits of thermal power generation.

According to the survey conducted by Japan comprehensive energy resources survey in 2010, the utilization rate of coal-fired power plants and gas-fired power plants in Japan is 72.3% and 52.8% respectively.[3]

The economic parameters in the process of investment and operation and maintenance are shown in table 7−3.

Table 7−3 Investment, operation and maintenance cost of coal-fired and gas-fired power plant

	Coal-fired power plant	Gas-fired power plant
Utilization ratio	50%-80% (average 72.3%)	50%-80% (average 52.8%)
Service life	30-40	30-40
Investment cost (10^4Yen/kW)	23	12
Fixed assets tax	1.4%	1.4%
Depreciation charge	5%	5%
Personnel wage (10^8 Yen/Year)	4.1	7.3
Repair cost (Yen/kW)	3450	2400
Other maintenance costs (Yen/kW)	3450	1080
Fuel cost (Yen/t)	1700	2200
Calorific value of fuel (MJ/kg)	25.7	54.6
Electric efficiency	42%	51%
Power consumption from the power plant	6.2%	2.0%

Table 7−4 Dynamic recovery period of coal-fired and gas-fired power plants

	Coal-fired power generation	Gas-fired power generation
Utilization ratio	Electricity selling price: 10.5 Yen/kWh	Electricity selling price: 13.5 Yen/kWh
80%	22.37	15.31
70%	29.37	19.52
60%	42.56	26.56
50%	Cannot be recycled	40.14

According to the economic parameters of power plant investment, operation and maintenance, the dynamic recovery cycle of power plant can be calculated under different feed-in tariff. As shown in table 7−4 above, the minimum feed in tariff that can be recovered within 40 years for coal-fired and gas-fired power plants is 10.5yen/kwh and 13.5yen/kwh respectively. As it is a large-scale investment project, 80% of the investment cost is considered to be bank loans. It can be seen that the minimum feed-in tariff of coal-fired power plants is lower than that of gas-fired power plants, and the main reason is that the fuel cost of gas-fired power plants is higher. However, the sensitivity of coal-fired power plant to equipment utilization is higher. Once the equipment utilization rate decreases, it will cause more serious economic losses.

(2) Including carbon tax

When the carbon tax is included in the calculation of economic benefits of coal-fired and gas-fired power plants, there will be a certain increase in the minimum feed-in tariff to cope with the carbon dioxide emissions generated in the process of power generation.

The minimum feed-in tariff after setting the carbon tax at 2.17, 6.52, 10.87 and 15.22 Yen/ kg-CO2 is shown in table 7-5 and table 7-6 below, respectively corresponding to the carbon tax forecast value in 2020-2040.

Table 7-5 Minimum feed-in tariff of coal-fired power plant with carbon tax.

	Carbon tax (Yen / kg-CO2)			
Utilization ratio	2.17	6.52	10.87	15.22
80%	11.97	16.44	20.91	25.38
70%	12.33	16.80	21.27	25.74
60%	12.81	17.28	21.75	26.22
50%	13.49	17.96	22.43	26.90

Table 7-6 Minimum feed-in tariff of gas-fired power plant with carbon tax

	Carbon tax (Yen / kg-CO2)			
Utilization ratio	2.17	6.52	10.87	15.22
80%	14.95	19.42	23.89	28.36
70%	15.14	19.61	24.08	28.55
60%	15.39	19.86	24.33	28.80
50%	15.74	20.21	24.68	29.15

It can be seen that there is a price gap of about 3 yen between coal-fired and gas-fired power plants, and both of them rise with the rise of carbon tax. Moreover, due to the low carbon emission of gas, the change of equipment utilization rate has a low impact on its economic benefits.

According to the average equipment utilization rate of coal-fired and gas-fired power plants of 72.3% and 52.8% respectively, the minimum feed-in tariff under different carbon taxes is calculated, and Fig 7-7 is obtained.

In the subsequent energy structure optimization, the feed-in tariff of thermal power generation will be calculated according to the lowest feed-in tariff in fig 7 and the proportion of coal-fired and gas-fired power plants.

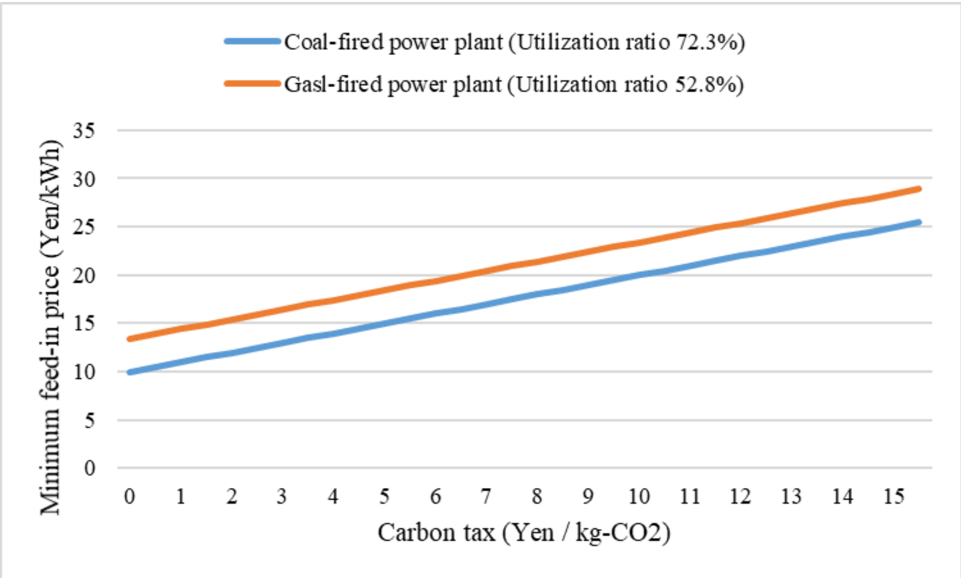

Fig 7−7 Minimum feed-in tariff under different carbon tax in coal-fired and gas-fired power plants

7.4.2 Optimization of energy structure

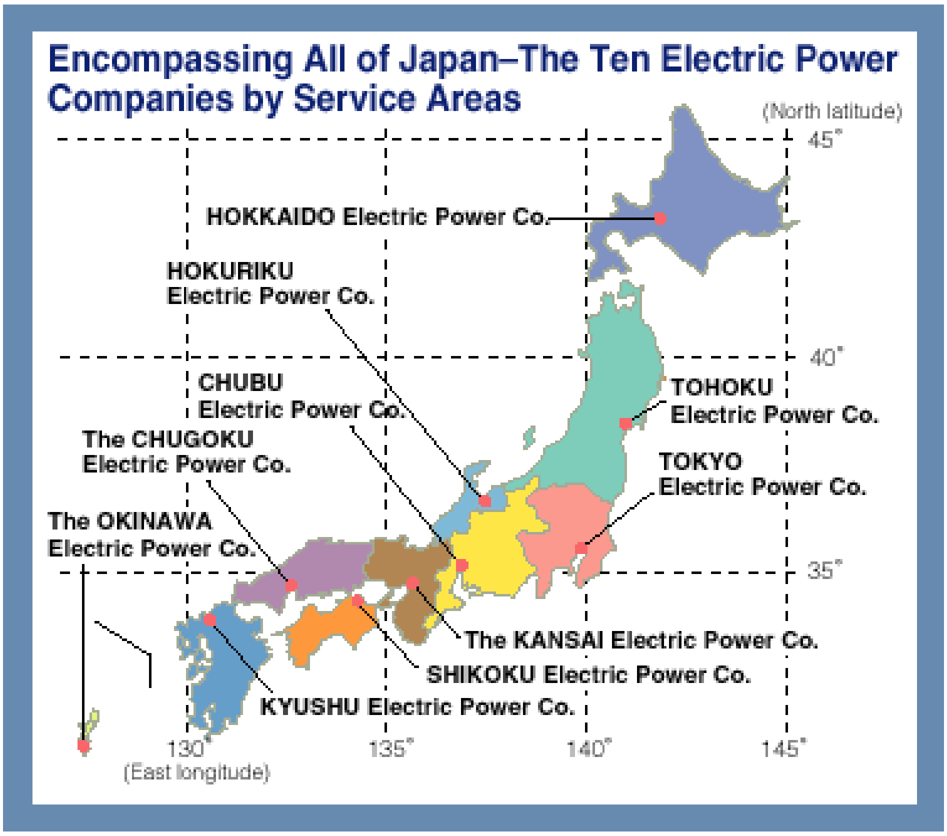

Fig 7-8 Distribution map of major power companies in Japan [4]

The research object of this article is ten power companies in Japan. The distribution and supply scope of each power company are shown in Figure 7-8 below. All power companies can supply about 92% of the electricity demand in Japan. Other electric power mainly comes from the small power suppliers newly added after the liberalization of the power market and the distributed power supply on the user side. Most of these small and distributed power sources are renewable energy, which does not affect the results of the research. Therefore, it is believed that the ten power companies studied in this article can reflect the power supply situation in Japan.

The power generation data of one year from April 2019 to March 2020 of ten electric power companies of Japan is selected as the calculation basis. The initial installed capacity of various energy sources and the proportion of power generation are shown in table 7-7 below.

Japan has ten power companies in this category, namely, Hokkaido Electric Power Company, Tohoku Electric Power Company, TEPCO, Chubu Electric Power Company, Hokuriku Electric Power Company, Kansai Electric Power Company, Chugoku Electric Power Company, Shikoku Electric Power Company, Kyushu Electric Power Company, and Okinawa Electric Power Company.

Table 7-7 Proportion of installed capacity of various energy sources of ten electric power companies

Company	Thermal power	Hydroelectric	Solar energy	Wind power	Nuclear, biomass and other sources
Hokkaido Electric Power Company	77.03%	11.83%	6.51%	3.73%	0.90%
Tohoku Electric Power Company	66.23%	15.67%	8.46%	3.52%	6.13%
Tokyo Electric Power Company	88.53%	4.52%	5.92%	0.37%	0.67%
Chubu Electric Power Company	83.05%	8.17%	8.39%	0.40%	0.00%
Hokuriku Electric Power Company	65.65%	27.75%	4.01%	0.75%	1.85%
Kansai Electric Power Company	67.79%	8.15%	5.02%	0.27%	18.77%
Chugoku Electric Power Company	81.84%	4.28%	10.10%	0.74%	3.05%
Shikoku Electric Power Company	51.96%	12.20%	11.68%	1.69%	22.47%
Kyushu Electric Power Company	43.38%	4.61%	12.37%	0.77%	38.86%
Okinawa Electric Power Company	94.08%	0.02%	5.01%	0.39%	0.49%
Total	75.93%	7.77%	7.29%	0.86%	8.16%

Among them, according to the data on the official website of Tokyo Electric Power Company, coal-fired and gas-fired power plants account for the vast majority of thermal power generation, except for 2% of oil-fired power plants. Therefore, according to the average equipment utilization rate of coal-fired and gas-fired power plants, the initial minimum online electricity price of thermal power generation without carbon tax is calculated as 12.3Yen/kWh. This price is used to represent the current economic level of Japanese thermal power plants.

Next, the lowest weighted feed in tariff under different carbon taxes and the corresponding energy structure will be calculated. Four assumptions are made for this optimization:

1) In order to simplify the model, the energy storage loss of pumped storage is approximately 0.3 from 0.2775, which is the same as that of hydrogen storage.

2) As we can see from the above comparison that the economic benefit of hydropower is the best, when the proportion of thermal power decreases, the proportion of hydropower will be expanded preferentially. However, due to the limitation of the objective environment, the maximum proportion of hydropower can reach 0.2 and 0.3 respectively. When hydropower reaches its maximum share, the economic best of onshore wind power and photovoltaic power will be used instead.

3) It is considered that renewable energy can replace thermal power generation in full, that is, when the maximum proportion of hydropower generation is reached, the remaining demand can be fully met by onshore wind power generation or photovoltaic power generation.

4) Considering that the initial stage is mainly pumped storage, when the pumped storage can not achieve peak cutting and valley filling in a day, the hydrogen storage system is used, which can span a long time and a long distance storage characteristics, to make up for the shortcomings of the pumped storage system.

7.4.3 Results analysis and discussion

When the carbon tax changes from 0-16Yen / kg-CO_2 and the maximum proportion of hydropower is 0.1, 0.2 and 0.3 respectively, the lowest weighted feed-in tariff is shown in Fig 7-9.

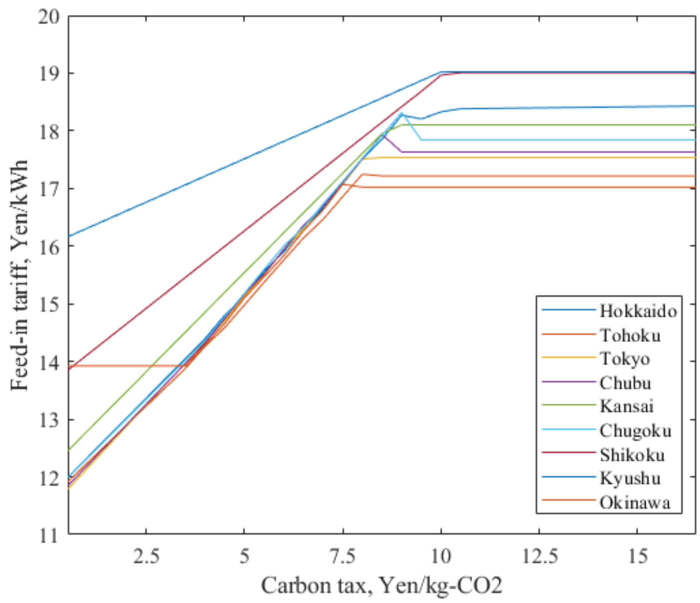

(a) Hydroelectric power generation = 0.2

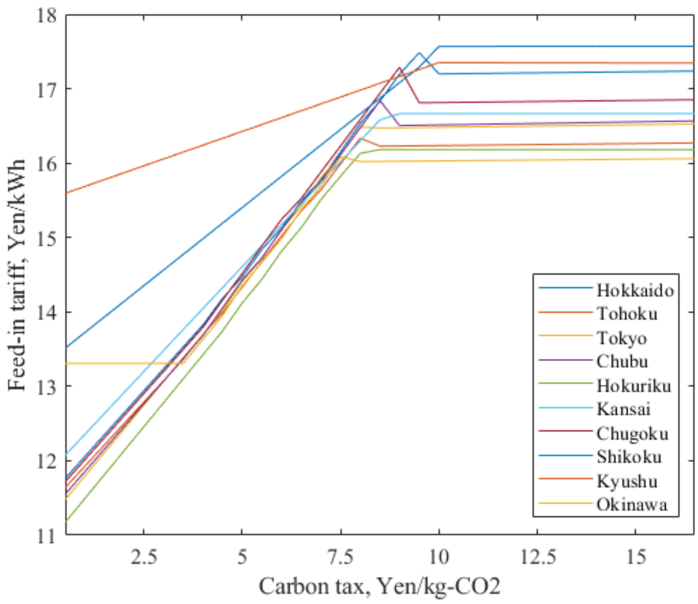

(b) Hydroelectric power generation = 0.3

Fig 7-9 The lowest weighted feed-in tariff under different carbon taxes

Taking the maximum power generation ratio of hydropower generation as 0.2 as an example, Fig 7-10 below shows the proportion of thermal power generation under different carbon taxes. It can be seen that the proportion of thermal power generation in most power companies come to zero under the carbon tax of 7.5-10Yen/kgCO2, that is, achieve 100% renewable energy supply.

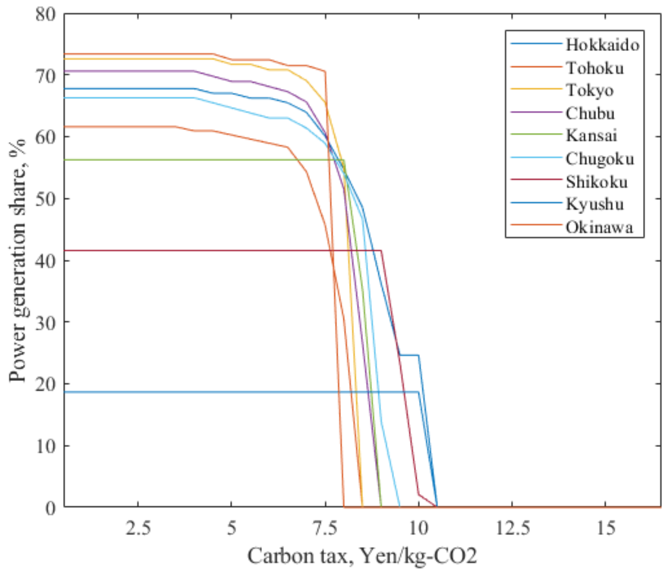

Fig 7-10 The proportion of thermal power generation under different carbon taxes

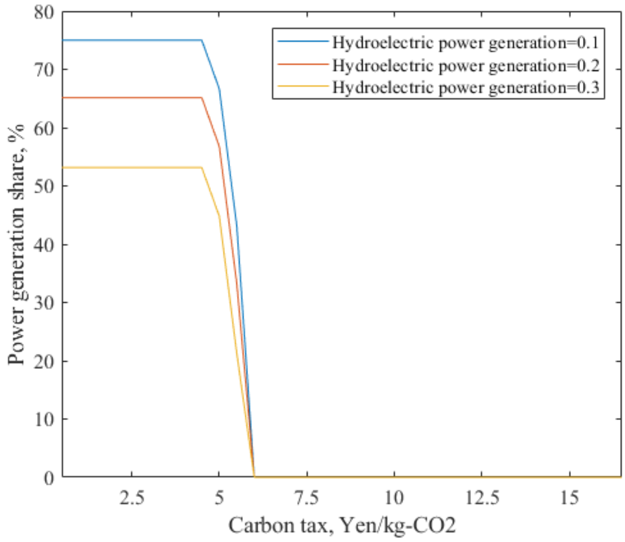

Fig 7-11 The proportion of thermal power generation under different carbon taxes and hydropower generation in Japan

Assuming that based on the characteristics of long-distance and inter-seasonal storage of hydrogen energy, Japan's renewable energy systems can be coordinated and dispatched. As a result, as shown in Fig 7-11, thermal power generation will reach zero before the carbon tax of 7.5 Yen/kgCO2. It can be seen that the introduction of hydrogen energy can help increase the proportion of renewable energy and accelerate the realization of 100% renewable energy supply. In addition, compared with the case of only pumped storage and without hydrogen storage (7-12), it can be seen that hydrogen storage technology can effectively reduce the weighted on-grid electricity price and accelerate the realization of 100% renewable energy supply.

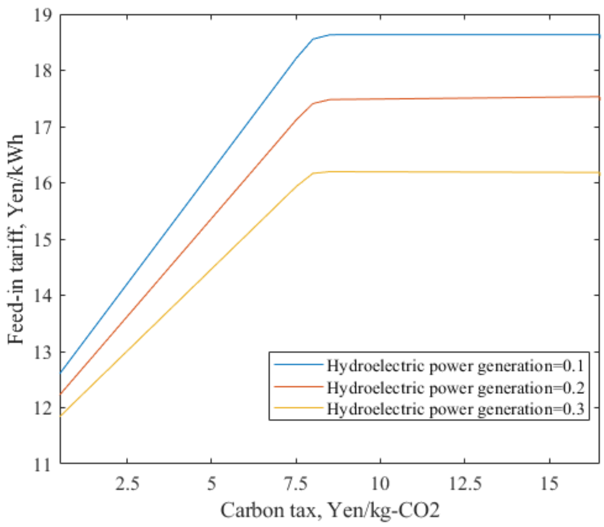

(a) Without storage

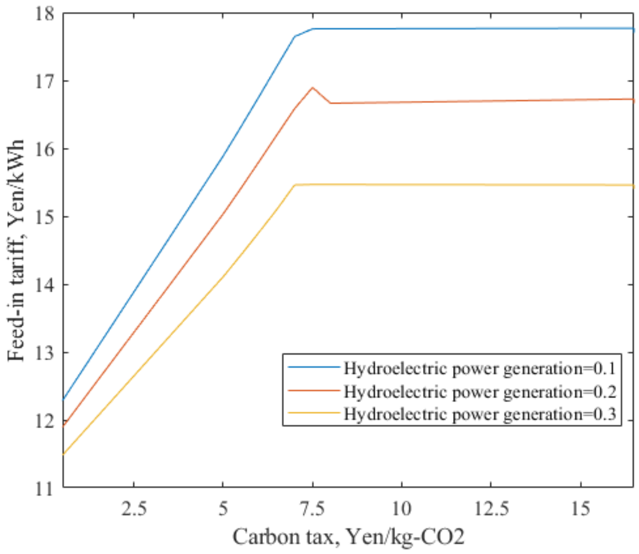

(b) Only pumped storage

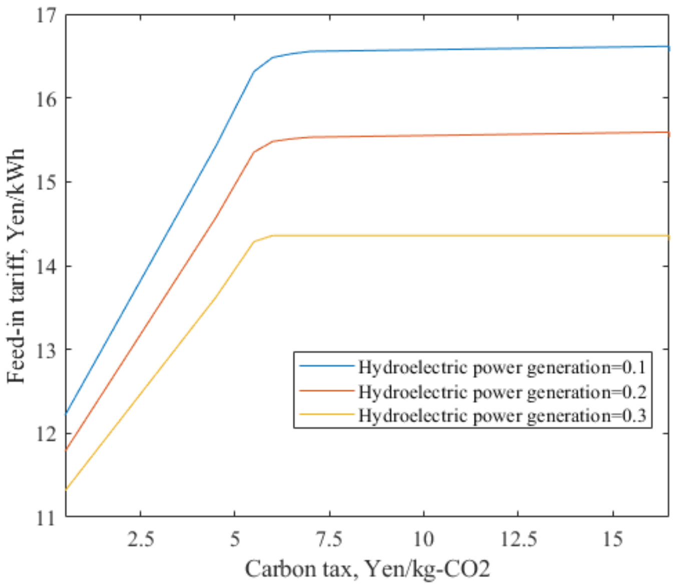

(C) With pumped and hydrogen energy storage

Fig 7-12 The lowest weighted feed-in tariff with different storage technology in Japan

7.5 Sensitivity analysis and discussion on the promotion of hydrogen energy

7.5.1 Sensitivity analysis of energy price

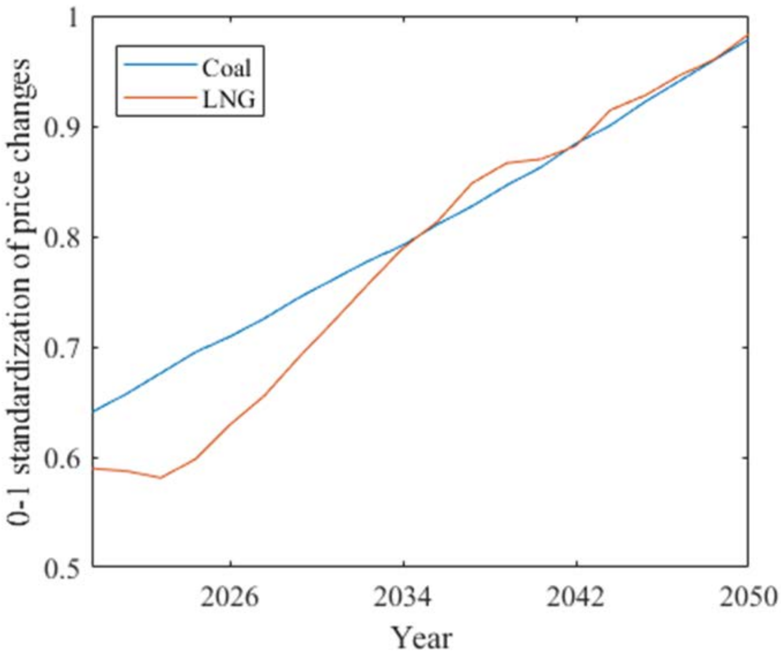

Fig 7-13 Energy price development trend forecasting [5]

Table 7-8 Setting of coal and LNG changes

Type	Base price	Target price	Increase ratio	Set change ratio
Coal	2.71	4.23	56.10%	0~60%
LNG	4.9	8.31	69.60%	0~70%

With the increasing global demand for clean energy, it is predicted that the prices of both coal and LNG will gradually increase. According to the forecasting of Energy Information Administration (EIA), the future price development of coal and LNG is obtained. (Fig 7-13)

Table 7-8 shows the basic price adopted by the article (2020) and the predicted price in the future (2040). According to the change rate of coal and LNG, set coal to change at 0-60%, LNG at 0-70%.

As shown in Fig 7-14, the results obtained show that the sensitivity of LNG is high. When the price increase reaches 70% of the existing one, 100% of the renewable energy supply can be achieved with a small carbon tax.

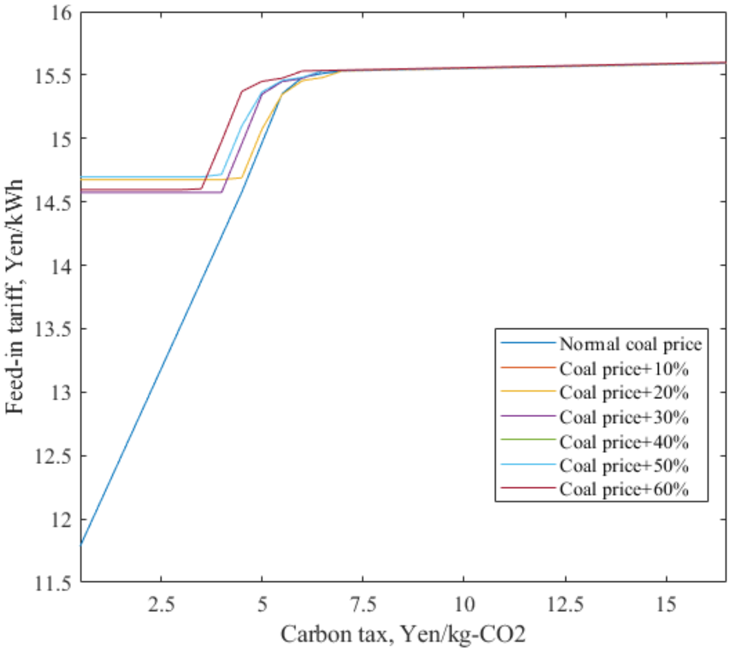

(a) Coal

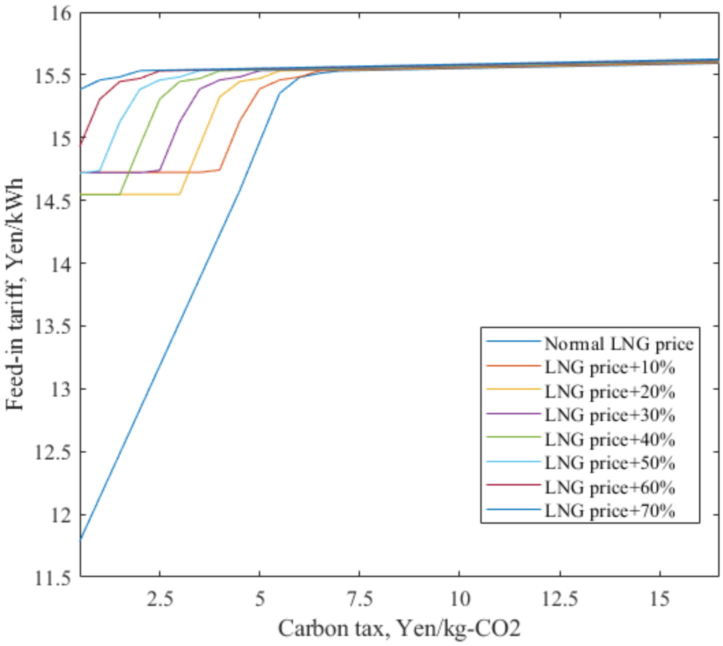

(b) LNG

Fig 7-14 The lowest weighted feed-in tariff under different carbon taxes with the change of coal and LNG price

7.5.2 Sensitivity analysis of energy equipment cost

According to Japan's strategic route of hydrogen energy [6], the price of hydrogen energy production equipment will drop by about 45%. It is believed that photovoltaic and wind power equipment will only fluctuate slightly, and the changes of the three equipment are shown in Table 7-9.

As shown in Fig 7-15, the results show that the price fluctuation of photovoltaic equipment has the highest sensitivity. Due to the impact of carbon taxes and price fluctuation intervals. Hydrogen energy production equipment fluctuated significantly when the price dropped by 10%. After that, within the range of 20%-50% price reduction, there was no significant change in the cost of electricity and electricity due to no significant reduction in renewable energy. The same situation appears in the sensitivity analysis of wind power generation equipment. It can be seen that the sensitivity of these two equipment is weak.

Table 7-9 Photovoltaic, wind power and hydrogen energy production equipment price changes

Type	Base price	Target price	Change ratio
Wind equipment	121000	-20%~+20%	
PV equipment	179000	-20%~+20%	
Hydrogen energy production equipment	400000	223000	44.25

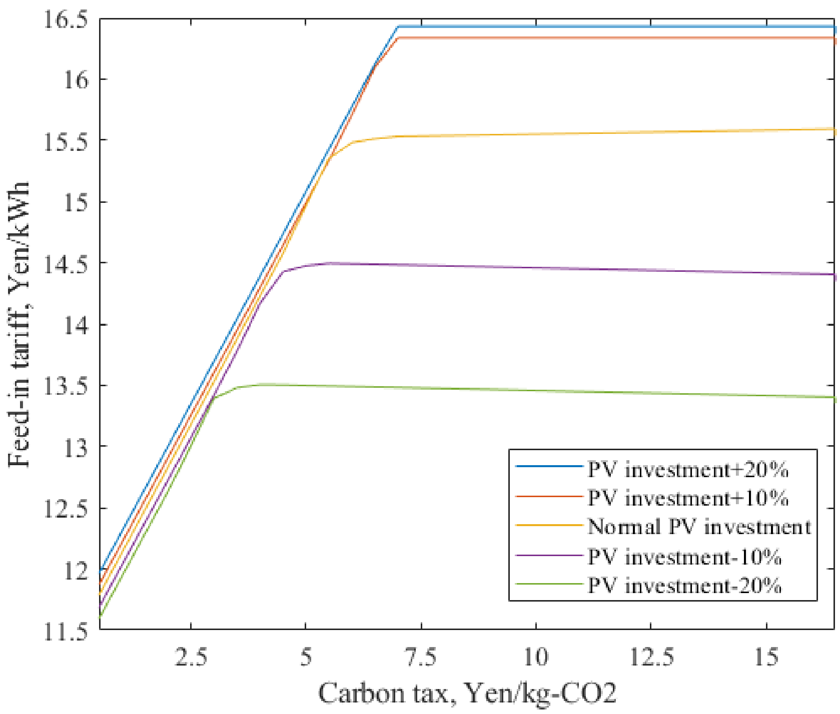

(a) Price changes in PV

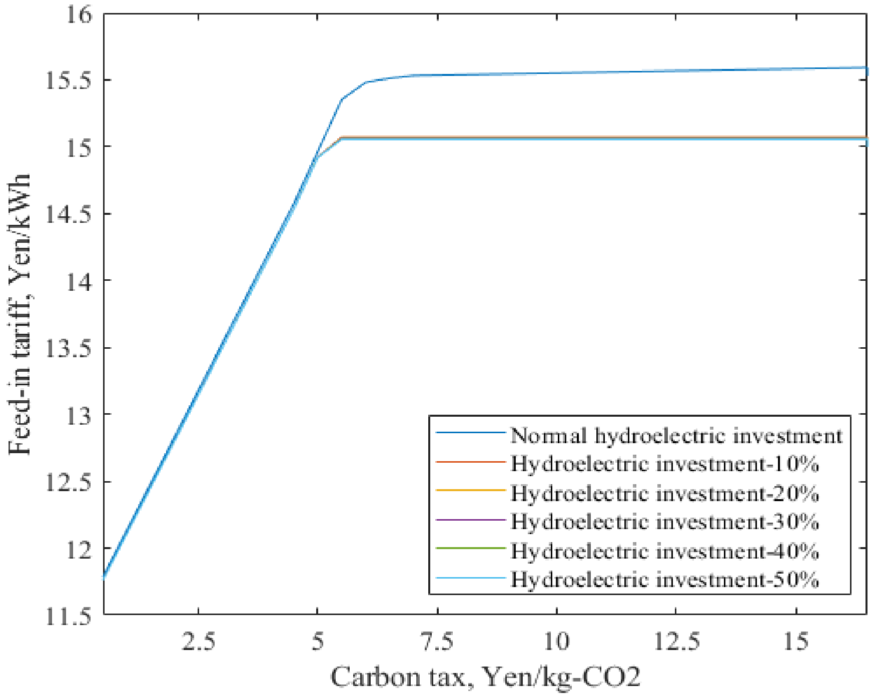

(b) Price changes in Hydrogen energy production equipment

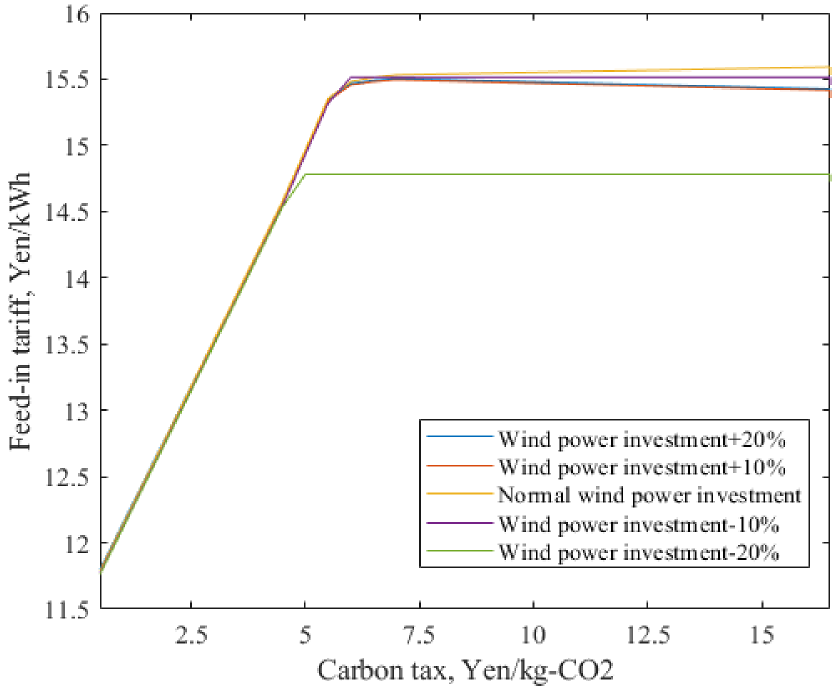

(c) Price changes in PV wind power

Fig 7-15 The lowest weighted feed-in tariff under different carbon taxes with different equipment price change

7.5.3 Discussion on the promotion of hydrogen energy

(1) Primary energy structure change and emission reduction effect analysis

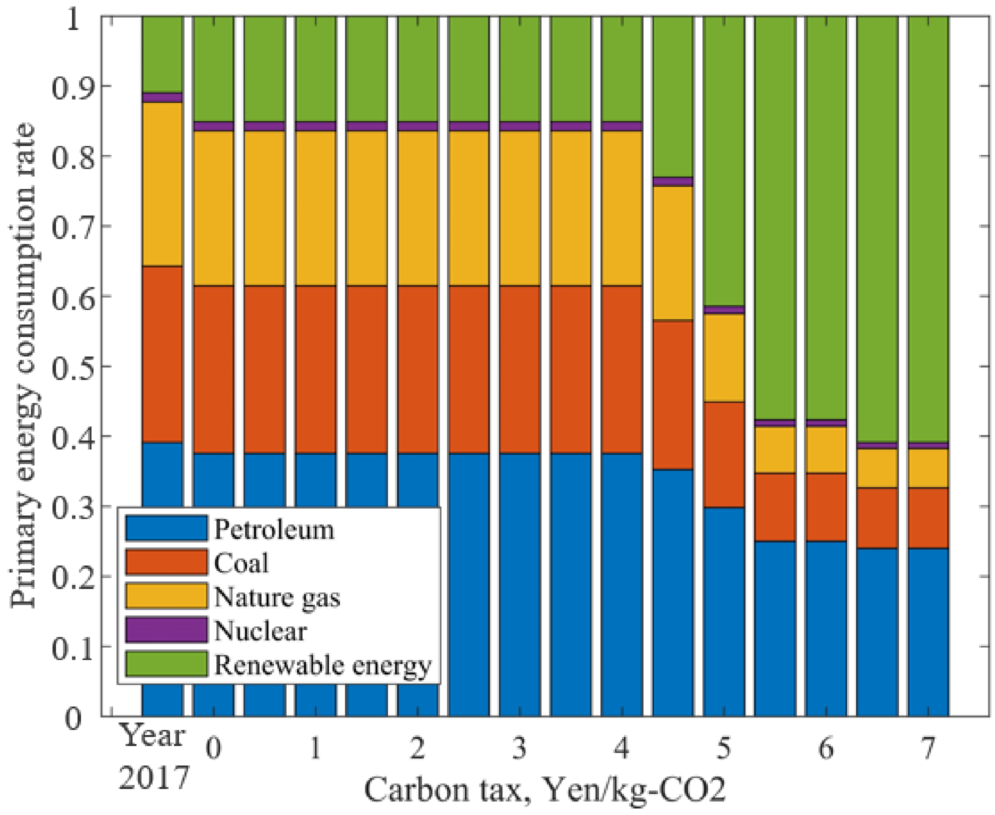

Fig 7-16 Primary energy consumption structure changed under different carbon tax

The concept of energy structure has been expanded from the field of power generation to primary energy consumption. If the energy consumption caused by demand-side management, equipment performance improvement and other energy-saving measures is not considered, the impact of structural changes in the field of power generation on primary energy consumption is shown in Figure 7-16 below. It can be seen that with the increase of carbon tax, the proportion of renewable energy will exceed 50% at 5Yen/kgCO2 and will eventually reach about 60%. Due to the impact of transportation and manufacturing, fossil fuels will still account for a certain proportion.

Japan's plan for reducing carbon emissions [7], and the final expected goals of other countries in the world are shown in Table 7-10. It can be seen that the emission reduction targets of other countries around the world are basically between Japan's 2030 and 2050 targets. Figures 7-17 show the carbon emissions calculated based on the primary energy consumption structure. It can be seen that the introduction of hydrogen energy can ultimately help Japan achieve the 2030 emission reduction target and reach the lowest level of the global emission reduction target.

Table 7-10 CO2 emission reduction targets for Japan in 2020.2030, 2050 and the world

Type	2020	2030	Global goal	2050
Target CO2 emissions (10^8 t)	13.44	10.78	4.22~8.45	2.86
Reduced difference (10^8 t)	Reached	1.69	3.94~8.17	9.58

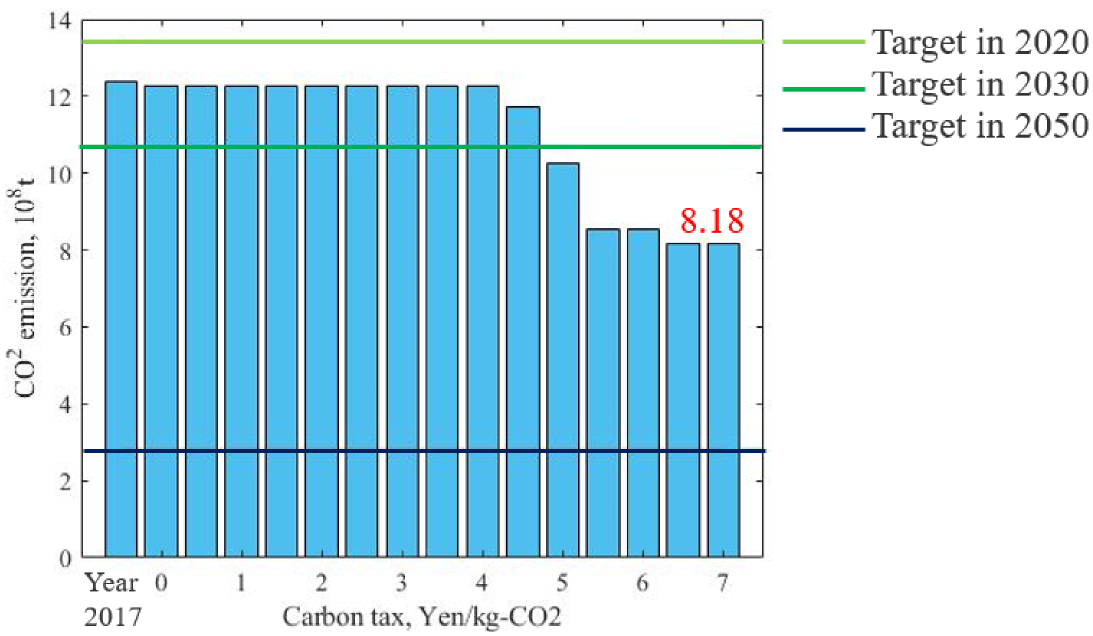

Fig 7-17 CO2 emissions under different carbon tax in Japan

(2) Analysis of the influence of hydrogen energy promotion

According to Japan's development plan for hydrogen energy and fuel cells [8], by 2030, the popularity of fuel cells will reach 5.3 million, and fuel cell vehicles will reach 800 thousand. At the same time compared with the European hydrogen energy plan, the scheme of mixing hydrogen into natural gas can reach 7.5% in 2030. Therefore, in addition to the reduction of CO2 emissions in the power industry, the effect of the introduction of hydrogen energy in other industries in 2030 can be achieved. (Table 7-11, Fig 7-18) It can be seen that among the three ways of promoting hydrogen energy, the way of natural gas doped with hydrogen can reduce the most CO2 emissions, followed by the popularity of fuel cells. But the effect of the three is relatively small compared to the overall effect of reducing emissions.

Table 7-11 Fuel cell, fuel cell vehicle and natural gas doped with hydrogen target in 2030 and emission reduction effect

Type	Base	Target in 2030	CO2 emissions reduce (10^8 t)
Fuel cell	1400000	5300000	0.045
Hydrogen fuel cell vehicle	40000	800000	0.01
Natural gas doped with hydrogen	0	7.50%	0.064
Total	0.119		

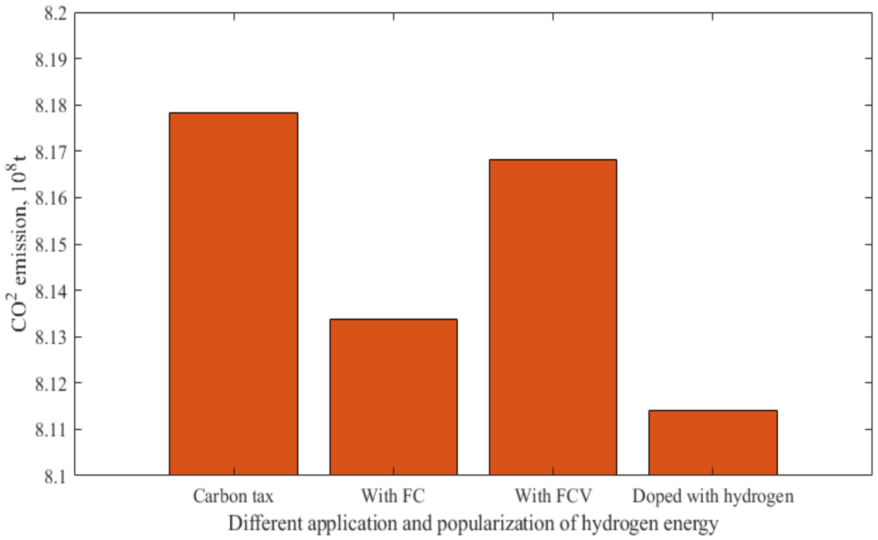

Fig 7-18 CO2 emission reduction effect analysis (2030)

According to Japan's goal of becoming the first country in the world to achieve a hydrogen society. Referring to the current Japanese car ownership and the number of houses, it is believed that the final three hydrogen energy promotion measures can achieve the effects shown in Table 7-12 and Figure 7-19.

Table 7-12 Fuel cell, fuel cell vehicle and natural gas doped with hydrogen target in 2030 and emission reduction effect

Type	Base	Hydrogen society	CO2 emissions reduce (10^8 t)
Fuel cell	1400000	60000000	0.67
Hydrogen fuel cell vehicle	40000	80000000	1.07
Natural gas doped with hydrogen	0	50%	0.43
Total	2.1		

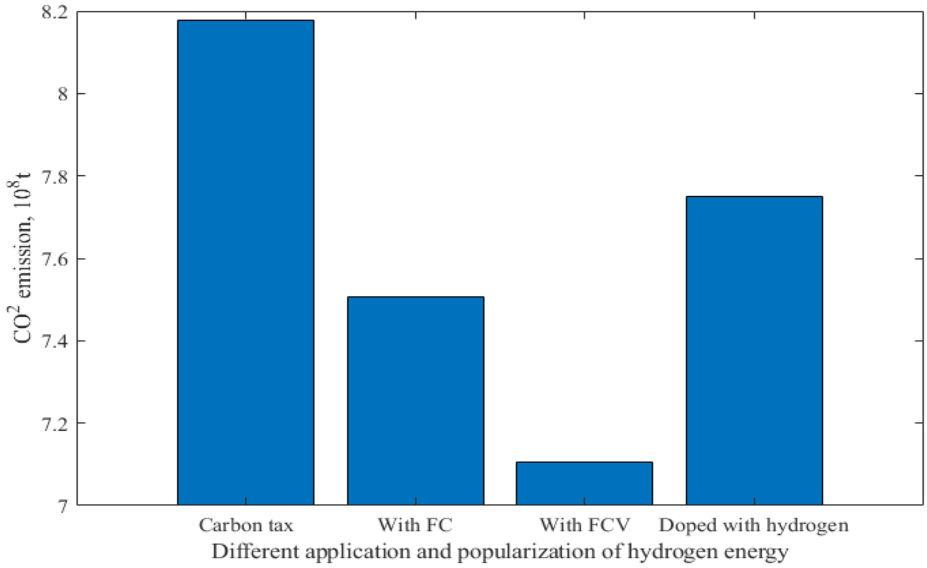

Fig 7-19 CO2 emission reduction effect analysis (hydrogen society)

It can be seen from the graph that the three measures can reduce CO2 emissions by 210 million tons. Combined with the impact of the carbon tax on the power energy structure, the introduction of hydrogen energy is expected to reduce 641 million tons of CO2 emissions. It can help Japan achieve 65% of its emissions reduction targets by 2050.

7.6 Summary

With the development of renewable energy, the phenomenon of wind and light abandonment is becoming more and more serious, and the shortcomings of pumped storage limited by the objective environment are more and more obvious. Hydrogen storage will become one of the important means to break through the bottleneck of renewable energy development in the future.

Through the comparison of hydrogen storage technology with conventional energy system, it can be seen that the current development limitation of hydrogen energy technology is mainly due to the high initial investment cost. At present, the establishment of carbon tax will be conducive to the promotion of fuel cell system. At the same time, in the field of renewable energy storage, hydrogen energy as a supplement means of pumped storage has begun to have practical application value.

Next, Japan’s ten power companies were taken as an example to study the optimal energy structure calculated according to the lowest weighted on-grid tariff under different carbon taxes. The proportion of thermal power generation of most power companies achieved zero under the carbon tax of 7.5-10Yen/kgCO2, that is, to achieve 100% renewable energy supply. Assuming that based on the characteristics of long-distance and inter-seasonal storage of hydrogen, Japan's renewable energy systems can be coordinated and dispatched. The result shown that these characteristics of hydrogen energy can accelerate the arrival of 100% renewable energy supply. According to the sensitivity analysis, the price of photovoltaics and the price of LNG are the most influential in this process.

After that, the research on electric energy structure was expanded to the overall primary energy structure. Analyze the role of hydrogen energy introduction through changes in energy structure and carbon emissions. The introduction of hydrogen energy can effectively increase the proportion of renewable energy. At the same time, it can help achieve the 2030 emission reduction target.

Finally, based on the promotion of hydrogen energy, in addition to the power system, three hydrogen energy promotion methods were proposed, including fuel cells, fuel cell vehicles, and natural gas dropped with hydrogen. According to Japan's promotion plan for the hydrogen energy system, by 2030, the three measures can reduce carbon dioxide emissions by about 12 million tons. It is assumed that in the future hydrogen energy society, FC and FCV will become the mainstream, and the proportion of natural gas doped with hydrogen will reach more than 50%. The results show that about 210 million tons of carbon dioxide emissions can be reduced. It can be seen that the promotion of carbon tax and hydrogen energy can help Japan achieve more than 65% of its emission reduction targets. It can be seen that even if other energy-saving and emission-reduction measures are not considered, the promotion of hydrogen energy in various fields will greatly reduce carbon dioxide emissions.

The research of this paper is mainly based on the calculation of system investment, operation and maintenance cost and corresponding dynamic investment payback period. In the calculation process, combined with the development planning and prediction of hydrogen energy and fuel cell in Japan and the United States, the corresponding parameters are estimated, and the results obtained have certain reference value. However, in the process of optimization, the calculation of energy storage loss and configuration of energy storage system is simplified. There is no in-depth analysis on the optimal operation strategy of energy storage system and renewable energy. Only from the macro point of view of the optimization of energy allocation and structure, there is still room for further study.

Reference

[1] Comprehensive Energy Survey, Ministry of Economy, Trade and Industry, Japan, 'Report on verification of power generation costs, etc. to the Long-term Energy Supply and Demand Outlook Subcommittee'.
https://www.enecho.meti.go.jp/committee/council/basic_policy_subcommittee/mitoshi/cost_wg/007/

[2] Technology Strategy Research Center (TSC), 'Toward the formulation of technical strategies in the field of electricity storage'. https://www.nedo.go.jp/content/100866310.pdf

[3] Natural Energy Institute, Japan, 'Business risk analysis of coal-fired power generation investment'. https://www.renewable-ei.org/activities/reports/20191003.php

[4] Electricity Review Japan : The Federation of Electric Power Companies / Japan. http://www.geni.org/globalenergy/library/national_energy_grid/japan/Electricity_Review_Japan.shtml

[5] Energy Information Administration, annual energy outlook 2020. https://www.eia.gov/outlooks/aeo/

[6] Japan Ministry of Economy, Trade and Industry, 'Hydrogen/fuel cell strategy roadmap'. https://www.meti.go.jp/press/2018/03/20190312001/20190312001.html

[7] Ministry of the Environment, Japan, 'Current status of greenhouse gas emissions and carbon/energy productivity in Japan'. https://www.env.go.jp/earth/ondanka/cp/arikata/conf07.html

Chapter 8

CONCLUSION AND PROSPECT

CHAPTER EIGHT: CONCLUSION AND PROSPECT

8.1 Conclusion

Hydrogen energy characteristics of long-distance and inter-seasonal transportation and storage can help renewable energy break through development bottlenecks and help various industries to decarbonize deeply. However, the current cost of the system restricts the rapid promotion of hydrogen energy. Therefore, based on the hydrogen energy characteristic of zero carbon emission when using, this study proposes to convert the environmental advantages of hydrogen energy into economic benefits through carbon tax. Although the large-scale popularization of hydrogen energy is bound to come according to the development plans of various countries, most of the current research is still based on the current energy supply and demand relationship and the demand for the environment. Considering the carbon tax will help to understand the application and development potential of hydrogen energy more clearly under more restrictive environmental conditions. This study will conduct research on the economic potential, impact analysis and development forecast of hydrogen energy based on carbon tax limitation from the three levels of equipment, system and region.

The main works and results can be summarized as follows:

In chapter one, RESEARCH BACKGROUND AND PURPOSE OF THE STUDY, analyzed the significance of hydrogen energy for renewable energy and global deep decarbonization. Then through the analysis of the characteristics of hydrogen energy, it shown the high safety of hydrogen energy. After that, the process of producing, storing, transporting and using hydrogen energy was explained. Finally, through the elaboration of the hydrogen energy development process and goals of the United States, the European Union, China and Japan, the importance of hydrogen energy in the energy strategies of various countries was highlighted. It can be seen that hydrogen energy has an important position in the energy strategies of countries around the world.

In chapter two, LITERATURE REVIEW OF HYDROGEN ENERGY SYSTEM, is mainly to sort out the research status of hydrogen energy. First of all, through the review of the research on the development of hydrogen energy by the policies of various countries, the current status and trends of the cost reduction of hydrogen energy systems were explained. Then it shown that the current research focus on hydrogen energy is the production of hydrogen energy and the performance improvement of fuel cells. Next, since the core of development based on hydrogen energy is to combine with renewable energy, the literature and compares the characteristics of hydrogen storage and other energy storage technologies was reviewed. Finally, according to the research object of this article, the research and combing of the application of fuel cell, fuel cell vehicle and hydrogen energy in regional energy system were carried out.

In chapter three, MODEL ESTABLISHMENT AND FORECASTING METHOD RESEARCH, is about methodological research and model building. Firstly, the research motivation and main research methods of the article, carbon tax, were expounded. Then the general load and equipment model to be used in the follow-up study were established. At the same time, different operating strategies based on regional energy systems were explained. Next, it was believed that load forecasting is the basis of follow-up research, so a new forecasting method of cold and hot load based on transfer learning was proposed and verified. The comparison with conventional prediction methods proves that the proposed method has high application value in the absence of sufficient actual data.

In chapter four, UTILIZATION POTENTIAL AND ECONOMIC ANALYSIS OF HYDROGEN ENERGY EQUIPMENT, the experimental data are obtained by the experiment table, and the regression equation can be made on the output current of the reactor and the flow of Methanol water according to the obtained data. Then the simulation model is built according to the equation, and the residual heat of the experiment table is simulated and analyzed. The results of the study show that the method of making hot water directly can maximize resource utilization. Finally, through the comparison of fuel cells, fuel cell vehicles and conventional systems under carbon tax restrictions, it can be seen that hydrogen energy equipment does not have economic advantages under the existing price system. With the cost reduction, by 2030 the price system and carbon tax level, hydrogen energy equipment does not require policy support to enter the mainstream energy market.

In chapter five, ECONOMIC AND POTENTIAL ANALYSIS OF FUEL CELL VEHICLE-TO-GRID SYSTEM, the potential of FCV2G was analyzed. Based on the electricity consumption data of a large shopping mall in Japan, a Monte Carlo simulation was used to obtain the impact of large-scale FCVs on the power load of the shopping mall. It proved that the introduction of FCVs can effectively reduce the power demand of the target shopping mall. After that, the effects of FCV2G were specifically analyzed through comparison with EV. With the increase of FCV import, the total income rises. Finally, the sensitivity analysis was performed with the FCV ratio of 15% as the benchmark. The results show that the overall benefits of FCV2G will develop in a better direction over time.

In chapter six, ECONOMIC AND POTENTIAL ANALYSIS OF REGION DISTRIBUTED HYDROGEN ENERGY SYSTEM, the economic potential of hydrogen in RDES was analyzed by considering introducing the concept of carbon tax to convert the environmental advantages of hydrogen energy into economic benefits. Firstly, five building types rely on hydrogen energy supply line in a demonstration area of hydrogen energy application of Kitakyushu, Japan were used as research cases, and the conventional RDES system including CCHP and PV-Battery was used as a comparative item for research and analysis. Then, the electrical load and the full-load equivalent running time method was used to forecast cooling and heating loads and curve shaping. After that, a total cost model including carbon tax was established for optimization. Finally, through the comparative analysis of different building types and buildings with varying load characteristics, it was found that with the increase of photovoltaic penetration rate, compared with conventional RDES, the economic benefit of hydrogen RDES is better and more obvious, that is, the fit with the photovoltaic system is higher. At the same time, it was found that the strong changes in the building load will inhibit the increase in the efficiency of hydrogen RDES, leading to a situation where the profitability is maximized within the photovoltaic penetration rate range of 20-40%. Therefore, it was considered that buildings with relatively gentle load changes are more suitable for large-scale introduction of hydrogen RDES systems. This result is consistent with the current demand-side management and energy consumption peak-shaving and valley-filling, which can achieve mutually beneficial effects.

In chapter seven, STUDY ON THE HYDROGEN IMPLICATION OF ENERGY STRUCTURE WITH CARBON TAX INTRODUCTION, hydrogen storage was compared with other conventional energy storage technologies. Next, Japan’s ten power companies were taken as an example to study the optimal energy structure calculated according to the lowest weighted on-grid tariff under different carbon taxes. The proportion of thermal power generation of most power companies achieved zero under the carbon tax of 7.5-10Yen/kgCO2, that is, to achieve 100% renewable energy supply. Assuming that based on the characteristics of long-distance and inter-seasonal storage of hydrogen, Japan's renewable energy systems can be coordinated and dispatched. The result shown that these characteristics of hydrogen energy can accelerate the arrival of 100% renewable energy supply. According to the sensitivity analysis, the price of photovoltaics and the price of LNG are the most influential in this process. Finally, the research on electric energy structure was expanded to the overall primary energy structure. Analyze the role of hydrogen energy introduction through changes in energy structure and carbon emissions. The introduction of hydrogen energy can effectively increase the proportion of renewable energy. At the same time, it can help achieve the 2030 emission reduction target. At the same time, the promotion of hydrogen energy, in addition to the power system, three hydrogen energy promotion methods were proposed, and the results shown that the promotion of carbon tax and hydrogen energy can help Japan achieve more than 65% of its emission reduction targets. That is, even if other energy-saving and emission-reduction measures are not considered, the promotion of hydrogen energy in various fields will greatly reduce carbon dioxide emissions.

In chapter eight, CONCLUSION AND PROSPECT have been presented.

To summary, this article introduced the concept of carbon tax to convert the environmental advantages of hydrogen energy into economic advantages. Comparative research on three different levels of equipment, system and region was conducted.

At the equipment level, equipment prices and carbon tax levels by 2030 will make hydrogen energy equipment market competitive without relying on policy support.

At the system level, fuel cell vehicles participate in the FCV2G system formed by V2G, and RDHES systems that have participated in the formation of regional distributed energy by hydrogen energy have great economic potential. Compared with V2G system, FCV2G system has larger schedulable space, which can make this technology more fully utilized. RDHES is more adaptable to photovoltaics. With the continuous promotion of distributed photovoltaic systems, RDHES will become the mainstream of distributed energy systems.

At the regional level, although the economic benefit of hydrogen storage is lower than that of batteries and pumped storage, it is not subject to objective environmental constraints and can be well used as an extension and supplement to existing energy storage technologies. As the penetration rate of renewable energy continues to rise, it will gradually become the main energy storage technology. At the same time, with the help of hydrogen energy, countries will also achieve their respective emission reduction goals more efficiently.

The introduction of carbon tax can effectively improve the economic benefits of the hydrogen energy system and help the promotion of the hydrogen energy system. At the same time, the popularity of hydrogen energy systems will also greatly accelerate the realization of global deep decarbonization. It is hoped that this research can provide new ideas for the promotion of hydrogen energy and provide theoretical reference for the research on the practical application of hydrogen energy.

8.2 Prospect

For prospect, as the scope of natural gas applications expands, the effect of reducing emissions through hydrogen doping will gradually increase. Therefore, there is still room for further research on the effect of hydrogen energy on emission reduction.

However, the use of hydrogen energy will not produce carbon emissions, but in the storage and transportation of hydrogen energy, energy consumption and carbon emissions still exist. The life cycle analysis of the use of hydrogen energy will help to understand the environmental and economic characteristics of hydrogen energy more clearly.

At the same time, the levels of hydrogen energy utilization in different regions are different, and the price system is different. This article is mainly aimed at the analysis of the application potential of hydrogen energy and the CO2 emission reduction effect under the Japanese energy and price system. The global promotion and application potential of hydrogen energy still needs in-depth research.